STUDIES ON THE HISTOPATHOLOGICAL EFFECTS OF *BACILLUS THURINGIENSIS* AND *NOSEMA POLYVORA* ON THE MALPIGHIAN TUBULES OF *PIERIS CANIDIA* LARVA

WANG JIAN BIN

Department of Biology

A thesis submitted in partial fulfilment of
the requirements for the degree of
Doctor of Philosophy
in
the Graduate School
The Chinese University of Hong Kong

October 1993

Acknowledgements

I would like to express my sincere thanks and deepest gratitude to my supervisor Dr. Wilkin W. K. Cheung, for his patient guidance, constant advice, discussion and enthusiastic encouragement during my Ph. D. study, and for his constructive comments and suggestions on this thesis.

I am also deeply grateful to Dr. Vincent E. C. Ooi and Dr. K. W. Chiu, Department of Biology, the Chinese University of Hong Kong, for their valuable advice and good suggestions to my study and research.

I am greatly indebted to all people who have kindly given me help, service, and information on my study and research. Special thanks are due to Ms. Denise F. Y. Ho who taught me electron microscopic techniques and photographic skills, and finally, I would like to give my hearty thanks to all staff of the Department of Biology, the Chinese University of Hong Kong, for their personal care as well as academic support to my studies in this Department.

CONTENTS

Abstract

Bacillus thuringiensis and *Nosema polyvora*, both act as biological control agents. The Malpighian tubules of *Pieris canidia* larvae had been used as a model for the study of their histopathological effects. The normal morphology of Malpighian tubules of *Pieris canidia* had six tubules. Each tubule could be conveniently divided into four regions: rectal lead, iliac plexus, yellow region and white region. The principal cells of all four regions had their apical surface folded to form microvilli, with mitochondria extending almost to their tips. Basally there were numerous infoldings forming intracellular channels extending deeply towards the apical surface. Many mitochondria, rough endoplasmic reticula, Golgi apparatus and vacuoles were found in the ground cytoplasm. The nucleus of each cell had scattered chromatin materials and an irregular outline. The yellow region had numerous electron dense granules which had been demonstrated to be mineral deposits. Then, the histochemical characteristics of Malpighian tubules were studied by various histochemical methods in order to understand their functions better.

Before examining the histopathological effects of *Bacillus thuringiensis* δ-endotoxin on the Malpighian tubules of *Pieris canidia*, the parasporal crystals were purified from laboratory cultured bacteria Thuricide supplied by Sandoz Company. Urografine solution was used as a separation medium. After centrifugation at 6000 rpm for two hours, spores were at the bottom of a centrifuge tube. Two bands were visible in the region of short gradients of urografine formed at the interface between the culture and the urografine solution. The crystals were in the lower band. After purification, the purified parasporal crystal δ-endotoxin was injected into the tubule lumen or applied

externally in the bathing medium of yellow region tubules. Mucosal and serosal exposure had different patterns of membrane disorganization, with those membranes closest to the site of application being disrupted first. The cytological alterations included enlargement of spaces in the cytoplasm and basal infoldings. The microvilli became slightly disorganized for mucosal treatment and the basal infoldings became slightly irregular in shape for serosal treatment. After 10 minutes toxin treatment, some of the microvilli appeared distorted and some of them appeared less affected. Most mitochondria were transformed into a condensed form. The nucleus enlarged and chromatin materials dispersed. The cytoplasmic spaces enlarged continually. By 20 minutes after toxin treatment, general disintegration was observed. Microvilli were completely disappeared and the apical membrane lysed. The rough endoplasmic reticula and Golgi apparatus vacuolated. The mitochondria were generally in the condensed form and almost round in shape. The basal infoldings were distorted and the basal lamina was damaged. These results indicated that *Bacillus thuringiensis* δ-endotoxin might bind to a plasma membrane receptor. The action of toxin was to generate small pores in the plasma membrane. Malpighian tubule cells swelled and eventually lysed.

The microsporidium *Nosema polyvora* had been described at the ultrastructural level. Its histopathological effects on the Malpighian tubules of *Pieris canidia* were then investigated. The ultrastructural changes included an enlargement of cytoplasmic spaces and some sort of mucus secretions appeared. In the central cytoplasm, the mitochondria, rough endoplasmic reticulum and Golgi apparatus appeared normal. The nuclei of Malpighian tubule cells became very irregular in shape. Mechanical damages to the host cells occurred with empty spaces formed in the cytoplasm. The basal infoldings appeared slightly disorganized, the cristae of mitochondria were modified and the microvilli were

distorted.

Part I. General Introduction

Bacillus thuringiensis is closely related to *Bacillus cereus*. The distinctive characteristic of *Bacillus thuringiensis* is the presence of a parasporal inclusion that exhibits insecticidal activity (Luthy *et al.*, 1982). During the last two decades, the histopathological effects of *Bacillus thuringiensis* on the insect midgut epithelia (Sutter and Raun, 1967; Endo and Nishiitsutsuji-Uwo, 1980; Ebersold *et al.*, 1980; Percy and Fast, 1983; Tojo, 1986; DeLello *et al.*, 1984; Gupta *et al.*, 1985; Oron *et al., 1985*; Lane *et al.*, 1989; Cheung *et al.*, 1990; Cheung and Lam, 1993), insect cell lines (Cooksey *et al.*, 1969) and embryonic cell (Johnson and Davidson, 1986) have been investigated extensively. However, the histopathological effects of *Bacillus thuringiensis* on Lepidoptera Malpighian tubules have not been reported on except the works of Reisner *et al.* (1989) on the skipper butterfly *Calpodes* larvae and Ryerse *et al.* (1990) on the tobacco budworm *Heliothis* larva. Insect Malpighian tubules possess a one cell thick epithelium generally similar to those of the midgut (Harvey *et al.*, 1983; Martoja and Ballan-Dufrancais, 1984). It is convenient to observe the cytological alterations of Malpighian tubules of *Pieris canidia* after *Bacillus thuringiensis* treatment.

Although many hypotheses have been proposed to explain the mode of action of *Bacillus thuringiensis* δ-endotoxin (Faust, 1968; Cooksey *et al.*, 1969; Fast and Donaghue, 1971; Fast and Morrison, 1972; Luthy, 1973; Traverse *et al.*, 1976; Nishiitsutsuji-Uwo *et al.*, 1979; Gupta *et al.*, 1985; Knowles and Ellar, 1987), the exact mechanism that causes the pathogenetic effects remains unclear. The histopathological study of *Bacillus thuringiensis* var. *kurstaki* δ-endotoxin on Malpighian tubules of *Pieris canidia* may provide insight into the tissue

specificity and cellular mode of action of the toxin.

The small cabbage white, *Pieris canidia* is a common butterfly in Hong Kong. Their larvae are serious pests in local vegetables (Hill *et al.*, 1982). It is possible to use *Bacillus thuringiensis* var. *kurstaki* for controlling this pest as the bacterium is a good alternative to solely using synthetic chemical pesticides (Faust and Bulla, 1982). In order to compare the structural changes induced by *Bacillus thuringiensis* with the normal structure and understand the functions of *Pieris* Malpighian tubules better, the normal structure of Malpighian tubules and their histochemical properties of *Pieris canidia* are first investigated.

Some protozoans such as Microsporidia, also hold potential as biological control agents for long-term suppression of pest (Ewen and Mukerji, 1980). Numerous studies on microsporidians have been undertaken. These include study of biology (Brooks, 1980; Andreadis, 1986; Hayasaka and Kawarabata, 1990; Zhao *et al.*, 1990; Solter *et al.*, 1991), life cycle (Ishihara, 1969; Kawarabata and Ishihara, 1984; Sleigh, 1989) and the fine structure of spores in different species (Liu and McEwen, 1977; Gorske and Maddox, 1978; Sato *et al.*, 1982; Avery and Anthony, 1983; Kline *et al.*, 1985; Larsson, 1989, 1990; Hsu *et al.*, 1991).

Microsporidian infections are widespread in insects and *Nosema* spp. have been discovered in many species (Liu and McEwen, 1977). The pathology of microsporidians has also been reported on by many authors (Malone and Wigley, 1981; Siegel *et al.*, 1986; Johnson and Pavlikova, 1986; Brooks, 1986; Solter *et al.*, 1990; Macvean and Capinera, 1991). However, the histopathological effects of protozoans on insects have received little attention. A study on the histopathology of *Nosema polyvora* on the Malpighian tubules of *Pieris canidia* will give better understanding of the action of protozoans on target insects.

Part II. Literature review

A. The structure and functions of insect Malpighian tubules

Survival in the terrestrial environment demands an osmoregulatory system that is efficient in conserving water and adapted to changes in environmental conditions. The insects have evolved a very flexible system that can cope with extremes on the humidity scale. Thus enables them to invade habitats ranging from the desert to the wettest parts of the tropical rain forest (Wall and Oschman, 1979). This system is one in which the digestive and excretory systems are coupled. The Malpighian tubules form a primary urine that enters the gut at the junction between the midgut and the hindgut. This primary urine in many way resembles a filtrate of the blood (Ramsay, 1958; Maddrell and Gardiner, 1974). By modifying the activities of the Malpighian tubules and the rectal absorptive cells, the water content of the faecal material can be adjusted from very wet to very dry. Hence the Malpighian tubule-rectum system functionally corresponds to the nephridia of Annelida and Onychophora and to the kidney of vertebrates (Wall and Oschman, 1979).

I. The excretory system of insects

1. Morphology of Malpighian tubules

In the majority of insects the excretory system consists of a number of Malpighian tubules. These tubules are elongated tubular structures which lie in the haemocoel (blood space) of the abdomen. One end of each tubule is closed

and the other end leads into the alimentary canal at the junction of the midgut with the anterior part of the hindgut (Chapman, 1975).

The Malpighian tubules are slender tubes arising from the junction between midgut and hindgut. In some insects, such as *Rhodnius*, there are special beaded structures separating the whole tubules into distal tubules and proximal tubules (Wigglesworth, 1972). The number of these tubules varies from 1 to 250 or more in different insects. When they are few, as in *Rhodnius*, they are often long. When they are numerous, as in *Periplaneta*, they are often short and grouped into bundles of equal size (Ross *et al.*, 1982).

2. Common types of Malpighian tubule system

Wigglesworth (1931) in his paper " the physiology of excretion in a blood-sucking insect, *Rhodnius prolixus* (Hemiptera, Reduvilidae)", described the four common types of Malpighian tubule system. These are basic type (A) with three variants (B), (C) and (D).

In the basic type of Malpighian tubule system (A), the tubules are long and convoluted, and each tubule is made up of walls one cell in thickness with four to six cells comprising the circumference. These tubules may lie more or less free in the body cavity, where they are bathed in the blood. However, some of the tubules are always closely associated with the fat body and digestive tract.

Tubules with the distal attachment are described as cryptonephric system (Lison, 1938). Tubules of this type are typical of the Coleoptera, in which there is no visible differentiation over the entire length, and they are represented by type (B). The Lepidoptera as type (D) also have cryptonephric tubules, but these tubules are roughly differentiated into two sections. the distal part is filled with a clear fluid, and the proximal part has solid particles that made it appear opaque.

Type (C) is typical of the Hemiptera, and through the extensive work of Wigglesworth (1931; 1972) with *Rhodnius*, this type has been thoroughly understood. This type of tubule has free distal end but shows a visible differentiation near the midpoint with the proximal half opaque and the distal half clear.

3. Morphology of hindgut

All of the alimentary tract posterior to the midgut in insects consists of cuticle-lined hindgut. The anterior portion of this is generally more narrow than the midgut and is termed ileum, while the posterior portion is usually expanded into a rectal sac (Chapman, 1975).

In most insects the ileum is an undifferentiated tube running back to the rectum, but in some termites it forms a pouch in which the flagellates concerned with cellulose digestion live, and in larval Scarabaeoidea there is a comparable fermentation chamber in which intima is produced into spines. In Heteroptera it is suggested that the ileum is concerned with the removal of water from the haemolymph (Goodchild, 1963), and in blowfly larvae certain cells are concerned in the excretion of ammonia (Waterhouse, 1957).

The rectum is often an enlarged sac and is thin walled except for certain region, the rectal pads, which have a columnar epithelium. There are usually six rectal pads and they may extend longitudinally along the rectum or they may be papilliform as in Diptera. The cells of the rectal papillae of *Calliphora* (Diptera) enclose extensive intercellular sinuses which are separated from the gut lumen by cell junctions and which connect only indirectly with the haemcoal. The cell membrane bounding these spaces form a series of flattened sacs which are closely associated with mitochondria. The apical membrane, beneath the cuticle

lining the rectum, is infolded in a series of parallel leaflets. In Odonata and Orthoptera each pad consists of a single layer of cells, but in Neuroptera, Lepidoptera and Hymenoptera there are two layers. The pads have a good tracheal supply (Chapman, 1975)

II. Structure of insect Malpighian tubules

Numerous studies on the structural features of insects Malpighian tubules of various larval and adult insects have been done, such as *Rhodnius prolixus* (Wigglesworth and Salpeter, 1962), the blowfly *Calliphora erythrocephala* (Berridge and Oschman, 1969), the stick insect *Carausius morosus* (Taylor, 1971a and b), the cicadas *Gaeana maculata* and *Cryptotympana mimica* and the spittle bug *Cosmoscarta abdominalis* (Marshall and Cheung, 1974), the housefly, *Musca domestica* (Sohal, 1974; Sohal *et al.*, 1976), the fruitfly *Drosophila melanogaster* (Eichelberg and Wessing, 1975), the skipper butterfly *Calpodes ethlius* (Ryerse, 1979), the brinefly, *Ephydra hians* (Yu *et al.*, 1988), the house cricket, *Acheta domesticus* (Hazelton *et al.*, 1988) and the midge *Chironomus tentans* (Jarial, 1988).

1. The general organization of the Malpighian tubules

The tubules consist of an epithelium which rests on a connective tissue sheath containing tracheoles. Circular muscular fibers are frequent, although they may be rare or absent (Crowder and Shankland, 1972; Eichelberg and Wessing, 1975). The basement membrane is composed of granular and fibrillar layers. The epithelial cells are jointed by septate, gap, and sometimes scalariform junctions. Whatever species, a cellular type that we term the principal Malpighian tubule

cell exhibits similar structural features associated with fluid secretion as well as storage processes. Other kinds of cells are present together with the principal ones (Martoja and Ballan-Dufrancais, 1984).

2. Structure of the principal Malpighian cell

This cell exhibits a structural polarity. The cells of all the tubule segments of *Drosophila* (Eichelberg and Wessing, 1975) principally exhibit a common polar structure. Each tubule cell shows a division into three regions: a basal, an intermediate, and an apical regions. The basal region which faces the body cavity, is separated from the haemolymph by the basement membrane. Deep folds of the cellular membrane, lying beneath the basement membrane, protrude into the cell body and building a tight mesh network of extracellular spaces, which enlarge the surface area. This is called the basal labyrinth. It extends from one quarter in *Periplanete americana* (Wall *et al.*, 1975) to three-quarters in *Calliphora erythrocephala* (Berridge and Oschman, 1969). Mitochondria are numerous, while microtubules, ribosomes, and rough endoplasmic reticulum are also present. Pinocytotic vesicles may occur along the membrane.

The basement membrane probably serve as a filter on the outside of the tubules to keep particles and cells from clogging the infolds of the basal cellular membrane. In *Calliphora erythrocephala* (Berridge and Oschman, 1969), the basement membrane also appears to be impermeable to large protein, while in others, *Drosophila melanogaster* (Eichelberg and Wessing, 1975) proteins such as horseradish peroxidase can penetrate this layer. The basal membrane of the upper Malpighian tubule of *Rhodnius prolixus* (Wigglesworth and Salpeter, 1962) contained higher concentrations of potassium than did the surrounding saline, so the polyanionic sites on the basal membrane might be cation-selective.

The basal plasma membrane of Malpighian tubules of *Rhodnius prolixus* (Wigglesworth and Salpeter, 1962) is highly folded into deep slits running perpendicular to the basal membrane. In thin section, dense plaques reminiscent of hemidesmosomes are observed on the cytoplasmic side of the basal membrane where it lies adjacent to the basal membrane. Three dimensional organization of the basal folds is maintained by an extensive cytoskeletal network inside the folds, consisting of both microtubules and microfilaments. The high degree of folding in the basal membrane is consistent with the multiple transport processes known to occur at this surface.

A brush border is characteristic for the apical region of *Drosophila* (Eichelberg and Wessing, 1975), which faces the lumen of the tubule. It is composed of more or less numerous finger-shaped protrusions of the cell which project into the lumen. These microvilli often contain a channel of the endoplasmic reticulum, which often has a connection to the reticulum of the intermediate cell region, and in some cases also communicates with the basal infoldings. Pinocytotic vesicles are frequent, but no cell coat can be observed.

The microvilli are thought to increase the membrane surface area available for salt and water transport between the cytoplasm and lumen. Microvilli, which are found throughout the animal kingdom, are tubular extensions of the cell cytoplasm, bounded by plasma membrane and containing microfilaments composed at least in part of action.

The intermediate region of the cells of *Drosophila melanogaster* (Eichelberg and Wessing, 1975) is characterized by diverse organelles. It is also transverse by channels of the endoplasmic reticulum; these channels can be connected with the numerous Golgi fields and can accumulate diverse substances in ampulla-like enlargements. Moreover, vesicles, multivesicular bodies and the polyploid nucleus are found in this region. The middle part of the cell contains the nucleus,

RER, few Golgi bodies, mitochondria and lysosomes. Mineral spherocrystals are frequently abundant. The principal cells sometimes sequester organic components such as granules containing calcium phosphates (Othoptera and Diptera), or flavins. Flavins have been described in Dictyoptera (*Blatella*), they are in the form of needles located in mitochondria or lysosomes. Such needles can be recognized in micrographs of the Malpighian tubules cells of *Periplaneta*, *Calpodes ethlius*, and *Calliphora* (Wall *et al.*, 1975; Ryerse, 1979).

Mineralized spherites (or dense bodies, or concretion) have been investigated by many authors (Wigglesworth and Salpeter, 1962; Cheung and Marshall, 1973a; Turbeck, 1974; Sohal, 1976; Yu *et al.*, 1988; Maddrell *et al.*, 1991). Most of these structural investigations have noted the existence of granular structures in the cytoplasm and the appearance of somewhat similar structures in the lumen. Several hypotheses have been proposed to explain the mode of origin of mineral spherite. Wigglesworth and Salpeter (1962) found that the Malpighian tubule cells of upper segment of *Rhodnius* were filled with spherical granules which appeared grayish yellow by transmitted light. Under the electron microscope, these abundant granules appeared to be mineralized deposits (presumably phosphates or carbonates of calcium and magnesium). They showed a concentric structure like diminutive calculi. From the observation, they concluded that the mineralized granules might possibly represent the final stage in the breakdown of mitochondria.

Cheung and Marshall (1973a) reported that areas of smooth endoplasmic reticula were frequently expended into wide cisternae, and it was within these that electron dense material appeared to be laid down. The endoplasmic reticulum was often in whorls, which was reflected by the appearance, in young cells, of spherites arranged in concentric circles. So they thought that mineral spherites might originate in cisternae formed from smooth parts of the

endoplasmic reticulum.

Sohal (1976) reported that the epithelium and lumen of the Malpighian tubules of the housefly , *Musca domestica* contained mineralized dense bodies called concretions. There were three types of concretions in the cytoplasm, which had been designated as type A, type B, and type C. Type A concretions were membrane bound spherical structures which might arise by the gradual intravacuolar accumulation of dense material. Type B concretions appeared to be related to multivescular bodies. Type C concretions were heteromorphic and morphologically resembled the residual bodies. They showed a positive localization of acid phosphatase reaction product. There was an age-associated increase in the distribution of type C concretions. In the cytoplasm of the tubules of newly emerged adult, dense bodies appeared as clear vacuoles which gradually accumulated electron opaque contents. In old flies relatively large area of the cytoplasm were occupied by dense bodies. Electron probe X-ray microanalysis of the dense bodies showed that they were rich in phosphorus, sulphur, chlorine, calcium, iron, zinc and copper. Dense bodies might play a role in achieving an effective excretion of these substances. The cytoplasmic dense bodies might become incorporated into the developing secondary lysosomes (Sohal, 1976).

Most electron microscopic researches have shown that the ultrastructure of the principal Malpighian tubule cells of insects are basically similar.

Minor variations in fine structure are obvious when considering the functional differentiation in different regions of one species or in different species. They mostly concern the development of microvilli, the number of mitochondria, and the occurrence of concretions. For example, the cells of the various regions of the *Drosophila melanogaster* (Eichelberg and Wessing, 1975) have some differences from the generalized picture. The distal tubule segment, its lumen is filled with primary urine consisting of solid concrements. The

epithelial cells of this region are very flattened; the basal and apical cellular membranes lie close together at some places. The cell barely has a brush border facing the lumen, only a few, poorly developed microvilli are discernible. The endoplasmic reticulum and Golgi fields are well developed. Many cytoplasmic vesicles which transport the substances from the heamolymph to the tubule lumen are characteristic for this region. The cells of the main part of the Malpighian tubules serve mainly for resorption, and thereby the formation of the secondary urine in the larva. The structure of the intermediate part is much more uniform than in the initial tubule region. The basal labyrinth is well developed. The mitochondria are scattered more or less throughout the entire cytoplasm. The central channels of the microvilli are connected with the endoplasmic reticulum. The ultrastructure of the cells of the main segment conforms with general ultrastructure of a tubule cell described before. Distal cells are very similar to those of the main tubule segment; however, along its length the ureter cell structure resembles more and more that of the midgut cells. In comparison to the cells of the main segment, the cells of the ureter only contain lipid deposits.

3. The structure of other cell types

In Dictyoptera, Lepidoptera, Diptera, and probably Homoptera, stellate cells are scattered among the principal ones (Martoja and Ballan-Dufrancais, 1984). In *Drosophila* the different segments of the Malpighian tubule are composed of one type of cell, but in salt fly *Ephydra riparia*, this does not apply (Eichelberg, 1973). There are two different types of cells in the main segment of the tubules of the species: the main cells (or principal cells) which are relatively large in size and due to their convex surface, give this segment of the tubules a beaded appearance; and the small accessory cells (or stellate cells) which have long

cellular processes radiating from the nuclear region along the junctions between the main cells. The accessory cells are so small, in comparison with the main cells, that they only make up about 5% of the total area of the tubule cross section.

The ultrastructure of the main cells of the tubules of *Ephydra* and those of the main segment of *Drosophila* are similar. The accessory cells are only third as high as the main cells. Their basal plasmalemma also forms a complex network of invaginations, which do not penetrate nearly as far as into the main cells but are limited to the basal region. The cytoplasm between the invagination possesses channels of the rough endoplasmic reticulum; only a few mitochondria are found here which are much smaller than in the main cells and show no polar alignment. Most of the mitochondria lie in the intermediate region of the cell. Here are also found a few Golgi field, vesicles, and channels of the rough endoplasmic reticulum. Unlike the main cells, an accumulation of pigments is completely lacking. Individual microvilli of the brush border are much shorter and relatively wider than main cells. This means that the accessory cells are not used for storage purposes. Mitochondria never penetrate them and are only seldom found at the base of the microvilli. Most of the microvilli are run through by a central channel.

The accessory cells show a close similarity to the cells described by Berridge and Oschman (1969) which are found in the posterior Malpighian tubules of *Calliphora erythrocephala*, and which are called stellate cells due to their star-shaped radiating cell processes. The stellate cells have an affinity for lead; that is , they can be selectively stained with lead salts. All these cells have a special significance in the selective transcellular passage of ions (Berridge and Oschman 1969).

Taylor (1971b) studied the fine structure of the type 2 cells in the

Malpighian tubules of the stick insect *Carausius morosus*, he reported that type 2 cells always localized beside the numerous type 1 cells. Type 2 cells are very similar in appearance to the stellate cells. However, the type 2 cells have much more highly developed granular endoplasmic reticulum, as well as Golgi fields and Golgi vacuoles. It can therefore be assumed that the type 2 cells, in addition to their possible activity in selective ion transport, also synthesize acid mucopolysaccharides, probably in the form of a mucoprotein.

In Dictyoptera and Othoptera, the tubules contain mucous cells. Their appearance is characteristic of secretory cells, with large vesicles containing a granular material. Rather similar to the Type 3 cell of certain Diptera which forms a proteinaceous secretion. Finally, in Homoptera, peculiar cells manufacture brochsomes which are bodies that contain lipids and proteins (Smith and Littau, 1960).

4. The cryptonephridial systems in the larvae of Lepidoptera and Coleoptera

In the so-called cryptonephric condition of the excretory system in insects the distal ends of the Malpighian tubules are closely applied to the rectum and enclosed with it in a special chamber, the perinephric space, separated from the rest of the body cavity by the perinephric membrane. The term `rectal complex' refers to this association of tubules and rectum. It is found in the larvae and adults of some Coleoptera, such as mealworm, *Tenebrio molitor* (Koefoed, 1971) and in the larvae (but not in adults) of most Lepidoptera. In some of the Coleoptera, but never in any of the Lepidoptera, the cryptonephric tubules make contact with the inner side of the perinephric membrane, which is paretically interrupted at the point of contact, and only a small window, known as a leptophragma, separates the lumen of the tubule from the haemcoal (Ramsay,

1976).

The leptophragma cells are composed of two parts: a thin, flat plate, with a deep bordering edge that is anchored to the rest of the tubule epithelia, and the cell body, which hang freely down into the lumen from one point of the border edge. The first part of the cell is an extremely thin cytoplasm layer. The outer surface is smooth, microvilli are developed on the inner side. Mitochondria never penetrate these microvilli, which coincides with the accessory cells of *Ephydra* and the stellate cells of *Callphora*. The microvilli of leptophragma cells are more loosely packed and are thinner than those of the normal tubule cells.

The body of the cell also possesses microvilli, which are free of mitochondria and which project into the lumen. In the cell body the following can be seen: the nucleus, many mitochondria, microtubules, free ribosomes, some small vesicles and sometimes Golgi fields. Large vacuoles contain electron-dense substances in the form of irregular aggregations of granules or as stacks of membranous materials.

Cryptonephridial systems occur especially among those beetles and butterfly larvae, which live in very dry biotops. It is expected that it serves for the reabsorption of water and perhaps some salts from the lumen of the hindgut through the rectal epithelium (Wigglesworth, 1931). Ramsay (1964) reported that the leptophragma cells were involved in a directional, selective transport of potassium ions.

Among some cicada, for example, *Euscelidius*, the proximal segments of the Malpighian tubules communicate through the fusion of their ends. These tubules are associated with the distal segment of the midgut (Munk, 1967). A tunica propria serves as the perinephric membrane of *Tenebrio molitor* (Ramsay, 1964). The tunica propria also forms a separate space between gut and body cavity, which could correspond to the perirectal chamber of *Tenebrio*. The tubules of the

cryptonephric region of cicadas show differences to the tubules of *Tenebrio*. In the region of cryptonephridium, the tubule is composed of only one type of cell (Eichelberg and Wessing, 1975). These cells are subdivided into three parts: a basal region with deep invaginations of plasmalemma; intermediate region and apical region with a well developed brush border.

From all above, the segment of the Malpighian tubules of insects can be composed of only one type of cell or by structurally different types, there are two cell types as a rule.

III. Functions of insect Malpighian tubules

The main role of the Malpighian tubules in excretion is to deliver to the hindgut a flow of fluid containing many of the haemolymph constituents at concentrations in proportions to their concentrations in the haemolymph. The hindgut reabsorbs those constituents required by the insect and rejects the others. In this way the composition and volume of the haemolymph is kept relatively constant or is adjusted to meet the needs of the insect (Maddrell, 1977).

1. Mechanism of fluid secretion by Malpighian tubules

1.1. Ion transport

Water movements across the walls of Malpighian tubules seem to be consequent upon ion movements. The movement of potassium ions into Malpighian tubules is clearly thermodynamically uphill. The rate of fluid secretion depends on the potassium concentration in the bathing saline. These facts suggested that potassium transport is active and important to fluid transport.

It seems that a potassium pump exists in the apical cell membrane. The pump has a higher affinity for sodium ions than for potassium ions. Such a pump will mainly pump the potassium ions which will enter the cell to replace those which are pump out across the luminal face. Potassium ions are pumped across the apical membrane passively. Chloride ions cross the tubule wall passively. When ions transport out across the apical membrane carries water molecules in the same direction (Maddrell, 1977).

1.2. Fluid transport

The rate of fluid flow produced by Malpighian tubules are in an inverse relationship to the osmotic concentration of bathing solution (Maddrell, 1977). Ion transport across the apical microvilli on the luminal side is likely to lead to locally raised osmotic concentration in the spaces between the microvilli. It has been suggested that such osmotic concentration differences could act to draw water through the cell membrane concerned. The cytoplasm close to the apical and basal membranes is also arranged as long thin channels or sheets. It has been argued that this could act to promote osmotic coupling between ion and water flow (Maddrell, 1977).

2. Active transport of organic compounds by Malpighian tubules

2.1. Organic anions

Insect Malpighian tubules could concentrate acidic dyes from dilute solutions. This ability is attributable to an organic anion transport system. Two types of compounds are handled by this system: acylamides and sulphonates. The

transport system has a high affinity for these substances. The ability of Malpighian tubules to transport organic anions probably serves to eliminate some of the products of metabolism of potentially harmful substances (Maddrell, 1977).

2.2. Organic cations

The ability of insect Malpighian tubules to secrete basic dyes have been investigated. The Malpighian tubules of larvae of *Chironomus* could rapidly concentrate neutral red, and the Malpighian tubules of larvae of *Manduca sexta* secreted such basic dyes as methyl green, methylene blue and neutral red (Maddrell, 1977).

Alkaloids occur in many plants. It is believed that alkaloids have been evolved as a protective measure against herbivores. Some insects can nevertheless thrive on a diet of such alkaloid containing plants. It turns out that the Malpighian tubules of several insects can remove such alkaloids as nicotine, atropine and morphine from the haemolymph at high rates and against steep concentration gradient. The ability of some insect Malpighian tubules to concentrate basic dyes may be attributable to the ability of the organic cation transport system (Maddrell and Gardiner, 1976).

3. Resorptive processes in Malpighian tubules

3.1. KCl resorption

Fluid secreted by the upper lengths of the Malpighian tubules is iso-osmotic with the haemolymph and is relatively high in potassium. The lower lengths of

the Malpighian tubules are largely responsible for the necessary alteration of the composition of the fluid that leaves the upper tubule (Maddrell and Phillips, 1975a). This suggests that the change in K^+ concentration causes the osmotic pressure change, possibly by a reabsorption of KCl without osmotically compensating amounts of water.

This resorptive system is controlled by hormone (Maddrell and Phillips, 1976) and is also affected by the concentration of K^+ in the fluid bathing the lower tubules. It may be that insects possess a form of autonomous control of excretion in which the system reacts directly to changes in the bathing it and responds appropriately.

3.2. Reabsorption of sugars

Insect Malpighian tubules are permeable structures and such useful substances as sugars and amino acids diffuse into the luminal fluid from the bathing solution. It has been also suggested that sugar might be reabsorbed in the anterior hindgut or in the rectum. Unexpectedly, it now appears that the Malpighian tubules themselves may act to reabsorb physiologically important sugar and so limit their loss from the haemolymph (Maddrell, 1977).

4. The passive permeability of Malpighian tubules

Malpighian tubules are permeable structure and many substances passively find their way into the secreted fluid by diffusion across the tubule wall (Maddrell, 1977). This permeable nature of the tubule wall is an essential feature in that it provides for the automatic removal of toxic material from the haemolymph. Some useful compounds as amino acids and sugar enter the

primary excretory fluid and have to be reabsorbed. In essence, compounds of mol. wt below about 400 freely cross the tubule wall while large compounds enter more slowly (Ramsay, 1958).

B. The biology and mode of action of *Bacillus thuringiensis*

I. Introduction

Bacillus thuringiensis is a bacterium that produces toxic protein crystals during sporulation. The specific toxicity of these crystals against pest insects provides the basis for the use of this organism as a biological insecticide (Adang, 1991). In the past years, many studies concerning about the pathology, toxicology, purification and mode of action of *Bacillus thuringiensis* were done. There has been an upsurge of interest in the molecular biology of *Bacillus thuringiensis*, particularly as it relates to toxin synthesis (Bulla *et al.*, 1980). The genetics of *B. thuringiensis*, the molecular cloning of δ-endotoxin gene and its regulation were intensively studied (Calabrese *et al.*, 1980; Yamamoto and Iizuka 1983; Aronson *et al.*, 1986; Whiteley and Schnepf 1986; Donovan *et al.*, 1988; Widner *et al.*, 1989; Pang and Mathieson, 1991).

II. Background

Bacillus thuringiensis is a crystalliferous sporeforming bacterium closely related to *B. cereus*. The term crystalliferous is applied to those *Bacillus* species that produce a discrete, characteristic inclusion within the sporangium in addition to the endospore (Bulla *et al.*, 1980). The first isolation of a *Bacillus thuringiensis* strain was reported at the beginning of this century by Ishiwata in 1902 (as cited in Aoki and Chegasaki, 1915). Later, the presence of inclusion bodies or "Restkorper" was described by Berliner (Berliner, 1915) and again by Mattes (1927) later. However, association of the inclusion with toxicity of

Bacillus thuringiensis to insects was not established until Hannay's rediscovery of the parasporal inclusion in 1953 (Hannay, 1953). At the same year, T. A. Angus, during his doctoral studies, found that juice of the silkworm midgut released a toxic substance from sporulating cells of *Bacillus thuringiensis*. He proved toxicity of the inclusions (Angus, 1953). Hannay , together with Fitz-James, discovered their proteinous nature (Hannay and Fitz-James, 1955). In the following years, many investigators actively studied crystalliferous entomocidal bacilli, particularly *B. thuringiensis*, both in the laboratory and in the field (Bulla *et al.*, 1980).

III. Cytology of germination, outgrowth and sporulation

The life cycle of *Bacillus thuringiensis*, like that of other bacilli, is characterized by several distinct steps (Bulla *et al.*, 1980) . These include: germination, outgrowth and sporulation. The cytological changes in different developmental stages are different.

Germination

The dormant bacterial spore is the ultimate stage of sporulation. Once completely formed, it represents a cryptobiotic state in which metabolic and developmental activity is at a minimum or is nonexistent (Bulla *et al.*, 1980). When environmental parameters evoke certain alterations in macromolecular configuration change, the dormant cells reverse itself metabolically and proceed toward vegetative growth (Bulla *et al.*, 1980).

Cytological changes in germination include: inter- and extrasporangial spores first lose the undercoat. In extrasporangia spore, this phenomenon is followed by

rapid and complete dissolution of the cortex. The spore nucleoid of both spore types goes from the electron-lucent to a fibrous condition and to the dispersed vegetation appearance. The dense vesicles and smooth plasma membrane observed in dormant spore are not present in germinated cells. Instead, the plasma membrane is irregular.

Outgrowth

Outgrowth is similar for both intra- and extra-sporangial spores, except intrasporangial spores are enclosed by the sporangial wall up though emergence. During outgrowth, the spore begins to swell and spore surface area increases about three and one half times over that for the dormant spore. Mesosomes are observed for the first time. Later, the sporoplast begins to elongate. During swelling and elongation, the fragmented outer fibrous spore coat becomes a dense band between the exosporium and the protoplast. The lamellar coat appears "stretched" around the developing vegetative cell wall. When most cells begin to emerge, the outer fibrous coat, exosporium, and lamellar spore coats are shed (Bulla *et al.*, 1980).

Sporulation

When bacilli are supplied with enough carbon, nitrogen and phosphorus, they grow vegetatively and the sporulation is repressed. At the end of vegetative growth, the exhaustion of the medium induces the initiation of sporulation. The cell starts a morphological transformation which leads, within a few hours, to the formation of a heat-resistant spore. The initiation of the sporulation process seems to be controlled by catabolite repression, but to date it has not been

possible to prove that what compound was responsible for the repression. Other compounds, such as ATP, 3', 5'-cyclic guanosine-5'-monophosphate, and high phosphorylated nucleotides, have been proposed as regulators of the initiation of sporulation (Luthy *et al.*, 1982).

The cytological changes of spore development in *Bacillus thuringiensis* is summarized by Bechtel and Bulla (1976) as seven stages: stage I-axial filament formation; stage II-forespore septum formation; stage III-engulfment, first appearance of ovoid inclusion and parasporal crystal, change in stainability of membranes and cytoplasm, and formation of forespore; stage IV to VI-formation of exsporium, primordial cell wall, cortex, and spore coats accompanied by transformation of the spore nucleoid; and stage VII-spore maturation and sporangia lysis.

One of the dramatic aspect of *B. thuringiensis* sporulation is the formation of the parasporal crystal (Bulla *et al.*, 1980). Ribier and Lecadet (1973) thought that the biogenesis of the crystal began during stage II. However, Bechtel and Bulla (1976) and Somerville (1971) indicated that the beginning of the biosynthesis of crystal should be placed in stage III.

IV. *Bacillus thuringiensis* and its toxins

Pathogenetic bacteria might cause diseases by the production of toxins . The toxin meant a poisonous or harmful material obtained from a living organism, or, in bacteriology, a specific class of antigenic poisons of cellular origin (Faust and Bulla, 1982).

Scientists have classified the toxins produced by bacteria by using one of several criteria (Bulla *et al.*, 1980):

(1). Anatomical location.

(2). The mode or site of action in the susceptible host.

(3). The chemical structure of molecule.

(4). Symbolic notations.

In *B. thuringiensis* strains, seven different toxins have been described (Faust and Bulla, 1982). They were:

(a). α-exotoxin

(b). ß-exotoxin

(c). τ-exotoxin

(d). δ-endotoxin

(e). Labile toxin

(f). A water soluble toxin

(g). A mouse factor exotoxin

Among all these toxins produced by *Bacillus thuringiensis*, the δ-endotoxin has been intensively investigated because it has a good potential for biological control of insect pests (Faust and Bulla, 1982).

The term endotoxin, generally applied to the haptenic portion of the cell walls of gram-positive bacteria, best known as containing the somatic or O antigens of the Enterobacteriaceae. This toxin of the parasporal crystal was designated an endotoxin because the crystal is formed during sporulation inside the vegetative cell and is not excreted to the outside in a soluble form (Faust and Bulla, 1982).

The protein crystal was usually bipyramidal or diamond in shape, but it might be cuboidal or amorphorus. In bipyramidal crystal, the protein subunits were arranged in stacked sheets which narrow from the equator towards the poles (Hannay and Fitz-James, 1955). The protein subunit was later determined to be the protoxin of δ-endotoxin.

From the study of fine structure of crystal, Labaw (1964) concluded that the

Bacillus thuringiensis crystal has a face centered cubic structure with a tetramolecular unit cell of 12.3 nm on an edge when dry. Individual molecule, being spherical, has a diameter of 8.7 nm. One year later, the X-ray diffraction techniques were used by Holmes and Munro (1965) to study the crystal structure in more details. They indicated that the units were not symmetrical and suggested a sheet packing through a fourfold screw axis in such a manner that each stria in the c-axis represents the distance between four layers. They replaced each pair of Labaw's spheres by an ellipsoid and the unit cell of the crystal became a body-centered tetragon with dimensions of 9.0 x 9.0 x 13.5 nm and contained eight asymmetrical molecular units each with a molecular weight in the region of 230,000. This calculation, along with the results of Bulla *et al.* (1977), indicated that the basic crystal asymmetric unit was a dimer of the 130,000-dalton monomer.

The native crystal is insoluble in aqueous solution at neutral or acidic pH, but soluble in high pH, reducing agents and urea. Complete solubilization of the glycoprotein of crystal can be achieved in several mixed solvent systems (Bulla *et al.*, 1979). SDS and ME or dithiothreitol were absolute requirements.

The protein crystal was composed of 95% protein and 5% carbohydrate (Bulla *et al.*, 1977, 1981). Glutamic acid and aspartic acid residues were the most abundant. Quantitative analysis of the neutral hexoses revealed that glucose was 3.8% and mannose was 1.8%. These accounted for all of the carbohydrate present. Based on molecular weight values, there were 20 glucose and 10 mannose residues per subunit (Bulla *et al.*, 1980). There were no detectable amino sugars, nor any lipids, nucleic acids, and sialic acid derivatives (Bateson and Stainsby, 1970).

V. Histopathological effects of *Bacillus thuringiensis* δ-endotoxin on

Lepidopterous larvae

The histopathology of *Bacillus thuringiensis* has been studied intensively in different insect species. The organs investigated include midgut and Malpighian tubule epithelia as well as different cell lines.

The earlier study was done by Heimpel and Angus (1959) on the silkworm *Bombyx mori* midguts. The cytological alterations included a general separation of the midgut epithelial cells from each other and from the basement membrane. Some cells were slough off into the lumen of the alimentary tract and possessed ruptured plasma membranes and a high degree of vacuolation. Then more detailed effects were reported by Endo and Nishiitsutsuji-Uwo (1980). They indicated that different ultrastructural changes were observed in the columnar and goblet cell after administration of the toxin. The deep infoldings of the cell membrane of some columnar cells became very irregular in shape and the mitochondria near the basal region were transformed into a condensed form. A few goblet cells showed relatively high electron density in the cytoplasm. With the passage of time, most mitochondria became condensed and endoplasmic reticulum assumed a vacuole-like configuration. The basal infoldings of the cell membrane almost disappeared. On the other hand, the cytoplasm of the goblet cells became very electron dense and granular. However, the mitochondria and the endoplasmic reticulum did not show any pathological deformation. Similar results were observed by Percy and Fast (1983). But in their paper, the changes on the microvilli were obvious. The microvilli became less consistently uniform in diameter; their organized internal microfilaments were disrupted and disappeared within 1 min after ingestion of toxin. The cisternae of rough endoplasmic reticula were enlarged and denuded of ribosomes. By 5 min after ingestion, microvilli of some columnar cells disappeared entirely. Mitochondria

in columnar cells were swollen but didn't exhibit the condensed configuration reported by Endo and Nishiitsutsuji-Uwo (1980).

European corn borer is one of the most serious indirect agricultural pests (Atkins, 1978). Biological control of European core borer by *Bacillus thuringiensis* is a good control method. The histopathological effects of *Bacillus thuringiensis* var. *thuringiensis* on this pest were studied by Sutter and Raun (1967). They reported that *Bacillus thuringiensis* var. *thuringiensis* caused the midgut epithelial cells to slough off into the lumen and thus expose area of the basement membrane to attack by vegetative rods. Bacterial spores germinated readily after they were ingested by the larvae. The vegetative rods penetrated the peritrophic membrane and attacked the disorganized midgut epithelium. General vacuolation of the midgut epithelium resulted from the disruption of microvilli in the goblet cells was observed. Globular cytoplasmic extrusion from infected epithelial cells also was reported. When the gut contents mixed with the haemolymph, the larvae died.

For the tobacco hornworm *Manduca sexta*, same works were done by several authors (DeLello *et al.*, 1984; Lane *et al.*, 1989). Lane *et al.* observed that tissues examined after only 1-5 min of exposure to the toxin, vacuoles associated with the golgi complex maturing face became enlarged and resulted in an increase in both vacuoles and the number of lysosomal bodies, many containing myelin like formations; some of these arose as autophagic vacuoles. The intercellular septate and gap junctions on the lateral borders were sometimes disrupted and with time often became internalized. All these findings were not reported in earlier.

Pieris brassicae and *Pieris canidia* are two closely related species. The histopathological effects of *Bacillus thuringiensis* on these two species also were investigated (Ebersold *et al.*, 1980; Cheung *et al.*, 1990; Cheung and Lam,

1993). Ebersold *et al.* (1980) reported that with the exception of the nuclear region, all intracellular components, such as endoplasmic reticulum, mitochondria and the golgi complex, underwent drastic structural changes in the presence of the δ-endotoxin. A considerable increase in the formation of autolytic vacuoles could be observed. The dictyosomes formed by the golgi complex contain enzymes for the supplementation of the gut juice, whereas the cytosegrosomes perform autolysis of intracellular components. A transmission electron microscopic study was performed on the gut of *Pieris canidia* by Cheung *et al.* in 1990. They revealed that the midgut microvilli, mitochondria, and endoplasmic reticulum were the primary targets of damage after the bacteria had penetrated the peritrophic membrane. There was extensive vacuolation and excretion of cellular contents. Numerous germinating bacterial cells were seen inside columnar cells in two hours post-treatment. The goblet cells, however, appeared to be less affected. After five hours of bacterial infection, the midgut epithelium was of severe damaged and became lysed. The mixing up of haemolymph and midgut contents would lead to the death of the insect larvae.

So far, only one paper has been reported on the changes in the fine structure of the Lepidopterous Malpighian tubules after *Bacillus thuringiensis* var. *kurstaki* infection (Reisner *et al.*, 1989). They described the histopathological effects from low dosage to high dosage of toxin treatment as stage 1, stage 2 and stage 3. In stage 1 changes involved enlargement of spaces in the cytoplasm and basal infolds whereas Stage 2 alterations included microvillar disorganization and lysis, mitochondrial alterations and continued enlargement of cytoplasmic spaces. Stage 3 changes included apical and basal membrane lysis, swelling of the rough endoplasmic reticulum and mitochondria, and leakage of cytoplasmic material into the tubule lumen.

From all these histopathological studies, it can be concluded that *Bacillus*

thuringiensis δ-endotoxin causes similar histopathological alterations in insect midgut and Malpighian tubules, such as the microvilli and basal infoldings become disorganized in the primary stage. The cell organelles appeared abnormal. Finally, the microvilli disappeared and the basal infoldings were damaged. These results demonstrated that the *B. thuringiensis* δ-endotoxin affected a fluid-transporting epithelium other than the midgut. The toxin acted by forming pores in cell membranes rather than by poisoning histospecific membrane protein (Reisner *et al.*, 1989).

VI. Mode of action of *Bacillus thuringiensis* δ-endotoxin

From numerous histopathological studies of *Bacillus thuringiensis* on different insect species, several hypotheses have been proposed to explain the mode of action of δ-endotoxin. These include: (1). They bind to a specific plasma membrane receptor and form lytic pore in plasma membrane (Knowles and Ellar, 1987). (2). They inhibit an epithelial K^+ pump (Gupta *et al.*, 1985). (3). They uncouple oxidative phosphorylation (Travers *et al.*, 1976). (4). They cause a general breakdown of cell permeability barriers (Nishiitsutsuji-Uwo and Endo, 1979).

An investigation was done by Travers *et al.* (1976) to determine the effects of the *Bacillus thuringiensis* var. *kurstaki* δ-endotoxin on mitochondria isolated from *Bombyx mori* midgut epithelium. The investigation revealed that *Bacillus thuringiensis* δ-endotoxin increased oxygen uptake by uncoupling oxidative phosphorylation in mitochondria and resulted in a low level of ATP production, the high demand for reduced coenzymes necessitated by increased oxygen uptake in a nonconservative electron transport system would at first increase the demand of the insect's catabolic process for glucose. Such stimulation of respiration by

the *B. thuringiensis* δ-endotoxin might explain the stimulation of glucose uptake during the first 5 minutes of intoxication. Meanwhile, in the cell the ratio of the diphosphate ester ADP and the triphosphate ester ATP controlled the rate at which NADH, the major reduced coenzyme in the cell, was used in the process of electron transport. When ATP levels fall because of the action of the uncoupler, the rate of NADH use increased dramatically. These results indicated that *B. thuringiensis* δ-endotoxin could act as an uncoupler of oxidative phosphorylation. Loss of ATP production caused by the action of the δ-endotoxin would lead to metabolic imbalance and possible cell death.

Nishiitsutsuji-Uwo *et al.* (1979) compared the cytological effects of valinomycin and *B. thuringiensis* δ-endotoxin by using TN-368 cell lines from *Trichoplusia ni*. The cytotoxic response was greatly affected by the ionic conditions of the solutions employed for the toxin test. Ions, in addition to K^+, seemed to participate in the cytotoxic expression of δ-endotoxin, if their concentration was sufficient. Mitochondria of the toxin treated cells were transformed into a form in which the matrix was very "condensed" and extraordinarily electron dense; those of valinomycin treated cells were transformed into the " swollen" form, they showed matrical swelling, the development of a markedly swollen, balloonlike appearance, with very low electron density. The cristae in the swollen mitochondria were narrow and tubular. Therefore, the cytotoxic effects of δ-endotoxin, unlike that of valinomycin, seemed to be a general breakdown of ion regulation on the cell level. Similar works were also done by Fast and Donaghue (1971) and Fast and Morrison (1972).

Gupta *et al.* (1985) used the electron probe X-ray microanalysis to study the effects of *Bacillus thuringiensis* var. *kurstaki* crystal on ions in an electrogenic K^+-transporting epithilium of *Manduca sexta*. The results revealed that the short-

circuit current, a precise measure of K^+ active transport, was inhibited by 78% in 10 min in *Bacillus thuringiensis* var. *kurstaki* treated midgut as compared to control. The average K^+ concentration in the goblet cell cavity was 129 mmol/kg wet wt in control midguts but only 37 mmol/kg wet wt in *Bacillus thuringiensis* var. *kurstaki* treated midguts. The elemental concentrations, including that of K^+, in other cell compartments were less affected by *Bacillus thuringiensis* var. *kurstaki*, but a rise in total cell calcium was suggested. It could be concluded that initially *Bacillus thuringiensis* var. *kurstaki* interacted specifically with the goblet cell apical membrane, which bounded the goblet cavity and contained the K^+ pump responsible for the short circuit current and high transepithelial potential difference. Such interaction resulted in a rapid disruption of K^+ transport across the goblet cell apical membrane, leading to dissipation of the K^+ gradient and loss of potential difference. This hypothesis also supported by Wood and Moreton (1978).

Recently, most people supported the hypothesis proposed by Knowles and Ellar (1987). They thought that a two step model in which, after binding to a specific plasma membrane receptor, the action of the δ-endotoxin was to generate small pores in the plasma membrane, either directly by inserting into the membrane, or indirectly by perturbing resident plasma membrane molecules. The creation of these pores would lead to colloid-osmotic lysis. i.e. an equilibration of ions through the pore resulting in a net inflow of ions, an accompanying influx of water, cell swelling and eventual lysis. Before this model was proposed by Knowles and Ellar (1987), a glycoprotein containing N-acetylgalactosamine was isolated from the plasma membrane of *Choristoneura fumiferana* cells. This protein bound to δ-endotoxin and was a good candidate for the cellular receptor (Ellar *et al.* 1986). Immunolocation of *Bacillus thuringiensis* var. *kurstaki* δ-endotoxin on the midgut and Malpighian tubules of the tobacco

budworm, *Heliothis virescens* was done by Ryerse *et al.* (1990). The latter authors suggested some sort of "receptors" for the *B. thuringiensis* var. *kurstaki* endotoxin were widely distributed on the apical surfaces of transporting epithelial cells.

Among all the above investigations, the hypothesis of Travers et al. (1976) has gained little support (Reisner *et al.*, 1989) . Data derived from ion movements and membrane potential in insect midgut (Ebersold *et al.*, 1978; Gupta *et al.*, 1985) and in insect cell lines (Ebersold *et al.*, 1980; English and Cantley, 1985) were most consistent with the criteria favoring the lytic pore formation hypothesis (Reisner *et al.*, 1989). Membrane lysis (Nishiitsutsuji-Uwo and Endo, 1979) and ion pump inhibition (Gupta *et al.*, 1985) were not mutually exclusive as potential mechanisms of action (Reisner *et al.*, 1989).

C. The biology and pathological effects of microsporidian protozoa

I. Life cycle of microsporidian protozoa

Microsporidian protozoans are intracellular parasites found in animals and protists (Canning and Lom, 1986; Larsson, 1986). They form unicellular spores which contain a single sporoplasm. The sporoplasm emerges from the everted polar filament directly into the cytoplasm of a host cell and grows to form a plasmodium. The plasmodium divides by merogony to produce merozoites that enter other host cells to repeat merogony or undergo sporogony to produce numerous sporoblasts which develop into spores (Sleigh, 1989).

The life cycle of *Nosema bombycis* was studied by Kawarabata and Ishihara in 1984. They indicated that *Antheraea eucalypti* cells were infected with sporoplasms of *Nosema bombycis* which had emerged from spores. The sporoplasms gradually increased in size and grew into elongated schizonts. The binary fissions of the schizont occurred in host cells. Usually, when single sporoplasm invaded the cells to multiply, four to six divisions of the schizonts were observed before spore formation started. After maximal multiplicative growth in host cells, the schizonts differentiated into sporonts. The sporont completed a single division and, normally, produced two sporoblasts. In the sporoblast, a refractive spot developed to a spherical body. The sporoblast cytoplasm stained deep blue with Giemsa as the sporoblast developed (phase I sporoblast) and the spherical body increased in size. Then, blue stained cytoplasm of the sporoblast disappeared and rearrangement of the spherical body started inside the faintly stained sporoblast (phase II sporoblast). After the

rearrangement of the spherical body in phase II sporoblasts had been completed, the nuclei inside the sporoblasts were not clearly visible. Finally, the compact nuclei were formed in the immature spore. Immature spore developed into mature spore. The mature spore differed from immature spore by the tightly packed nuclei and more refractile cell wall.

II. Germination of microsporidian protozoa

After the spores are ingested by the host, the spores germinate in the midgut of the host, in response to the necessary stimuli, the internally coiled polar filament everts explosively from the spore. The hollow polar filament pierces the gut wall, facilitating the transfer of the infective sporoplasm into the susceptible host tissue (Whitlock and Johnson, 1990).

Considerable attention has been given to the questions concerning microsporidian germination and much emphasis has been placed on the optimum pH, ionic, and osmotic conditions for germination of various microsporidian species (Malone, 1984; Undeen and Avery, 1984). Olsen *et al.* (1986) studied *in vitro* germination of *Nosema apis* spores. They reported that germination was associated with the extruding polar tube. Germination of individual spore was complete, including sporoplasms formation, granular cytoplasmic contents of the sporoplasms were visible and were highly active. Sporoplasm appeared at the distal end of the polar tube as a ballooning of the sporoplasm membrane and remained attached to the polar tube. A relatively dense spherical body, external to the membrane of the sporoplasm at the site of polar tube attachment, was seen. Then, Iwano and Ishihara (1989) demonstrated that spore germination often occurred in cultured cells earlier postinoculation.

Factors influencing the germination of spore were also investigated by some

authors. Whitlock and Johnson (1990) reported that when exposed to solutions of monovalent salts, spores of the microsporidian *Nosema locustae* germinated in the presence of sodium and potassium, at pH 9.2, but not in the presence of lithium. Between 12 and 16% of spores could also be induced to germinate following a 1 month long inoculation in polyethylene glycol before being transfered to Tris-NaCl resulted in 30.5% germination. In contrast, freeze-drying inhibited germination, as did a 5-min exposure to UV light, while germination was also adversely affected by exposure to temperatures above 40°C for even brief periods.

Undeen and Epsky (1990) reported that spores of *Nosema locustae* were induced to germinate in vitro by a two-step procedure. Spores were first activated by drying in air, dehydrated in hyperosmotic solutions of sucrose or polyethylene glycol 400, or by extended treatments in low concentrations of PEG. Germination occurred after transfer of the activated spores to an alkaline salt solution, with a pH optimum of 9.0-10.0.

The spore is the final stage of the life cycle of microsporidian protozoa. Normally, the spore wall is very thick. It has a great resistance to the unsuitable environment condition (Hsu *et al.*, 1991). When the environment condition turns to good for the germination of spores, the polar tube extrudes from the spore. The spore plasma appears at the distal end of the polar tube and attaches to the polar tube. So it can be concluded that a number of stimuli (or the interactions) are required to induce germination, some of which are yet to be elucidated (Whitlock and Johnson, 1990).

III. The fine structure of microsporidian protozoa

Acting as biological control agents for many microsporidian protozoa, the

classification and identification of different species are very important. In the past year, the turns and the coiling tilt of the polar filament of the spore generally served as important criteria for classification and identification (Sato *et al.*, 1982). Because appearance of polar filament in different sections and different developmental stages varied. These features were not suitable as criteria in taxonomy (Hsu *et al.*, 1991). The revision of the Thelohania-like Microsporidia by Hazard and Oldacre (1975) was a milestone in microsporidiology. For the first time ultrastructural characteristics were used more extensively for taxonomic purposes (Larsson, 1990). The fine structures of microsporidian species have been studied by many authors (Liu and McEwen, 1977; Gorske and Maddox, 1978; Sato *et al.*, 1982; Avery and Anthony, 1983; Kline *et al.*, 1985; Larsson, 1989, 1990; Hsu *et al.*, 1991; Iwano and Ishihara, 1991). *Nosema blissi* was described from the Malpighian tubules of adults of *Blissus leucopterus hirtus* (Liu and McEwen, 1977). Spores were packed in the host cell in direct contact with the cytoplasm. No pansporoblastic membranes were observed. The polar filament lay in 37 to 40 coils, arranged in a single layer in the posterior portion of the spore, and in seven layers in the anterior portion. The sporont presented the typical diplokaryon arrangement of the nuclei and was distinguished from a schizont by the presence of a wall in addition to the plasma membrane. The schizont possessed a plasma membrane only. Sporoblasts were not surrounded by a pansporoblastic membrane. The early sporoblast possessed a thick wall than the sporont and was also recognized by the developing polar filament and parallel arrangement of the endoplasmic reticulum. The developed sporoblast was characterized by a more electron dense cytoplasm, a fully-formed polar filament, and the possession of the vesicles.

The early development of *Nosema algerae* in *Anopheles albimanus* was described by Avery and Anthony in 1983. They reported that sporoplasm were

binucleate, although the nuclei were not always in diplokaryotic arrangement and were enclosed by double membrane. The most striking feature of these early sporoplasm was the whorled vesicles in the cytoplasm and the fibrous protrusion on the limiting membrane. Meronts were elongate and the fibrous protrusions had coalesced to produce a thick-pitted plasmalemma. Dark spherical granules were seen in the host tissue surrounding the dividing meronts. The sporonts shrank away from the host tissue due to condensation of the cytoplasm, leaving a clear area between the sporont and the host tissue. The spore had a similar structure with that of *Nosema bilissi* reported by Liu and McEwen (1977).

Based on the past studies, Sato *et al.* (1982) reported the internal ultrastructure of the spore of *Nosema bombycis* in details. The polar filament had about 12 coils, with an angle of tilt of at least 49°C. The filament contained a central core surrounded by four concentric layers. The core was surrounded by a relatively electron-lucent layer with a substructure consisting of about 16 small granules. The next layer and the outmost layer were translucent like the membranes of the endoplasmic reticulum or nucleus and between the two layers was an electron-dense layer. The polaroplast consisted of two morphologically different components, an anterior part composed of laminated membranes, which might be tightly flattened sacs, of horseshoe shape in a longitudinal section of the spore, and a posterior part made up of loosely flattened sacs of lozenge shape. Two nuclei, slightly elongate in the direction of the minor axis of the spore, were found in the posterior half of the spore. The posterior vacuole, enclosed by double membranes, occurred near the posterior pole of the spore. Occasionally, near the vacuole had vesicles along its side. These vesicles separated from the vacuole in a spore.

The detained structures of spore wall and polar filament were reported by Larsson (1989, 1990) in *Hyalinocysta expilatoria* and *Napamichum aequifilum*.

He indicated that the spore wall was fairly thick. The normal three layers of the spore wall were well developed: an internal plasma membrane of unit membrane construction, a thick median translucent endospore, and a complex exospore. The exospore was distinctly stratified with an external fine granulation, a translucent layer; a double layer resembling a unit membrane; a prominent, highly electron-dense layer of uniform texture; and bordering to the endospore, a diffuse granular layer. The granular border zone to the endospore and the endospore layer were reduced at the anterior pole of the spore. The polar filament was attached to an anchoring disk at the apex of the spore. The umbrella-like polar sac was distinct, but fairly weakly developed. The coiled part began at the middle of the spore. The angle of tilt of the anterior filament coil to the long axis of the spore was 70°-75°. The transversely sectioned filament revealed concentric layers of varying electron density, in the outward direction: a central moderately electron-dense zone with concentric bands, a moderately dense zone suggeting longitudinal fibrils, a prominent, dense zone interrupted by a less dense area, and a surface layer resembling an unit membrane. The same layered structure of polar coil also reported in *Nosema* sp. M11 and *Nosema* M12 (Sato *et al.*, 1982). So the structure of polar coils for most microsporidia were in the concentric layers of varying electron density.

From all these ultrastructural studies of microsporidian protozoa, it can be concluded that in different species of microsporidian protozoa, some structures are similar, but some structures are different. For example, the spores were generally pyriform in shape. The spore wall was fairly thick and composed of three layers, The polar filament was attached to an anchoring disc and the polar sac was formed. Two nuclei were observed in the cytoplasm. But other structures such as the number and structure of polar coils may be different. In recent year, microsporidians pathogenic to insects have been recorded

incuriously from various groups. Spores have been used extensively to study microsporidians, and spore morphology is one of the most reliable characteristics used for taxonomy (Hayasaka and Kawarabata, 1990). Spore length and width, and spore surface antigens (Kawarabata and Hayasaka, 1987) have also been employed to distinguish species.

IV. Mass production and storage

Although some protozoa have been considered as microbial control agents, however, most entomophilic protozoa are obligate parasites and must be cultured in the living cells of their hosts. Thus the production of such pathogens *in vitro* is inherently more difficult and expensive (Ignoffo, 1966).

Spores of most protozoa have been extracted from their hosts by homogenization of entire insects or appropriate tissue in a tissue grinder or blender to disrupt the host cells. The homogenate is strained through several layer of cheesecloth to filter out the larger particles of cellular debris. The filter is resuspended in sterile distilled water and centrifuged slowly to form a pellet of spores. Two or three repeated washing and centrifugations of the spores have been adequate to give a relatively pure suspension of spores sufficient for field use. Extremely pure spores have been obtained by the technique of trigulation or through the density gradient method using Ludox (Brooks, 1980). Spore concentrations are generally determined by the use of bacterial counting chamber.

Production of Microsporidia by oral infection has been described by many investigators. Mclaughlin (1971) reported that spores of *Nosema gasti* were mass-produced. The original inoculum was centrifuged twice in sterile distilled water at a low centrifugal force to separate the spores from most of the tissues

and the smaller microbial debris. The spores were then treated with a concentrated solution of quarternary ammonium salt for 15 minutes at room temperature to reduce microbial contamination. Spores were then pelleted by centrifugation. Then spores of *N. gasti* were fed to second instar larvae of boll weevil and were harvested from infected adults about 2-4 days after they emerged.

The centrifugation technique also was used for collecting the spores of *Nosema apis* from the midgut of artificially infected cage bees (Olsen *et al.*, 1986). Midguts of *N. apis* were mascerated in phosphate buffered saline and the resultant suspension was filtered over loose cotton wool. Filtrate containing the spores was diluted and washed three times by centrifugation in PBS, then resuspended and poured into a column and allowed to settle by gravity at 4°C. Settling resulted in banding which allowed heavier debris to be removed from the bottom and pollen, germinated spores, and light debris to be removed from the top. Collected spores were washed a further four times in PBS, resuspended in deionized water, and stored at 4°C for at least 1 week before commencing germination procedures.

The spores of *Nosema bombycis* were propagated in silkworm larvae (Hayasaka and Kawarabata, 1990). Spores for inoculating insect cell culture were prepared by single step gradient centrifugation on Percoll. Usually, 1 volume of the spore suspension was layered on 9 volumes of Percoll in a small glass test tube. The tube were centrifuged at 3000 rpm for 20 min at 4^0C and the sedimented spores were resuspended in distilled water. This was repeated three times and purified in distilled water. Purified spores were stored at 4°C for no more than two days.

Most investigators have stored the spores of various Microsporidia or neogregarines in water at temperatures slightly above freezing of 0-6°C,

generally for only a few weeks. Spore viability is usually good and in most cases infectivity is not significantly different from that of fresh suspension (Brooks, 1980). The spores of some species in aqueous suspension remain viable up to seven to ten years when kept at a low temperatures. However, the infectivity of most species declines dramatically after only a few months, especially at higher temperatures, and no completely satisfactory method is known to preserve spore viability for prolonged periods (Brooks, 1980). On the other hand, a few species of Microsporidia survive well for extended periods when stored in small quantities in liquid nitrogen (Vavra and Maddox, 1976).

Several alternative methods for preserving the infectivity of protozoan spores have also been studied. To avoid premature germination, spores of some species, such as *Nosema whitei*, must be stored dry, i.e., either in dried host cadavers or mixed with flour (Brooks, 1980)

The spores of some species of Microsporidia are lyophilized successfully either in host tissue or in water (Fuxa and Brooks, 1979). Although some spores remain viable for up to two years, there is usually a significant decrease in spore viability immediately following lyophilization. The infectivity of lyophilized spores may not be better than that of spores stored in aqueous suspension at low temperatures (Vavra and Maddox, 1976).

V. Pathology of microsporidian protozoa

Protozoa infections are usually chronic, some may be severe and fatal, and probably are of more important than is generally realized (Wilson, 1982). Microsporidia generally invade the muscles, intestinal epithelium, lymphocytes and adipose tissue of invertebrates, especially insects (Sleigh, 1989).

The pathological effects of Microsporidia on the insects have been widely

investigated (Malone and Wigley, 1981; Siegle *et al.*, 1986; Johnson and Pavlikova, 1986; Brooks, 1986; Onstad and Maddox, 1989; Armstrong and Bass, 1989; Solter *et al.*, 1990; Macvean and Capinera, 1991). The Microsporidia were known to deplete the nutritive reserves normally used for reproduction, reducing fecundity (Smirnoff and Chu, 1968), fertility (Tanabe and Tamashiro, 1967), and longevity (Gaugler and Brooks, 1975). The pathogenicity of *Nosema carpocapsae* for codling moth was studied by Malone and Wigley in 1981. They reported that the infection did not cause mortality but did reduce the fecundity and fertility of infected moths. *Nosema carpocapsae* was transmitted transovarially as well as horizontally. Infected female mated with infected males generally produced fewer eggs than healthy pairs.

Siegel *et al.* (1986) reported that the corn borer adults infected with *N. pyrausta* laid 33% fewer eggs than uninfected larvae. Mortality was linked to the ovipositional sequence of the egg masses. Larvae from infected egg masses laid after the fourth day of oviposition experienced greater mortality than those from infected egg masses laid during the first 2 days of oviposition. Both cold stress and crowding stress increased mortality of infected larvae.

Brooks (1986) compared the histopathological effect of *Nosema epilachnae* and *Nosema varivestis* on the Mexican bean bettle. They indicated that *Nosema epilachnae* was decidedly more virulent than *Nosema varovestis*, with the lowest dosage rate of *N. epliachnae* resulting in an adult emergence rate of only 50% in contrast to a 96.3% survival rate of larvae exposed to the highest dosage rate of *N. varivestis*. Both species produced significant reductions in adults longevity and fecundity.

The purpose of insect control is to reduce crop losses caused by insect damage to plant tissue. Most control measures are designed to kill sufficient numbers of insects so that the total amount of feeding is reduced to an acceptable

level. Insecticides can be effective in protecting crops for a number of other reasons, including effects on consumption, development, reproduction, and activity (Johnson and Pavlikova, 1986). In the latter reference, Johnson and Pavlikova reported that rate of inoculation was a significant factor in suppression of feeding after correction for the effects of developmental stage, sex, and body weight. The quantity of dry matter consumed decreased linearly with increasing rate of spore ingestion.

The serious economic losses caused by two species of the genus *Nosema* must mentioned here. One is *Nosema apis*, it may be found in the cells of midgut and Malpighian tubules of adults of honey bees, in which this parasite causes the destructive nosema disease . Another is *Nosema bombycis*. It is responsible for pebrine disease of silkworms, in which tissue cells of any type may be infected at any stage of growth, so that even eggs may be infected and larvae may die without spinning silk cocoons (Sleigh, 1989).

Nosema pyrausta is a common and wide spread microsporidian parasite of the European core borer, *Ostrinia nubilalis*. It produces a chronic disease that reduces adult longevity and fecundity (Windels *et al.*, 1976) but may also cause larval mortality under conditions of environmental stress (Lewis and Lynch, 1976). It is both vertically and horizontally transmitted and appeared to be an important biological mortality factor that helps regulate corn borer populations in nature (Hill and Gary, 1979; Andreadis, 1984). Solter *et al.* (1990) investigated the timing of disease-influenced processes in the life cycle of *Ostrinia nubilalis* infected with *Nosema pyrausta*. They indicated that mean developmental times of infected and uninfected insects reared at 30°C were not significantly different; however, the disease significantly slowed the development of second to fifth instar larvae and pupae reared at 24°C. A finding which might indicate that the pathogen developed more quickly at lower temperatures than at higher

temperatures.

A number of authors have suggested that *Nosema locustae* holds potential as a biocontrol agent for long term suppression of acridids, by virtue of population reductions within the season of inundative release and suppression in the following season (Ewen and Mucerji, 1980), as well as sublethal effects such as reductions in feeding and growth as a result of infection (Johnson and Pavikova, 1986). Macvean and Capinera (1991) reported that *Nosema locustae* did not produce detectable infections in Mormon crickets in any stage of development, while nymphal development was retarded among insects inoculated as first to third instars with high spore concentrations. A new species of *Vairimorpha* n. sp. produced significant mortality among first to third instar Mormon crickets. *Vairimorpha* n. sp. appeared to be a promising biocontrol agent for both short term host density reductions and long term reductions in host development coupled with enhanced transmission potential.

Most species of the entomophilic protozoa have been considered as important natural mortality factors but of only limited value as candidates for short term, microbial insecticides, several species have been evaluated for use in applied pest control programs (Brooks, 1986). There is increasing evidence to indicate the promise of entomophilic protozoa as microbial control agents. Suitable techniques are available for mass production and storage of a number of species, especially Microsporidia (Brooks, 1980).

Part III. Light and electron microscopic studies of the Malpighian tubules of *Pieris canidia* larva (Lepidoptera)

Summary

The small cabbage white *Pieris canidia* Spar. larva has six Malpighian tubules. Each tubule can be conveniently divided into four regions: rectal lead, iliac plexus, yellow region and white region. The principal cells of all four regions have their apical surface folded to form microvilli (particularly the iliac plexus, having canaliculi formed) with mitochondria extending almost to the microvilli tips. Basally there are numerous infoldings forming intracellular channels extending deeply towards the apical surface. Many mitochondria, rough endoplasmic reticula and vacuoles are found in the ground cytoplasm. The nucleus of each cell has scattered chromatin materials and an irregular outline. The yellow region has numerous electron dense granules which have been demonstrated to be mineral deposits. The possible functions of each of the above regions are discussed in this chapter.

Introduction

Insect Malpighian tubules are elongated tubular structures which lie in the haemocoel of the abdomen. One end of each tubule is closed and the other end leads into the alimentary canal at the junction between the midgut and the anterior part of the hindgut. In the larvae and adults of some Coleoptera and the larvae (but not in the adults) of most Lepidoptera, the distal ends of the Malpighian tubules are closely applied to the rectum and enclosed within it in a

special chamber, the perinephric space,separated from the rest of the body cavity by the perinepheric membrane. The term "rectal complex" refers to this association of tubules and rectum (Ramsay, 1976).

Numerous studies on insect Malpighian tubules have been done (see reviews by Maddrell, 1977; Martoja and Ballan-Dufrancais, 1984; Bradley, 1985). For Lepidopterous larvae, the Malpighian tubules studied so far include those of the rice moth *Corcyra cephalonica* (Srivastava, 1962), the skipper *Calpodes* (Irvine, 1969; Ryerse, 1979), silkworm *Bombyx mori* (Teigler and Arnott, 1972), the tobacco hornworm *Manduca sexta* (Ramsay, 1976) and the common cabbage white *Pieris brassicae* (Nicolson, 1976). All these studies are mainly associated with physiology of Malpighian tubules. Just Ryerse' paper (Ryerse, 1979) studied the structural changes which occur in the Malpighian tubule yellow region principal cells during larval-pupal-adult development of *Calpodes* . However, the structure of the Malpighian tubules of the small cabbage white *Pieris canidia* larva has not been reported on.

During the course of studying the histopathological effects of *Bacillus thuringiensis* on the Malpighian tubule cells of *Pieris canidia* larva I find it worthwhile to study the fine structure of *Pieris canidia* larvae in detail so as to understand the structural differentiation of Lepidoptera Malpighian tubules better.

Materials and methods

Adults of *Pieris canidia* Spar. (Lepidoptera) were collected from Chek Nai Ping and the Chinese University campus in the New Territories of Hong Kong. Under captivity in a rearing box, they were supplied with 5% sucrose solution for their daily diet, and a small cabbage plant, *Brassica parachinesis* B. for

oviposition. Fourth instar larvae were used for dissection. Dissections were made in 0.2 M phosphate buffer, pH 7.2, and four regions (yellow region , white region , iliac plexus and rectal lead) were fixed in 2.5 % glutaraldehyde in 0.2 M phosphate buffer, pH 7.2, at 4° C, for 1 hour respectively and post-fixed in 1% osmium tetroxide in phosphate buffer. Tissues were dehydrated in ascending series of alcohol, infiltrated with acetone and resin (1:1) at room temperature for 1 hour and then embedded in spurr resin.

For transmission electron microscopy, sections were cut with a Reichart ultratome and were stained with uranyl acetate and lead citrate. Sections were observed in a Zeiss EM 9S-2 electron microscope.

For light microscopy, thick sections (1μm) were also cut with a Reichart ultratome and were stained in 1% toluidine blue in 1% borax.

For reference purpose, the distal Malpighian tubules (known to accumulate large amounts of minerals for storage excretion by Dr. W. W. K. Cheung) of the lantern bug *Pyrops candelaria* Linn. were also fixed and sectioned for electron microscopic examination.

Results

General morphology

The general organization of *Pieris canidia* Malpighian tubules is shown diagrammatically in Fig. 1. There are six Malpighian tubules , and each has its distal end embedded in the rectum to form the cryptonephridial condition. Together with the rectum, the latter has been referred to as the "rectal complex". Each tubule may be conveniently divided into four portions based on external appearance, namely, the rectal lead, iliac plexus, yellow region and white region

respectively. The rectal lead is the portion emerging from the rectum. It is relatively short and straight , giving way to the highly convoluted iliac plexus closely attached to the colon by ligaments. From here it continues as the straight yellow region, with its name derived from its color appearance. It runs anteriorly over the surface of the midgut well beyond halfway and then turns and runs posteriorly as the white region. At the pyloric junction of midgut and ileum the white regions of the three tubules on each side unite into a small pulsating urinary bladder for emptying the Malpighian tubule fluid.

For convenience sake the internal Malpighian tubules (embedded inside the rectum) and the urinary bladder have been excluded in this study.

Histology and ultrastructure

In the light microscope the rectal lead Malpighian tubule consists of a one cell thick epithelium of several flattened cells. The apical brush border measures 3 μm in length and there are extensive basal membranous infoldings extending 1/2 distance towards the apical surface (Fig. 2).

Under the electron microscope the brush border can be seen to consist of microvilli having mitochondria extending to the tips of them . The nucleus is irregular in outline and consists of scattered chromatin materials (Fig. 3). The ground cytoplasm consists of scattered rough endoplasmic reticulum, golgi apparatus and mitochondria . Occasionally there are extracellular spaces which may be extensions from the basal plasma membrane (Fig. 4). A tight cell junction (probably desmosome) between adjacent cells ran down two-third distance from the apical border (Figs. 5, 6, 7). The basal membrane is 0.3 μm in thickness.

In the light microscope the iliac plexus Malpighian tubule consists of a much

folded epithelium forming canaliculi at various places. The basal infoldings are very extensive, extending almost towards the tip of the apical surface. Extracellular spaces can also be clearly seen just below the apical plasma membrane, which forms numerous microvilli (Fig. 8).

Under the electron microscope, a Malpighian tubule cell can be seen to consist of numerous basal infoldings randomly distributed in the entire cell (Fig. 9) . The nucleus has an irregular outline. The ground cytoplasm has scattered rough endoplasmic reticulum and numerous vacuoles and extracellular spaces (Fig. 10). The basement membrane is 0.3 μm in width.

In the light microscope a Malpighian tubule cell of the yellow region consists of osmiophilic granular deposits. These granules are mineral spherites and cytochemically they consist of calcium, magnesium, ferric iron and phosphate deposits (see next part). The brush border is 5 μm in width, and the basal infoldings extend to 1/2 distance towards the apical surface (Fig. 11).

Under electron microscope there are numerous mineral spherites, multivesicular bodies and mitochondria (Figs. 12, 13). The mineral spherites are oval-shaped and sometimes their contents drop off from sections. Mineral spherites appear to be formed from secondary lysosomes or multivesicular bodies. Minerals first appear to be laid down in the center of these in a concentric manner (Fig. 14). Heavy accumulation of minerals would result in a concentric sphere (Fig. 15). In between adjacent Malpighian tubule cells a septate desmosome can be seen running 1/3 distance from the apical border.

In the light microscope, the white region Malpighian tubule consists of a thin epithelium having a brush border of 6 μm in width. The basal infoldings extend 1/2 distance towards the apical border. Occasionally, patches of extracellular space can be seen. The lumen is sometimes filled with deposits of white substance which cytochemically demonstrated to consist of calcium phosphate

(see next part) (Fig. 16).

Under the electron microscope, sparse mineral spherites may also occur in the cytoplasm though less extensive as the yellow region. The nucleus has an irregular outline (Fig. 17). The ground cytoplasm has scanty rough endoplasmic reticulum (Fig. 18), mitochondria, golgi apparatus and vacuoles (Fig. 19).

Discussion

Functional differentiation of the Malpighian tubules occurs in many insects whereby the Malpighian tubules fluid is modified in chemical composition before draining into the hindgut (Cheung, 1981). For example, in the larvae of *Calpodes ethlius*, the distal iliac-plexus and rectal lead region actively transport K^+ into the tubule lumen which drive the flow of water and other solutes to form a primary urine. The proximal yellow and white regions secrete Na^+ and absorb K^+ and water (Irvine, 1969). Similar results were also observed in *Rhodnius* (Wigglesworth and Salpeter, 1962), *Cenocorixa* (Jarial and Scudder, 1970) and *Pyrops* (Cheung, 1981). Generally, the distal tubules function in fluid and wastes secretion while the proximal tubules are concerned with reabsorption of useful products (Ramsay, 1976; Bradley, 1985).

In *Pieris canidia* and also other Lepidopterous larvae such as *Calpodes* (Irvine, 1969) and *Pieris brassicae* (Nicolson, 1976), the larval Malpighian tubules are arbitrarily divided into four regions externally. Fluid secretion is mainly carried out by the rectal lead and iliac plexus. This function is in accord with the ultrastructure of these two regions. For *Pieris canidia* rectal lead and iliac plexus , the principal cells have numerous basal infoldings forming long narrow intracellular channels extending deeply into the cells, the apical surfaces are amplified by packed microvilli. The numerous mitochondria are closely

associated with the basal infoldings and brush border respectively. This indicates the sites of maximal energy requirements in the cell. Active transport of ions and water may occur here.

For the white region and yellow region, the basal membrane of principal cells also form basal infoldings and the apical surface form brush border. For other insects such as *Pieris brassicae* , Na^+ secretion occurs in the yellow region and white region. K^+ is absorbed in the white region (Nicolson, 1976). It is possible for yellow and white regions that some useful materials could be reabsorbed into the haemolymph.

Berridge and Oschman (1969) reported that the principal cells of *Calliphora* had long narrow basal infoldings and a microvillate luminal border, both were intimately associated with mitochondria. For the principal urine-secreting cells of the Malpighian tubules of *Carausius* (Taylor, 1971b), mitochondria are arranged in two bands of about equal volume near to the basal and apical surfaces , suggesting active processes occur at both surfaces. Basal infoldings and apical microvilli which greatly amplify the cell surface are probably primarily devices to increase the passive permeability of the tissue to solutes. The extensive endoplasmic reticulum is locally differentiated into several components and ramifies between the infoldings and along microvilli but probably is not an intracellular conduit for the majority of urinary constituents. The epithelium of the Malpighian tubules in the housefly is comprised of four distinct cellular types. Type I cells are characterized by the presence of intimate associations between infoldings of basal plasma membrane and mitochondria. On the luminal surface, cytoplasm is extended into microvilli which contain mitochondria. Membrane bound vacuoles in the cytoplasm seem to progressively accumulate granular material. Type II cells have dilated canaliculi. Microvilli lack mitochondria. The type III cell has not been reported previously in

Malpighian tubules. It has very well developed granular endoplasmic reticulum which contains intracisternal bundles of tubules. Cytoplasm contains numerous electron dense bodies. Type IV cells, mitochondria do not extend into the microvilli (Sohal, 1974). From Sohal' results, the type I cell has a similar structure with the principal cells.

The basic structure of the principal cells of different species are similar in that each cell is divided into three regions: a basal, an intermediate, and an apical region. The basal region which faces the body cavity, is separated from the haemolymph by the basement membrane. Cellular membrane fold deeply to form basal infoldings. A brush border is characteristic for the apical region which faces the lumen of the tubule. It is composed of numerous microvilli. For basal infoldings and apical microvilli, both are intimately associated with mitochondria. The intermediate region is characterized by diverse organelles such as endoplasmic reticulum, golgi apparatus, vesicles, multivesicular bodies and polyploid nucleus (Eichelberg and Wessing, 1975). But some other structures may be different, for example, the mineral spherites are found in the central cytoplasm of Malpighian tubule of *Pieris canidia*. This structure was also found in *Rhodnius* (Wigglesworth and Salpeter, 1962), *Gaeana* (Cheung and Marshall, 1973a), *Musca* (Sohal, 1976) and *Calpodes* (Ryerse, 1979).

In *Pieris canidia*, the mineral spherites are oval-shaped and their contents are in a concentric manner. Cytochemical tests indicate that they consist of calcium, magnesium, ferric iron and phosphate deposits (see next part). In *Rhodnius*, mineral granules, presumably phosphates or carbonates of calcium and magnesium, appear grayish yellow by transmitted light. They show a concentric structure. The mineralized granules may possibly represent the final stage in the breakdown of mitochondria (Wigglesworth and Salpeter, 1962). In *Gaeana*, the areas of smooth endoplasmic reticulum are expended into wide cristernae, and it

is within these that electron dense material appear to be laid down. In young cells, the mineral spherites arrange in concentric circles (Cheung and Marshall, 1973a). In *Musca domestica*, three types of mineral spherites are observed (Sohal *et al.*, 1976). Type A concretions are membrane-bound spherical structures which may arise by the gradual intravacuolar accumulation of dense material. Type B concretions appear to be related to multivesicular bodies. Type C concretions are heteromorphic and morphologically resemble the residual bodies. They show a positive location of acid phosphatase reaction product. X-ray microanalysis of intracytoplasmic and intraluminal concretions reveal the presence of phosphorus, sulphur, chlorine, calcium, iron, zinc and copper (Sohal *et al.*, 1976).

By now, relatively little is known about the origin of the mineral spherites. According to different authors' suggestions, these can be summarized as follows:

(1). Mineral spherites may arise by the mineralization of degenerating mitochondria (Wigglesworth and Salpeter,1962).

(2). Mineral spherites may arise from membrane bound vacuoles, multivesicular bodies, and the secondary lysosomes or residual bodies (Sohal et al., 1976).

(3). Mineral spherites may originate in the cisternae formed from smooth parts of the endoplasmic reticulum (Cheung and Marshall,1973a).

For *Pieris canidia*, the multivesicular bodies were seen to be gradually mineralized. A heavy accumulation of minerals would result in a spherical globule of electron dense minerals or mineral spherites. So the second mechanism was the dominant one for *Pieris canidia.*

With the formation of the rectal complex and the differentiation of Malpighian tubules in *Pieris canidia*, useful materials and water can be reabsorbed into the haemolymph. This will ensure its survival in relatively dry

environment.

Part IV. Histochemical studies on the *Pieris canidia* larval Malpighian tubules

Summary

Histochemical studies on the four portions of *Pieris canidia* larval Malpighian tubules have been investigated by various histochemical methods. The carbohydrates, proteins, lipids, enzymes, several mineral ions and uric acid have been tested. Results showed that the rectal lead and iliac plexus cells yielded positive results with tests for Succinic Dehydrogenase, ATPase and Acid Phosphatase. The reaction products were mainly localized in the basal cytoplasm. It is possible that secretion of ions could occur here. For the white region and yellow region cells, reaction products for ATPase, Alkaline Phosphatase and Succinic Dehydrogenase were associated with the brush border. The basal and apical cytoplasm also produced positive results for these enzymes. Some sort of resorption of solutes could occur here. The tubule cells were stained intensively positive with Mercury-Bromophenol Blue, indicating that mucoprotein or other proteinaceous materials could be present in the microvilli, apical and basal cytoplasm. Positive reaction was also produced by Sudan Black B, indicating the existence of phospholipids in microvilli , apical and basal cytoplasm. Tests for carbohydrates showed that the white region cells gave a positive reaction with Toluidine Blue and PAS. A positive reaction was also found at the microvilli of the yellow region. Toluidine Blue test gave a positive results for both iliac plexus and rectal lead cells, while PAS just produced a positive result for the apical cytoplasms of these two portions. Tests for calcium, magnesium, phosphate showed that the apical cytoplasm of yellow region yielded very strongly positive

reactions. These results indicated that the minerals consisted of calcium, magnesium and phosphate and were mainly stored in this portion. Tests for uric acid and carbonate gave negative results. The relationship between histochemical studies and ultrastructural observations (see previous chapter) of Malpighian tubules of *Pieris canidia* is also discussed in this part.

Introduction

Histochemical tests have been done by different authors in different insect tissues. For example, the midgut of cercopid larvae and adults (Gouranton, 1968a), the midgut of *Fulgora candelaria* (Marshall and Cheung, 1970), the midgut of cicadoids (Cheung and Marshall, 1973a), the midgut of *Pieris canidia* (Cheung and Lam, 1993).

The histochemical characteristics of Malpighian tubules have also been studied in several insects, e.g. studies on water and ion transport in *Gaeana maculata*, *Cryptotympana mimica* and *Cosmoscarta abdominalis*. Marshall and Cheung (1974) reported that the structure and cytochemistry of the filter chamber indicating water flows from filter chamber proper to internal midgut and internal Malpighian tubules by passive osmosis. The external Malpighian tubules appear to be structurally and chemically adapted for ion secretion and possibly for reabsorption in the Malpighian duct segment.

The cytochemical tests for the distal tubule cells of Malpighian tubules of *Pyrops* revealed that the presence of enzymes such as ATPase, Cytochrome Oxidase and Succinic Dehydrogenase. These enzymes were related to transport and metabolism and indicated that secretion of ions could occur here. In the ground cytoplasm of proximal tubule cells, transporting and metabolic enzymes such as ATPase, Glucose-6-Phosphatase, Cytochrome Oxidase, and Succinic

Dehydrogenase also were found. It might be conjectured that some sort of resorption of solutes occur here (Cheung, 1981). Other studies on the cytochemistry of the Malpighian tubules of *Aphrophora alni*, *Philaenus spumarius* and *Cicadella viridis* were investigated by Gouranton (1968b). The ultrastructure of the Malpighian tubules of *Pieris canidia* was studied (see previous part), but the histochemical tests on the Malpighian tubules of *Pieris canidia* have not been investigated yet.

The aim of this study is to find out the histochemical characteristics of the Malpighian tubules of *Pieris canidia*. This information is useful for understanding the structure and function of the excretory system of this insect. This information might also be useful in understanding the histopathology of the Malpighian tubules after infection with *Bacillus thuringiensis* and the protozoan *Nosema polyvora*.

Materials and methods

Adults of the small cabbage white *Pieris canidia* Spar. larvae were reared in an insectary on potted Chinese flowering cabbage *Brassica parachinensis* B. at $23\pm1°C$ with L/D=14/10 photoperiod. Fourth instar larvae were used for dissections. The four regions of a Malpighian tubule: rectal lead, iliac plexus, yellow region, and white region were dissected separately from the body cavity in 0.2 M phosphate buffer (with sucrose added). Malpighian tubules were then fixed in formal saline, formal calcium or Bouin's fluid. The tissues were washed in distilled water and dehydrated in ascending alcohol series: 50%, 70%, 90%, 95%, 100% alcohol (two times), each for 10 minutes. The tissues were cleared in xylene. For filtration, the tissue were put into 1/3 wax with 2/3 xylene at 56^0 C, for 30 minutes, and then removed to 1/3 xylene with 2/3 wax at 56^0 for

another 30 minutes, and finally to pure wax for 2 hours. After embedding in paraffin wax, the rectal lead, iliac plexus, yellow region, and white region were blocked separately.

All four regions of Malpighian tubules were sectioned in a microtome at the thickness of 5 μm. The slides were put onto a hot plate for drying. Dried slides could be used for various histochemical tests. Freeze-substituted methods were used when appropriate. Fresh whole Malpighian tubules were also used for certain histochemical tests.

The larval Malpighian tubule epithelia of *Pieris* were subjected to the following histochemical tests:

a. Carbohydrates: Aqueous Periodic Acid-Schiff (PAS) reagents were used to demonstrate glycogen and other polysaccharides (Pearse, 1968). Enzymatic treatment of control tissues involved incubating in 1% diastase at 37^0 C for 30 minutes. Acid mucoproteins were identified by staining with Toluidine Blue to detect the degree of metachromasia induced (Pearse, 1968). Alcian Blue method (Pearse, 1968) was also used to study mucins.

b. Proteins: The Mercury-bromophenol Blue method was used to demonstrate general proteins (Bonhag, 1955). Basic proteins were stained with Acid Solochrome Cyanine method (Pearse, 1968).

c. Lipids: Tests for the presence of phospholipids were carried out on formalin-fixed materials. Sections were subjected to Sudan Black B method (Pearse, 1968).

d. Enzymes

1). ATPase: This enzyme was tested with lead method described by Wachstein and Meisel (1957).

2). Alkaline phosphatase: This enzyme was detected with the method of Fredricsson (1952).

3). Acid phosphatase: This enzyme was tested according to the method of Barka and Anderson (1963).

4). Succinic dehydrogenase: This enzyme was detected by the method of Barka and Anderson (1963).

5). Glucose-6-phosphatase: This enzyme was tested by the method described by Pearse (1968).

6). ß-glucuronidase; This enzyme was detected by the method of Seligmen *et al.* (1954).

e. Ions: The ions including calcium, magnesium, phosphate, ferric iron, and carbonate were tested by the methods described by Pearse (1968).

f. Uric acid: This secreted material was tested by Hexamine Silver method described by Pearse (1968).

Every test was repeated at least four times until the results were reliable.

Results

The light and electron microscopic studies on the Malpighian tubules of *Pieris canidia* larvae have been performed as reported in the previous chapter. Results of present histochemical tests were correlated with the results obtained earlier.

Histochemical properties of the rectal lead

a. Carbohydrates: The rectal lead cells were stained by Toluidine Blue (Fig. 20). The apical cytoplasm was stained by PAS. Most of the PAS positive substances, probably mucopolysacchrides or mucoproteins, were located on the brush border. The microvilli and basal cytoplasm were not stained by PAS .

Diastase digested control sections were negatively stained. They were not stained by Alcian Blue.

b. Proteins: The general proteins present in the Malpighian tubules cells were stained by Mercury-Bromophenol Blue (Fig. 21) and Acid Solochrome Cyanine method. The rectal lead cells were stained positive by Acid Solochrome Cyanine and Mercury Bromophenol Blue. Especially, the microvilli of rectal lead cells were stained strongly by these two reagents. These results indicated that mucoprotein or other proteinaceous materials could be associated with the brush border.

c. Lipids: Phospholipids were detected by Sudan Black B method. Results showed that the rectal lead cells gave a positive reaction. In general, membraneous structures of cells were stained positive, indicating the presence of phospholipids in these areas.

d. Enzymes: The rectal lead cells yielded positive results with tests for ATPase, Alkaline Phosphatase, Succinic Dehydrogenase, Acid Phosphatase and Succinic Dehydrogenase. The reaction products were mainly localized in the basal cytoplasm of the cells, indicating the presence of transporting function at these sites. Glucose-6-Phosphatase gave positive result for the apical cytoplasm of the tubule cells. Just for the apical and basal cytoplasms of the cells of this portion yielded positive result with test for ß-glucuronidase.

e. Ions: Tests for calcium, magnesium, phosphate, carbonate and ferric ion gave negative results except that the apical cytoplasm yielded slightly positive result with tests for calcium, ferric ion and the basal cytoplasm produced a positive result for phosphate.

f. Test for uric acid gave a negative result for the Malpighian tubule cells.

Table 1 summaries the histochemical properties of the rectal lead cells.

Histochemical properties of the iliac plexus

Tests for carbonates, proteins, lipids and ions gave similar results as those for the rectal lead (Fig. 22). Test for ATPase showed that just the microvilli gave positive result. Glucose-6-Phosphatase produced positive staining for both apical and basal cytoplasms (Fig. 23). But test for ß-Glucuronidase gave a negative result.

Table 2 summarizes the histochemical properties of the iliac plexus.

Histochemical properties of the yellow region

a. Carbohydrates: The microvilli were stained by PAS and Toluidine Blue (Fig. 24). However, tests for apical and basal cytoplasms gave negative results. The results showed that acid mucopolysaccharides or mucoproteins were located on the brush border. Alcian Blue gave a negative result.

b. Proteins: The microvilli and apical cytoplasms were stained strongly positive by Acid Solochrome Cyanine and Mercury-Bromophenol blue. The basal cytoplasm was stained lightly.

c. Lipids: The microvilli of yellow region cells yielded strongly positive results with test for Sudan Black B. Weakly positive reactions were obtained with basal and apical cytoplasm.

d, Enzymes: Tests for Alkaline Phosphatase, ATPase (Fig. 25), and Succinic Dehydrongenase showed that the strong reaction products were associated with the brush border and apical cytoplasm. So very active transporting materials took place in these places. This phenomenon is closely related to the ultrastructural observation that many mitochondria were associated with microvilli (see previous chapter). Glucose-6-Phosphatase gave positive result to the apical cytoplasm and

negative results to the microvilli and basal cytoplasm. Acid Phosphatase gave a slightly staining for apical and basal cytoplasms. Test for ß-Glucuronidase indicated a negative result.

e. Ions: The apical cytoplasm of cells of this region gave a very strong positive reactions with tests for calcium (Fig. 26), magnesium, and phosphate (Fig. 27), a slightly positive result for ferric iron (Fig. 28), indicating that the minerals consisted of calcium, magnesium, phosphate, and iron were mainly stored in the cytoplasm of this region. These results were associated with mineral spherites observed under the electron microscope (see previous chapter). But the microvilli gave negative results for calcium, magnesium, phosphate and iron. Test for carbonate produced a negative result.

Table 3 summarizes the histochemical properties of the yellow region.

Histochemical properties of the white region

a. Carbohydrates: The microvilli of the white region cells were stained positive by PAS (Fig. 29) and Toluidine Blue (Fig. 30). The apical and basal cytoplasm were also stained slightly positive by PAS and Toluidine Blue. They were not stained by Alcian Blue.

b. Proteins: The microvilli of white region tubule cells were stained positive by Acid Solochrome Cyanine, especially stained strongly by Mercury-Bromophenol Blue, For the basal and apical cytoplasms of white region cells were stained positive for Mercury-Bromophenol Blue, but negative for Acid Solochrome Cyanine.

c. Lipids: The microvilli of the white region cells produced strongly positive reaction with test for Sudan Black B (Fig. 31). The apical and basal cytoplasm gave slightly positive staining.

d. Enzymes: The white region tubule cells yielded strongly positive results with tests for ATPase, Succinic Dehydrongenase (Fig. 32) and Alkaline Phosphatase (Fig. 33). The reaction products are mainly localized in the brush border of the cells, indicating the presence of transporting function at these sites. Weakly positive reactions were obtained with tests for the above enzymes for basal and apical cytoplasms. Glucose-6-Phosphatase and Acid Phosphatase (Fig. 34) gave positive results for the apical cytoplasm of the tubule cells. ß-Glucuronidase gave a negative result.

e. Ions: Tests for calcium, phosphate and ferric ion produced slightly positive results for apical cytoplasm. However, tests for magnesium and carbonate gave negative results.

f. Test for uric acid gave a negative result for the Malpighian tubule cells.

Table 4 summarizes the histochemical properties of the white region.

Discussion

Functional differentiation of the Malpighian tubules occurs in many insects whereby the Malpighian tubule fluid is modified in chemical composition before draining into the hindgut (Cheung, 1981). Examples are *Rhodnius* (Wigglesworth and Salpeter, 1962) and *Calpodes* (Irvine, 1969). Water conservation is thus successfully achieved.

Such functional differentiation in the Malpighian tubule is correlated with the structural differences. Based on studies on the Malpighian tubules of *Calliphora*, Berridge (1968) suggested that the basal invaginations and the apical microvilli were important for urine formation in insects. Within the channels of the basal infoldings, a hypotonic fluid is created towards the closed end of the channels. Hypotonicity within the channel provides the osmotic gradient for passive

movement of water into the cell. Similar mechanisms are supposed to be involved in the urine secretion process of the apical microvilli (Berridge and Oschman, 1969; Oschman *et al.*, 1971).

The histochemical results are also related to the functional differentiation. The ultrastructure and cytochemistry of the distal region of the Malpighian tubules was consistent with the suggestion that ion transport took place from haemolymph to lumen by active transport mechanism. This was also true of cercopoid Malpighian tubules although they were highly specialized for protein secretion (Marshall, 1974). The Malpighian tubules had cells with basal leaflets containing mitochondria and the basal region was rich in ATPase (Marshall and Cheung, 1974). For the Malpighian tubules of *Pieris canidia*, there are six Malpighian tubules and each tubule might be conveniently divided into four portions, namely, white region, yellow region, iliac plexus and rectal lead. For the rectal lead and iliac plexus cells, histochemical tests yielded positive results with tests for ATPase, Alkaline and Acid Phosphatases, and Succinic Dehydrogenase. The reaction products was mainly localized in the basal cytoplasm of the cells. The presence of all these enzymes, which are related to transportation and metabolism, indicate that secretion of ions could occur here. The primary urine formation begins at the distal segments. Similar findings were also observed in the Malpighian tubules of *Pyrops* by Cheung (1981).

The electron microscopic studies indicate that the distal tubule cells of *Pieris canidia* have numerous basal infoldings, forming long narrow intracellular channels extending deeply into the cells. Many mitochondria are associated with these channels (see previous part). They can supply energy for cellular metabolism. This result agrees with the histochemical results.

For the white region cells of *Pieris canidia*, the apical membrane infolded to form microvilli, the mitochondria extended to the tips of them. Histochemical

tests show that the reaction products produced by ATPase, Succinic Dehydrogenase are associated with the brush border and apical cytoplasm. This result is just the same as those in other insects, e.g. *Pyrops* (Cheung, 1981). So some sort of resorption of solutes could occur here. The yellow and white regions, together with the rectum, ensure that all useful materials are reabsorbed back into the haemolymph.

For the microvilli of every region, the histochemical tests show that the Alkaline Phosphatase is mainly associated with them, and may be essential for maintaining a proper water and ion balance in haemolymph (Cheung and Lam, 1993). The positive results for proteins indicate that there is an active synthesis of these products (Cheung and Lam, 1993). A positive reaction of Toluidine Blue associated with microvilli, indicates that there is mucoprotein on the mucosal surface. Positive reactions produced by Acid Solochrome Cyanine and Mercury-Bromophenol Blue are also associated with microvilli and apical cytoplasm. So general and basic proteins exist in the mucosal surface. The microvilli are stained intensively positive with Sudan Black B indicating that phospholipids exist in the microvilli. Because the major components of cell membrane are polar lipids and proteins (Lehninger, 1982), it can be concluded that the microvilli are formed from the apical membrane.

In the light microscope, a principal cell of the yellow region contained numerous osmiophilic granular deposits. Most of these granules were mineral spherites. Under the electron microscope, the mineral spherites were oval-shaped and sometimes their contents dropped off from sections (see previous part). The histochemical tests further confirm this observation. Because the apical cytoplasm of yellow region had yielded a very strongly positive reactions with tests for calcium, magnesium, phosphate, and a slightly positive result for ferric ion histochemically, so the mineral spherite is composed of all these materials.

The mineral spherites (or granules) were also studied by other authors cytochemically. Gouranton (1968a) studied the granules of the midgut epithelium of cercopid larvae and adults by cytochemical methods and by electron microscopy. He reported that the granules had a diameter up to about 2μ and contained calcium, magnesium, iron, carbonates, and phosphates. Protein and mucopolysaccharide had also been detected. A chromatographic study showed that uric acid and guanine were not present. The mineral spherites could be clearly seen under the electron microscope. The distal tubule cells of the Malpighian tubules of the lantern bug *Pyrops candelaria* were also capable of mineral storage excretion. The spherites shown in light and electron micrographs were stained positively with tests for calcium, magnesium and phosphate (Cheung, 1981). These mineral spherites did not contain uric acid, and were comparable to those in the distal tubules in *Rhodnius* (Wigglesworth and Salpeter, 1962). These mineral spherites had also been observed in other insects. Examples are *Musca domestica* (Sohal, 1974; Sohal *et al.*, 1976); *Calpodes ethlius* (Ryerse, 1979); *Ephydra hians* (Yu *et al.*, 1988); *Acheta domesticus* (Hazelton *et al.*, 1988) and *Rhodnius prolixus* (Maddrell *et al.*, 1991).

Little is known about the mode of origin of the mineral spherites in insect cells. Several hypotheses have been proposed by different authors (Wigglesworth and Salpeter, 1962; Sohal *et al.*, 1976; Cheung and Marshall, 1973a). Further studies on these structures are necessary so as to understand their exact mode of formation.

Part V. Separation and Purification of parasporal crystals of *Bacillus thuringiensis* var. *kurstaki*

Summary

A spore-free parasporal crystals suspension was prepared from *Bacillus thuringiensis* var. *kurstaki* by using urografine solution as a separation medium. After centrifugation at 6000 rpm for two hours, spores were at the bottom. Two bands were visible in the region of the short gradient of urografine formed at the interface between the culture and the urografine solution. The crystals were in the lower band. Protein composition of parasporal inclusion bodies was determined by sodium dodecyl sulfate-polyacrylamide gel electrophoresis (3% stacking gel and 7.5% resolving gel). Two proteins, P1 (134 KDa) and P2 (63 KDa), were found.

Introduction

Bacillus thuringiensis var. *kurstaki* is an effective microbial insecticide for the control of Lepidopterous pests. During sporulation, this bacterium synthesizes a proteinaceous crystalline inclusion within the sporangium. This inclusion, known as the crystal δ-endotoxin, displays insecticidal activity towards Lepidopterous larvae (Knowles and Ellar, 1987). Current studies of parasporal crystals of *Bacillus thuringiensis* require that the crystals are effectively and completely separated.

Many techniques have been used in separating parasporal crystals from the

spores. The first techniques for isolating the crystals consisted in the elimination of the spores from the mixture harvested in the last stage of culture, either through mechanical disruption (Fitz-James, 1953), or through spontaneous germination followed by autolysis (Hannay and Fitz-James, 1955). The crystals were then free from the debris through repeated washing and differential centrifugation. These techniques, time consuming and difficult, gave a very poor yield. Angus (1956) devised a technique of extraction and purification of *B. thuringiensis* var. *sotto* toxin. A first extraction by 0.05 *N* sodium hydroxide was followed by dialysis against water and precipitation at pH 4.4. The precipitate was redissolved in 0.01 *N* sodium hydroxide and the solution was reprecipitated through continued dialysis against distilled water. The final precipitate is freeze dried. With this method it is relatively easy to obtain large quantities of toxin. Yet purification is not sufficient to ensure that protein contaminants from spores do not exist. The technique of emulsion in organic solvents was firstly devised by Angus (1959), who used a fluorocarbon. The aqueous suspensions of spores and crystals, harvested after 14 days of culture on Difco agar at 28^0C were added to the solvent at a ratio of 9:1 (volume) and emulsified in a high speed mixer. After shaking, the emulsion was separated into two phases; an aqueous upper phase which contained almost exclusively crystals, and a lower organic phase which contained hydrophobic spores. Treatment of the aqueous phase must be repeated several times until less than 1% of spores remains. The residual spores were eliminated through germination and autolysis before a final treatment with the solvent. This technique, theoretically very effective, involved several extractions, one after another, with the solvent, and its yield was low. It had been modified by Bateson (1965), who added 1% sodium sulfate to the aqueous phase and n-butyl citrate to the fluorocarbon of the emulsion. With this method it is possible to obtain preparation with 99% of the crystals after only one solvent

treatment. Church and Halvorson (1959) used sucrose as a supporting medium in experiments. Because of the high density of the spores, however, most of the preparation was recovered as a pellet and was therefore less adequately characterized. The diphasic system described by Albertsson (1960) using dextran sulfate and polyethylene glycol is frequently used to free the preparation of spores. Lewis *et al.* (1964) used the lead chelate of N, N'-(dihydroxyethyl)-N,n'-(dicarboxymethyl) ethylenediamine as a supporting medium for a gradient and were able to separate distinct spores. However, the spores were not tested for viability, and thus it is not known whether they were damaged by the high concentration of lead. Bateson (1965), who added 1% sodium sulfate to the aqueous phase and n-butyl citrate to the fluorocarbon of the emulsion. Lecadet (1965) used tetrabromoethane and Pendleton and Morrison (1966) used carbon tetrachloride after previous filtration on Whatman paper to obtain more crystals. Murray and Spencer (1966) obtained a very satisfactory yield by emulsifying with chloroform and filtering through Millipore filter membranes. Their crystal preparations contained approximately one spore per three thousand crystals. Goodman *et al.* (1967) distributed dextran sulfate 500 and polyethylene glycol 6000 into two phases in a previously determined proportion so that the spores went preferentially into the phase richer in polyethylene glycol. Through the repetition of this procedure, followed by repeated washing and differential centrifugation, the investigators obtained very pure preparations with 99.94% of crystals and a yield of 250 mg/10gm of the spore-crystal mixture. This yield is rather low, but the method avoids the risks associated with treatment with solvents. Cooksey *et al* (1969) described a technique of purification in which the solution in sodium hydroxide and the preparation at pH 4.4 was followed with fractionation on Sephadex G 200, precipitation with ammonium sulfate, and a second fractionation on Sephadex. The preparation thus obtained contained only

the soluble components from the crystal; the purification was followed by electrophoresis on polyacrylamide gel. This time-consuming technique could be used only to provide small amounts of products for structural studies.

Schatz *et al.* (1964) reported the use of urografine, a compound with high density and relatively low viscosity, as a supporting medium for a density gradient. Their successful isolation and characterization of functional mitochondria from such gradients indicated that this compound might be without toxic effect on bacteria. Urografine gradients had been used by Tamir and Gilvarg (1966) to separate spores of *Bacillus megaterium* from vegetative cells and by Wise *et al.* (1967) to obtain spores of altered dipicolinic acid content. Sharpe (1975) used urografine as a supporting medium to separate spores and crystals of *Bacillus thuringiensis*. The spores and crystals of *Bacillus thuringiensis* var. *dendrolimus*, grown in the medium, were washed in water. About 0.3 ml of the final water suspension was layered onto 11 ml of a linear water-urografine gradient in thick walled glass tubes and centrifuge for two hours at 10000 rpm in swinging bucket rotor. Bands of crystals and spores were harvested with a Pasteur capillary pipette after first removing the above liquid. Urografine was also used by Milne *et al.* (1977) and Meenakshi and Jayaraman (1979) as a linear or a discontinuous gradient to separate crystals from spores. Mahillon and Delcour (1984) used urografine for purification of parasporal crystals from *Bacillus thuringiensis*. Urografine is the European commercial name of Renografin. Renografin is the X-ray contrasting agent methylglucamine 3,5-diacetylamino-2,4,6-triiodobenzoate.

Comparing all the above procedures, the most widely used is the centrifugation of the X-ray contrasting agent urografine as a supporting medium. This technique is rapid, simple and has been reported to give high purity preparations of crystals and spores. The procedure given below will be a

convenient method for separating the spores and crystals for studying the latter's histopathological effects on *Pieris canidia* larva.

Materials and methods

Culture material

Bacillus thuringiensis var *kurstaki* (HD-1) was provided by Sandoz company, under the trade name Thuricide. The bacterial preparation was in the form of spore-crystal mixture, with potency 16,000 international units per gram.

Isolation of the crystals from the Spore/crystal mixture

The bacterium was grown in the modified CHES medium (Chestukina *et al.*, 1980). The composition of the nutrient medium was as follows:

Casamino acid----------0.5%

Yeast extract----------0.4%

Glucose----------0.2%

NaCl----------0.5%

$MgSO_4 . 2H_2O$----------0.01%

$CaCl_2 . 2H_2O$----------0.05%

pH----------7.4

Firstly, the bacteria were grown in CHES medium (50 ml in 250 ml flasks) with shaking (150 rpm) at 28°C for 7 hours. After preculture, the CHES medium (50 ml in 250 ml flasks) was inoculated with 1% (v/v)of a *Bacillus thuringiensis* preculture and was incubated at 28°C in a shaker at 150 rpm for 12 hours. This culture was centrifuged at 8000 rpm, 20°C for 15 minutes (GSA rotor). The

pellets were resuspended in the initial volume of sterile distilled water (50ml). This culture was incubated at 28^0 in a shaker at 150 rpm for 4 days for sporulation and autolysis. After 4 days incubation, the culture was examined under phase contrast microscope to ensure that sporangia had lysed and free spores and crystals could be seen. A centrifuge tube (50 ml) was prepared and 20 ml of 67% urografine solution was dispensed into it. A pipette was used for layering carefully 20 ml of the spore-crystal suspension onto the urografine solution. The solution was centrifuged at 6000 rpm, 4^0C for 2 hours. After centrifugation, the tube was examined. Spores were at the bottom and two bands were visible in the region of the short gradient of urografine formed at the interface between the culture and urografine solution. The parasporal crystals were in the lower band. The band was removed with Pasteur pipette and examined under phase-contrast microscope. The crystals were resuspended in distilled water and centrifuged at 15,000 rpm, 4^0 for 30 minutes. The pelleted crystals were ready for use and analysis. The crystals could be lyophilized and stored at -20^0 until use. However, the crystals should be avoided thawing and freezing repeatedly as these tended to make the crystals more difficult to resuspend. Furthermore, the composition might change due to protease action. The purity of the crystals were monitored by examining samples of these by scaning electron microscopy.

Solubilization of crystal δ-endotoxin

Complete solubilization was accomplished by incubating the crystals in 1% (wt/vol) sodium dodecyl sulfate (SDS); 2% (vol/vol) ß-mercaptoethanol (ME); 6 M urea and an equimolar (0.01 M) ratio of NaH_2PO_4 and Na_2HPO_4 (pH 7.2) for 1 hour at 28^0C. Soluble toxic material was obtained in the following manner. A suspension of crystals (0.4%, wt/vol) was titrated to pH 12 with 1 N NaOH at

28^{0}C. The crystals suspension was allowed to stay at this pH for 5 hours and then dialyzed against 0.02 N phosphate at pH 7.5. Protein concentration was determined by absorbance at 280 nm using an extinction coefficient of 1.1 absorbance units equal to 1 mg of protein per ml (Tyrell *et al.*, 1981).

Sodium dodecyl sulphate-polyacrylamide gel electrophoresis (SDS-PAGE)

Protein composition of parasporal inclusion bodies was determined by modifying the SDS-PAGE procedure of Laemmli (1970). A 3% stacking gel and a 7.5% resolving gel were run on a Mini-protein II electrophoresis cell (Bio-Rad Instrument) for 10 minutes at 50 volts and 1 hour at 100 volts respectively. Protein standards used for molecular masses (KDa) were used the Bio-Rad, SDS-PAGE molecular weight standards, high range specification, including myosin (200), ß-galactosidase (116.25), phosphrylase B (97.4), bovine serum albumin (66.2) and ovalbumin (42.699). Gels were stained with Coomassie Brilliant Blue R 250 for 4 hours and destained by washing in methanol/H_2O/acetic acid (vol/vol/vol=45/45/10) for 4-8 hours. The gels were stored in water containing 20% glycerol.

Scanning electron microscopy

Crystal morphology was detected by scanning electron microscope. Purified HD-1 strain crystals were dissoved in double distilled water. The suspensions were placed on copper mounts and air dried. Samples then were coated with gold, examined and photographed with a JSM 5300 scanning electron microscope at a voltage of 15 kV.

Results

Bacillus thuringiensis var. *kurstaki* was precultured and grown in the CHES medium. After centrifugation at 6000 rpm using urografine as supporting medium, the parasporal crystals could be separated from spores and cell debris. Two bands could be seen in the centrifuge tube. The first band is cell debris and the second band is crystals (Fig. 35). The spores were accumulated in the bottom of the centrifuge tube. The method of centrifugation at 6000 rpm for 90 minutes was firstly used, but the two bands were not separated very well. When the centrifugation time was increased to 120 minutes, two bands were separated well. It was simple to remove the crystals band from the solution with a Pasteur pipette.

Complete solubilization was accomplished by Tyrell's method. Solubilized proteins were analyzed by SDS-polyacrylamide gel electrophoresis. Two major bands of 134 and 63 KDa were found (Fig. 36).

The morphology of the purified crystals were examined by scanning electron microscope. Two kinds of crystals were produced by the HD-1 (kurstaki) strain (Fig. 37). One was a bipyramidal crystal containing a 134 kDa protein (P1) (Fig. 38). Another was a cuboidal crystal containing a 63 kDa protein (P2) (Fig. 39).

Discussion

A purified insecticidal toxin from *Bacillus thuringiensis* var. *kurstaki* was isolated. Its molecular weight is approximately 63 KDa as determined by SDS-polyacrylamide gel electrophoresis. The parasporal crystal of *Bacillus thuringiensis* is composed of a repeating subunit that is converted to a smaller toxic component by dissolution with denaturing agent (Bulla *et al.*, 1979). But

from the SDS-polyacrylamid gel electrophoresis result, after solubilization of parasporal crystals, small quantity of protoxin also exists in the solution. For the susceptible insect larvae, firstly, the δ-endotoxin is contained in the parasporal protein crystals of *Bacillus thuringiensis* as an inactive protoxin . After the protein crystal is ingested by Lepidopterous larvae, it is dissolved by the alkaline gut juice. The crystal dissociates and the protoxin releases. The dissolved protoxin is further digested by the protease in the insect midgut to form the active toxin (Luthy *et al.*, 1982).

Although several methods have been used for purification of parasporal crystals of *Bacillus thuringiensis*, the most widely used method is the centrifugation on urografine gradient. Why do so many people use this method ? Because the major problem for the purification methods used by Fitz-James (1953, 1955), Angus (1959), Goodman (1967) and other persons have low yield for purified crystals. With the method used by Lewis *et al.* (1964), the purified spores and crystals were not tested for viability. Comparing the method used by Sharpe (1975) with the ours, there are some disadvantages for the Sharpe's method: (1). Before centrifugation, the spores suspension must be treated by sonication. (2). The separation easily becomes unclear and there is clumping. The current described method using urografine as supporting medium is simple, rapid and gives high purity of crystals. Obviously, this method could easily be adapted to specific strains, if necessary, by changing the concentration of urografine in order to adjust to different crystals and spore densities. The purified δ-endotoxin has been used in the studies on the histopathological effects of *Bacillus thuringiensis* var. *kurstaki* on the Malpighian tubules of *Pieris canidia* larvae in my study.

Part VI. Histopathological effects of *Bacillus thuringiensis* var. *kurstaki* δ-endotoxin on the Malpighian tubules of *Pieris canidia* larva

Summary

The histopathological effects of *Bacillus thuringiensis* var *kurstaki* δ-endotoxin on the Malpighian tubule cells of *Pieris canidia* larva had been studied. The tubule was treated by the toxin mucosally and serosally. Tissues examined after 1 minute of exposure to the toxin already revealed fine structure alterations. These included enlargement of spaces in the cytoplasm and basal infoldings. The microvilli became slightly disorganized for mucosal treatment and the basal infoldings became slightly irregular in shape for serosal treatment. After 10 minutes treatment of toxin, some of the microvilli appeared distorted and showed blebbing, but some appeared less affected. Most mitochondria were transformed into a condensed form. The nucleus enlarged and chromatin materials dispersed. The cytoplasmic spaces enlarged continually. By 20 minutes after toxin treatment, general disintegration was observed. Microvilli disappeared completely and the apical membrane lysed. The rough endoplasmic reticula and Golgi apparatus vacuolated. The mitochondria were generally in the condensed form and almost round in shape. Basal infoldings were also disorganized and the basal lamina was damaged. The results indicated that *Bacillus thuringiensis* δ-endotoxin might bind to a plasma membrane receptor. The action of toxin might be generate small pores in the plasma membrane. Cells swelled and eventually lysed.

Introduction

Bacillus thuringiensis is a widely distributed, sporeforming, gram-positive microorganism closely related to *Bacillus cereus* (Faust and Bulla, 1982; Whiteley and Schnepf, 1986). It produces one or more parasporal crystals during the sporulation cycle and is pathogenic to Lepidopterous larvae (Couch and Ross, 1980). When the protein crystal is ingested by the susceptible insect larvae, it is dissolved by the alkaline gut juice. The crystal dissociates and the protoxin is released. The dissolved protoxin is further digested by the protease in the insect midgut to form the active toxin (Heimpel and Angus, 1959). Histopathological studies on insect midgut *in vitro* show that the primary target of the activated toxin is the epithelial cells which swell and lyse resulting in severe disruption of the gut epithelium (Heimpel and Angus, 1959; Ebersold *et al.*, 1978; Cheung *et al.*, 1990).

Although the site and mode of action of the *Bacillus thuringiensis* δ-endotoxin are not fully understood, many theories have been proposed to explain the mechanism that cause the pathogenic effects (Travers *et al.*, 1976). These include: (1). It binds to a specific plasma membrane receptor and form lytic pores in plasma membrane (Knowles and Ellar, 1987). (2). It uncouples oxidative phosphorylation (Travers *et al.*, 1976); (3). It inhibits an epithelial K^+ pump (Gupta *et al.*, 1985). (4). It specifically affects Na^+ and/or K^+ transport (Himeno *et al.*, 1985). (5). It causes a general breakdown of cell permeability barriers (Nishiitsutsuji and Endo, 1979). Immunolocation of *Bacillus thuringiensis* var. *kurstaki* δ-endotoxin on the midgut and Malpighian tubules of Lepidopterous larva *Heliothis* indicated that receptors for the *Bacillus thuringiensis* var. *kurstaki* endotoxin are widely distributed on the apical surfaces of transporting epithelial cells (Ryerse *et al.*, 1990).

There were many histopathological studies carried out on Lepidopterous midgut epithelia (Sutter and Raun, 1967; Endo and Nishiitsutsuji-Uwo, 1980;

Ebersold *et al.*, 1980; Percy and Fast, 1983; Tojo, 1986; DeLello, 1984; Gupta *et al.*, 1985; Lane *et al.*, 1989; Cheung *et al.*, 1990) and on insect cell lines, such as nerve cells of cockroaches (Cooksey *et al.*, 1969). So far, only one paper has reported the changes in the fine structure of the Lepidopterous Malpighian tubules after *Bacillus thuringiensis* var. *kurstaki* infection (Reisner *et al.*, 1989) and the histopathological effects of *Bacillus thuringiensis* var. *kurstaki* on the Malpighian tubules of *Pieris canidia* larva have not been investigated yet. Insect Malpighian tubules possess a one cell thick epithelium generally similar to those of the midgut (Wigglesworth, 1953; Harvey *et al.*, 1983). Thus, the utilization of insect Malpighian tubules for studying the histopathological effects of *Bacillus thuringiensis* var. *kurstaki* δ-endotoxin may provide insight into the tissue specificity and cellular mode of action of *Bacillus thuringiensis* δ-endotoxin.

The ultrastructure of the Malpighian tubules of *Pieris canidia* larva was studied in the previous chapter of this thesis. The purified *Bacillus thuringiensis* var. *kurstaki* δ-endotoxin was used for treating the Malpighian tubules of *Pieris canidia* mucosally and serosally. Histopathological changes in Malpighian tubule cellular structure are discussed in this chapter.

Materials and Methods

Separation and purification of parasporal crystals of *Bacillus thuringiensis kurstaki*

The method for purification of parasporal crystals was described in previous chapter of this thesis.

Activation of Toxins

Five milligrams of purified crystal was weighed. The crystal was suspended in 1 ml 1% protease (containing trypsin) and 0.2% dithiothreitol (DTT) in 0.2 M CAPS (3-[cyclohexylamino] propanesulphonic acid) buffer, pH 10.5, and incubated at 28^{0}C on a rotary shaker for 24 hr. The suspension was then centrifuged and the supernatant was collected. No further purification need to be carried out. The protein concentration of the activated toxin was determined by the Bio-Rad microassay dye method.

Bio-Rad protein centrifugation assay

The Bio-Rad protein standards were used for making the standard curve (Fig. 40). Firstly, several dilutions of bovine serum albumin: 4 μg/ml, 8 μg/ml, 12 μg/ml, 16 μg/ml, 20 μg/ml were prepared. Then 0.8 ml of every standard dilution and 100 times diluted samples were placed in clean, dry test tubes. 0.8 ml CAPS buffer was placed in "blank" test tube. 0.2 ml reagent concentrate was added. The test tubes were mixed several times by gentle inversion. After a period of 5 minutes to one hour, OD_{595} was measured versus reagent blank. The standard curve was made by plotting OD_{595} versus concentration of standards. Unknowns were read from the standard curve.

After assay, the concentration of sample one was 1.007 mg/ml, and sample two was 1057 mg/ml (Table 5). Appropriate sample dilutions were prepared for treatment of Malpighian tubules of *Pieris canidia*.

Experimental animals and tissue treatment

The small cabbage white *Pieris canidia* larvae were reared in an insectary at 23$\pm$1°C with a L/D = 14/10 photoperiod. Fourth instar larvae were used for

dissection. Malpighian tubules were dissected in 0.2 M phosphate buffer (with sucrose added).

Each Malpighian tubule of *Pieris canidia* could be conveniently divided into four regions based on external appearance. Only the yellow region was reported in this study.

After opening the body cavity of the larvae, the purified toxin or control solution was applied. For serosal treatment, microliter quantities of toxin or control CAPS buffer were added to 10 ml dissecting phosphate buffer. The final concentration of toxin was 0.001 μg/ml. For mucosal treatment, the toxin solution or control CAPS buffer were injected into the yellow region lumen with a micropipette. The injected solution containing 2% neutral red for indicating the solution passed through the tubule lumen completely. The concentration of toxin for mucosal treatment was 0.00001 μg/ml. The treatment times for both mucosal and serosal treatments were 1 minute (stage 1), 10 minutes (stage 2) and 20 minutes (stage 3) respectively.

After different treatment intervals, the tissues were fixed in 2.5% glutaradehyde in 0.2 M phosphate buffer (with sucrose added) and were postfixed in 1% osmium tetroxide. Tissues were dehydrated in alcohol series and were finally embedded in Spurr resin. Sections were stained with uranyl acetate and lead citrate and were observed under a JEOL JEM-CXII electron microscope.

For light microscope studies, thick sections of 1 μm thickness were also cut. They were stained in 1% toluidine blue in 1% borax for observation.

Results

Mucosal treatment of Malpighian tubules with control buffer

The principal cells of yellow region injected with control CAPS buffer, possessed structural features similar to those for normal yellow region principal cells (Fig. 41). The brush border consisted of microvilli having mitochondria extending to the tips of them. The ground cytoplasm, had scattered rough endoplasmic reticula, Golgi apparatus, vacuoles and mitochondria. Occasionally, there were cytoplasmic spaces in the cytoplasm. Well-organized basal infoldings containing mitochondria extended halfway toward the apical region.

Mucosal treatment of Malpighian tubules with δ-endotoxin

For mucosal treatment method, the toxin concentration used was 0.00001 μg/ml and was constant for various stages in treatment. The treatment times were 1 minute, 10 minutes and 20 minutes respectively. When treatment time was short, there were less damages seen. With the increase of treatment time, cytological changes became more serious. Finally, the principal cells exhibited gross structural damage. So the manifestation of toxic effects depended on the toxin treatment time and dosage of toxin. From the observation of many sections in different stages, the experimental results could be summarized as follows:

Stage 1. The basic structure of treated principal cell had small difference from those of control cell (Fig. 42). The fine structural alterations included that microvilli became slightly disorganized (Fig. 43). Many cytoplasmic spaces formed in basal region and central cytoplasm. The rough endoplasmic reticula appeared normal and mitochondria had no abnormalities and were evenly distributed throughout the cell (Fig. 44). The chromatin materials of nucleus became dispersed (Fig. 45). Intercellular tight cell junctional membranes remained closely apposed (Fig. 44). The basal infoldings were little affected by the toxin.

Stage 2. Cytological changes were more obvious (Fig. 46). These changes were: microvilli appeared distorted and showed blebbing and some of them appeared damaged (Fig. 47). The cytoplasmic spaces enlarged continuously. Most of the mitochondria had condensed and the intracristal spaces were irregularly enlarged. The basal infoldings became disorganized. The apical membrane was lysed occasionally (Fig. 48).

Stage 3. General disintegration of the principal cell had clearly begun in this stage (Fig. 49). Microvilli were completely damaged and the apical membrane lysed. Cytoplasmic materials including some organelles extruded into the tubule lumen (Fig. 50). The cytoplasm was less electron dense than control cell. The compartments formed by basal infoldings of the cell membrane deformed and had a vacuole-like configuration. The rough endoplasmic reticula and Golgi apparatus vacuolated (Fig. 51). The mitochondria were completely swollen and almost round in shape. The basement membrane had been eroded to some extent (Fig. 52). The intercellular septate junctional membranes appeared to be pulled apart. But the tight cell junction appeared normal (Fig. 53). Some multivesicular bodies could also be found in the cytoplasm (Fig. 54).

Serosal treatment of Malpighian tubules with control buffer

The control principal cell also have a similar structure to the normal yellow region principal cell (Fig. 55).

Serosal treatment of Malpighian tubules with δ-endotoxin

Stage 1. The basic structure had small difference from the control cell (Fig. 56). The ultrastructural changes were: the cytoplasm vacuolation appeared (Fig.

57) and the basal infoldings became slightly disorganized (Figs. 58). However, the microvilli appeared normal. The rough endoplasmic reticulum vacuolated and mitochondria appeared normal. The tight cell junction was not affected by the toxin.

Stage 2. The basal infoldings became disorganized significantly. Some of the mitochondria were condensed and some had their cristae damaged (Figs. 59). Some of the microvilli became disorganized (Fig. 60). Some mitochondria in the central cytoplasm also appeared normal (Fig. 61). The nucleus became enlarged and the chromatin materials dispersed (Fig. 62). Numerous vesicles and cytoplasmic spaces were also found in the ground cytoplasm.

Stage 3. Most of the cytological changes were similar to those of mucosal treatment stage 3 (Fig. 63). The nucleus together with other cytoplasmic materials were extruded into the lumen (Fig. 64). But in the central cytoplasm, the multivesicular bodies could be seen. Some sort of dense bodies, containing minerals also were found. The rough endoplasmic reticula were lysed (Fig. 65). Myelin figures were seen in the cytoplasm (Fig. 66). The nucleus was swollen and there were more nuclear pores formed in the nuclear membrane than those in the healthy cell (Fig. 67). Occasionally, the principal cells were detached from the basal lamina.

Discussion

In the present study, the histopathological effects of *Bacillus thuringiensis* var. *kurstaki* δ-endotoxin were examined. The experimental results indicated that the action of parasporal crystal δ-endotoxin on the cells of Malpighian tubules was rapid. At 1 minute after mucosal and serosal toxin treatments, there were cytological alterations observed. The cytoplasmic spaces enlarged. Although some

organelles in the cytoplasm were not affected obviously in stage 1, the microvilli became disorganized firstly for mucosal treatment and the basal infoldings became disorganized firstly for serosal treatment. The mucosal and serosal treatments had different patterns of membrane disorganization, with those membranes closest to the site of toxin application being disrupted first. This phenomenon also observed by Reisner *et al.* (1989) in the skipper larva, *Calpodes ethlius*. With the passage of time, the microvilli appeared distorted and swollen. Finally, they disappeared from the apical surface. The mitochondria became condensed and the rough endoplasmic reticulum dilated. The basal infoldings also became disorganized.

Reisner *et al.* (1989) studied the histopathological effects of *Bacillus thuringiensis* var. *kurstaki* δ-endotoxin on the Malpighian tubule cells of *Calpodes ethlius*. They reported that the treatment time was constant (1 hour) for both mucosal and serosal exposures, but toxin dosages varied from low concentration 1.6 μg/ml to high concentration 314 μg/ml in different stages. The treatment method used by Reisner *et al* was different from the method used in this work. They reported that after 1 hour exposured to the toxin, the principal cell exhibited variable cytopathological changes with a progression of severity from low to high toxin concentration. Stage 1. changes involved enlargement of spaces in the cytoplasm and basal infolds. But in *Pieris canidia* stage 1 , the microvilli became slightly disorganized for mucosal treatment and the basal infoldings became slightly disorganized for serosal treatment. Stage 2. For *Calpodes*, alterations included microvilli disorganization for mucosal exposure and basal infoldings became disorganized for serosal exposure. Microvilli lysed. But in *Pieris canidia*, some microvilli lysed and some were less affected. Similar results were also reported by Lane *et al.* (1989) in silkworm midgut cells. They reported that the Golgi apparatus vacuolated after toxin intoxication. The dense

bodies and multivesicular bodies were observed in the central cytoplasm. The tight cell junction appeared to be unaffected by toxin. The Malpighian tubule principal cells of *Calpodes* were affected by toxin at concentration of 1.6 μg/ml for 1 hour. But the Malpighian tubule principal cells of *Pieris canidia* were affected by toxin at a low concentration of 0.00001 μg/ml for 1 minute. The midgut epithelial cells of *Pieris canidia* larva were affected by the toxin after 20 minutes treatment (Cheung *et al.*, 1990). The midgut cells of silkworm were affected by the toxin as soon as 1 minute after treatment (Percy and Fast, 1983) whereas Lane *et al.* (1989) showed that fine structural alterations of midgut were observed only 1-5 minutes of exposure to the toxin. Therefore, the sensitivities of the same organ in different species and different organs in the same species to toxin might be different.

The manifestation of toxin effects is variable, depending on dose of toxin, developmental stage (Endo and Nishitsutsuji-Uwo, 1980) and toxin treatment time.

The observed morphological changes also reported on midgut epithelial cells after *Bacillus thuringiensis* infection. A closely related study was done on the midgut of *Pieris canidia* by Cheung *et al.* 1990. They reported that the midgut microvilli, mitochondria, and endoplasmic reticulum were the primary targets of damage after the bacteria had penetrated the peritrophic membrane. A columnar cell had the apical cytoplasm bulging, with some of the microvilli being destroyed. More vacuoles than in the control midgut were seen. The nucleus became irregular in shape after 20 minutes of toxin treatment. There was extensive vacuolation and excretion of cellular contents. Numerous germinating bacterial cells were seen inside columnar cells in two hours post-treatment. The goblet cells, however, appeared to be less affected. After five hours of bacterial infection, the midgut epithelium was of severe damage and became lysed. The

mixing up of haemolymph and midgut contents would lead to the death of the insect larva.

In other species, an earlier report was done on *Bombyx mori* by Heimpel and Angus (1959). The histopathological changes were a general separation of the midgut epithelial cells from each other and from the basement membrane. Some cells were sloughed into the lumen of the alimentary tract and possessed ruptured plasma membrane and a high degree of vacuolation. The latter was also observed in the present work in stage 3.

Endo and Nishiitsutsuji-Uwo (1980) reported that shortly after the ingestion of the toxin by silkworm, the deep infoldings of the basal cell membrane of some columnar cells became very irregular in shape. Most mitochondria were transformed into a condensed form and the endoplasmic reticulum assumed a vacuole-like configuration. The cytoplasm of the goblet cells became very electron dense and granular.

Percy and Fast (1983) described the ultrastructural changes of silkworm *Bombyx mori* within 1 minute after toxin ingestion. Microvilli became less constantly uniform in diameter; their organized internal microfilments were disrupted and disappeared. The cristae of rough endoplasmic reticulum were enlarged and denuded of ribosomes. By 4 minutes after ingestion, the number of microvilli had considerably decreased. The microvilli were replaced by small bulbous eversions. For *Pieris canidia* principal cells, after 1 minute treatment of toxin (mucosal), the microvilli became slightly disorganized. With the increase of toxin treatment time, microvilli became blebbing and finally disappeared completely. No bulbous eversions were found. For silkworm, by 5 minutes after ingestion of *Bacillus thuringiensis* crystal toxin, gross ultrastructural changes were observed in silkworm midgut cells (Percy and Fast, 1983). Mitochondria were swollen but did not exhibit the condensed configuration as shown in *Pieris*

canidia in stage 3.

The midgut epithelium of tobacco hornworm *Manduca* examined after only 1-5 minutes of exposure to the toxin already revealed fine structural alterations (Lane *et al.*, 1989). Vacuoles associated with Golgi bodies' maturing face became enlarged. This effect was intensified with more-extensive exposure to the toxin, resulting in an increase in both vacuoles and the number of lysosomal bodies. In this work, the number of vacuoles associated with Golgi apparatus increased and the vacuoles enlarged.

Bacillus thuringiensis δ-endotoxin caused similar histopathological alterations in insect midgut and Malpighian tubules, such as the microvilli and basal infoldings became disorganized initially. The cell organelles appeared abnormal. Finally, the microvilli disappeared and the basal infoldings were disorganized. These results demonstrated that the *Bacillus thuringiensis* δ-endotoxin affected a fluid-transporting epithelium other than the midgut. Of the many theories proposed (see introduction), the binding of δ-endotoxin to membrane receptors was the most accepted explanation.

After binding to specific plasma membrane receptors, the primary action of the δ-endotoxins may generate small pores in the plasma membrane, either directly by inserting into the membrane or indirectly by perturbing resident plasma membrane molecules. The creation of these pores leads to the phenomenon of colloid osmotic lysis i.e. equilibration of ions through the pores results in a net influx of ions, an accompanying inflow of water, cell swelling and eventual lysis (Ellar *et al.*, 1986). From the present results, the microvilli became disorganized in stage 1. In this time, δ-endotoxin might be bound to the specific membrane receptors. When some of the microvilli lysed in stage 2, this resulted in forming small pores in the membrane. Then cellular organelles in the cytoplasm were affected. The Malpighian tubule cells swelled and eventually lysed

(Ellar *et al.*, 1986). So *Bacillus thuringiensis* δ-endotoxin could act by forming pores in cell membranes rather than by poisoning histospecific membrane proteins (Reisner *et al.*, 1989).

Part VII. The fine structure of a Microsporidian *Nosema polyvora* from the cabbage white *Pieris canidia*

Summary

The ultrastructure of *Nosema polyvora* in *Pieris canidia* was studied by electron microscopy. The presporal stages included trophozoite and sporoblast had been described. The trophozoite, seen as a small plasmodium, possessed a pair of closely appressed nuclei-diplokaryon and a unit membrane of normal type. The sporont formed two sporoblasts. The sporoblast also had one layer of cell membrane and recognized by the developing polar filament. The fine structure of mature spore was complex. The spore wall was 66 nm thick. It was composed of three layers: exospore wall, endospore wall and plasma membrane. The exospore wall consisted of three sublayers. The polaroplast consisted of two morphologically different regions: a lamellar region, consisted of laminated membranes, was in the former; a vesicular region, consisted of loosely flattened sacs, was in the latter. The polar filament had 11 polar coils and the angle of tilt of the polar filament coils to the long axis of the spore was about 10^0-15°. Two nuclei were surrounded by endoplasmic reticulum, located in the posterior part of the spore. The posterior vacuole, enclosed by double or more membranes, occurred near the posterior pole of the spore. The results of this study might provide some useful information for classification and identification of the Microsporidia.

Introduction

The pathogenic protozoa species associated with insects are found in all of major protozoa subgroups. However, the majority of the described species of entomophilic protozoa are in the order Microsporidia and it has been estimated that most insect species have at least one microsporidium as a pathogen (Weiser, 1976).

A number of authors had suggested that *Nosema* sp. held potential as a biological control agent for long-term suppression of pest (Ewen and Mukerji, 1980), as well as sublethal effects such as reduction in feeding and growth as a result of infection (Johnson and Pavlikora, 1986). For every new species, the identification of species name is very important. In the past year, the turns and the coiling tilt of the polar filament of the spore generally served as important criteria for classification and identification (Sato *et al.*, 1982). Because appearance of polar filament in different sections and different developmental stages varied, these features were not suitable as criteria in taxonomy (Hsu *et al.*, 1991). The revision of the Thelohania-like Microsporidia by Hazard and Oldacre (1975) was a milestone in microsporidiology. For the first time ultrastructural characteristics were used more extensively for taxonomic purposes (Larsson, 1990).

The fine structures of microsporidian species have been studied by many authors (Liu and EcEwen, 1977; Gorske and Maddox, 1978; Sato *et al.*, 1982; Avery and Anthony, 1983; Kline *et al.*, 1985; Larsson, 1989; Larsson, 1990; Hsu *et al.*, 1991; Iwano and Ishihara, 1991). However, the fine structure of *Nosema polyvora* has not been examined (Blunck, 1954). In this chapter, the ultrastructure of *Nosema polyvora in vivo* from the presporal stages to mature spore stage will be described. The differences and similarities for different species also have been discussed here. The results of this study might provide some new information for classification and identification of the Microsporidia.

Materials and methods

Adults of the small cabbage white *Pieris canidia* larvae were collected from Chek Nai Ping in May of 1991 for laboratory rearing. Because the weather of Hong Kong in May was very warm, it was easy for protozoa infection. Larvae were reared in an insectary on potted *Brassica parachinenisis* at 23±1°C with L/D=14/10 photoperiod. Fourth instar larvae were used for dissection. Four regions of Malpighian tubule, namely rectal lead, iliac plexus, yellow region and white region were dissected out from the body cavity in 0.2M phosphate buffer (with sucrose added), fixed in 2.5% glutaradehyde in 0.2M phosphate buffer and postfixed in 1% osmium tetroxide. Tissues were dehydrated in alcohol series and were finally embedded in Spurr resin. Sections were stained with uranyl acetate and lead citrate and were observed under a Zeiss EM 9S-2 or JEOL-CXII electron microscope. The observations on the Malpighian tubule cellular structure of these larvae proved that they were infected by *Nosema polyvora* (Blunck, 1954). So *Pieris canidia* were infected by protozoa naturally. The infected larvae were used for ultrastructural studies.

Results

Presporal stages

Trophozoite stage: The merogonial stage of *Nosema polyvora* was seen as a small plasmodium. The plasmodium possessed diplokaryon-a pair of closely appressed nuclei and a dividing plasmodium had 4 nuclei (Fig. 68). The cytoplasm was electron-dense with numerous free ribosomes. One layer of cell

membrane could be observed. This membrane was a unit membrane of the normal type. The membrane of the trophic stage was usually in direct contact with host cytoplasm. There were no mitochondria in the ground cytopasm.

Merogony: The plasmodium multiplied within host cells by binary fission to produce merozoites (Fig. 69). The merozoites could enter other host cells for further infection. When the merozoites matured to sporonts, the ribosomes and rough endoplasmic reticula became prominent (Fig. 70).

Sporogony: The merozoites underwent sporogony to produce numerous sporoblasts. Sporoblasts were observed to lie singly in the host cytoplasm. The sporoblast also possessed one layer of cell wall and recognized by the developing polar filament (Figs. 70, 71). With development, the cytoplasm of sporoblast became more electron-dense. The sporoblast shrank away from the host tissue due to condensation of the cytoplasm, leaving a clear electron translucent space between the sporoblast and the host tissue. Some dark granules were observed in the cytoplasm of a sporoblast (Fig. 70). Granules accumulated together to form a network structure (Figs. 71, 72, 73). It was possible that the cytoplasm condensed firstly at some site in the form of dark granules. When more and more granules were accumulated in the cytoplasm, the cytoplasm would become more electron-dense. Therefore, the cytoplasm of mature spore was denser than that of the trophozoite stages. Because different developmental stages of protozoa existed within one host cell, plasmodium, sporoblasts, immature spores and mature spores could be seen in a Malpighian tubule cell at the same time (Figs. 69, 74, 75).

The mature spore: Mature spores were variable in shape but generally pyriform,

with round ends (Fig. 76). The spore wall was fairly thick of 66nm thick. However, at the anterior pole, the thickness was less than 25nm. It consisted of three layers: the exospore wall was electron-dense layer at the outside, a median thick electron-lucent endospore and an internal plasma membrane of unit membrane construction. The endospore wall became thinner at the anterior pole. During the development of *Nosema polyvora*, the thickness of endospore wall varied and increased with spore maturation. The exospore wall was clearly divided into three sublayers: a electron-dense layer of uniform membrane at the outside of spore, a median almost translucent layer and a granular internal border to the endospore (Fig. 77, 78).

The polar filament was attached to an anchoring disc at the apex of the spore (Fig. 77). The umbrella-like polar sac was not very clear. The filament widened successively toward the anchoring disc (Figs. 76, 77). The polaroplast consisted of two morphological different regions: lamellar region and vesicular region. The lamellar region located in the anterior part of spore, was composed of laminated membranes. In longitudinal section, the whole region was in a horseshoe-like shape. These lamellar membranous structure extended toward the posterior approximately to one-third of the cytoplasm. The vesicular region was composed of loosely flattened sacs. The manubrium of polar filament passed through the lamellar region (Fig. 77). The polar filament extended toward posterior part and coiled around the cytoplasm. The polar coils were formed from the transverse section of polar filament. For *Nosema polyvora*, the polar filament had 11 coils. the angle of tilt of the polar coil to the long axis of the spore was 10°-15° (Fig. 76). The polar coil was in a concentric manner. It was composed of four parts: a central, moderately electron-dense zone; then a translucent layer; a more electron-dense layer around them; a layer of unit membrane construction at the outside of polar coil (Fig. 79).

Two nuclei were located in the posterior part of spore. At the outside of typical diplokaryon, rough endoplasmic reticula were found (Fig. 80).

The posterior vacuole, enclosed by double or more membranes, occurred near the posterior pole of the spore (Fig. 81). There were one or more posterior vacuoles in *Nosema polyvora* spores (Fig. 82). The cytoplasmic groove appeared in the cytoplasm (Fig. 76).

Discussion

The fine structure of *Nosema polyvora* has been studied. The structure of presporal stages were basically similar to that of other species in Microsporidia. For prespore stages, the trophozoite possessed one layer of cell membrane and diplokaryon. The cytoplasm was electron-dense, with ribosomes distributed in it. The sporont formed two sporoblasts. The sporoblast also had one layer cell membrane and a polar filament was developed. The disploroblastic development was common for the genus *Nosema* (Kline *et al.*, 1985). Larsson (1989) studied the ultrastructure of *Hyalinocysta expilatoria* (Microspora, Thelohaniidae). He reported that when the merozoites matured to sporonts, the membrane associated ribosomes and the endoplasmic reticulum both became more prominent. This was also observed in *Nosema polyvora*. Electron dense material, secreted externally to the plasma membrane, generated blister-like protuberances, which enlarged and became confluent, forming the envelope of the sporophorous vesicle (Larsson, 1989). This vesicle was not observed in *Nosema polyvora*. Iwano and Ishihara (1991) reported that the sporoblasts of *Nosema* spp. characterized by the presence of unstained areas either at both ends or only at the posterior end. The densely stained cytoplasm obscured the site of the nuclei. In electron microscope preparations, sporoblasts contained a network structure that was associated with

lacuna. All these structures were not found in the sporoblast of *Nosema polyvora*. For *Nosema polyvora*, some dark granules were found in the cytoplasm of sporoblast. In some sporoblast, the granules accumulated together to form network structure. This network structure was different from the network structure reported by Iwano and Ishihara (1991) and was not found in other species of Microsporidia.

The ultrastructure of spores of Microsporidia have been studied in detail by many authors (Gorske and Maddox, 1978; Sato *et al.*, 1982; Avery and Anthony, 1983; Kline *et al.*, 1985; Larsson, 1989; Larsson, 1990; Hsu *et al.*, 1991; Iwano and Ishihara, 1991). The fine structural characteristics were used more extensively for taxonomic purpose (Larsson, 1990). Generally, the spores of *Nosema* spp. are pyriform in shape. The spore wall is fairly thick and composed of three layers. The polar filament is attached to an anchoring disc and polar sac is formed. The polar coil is formed from the transverse section of polar filament. Two nuclei are observed in the cytoplasm. But other structures may be different for different species. The exospore wall of *Nosema polyvora* was three layers: a electron-dense layer of uniform membrane at the outside of spore, a median almost translucent layer and a granular internal border to the endospore. However, the exospore wall of *Hyalinocysta expilatoria* was five layers: an almost translucent layer; a double layer resembling a unit membrane; a prominent, highly electron-dense layer of uniform texture; and, bordering to the endospore, a diffuse granular layer. The same structure was reported in *Limnochares aquatica* by Larsson in 1990.

The coiled part of *Napamichum aequifilum* began approximately one third from the anterior pole. The six or seven 149-165 nm wide coils were packed in a single layer close to the spore wall. The angle of tilt of the anterior coil to the spore was about 40° (Larsson, 1990). In *Hyalinocysta expliatoria*, the coiled part

began at the middle of the spore, with 5-6, 245-275 nm wide, anterior coils, and 2-1, 165 nm wide, posterior coils. The angle of tilt of the anterior filament coil to the long axis of the spore was 70°-75°. The spore of *Nosema pilicornis* had 11 or 12 polar filament coils of uniform size lying in a single line along the posterior side of the spores. The polar filament was located in the extreme posterior end of spore. The polar filament had an angle of tilt of about 80° (Gorske and Maddox, 1978). The polar filament of *Nosema bombycis* had about 12 coils, with an angle of tilt of at least 49° (Sato *et al.*, 1982). The polar filament of *Nosema* sp. M11 had about 11 coils, with an angle of tilt of at least 39°. The polar filament of *Nosema* sp. M12 had about 15 coils, with an angle of tilt of at least 43°. The number of coils in the polar filament of *Pleistophora* sp. was about 8, with an angle of tilt of at least 39° (Sato *et al.*, 1982). But the polar filament of *Nosema polyvora* had 11 polar coils. The angle of tilt of the polar filament to the long axis of the spore was 10°-15 °. The coil part began at the middle of the spore.

The structure of polar coils for most Microsporidia were in the concentric layers of varying electron density. They had generally a central moderately dense zone with concentric bands, but the number of concentric layers surrounding the zone might be different. The transversely sectioned filament of *Napamichum aequifilum* revealed concentric layers of varying electron density, in the outward direction: a central, moderately dense zone suggesting longitudinal fibrils, a prominent, dense zone interrupted by a less dense area, and a surface layer resembling an approximately 5 nm thick unit membrane (Larsson, 1990). This structure of a central zone surrounded by four concentric layers was also reported in *Nosema bombycis* (Sato *et al.*, 1982). The polar coil of *Nosema polyvora* was composed of a central, moderately electron-dense zone, enveloped by a translucent layer. Then a more electron-dense layer surrounded them. A layer of unit membrane construction was located at the outside of polar coil. This

kind of structure was also reported in *Nosema* sp. M11 and *Nosema* M12 (Sato *et al.*, 1982) and *Hyalinocysta expilatoria* (Larsson, 1989).

The posterior vacuoles, enveloped by double or more membranes, were observed in *Nosema polyvora*, *Nosema bombycis* (Sato *et al.*, 1982) and *Nosema* sp. from the tobacco cutworm *Spodoptera litura* (Hsu *et al.*, 1991). For *Nosema bombycis* and *Nosema* sp. from tobacco cutworm, only one posterior vacuole was found. But for *Nosema polyvora*, one or more posterior vacuoles were found. In *Nosema bombycis*, occasionally, the posterior vacuole had vesicles along its side. These vesicles had been observed separating from the vacuole in a spore (Sato *et al.*, 1982). This kind of vesicle was not found in *Nosema polyvora* and other species of Microsporidia.

The polaroplast of *Nosema polyvora* consisted of two morphologically different regions: Lamellar region in the former and vesicular region in the latter. This same structure also was reported in *Nosema* sp. from tobacco cutworm (Hsu *et al.*, 1991). Sato (1982) reported that the polaroplast of *Nosema bombycis* had two different components, an anterior part composed of laminated membranes, which might be tightly flattened sacs, of horseshoe shape in a longitudinal section of the spore, and a posterior part made up of loosely flattened sacs of lozenge shape. But the polaroplast of *Hyalinocysta expilatoria* appeared to be uniformly lamellar. Each lamella was delimited by a unit membrane. The polaroplast surrounded the anterior part of the polar filament to the level of the anterior coil (Larsson, 1989).

A phenomenon was observed in this study and also reported in other species. The most stages of development, including sporoplasm, sporoblast, immature spore and mature spore were presented within one infected cell at the same time. At this point, after some time infection, the development of the Microsporidia was no longer synchronous (Avery and Anthony, 1983).

Based on the developmental stages of *Nosema polyvora* observed, the available information was sufficient to put this organism into the genus *Nosema* (Blunck, 1954). This evidence included (1). persistence of nuclei in diplokaryotic configuration. (2). development of two sporoblasts from each sporont (Kline *et al.*, 1985). This disporoblastic development was common for the genus *Nosema* (Gorske and Maddox, 1978).

Wilson (1974a, 1977) reported that *Nosema fumiferanae* could be transferred within a host population by transovarial transmission. In this study, the adults of *Pieris canidia* were collected from the field. The observation on the Malpighian tubules of fourth instar larvae at the ultrastructural level proved that they had been infected by *Nosema polyvora*. So the adults captured from outside had been infected by protozoa. The parasite was transovarially transmitted to the larvae of any surviving infected females. Eggs laid by infected females were usually infected. The embryos of partially developed eggs, as well as newly hatched larvae, contained spores (Gorske and Maddox, 1978).

In the past year, the criteria for classification were mainly based on the size, shape of spores, Giemsa staining and life cycle. All these work were done under the light microscope. As criteria for classification, the size and shape of spores varied in different physiological conditions, they were not suitable for classification (Hsu *et al.*, 1991). Recently, the turns and coiling tilt of the polar filament of the spore could serve as important criteria for classification and identification. Because appearance of polar filament in different sections and different developmental stages varied, they were not suitable as only criteria for classification (Hsu *et al.*, 1991). In this study, the polar filament, as shown in figure 76, had 11 polar coils and the angle of tilt of polar filament to long axis of spore was 10°-15°, but in figure 82, it had 9 polar filament coils and the angle of tilt was about 20°. Now, many authors have used the fine structure of spores as

the criteria of classification of Microsporidia (Larsson, 1989, 1990). This study was based on this point of view, which could provide some useful information for classification.

Part VIII. Histopathological effects of *Nosema polyvora* on the Malpighian tubules of *Pieris canidia* larva

Summary

Field-collected adults of the small cabbage white *Pieris canidia* were found to be infected with a microsporidium *Nosema polyvora*. Fourth instar larvae were used for studying the histopathological effects of *Nosema polyvora* on the Malpighian tubules of *Pieris canidia*. The cytological alterations included that cytoplasmic spaces enlarged firstly in the basal region and central cytoplasm after protozoan infection. Some vacuole-like structures were found in the cytoplasm. Then some sort of mucus secretions induced by the protozoa appeared. These were abnormal secretions of unknown purpose. In the central cytoplasm, mitochondria, the rough endoplasmic reticulum and Golgi apparatus appeared normal. The nuclei of Malpighian tubule cells became very irregular in shape. Mechanical damages to the host cells occurred when numerous sporoblasts and spores existed in the cytoplasm, then empty spaces were formed in the cytoplasm. The basal infoldings appeared slightly disorganized, the cristae of mitochondria were modified. Microvilli also became disorganized.

Introduction

Despite the chronic nature of the infections they cause, several species of Microsporidia offer a good potential as microbial control agents, particularly against insect pests of high economic threshold (Brooks, 1980). Since relatively few of the entomophilic protozoa are highly virulent or fast acting, they have

most often been considered to offer little potential as short-term, quick-acting microbial insecticide and to be more appropriate as agents for long term application or introduction programs (Mclaughlin, 1971)

Numerous studies on Microsporidia have been undertaken. These included the study of the fine structures of spore in different species (Liu and McEwen, 1977; Gorske and Maddox, 1978; Sato *et al.*, 1982; Avery and Anthony, 1983; Kline *et al.*, 1985; Larsson, 1989, 1990; Hsu *et al.*, 1991), life cycle (Ishihara, 1969; Kawarabata and Ishihara, 1984; Sleigh, 1989), biology (Brooks, 1980; Andreadis, 1986; Hayasaka and Kawarabata, 1990; Zhao *et al.*, 1990; Solter *et al.*, 1991).

Microsporidian infections are widespread in insects and *Nosema* spp. have been discovered in many species (Liu and McEwen, 1977). The pathological effects of Microsporidia on the insects have also been widely investigated (Malone and Wigley, 1981; Siegel *et al.*, 1986; Johnson and Pavlikova, 1986; Brooks, 1986; Onstad and Maddox, 1989; Armstrong and Bass, 1989; Solter *et al.*, 1990; Macvean and Capinera, 1991). Malone and Wigley (1981) reported that the infection of *Nosema carpocapsae* did not cause mortality but did reduce the fecundity and fertility of infected moths. *Nosema carpocapsae* was transmitted transovarially as well as horizontally. Brooks (1986) reported that *Nosema epilachnae* and *Nosema varivestis* significantly reduced the longevity and fecundity of the adults. But corn borer adults infected with *Nosema pyrausta* experienced higher mortality than uninfected larvae. Mortality was linked to the ovipositional sequence of the egg masses (Siegel *et al.*, 1986). Like most species of the entomophilic protozoa, Microsporidia generally produce chronic, sublethal infection in their hosts characterized by such symptoms as irregular growth, retarded larval development, incomplete metamorphosis, and reduced adult vigor, fecundity, and longevity (Brooks, 1974). So all these pathological studies

were mainly concerned with biological changes. The cytological alterations after the protozoa infection on their hosts have not been investigated. In order to understand the mechanism of action of *Nosema* on the target insect, the histopathological effects of *Nosema polyvora* on Malpighian tubule cell structure of *Pieris canidia* larva have been studied.

Materials and methods

Adults of small cabbage white *Pieris canidia* larvae were collected from the fruit garden (with the Chinese cabbage *Brassica parachinenisis* growing) of Chek Nai Ping in May of 1991 for laboratory rearing. Because the weather of Hong Kong in May was humid and warm, it was easy for protozoa to multiply and get their hosts infected. Larvae were reared in an insectary on potted *Brassica parachinenisis* at 23±1°C with L/D=14/10 photoperiod. Fourth instar larvae were used for dissection. Four regions of Malpighian tubule, namely rectal lead, iliac plexus, yellow region and white region were dissected out from the body cavity in 0.2M phosphate buffer (with sucrose added), fixed in 2.5% glutaradehyde in 0.2M phosphate buffer and postfixed in 1% osmium tetroxide. Tissues were dehydrated in alcohol series and were finally embedded in Spurr resin. Sections were stained with uranyl acetate and lead citrate and were observed under a Zeiss EM 9S-2 or JEOL-CXII electron microscope. The observations on the Malpighian tubule cellular structure of these larvae proved that they had been infected by *Nosema polyvora*. So *Pieris canidia* were infected by protozoa naturally. The infected larvae were used for histopathological studies.

Results

After protozoa infection, there were many cytoplasmic spaces formed in the basal region and central cytoplasm of Malpighian tubule cells (Fig. 74). Some vacuole-like structures were also found in the central cytoplasm and the basal region of the microvilli (Fig. 75). For the normal structure of the Malpighian tubule cells, extracellular spaces were found and distributed throughout the cell. But in infected cell, extracellular spaces were located mostly around the protozoa (Fig. 83). In the central cytoplasm and apical region, some sort of mucus secretions induced by the protozoa appeared (Figs. 84, 85). The morphology of these secretions was different from that of the extracellular spaces. Normally, the extracellular spaces, as extensions of the basal infoldings, were located near the basal region of the cell. But the mucus secretion distributed throughout the cell. The trophozoite stage of *Nosema polyvora* was seen as a small plasmodium. The plasmodium proliferated inside the cytoplasm of the Malpighian tubule cells (Fig. 75). With development, the sporoblast and spore shank away from the host cytoplasm, leaving a clear electron translucent space between the protozoan and the host tissue (Figs. 70, 86). The plasmodium divided by binary fission to produce numerous merozoites or sporoblasts which developed into spores (Fig. 69). When most of the cytoplasm was occupied by the sporoblasts and spores, mechanical damages to the host cells occurred, then empty spaces were formed in the cytoplasm (Fig. 87). After infection for generations, different developmental stages of *Nosema*, including trophozoite, sporoblast and mature spore, were found within one cell at the same time (Figs. 74, 75). As a result, less organelles such as mitochondria were found in the central cytoplasm of infected cell than that of normal Malpighian tubule cell (Fig. 86). Upon heavy infection by protozoa, the basal intracellular channels enlarged continually and appeared slightly disorganised (Fig. 68). The apical microvilli became loose and

some part of them became detached from the apical border (Fig. 88). The cristae of mitochondria in the basal infoldings were modified (Fig. 89). In the central cytoplasm, the rough endoplasmic reticula were found to be disorganised. The nuclei of Malpighian tubule cells became very irregular in outline (Fig. 90). Much cytoplasmic spaces were formed in the cytoplasm. Eventually, cell eruption was observed.

Discussion

The histopathological effects of *Nosema polyvora* on the Malpighian tubule cell of *Pieris canidia* was studied. The results showed that *Nosema polyvora* and *Bacillus thuringiensis*, both as biological control agents, cause some comparable yet different histopathological effects. After protozoa infection, many cytoplasmic spaces were formed in the basal region and central cytoplasm. In the central cytoplasm, the rough endoplasmic reticulum and Golgi apparatus were also found and they were not damaged by the protozoa. The microvilli also became disorganized. The tight cell junction was not damaged by protozoa. All these results were similar to that of *Bacillus thuringiensis* var. *kurstaki* treatment at stage 1. After the Malpighian tubule was treated with *Bacillus thuringiensis* mucosally or serosally, the cytological alterations included the cytoplasmic spaces enlarged, the rough endoplasmic reticulum appeared normal and the mitochondria had no abnormalities and were evenly distributed throughout the cell. The tight cell junction was not damaged by the toxin. But for *Bacillus thuringiensis* treatment at stage 1, the microvilli became slightly disorganized and the basal infoldings were little affected for mucosal treatment. The basal infoldings became slightly disorganized and the microvilli appeared normal for serosal treatment. The chromatin of nucleus became dispersed after *Bacillus*

thuringiensis treatment. This result was not observed for protozoa infection. The nuclei of Malpighian tubule cell became very irregular in shape. The mechanical damages to the host cells occurred, then empty spaces were formed in the cytoplasm when numerous sporoblasts and spore existed in the cytoplasm of host cells. This was not found for *Bacillus thuringiensis* treatment. After protozoa infection, some sort of mucus secretion induced by protozoa appeared. This was not found in the *Bacillus thuringiensis* treatment. So the ultrastructural changes after *Nosema polyvora* infection and *Bacillus thuringiensis* treatment at stage 1 were basically similar. However, when treatment time of *Bacillus thuringiensis* was increased, more serious damages were caused in Malpighian tubule cells. For example, at stage 2, the microvilli appeared distorted. The basal infoldings became disorganized. Most of the mitochondria condensed. At stage 3, the general disintegration of the principal cell had clearly began. The microvilli were completely disappeared and apical membrane lysed. Cytoplasmic materials including some organelles extruded into the tubule lumen. The basal infoldings were damaged. All these did not happen for protozoa infection. Protozoans generally produce chronic rather than acute diseases and , therefore, as control agents do not create as dramatic results as do some of viruses and bacteria (Wilson, 1982). Microsporidia generally invade the muscle, intestinal epithelium, lymphocytes and adipose tissue of invertebrates, especially insects (Sleigh, 1989). The Microsporidia were known to deplete the nutritive reserves normally used for reproduction, reducing fecundity (Smirnoff and Chu, 1968), fertility (Tanabe and Tamashiro, 1967), longevity (Gaugler and Brooks, 1975), and mating success (Gaugler and Brooks, 1975).

In the primary stage of protozoa infection, the Malpighian tubule cell of *Pieris canidia* produced some sort of mucus secretions of unknown function. In other species, different cell defense mechanisms were found. Ratcliff and Rowley

(1987) reported that the cellular defense reactions of insects to microbial invaders consist primarily of phagocytosis of small numbers of such particles, while nodule (granuloma) formation deals with larger particulate insults. Grace (1962) demonstrated the development of a cytoplasmic polyhedrosis in cultured *Antheraea eucalypti* cells following *in vitro* phagocytosis of the polyhedra. He filmed the elimination of dead cells by phagocytosis in Lepidopteran cell culture. The bactericidal capacity of the cockroach *Blaberus craniifer* was assayed by Anderson *et al.* in 1973. Hemocytes, maintained in short term culture, were capable of phagocytizing and destroying 5 species of bacteria. Rahmet-Alla and Rowley (1989) reported that nodules were formed in the Mederia cockroach, *Leucophaea maderae*, in response to injections of low doses of three strains of bacteria. Histologically, the nodules formed in response to all bacterial species employed were similar, with a central necrotic core enclosing cell debris and occasional bacteria, and an outer, thin sheath of plasmatocyte-like hemocytes.

Schwemmler and Muller (1986) reported that the invading of bacteria on the leafhopper *Euscelidius* could be digested by enzymes contained in lysosomes. This reaction was also observed by Cheung and Purcell (1993) in the leafhopper *Euscelidius variegatus*. They reported that there were a large numbers of lysosomes produced at the apical cytoplasm of epithelium cells to surround the proliferating bacteria. In fact, BEV bacteria under various stages of digestion by lysozymes were seen, with the remains of the final digested products appearing as membranous whorls.

The epithelium cells of *Euscelidius variegatus* that were fully occupied by bacteria could be shed to the gut lumen by an eruption process. These bacteria might be passed out of the insect body together with its excrement. The reduced longevity of *E. variegatus* infected by BEV might be due in part to diminished gut function caused by degeneration of midgut cells occupied by bacteria in

phagosomes or in the cell cytoplasm (Purcell and Suslow, 1987).

In this study, the adults of *Pieris canidia* were collected from outside field in summer of 1992. The larvae reproduced by the adults appeared normal, no distinct external characteristics proved larvae infected by protozoa. The observations on the Malpighian tubule cellular structure of these larvae proved that they have been infected by *Nosema polyvora*. Eggs laid by infected females were usually infected. The embryos of partially developed eggs, as well as newly hatched larvae, contained spores (Gorske and Maddox, 1978). Larsson (1990) also found this phenomenon in the aquatic mite *Limnochares aquatica* after microsporidium *Napamichum aequifilum* infection. He reported that there were no external signs of infection. The mite appeared to be healthy. The microsporidium was detected when the mite was routinely squashed on a microscope slide. *Nosema locustae* did not produce detectable infections in Mormon crickets in any stage of development (Macvean and Capinera, 1991). So the adults of *Pieris canidia* were infected by protozoa naturally. When further infection caused, the cytoplasmic spaces enlarged firstly, then cytoplasmic secretion induced by protozoa appeared. Nuclei of cells became irregular in shape and finally microvilli became disorganized. All these cytological alterations would result in loss of functions of digestive and excretory systems. Histopathological effects of *Nosema polyvora* on the Malpighian tubule cells of *Pieris canidia* also showed that the target of *Nosema* was gut epithelium or Malpighian tubule cells.

There is increasing evidence to indicate the promise of entomophilic protozoa as microbial control agent. Because less works have been done on the histopathological effects of protozoa on host tissue, further research is needed on the mode of entry of the parasite into the intestinal cells and mode of action of microbial insecticide.

Part IX. General discussion

In the majority of insects the excretory system consists of a number of Malpighian tubules. The main role of the Malpighian tubules in excretion is to deliver to the hindgut a flow containing many of the haemolymph constituents at concentrations in proportion to their concentrations in the haemolymph. The hindgut reabsorbs those constituents required by the insect and reject the others. In this way the composition and volume of the haemolymph is kept relatively constant or is adjusted to meet the needs of the insect (Maddrell, 1977).

This study has shown that *Bacillus thuringiensis* and *Nosema polyvora* affect insect Malpighian tubules by inducing cytological alterations. Their modes of action, however, differ greatly. The histopathological effects of *Bacillus thuringiensis* δ-endotoxin on Malpighian tubules of *Pieris canidia* were observed after 1 minute post-treatment. The Malpighian tubule cells of *Calpodes* exhibited variable cytological changes after 1 hour exposure to the toxin (Reisner *et al.*, 1989). There were some caterpillars' midgut epithelia which showed immediate response to *Bacillus thuringiensis* treatment. The midgut cells of silkworm were affected by the toxin as soon as 1 minute after toxin treatment (Percy and Fast, 1983). Similarly, Lane *et al.* (1989) reported that fine structural alterations of midgut of *Manduca* were observed 1-5 minutes of exposure to the toxin. The midgut epithelial cells of *Pieris canidia* larvae were affected by toxin after 20 minutes exposure (Cheung *et al.*, 1990). Thus there exists variations in the response of the host to toxin action.

From all these histopathological descriptions, the *Bacillus thuringiensis* δ-endotoxin causes comparable cytological changes in insect midgut and Malpighian tubules. So the *Bacillus thuringiensis* δ-endotoxin affects a fluid-

transporting epithelium other than the midgut (Reisner *et al.*, 1989).

In order to explain the mode of action of δ-endotoxin, several hypotheses have been proposed by different authors (Travers *et al.*, 1976; Nishiitsutsuji and Endo, 1979; Gupta *et al.*, 1985; Himeno *et al.*, 1985; Knowles and Ellar, 1987). Since the present results showed that both the apical microvilli and the basal infoldings were much eroded after *Bacillus thuringiensis kurstaki* δ-endotoxin treatment, the most likely mode of action of the toxin would be its binding to specific membrane areas or receptors on cell membranes. This would create lytic pores that would lead to osmotic lysis of cellular contents. Further research is needed on the isolation of this receptor from the Malpighian tubules epithelium of *Pieris canidia*, and the structure of the receptor can be analyzed by biochemical methods. All these works will be helpful for understanding the mode of action of *Bacillus thuringiensis* δ-endotoxin.

Some authors used the spores and crystals mixture to determine the toxicity of *Bacillus thuringiensis* (Mohd-Sallen and Lewis, 1982; Moar *et al.*, 1989). But most authors used the purified crystals to study the toxicity of *Bacillus thuringiensis* toxin (Ellar *et al.*, 1986, 1987; Reisner *et al.*, 1989; Rie *et al.*, 1990) because the insecticidal activity was due to the activated toxin (Angus, 1956; Lacadet, 1970; Kurstak and Tijssen, 1982; Aronson *et al.*, 1986).

Many techniques have been used in the separation of parasporal crystals from the spores (Ibarra and Federici, 1956; Church and Halvorson, 1959; Gingrich, 1968; Fast, 1972; Sharpe *et al.*, 1975; Milne *et al.*, 1977; Bulla *et al.*, 1979; Yamamoto and Mclaughlin, 1981; Bulla *et al.*, 1981; Mahillon and Delcour, 1984; Moar *et al.*, 1989). By reason of low yield of purified crystals, activity loss of toxin and too complex of techniques for other purification methods, the method using urografine as a separation medium for purification of parasporal crystals have been used by more and more people. The method used

in this study is simple, rapid and gives high purity of crystals.

Recently, the fine structure of protozoa was used as a classification criterion (Hazard and Oldacre, 1975), so many works have been done especially on microsporidian protozoa. For different species, the general structures are similar, for example, the spore consists of spore wall, polaroplast and polar filament. There are endoplasmic reticulum and diplokaryon in the cytoplasm. However, some detailed structures are different in different species, such as the number and structure of polar coils and the angle of tilt of the polar coils to the spore may be different in different species. There are 11 polar coils for *Nosema polyvora*, and the angle of tilt of the polar filament to long axis of the spore was 10°-15°. The spore of *Nosema pillicornis* had 11 or 12 polar coils of uniform size. The polar filament had an angle of tilt of about 80° (Gorske and Maddox, 1978). The polar filament of *Nosema bombycis* had about 12 coils, with an angle of tilt of at least 49° (Sato *et al.*, 1982). The arrangement of polar coils for most microsporidian were in a concentric manner of varying electron density. But the number and structure of concentric layers surrounding the zone might be different in different species. There are three layers for *Nosema polyvora*, but four layers for *Napamichum aequifilum* (Larsson, 1990) and *Nosema bombycis* (Sato *et al.*, 1982). All these structural differentiation was used for classification of protozoa.

Although numerous studies on microsporidian have been undertaken (Ishihara, 1969; Liu and McEwen, 1977; Avery and Anthony, 1983; Kawarabata and Isihara, 1984; Hayasaka and Kawarabata, 1990), the histopathological effects of protozoa on insects have not been reported yet. This study shows that the protozoa can also infect the insect by causing damages to epithelial cells. They cause different histopathological effects to Malpighian tubules cells with those caused by *Bacillus thuringiensis*. However, the infection to insect is normally so

light that it cann't be detected by external features.

During evolution, insects have developed some defense reactions by which they defend themselves against other pathogens (Gotz and Boman, 1985). For examples, phagocytosis, nodule formation, cellular and humoral encapsulation. The cellular defense mechanisms of insects to microbial invaders consist primarily of phagocytosis of small number of such particles, while nodule formation deals with larger particulate insults (Ratcliff and Rowley, 1987). The cellular encapsulation is a reaction of haemocytes to living or non-living foreign objects, which leads to a multicellular envelope surrounding this object (Gotz and Boman, 1985). Humoral encapsulation is an unusual type of defense reaction to foreign material. The deposition of minute particles of pigmented material results in a continuous layer that completely enclosing the foreign material. Following this deposition, haemocytes are accumulated (Gotz and Boman, 1985). However, in this study, some sort of mucus secretions were found in the Malpighian tubule cells of *Pieris canidia* after protozoa infection. These secretions were probably for cell defense.

Spores of some protozoa have been extracted from their host by centrifugation techniques (Wilson, 1982). The spore of *Nosema polyvora* have not been extracted from the insect tissue, because the Malpighian tubules of *Pieris canidia* used in this histopathological study were infected by *Nosema polyvora* naturally. Further research is needed on the extraction of *Nosema polyvora* spores from infected Malpighian tubules or midgut of *Pieris canidia*. The extracted spores can be used for biological study of *Nosema polyvora* or other purposes.

Part X. Conclusion and Summary

The histopathological effects of *Bacillus thuringiensis* and *Nosema polyvora* on *Pieris canidia* larva have been investigated. The damages caused by *Bacillus thuringiensis* infection were fast and serious because the cytological alterations were observed after 1 minute post-treatment. The principal cells exhibited variable cytopathological changes with a progression of severity from short time to long time toxin treatments. However, mucosal and serosal exposures had different patterns of membrane disorganization, with those membranes closest to the site of application being disrupted first. In stage 1, there were numerous vacuoles in the ground cytoplasm and the cytoplasmic spaces enlarged. The mitochondria did not show notable damage. The nucleus had chromatin materials dispersed and the rough endoplasmic reticulum got swollen. The microvilli became slightly disorganized for mucosal treatment and the basal infoldings became slightly irregular in shape for serosal treatment. In stage 2, the cristae of mitochondria had been seriously damaged. The cytoplasmic spaces enlarged continually. The mucosal exposure of principal cells showed extensive microvilli damage and there was extrusion of apical cytoplasm. Serosal treatment of the cells had the basal membranous channels become disorganized resulting in large vacuoles in the ground cytoplasm. In stage 3, general disintegration of cells was observed. The apical microvilli were completely damaged. All the mitochondria had their cristae impaired and they became very much swollen. The cytoplasm had vacuolated to such an extent that no visible rough endoplasmic reticulum could be recognized. The basal infoldings were also disorganized and the basal lamina was damaged. So the Malpighian tubule epithelium was of severe damage and became lysed. The mixing up of heamolymph and Malpighian tubule

contents would lead to ionic imbalance, eventually death of the insect larvae.

Comparing with infection caused by *Bacillus thuringiensis*, the infection caused by protozoa was chronic and light. After protozoa infection, the cytoplasmic spaces enlarged in basal region and central cytoplasm. Some vacuole-like structures were found in the cytoplasm. Then some sort of mucus secretions induced by the protozoa appeared. These secretions were probably for cell defense. This reaction was not observed in the *Bacillus thuringiensis*-treated Malpighian tubules. But the cell organelles such as mitochondria, rough endoplasmic reticula and golgi apparatus did not appear abnormal except the nucleus became very irregular in shape. The basal infoldings and apical microvilli also became slightly disorganized, but they did not lyse.

Results of the present study indicate the promise of *Bacillus thuringiensis* and *Nosema polyvora* as good biological control agents for Lepidopterous larvae even though the action of protozoa is chronic and the creation of an epizootic is slow.

References

Adang, M. J. 1991. *Bacillus thuringiensis* insecticidal crystal proteins: Gene structure, action, and utilization. In " Biotechnology for biological control of pests and vectors" (Maramorosch, K. Ed.), pp.3-24. CRC Press, Boston and London.

Albertsson, P. A. 1960. Partition of cell particles and macromolecules. Wiley, New York.

Anderson, R. S., B. Holmes and R. A. Good. 1973. In vitro bactericidal capacity of *Blaberus craniifer* hemocytes. J. Invert. Pathol. 22: 127-135.

Andreadis, T. G. 1986. Dissemination of *Nosema pyrausta* in feral populations of the European corn borer, *Ostrinia nubilalis*. J. Invert. Pathol. 48: 335-343.

Ang, B. J. and K. W. Nickerson. 1978. Purification of the protein crystal from the *Bacillus thuringiensis* by zonal gradient centrifugation. Appl. Environ. Microbiol. 36: 625-626.

Angus, T. A. 1953. Studies of *Bacillus* spp. pathogenic for silkworm, Progress Report, Forest Biology Division, Canada Department of Science and Service. 9: 6.

Angus, T. A. 1956. Extraction, purification and properties of *Bacillus scotto* toxin. Can. J. Microbiol. 2: 122-131.

Angus, T. A. 1959. Separation of bacterial spores and parasporal bodies with a fluorocarbon. J. Invert. Pathol. 1: 97-98.

Aoki, K. and Y. Chegasaki. 1915. Uber die pathogenitat der sog. *Sotto Bacillen* (Ishiwata) bei seiden rauven. Mitt. Med. Fak. Kais. 13: 419.

Armstrong, E. and L. Bass. 1989. Effects of *Nosema kingi* on the development and weight of adult *Drosophila melanogaster* (OR-R-Strain). J. Invert. Pathol. 53: 102-106.

Aronson, A. I., W. Beckman and P. Dunn. 1986. *Bacillus thuringiensis* and related insect pathogens. Microbiol. Rev. 50: 1-24.

Atkins, M. D. 1978. Insects in perspective. Macmillan, New York. pp. 326-328.

Avery, S. W. and D. W. Anthony. 1983. Ultrastructural study of early development of *Nosema algerae* in *Anopheles albimanus*. J. Invert. Pathol. 42: 87-95.

Barka, T. and P. J. Anderson. 1965. Histochemistry: Theory, practice, and bibliography. Harper & Row, New York.

Bateson, J. B. 1965. Isolation of the crystalline parasporal bodies of *Bacillus thuringiensis*. Nature 205: 622-623.

Bateson, J. B. and G. Stainby. 1970. Analysis of the active principle in the biological insecticide *Bacillus thuringiensis* Berliner. J. Food Technol. 5: 403.

Bechtel, D. B. and L. A. Bulla, Jr. 1976. Electron microscope study of sporulation and parasporal crystal formation in *Bacillus thuringiensis*. J. Bacteriol. 127: 1472.

Berliner, E. 1915. Uber die schlaffsucht der mehlmottenraupe (*Ephestia kuhniella* Zell.) und ihren erreger *Bacillus thuringiensis*, n. sp. Z. Angew. Entomol. 2: 29.

Berridge, M. J. 1968. Urine formation by the Malpighian tubules of *Calliphora*. I. Cations. J. Exp. Biol. 48: 159-174.

Berridge, M. J. and J. L. Oschman. 1969. A structural basis for fluid secretion by Malpighian tubules. Tissue & Cell 1: 247-272.

Blunck, H. 1954. Mikrosporidien bei *Pieris brassicae* L. ihren Parasiten und Hyperparasiten. Zeitsch. angew. Ent. 36: 316-333.

Bonhag, P. F. 1955. Histochemical studies of the ovarian nurse tissues and oocytes of the milkweed bug, *Oncopeltus fasciatus* Dallas. II. Sudanophilia, phospholipids, and cholesterol. J. Morphol. 97: 283.

Bradley, T. J. 1985. The excretory system: Structure and function. In "Insect physiology, biochemistry and pharmacology" (Kerkut, G. A. and L. I. Gilbert, Eds.). Vol. 4. pp. 421-465. Pergamon Press, Oxford.

Brooks, W. M. 1974. Protozoan infection. In "Insect Diseases" (Cantwell, G. E. Ed.), Vol. 1. pp. 237-300. Marcel Dekker, Inc. New York.

Brooks, W. M. 1980. Production and efficacy of Protozoa. Biotech. Bioengin. 110: 1415-1440.

Brooks, W. M. 1986. Comparative effects of *Nosema epilachnae* on the mexican beetle, *Epilachna varivestis*. J. Invert. Pathol. 48: 344-354.

Bulla, L. A. Jr., D. B. Bechtel, K. J. Kramer, Y. I. Shethna, A. I. Aronson and P. C. Fitz-James. 1980. Ultrastructure, physiology, and biochemistry of *Bacillus thuringiensis*. CRC Critical Reviews in Microbiol. pp. 147-204.

Bulla, L. A. Jr., L. I. Davidson, K. J. Kramer and B. L. Jones. 1979. Purification of the insecticidal toxin from the parasporal crystal of *Bacillus thuringiensis* subsp. *kurstaki*. Biochem. Biophys. Res. Commun. 91: 1123-1130.

Bulla, L. A. Jr., K. J. Kramer, D. J. Cox, B. L. Jones, L. I. Davidson and G. L. Lookhart. 1981. Purification and characterization of the entomocidal protoxin of *Bacillus thuringiensis*. J. Biol. Chem. 256: 3000-3004.

Bulla, L. A. Jr., K. J. Kramer and L. I. Davidson. 1977. Characterization of the entomocidal parasporal crystal of *Bacillus thuringiensis*. J. Bacteriol. 130: 375.

Calabrese, D. M., K. W. Nickerson and L. C. Lane. 1980. A comparison of protein crystal subunit sizes in *Bacillus thuringiensis*. Can. J. Microbiol. 26: 1006-1009.

Canning, E. U. 1982. An evaluation of protozoal characteristics in relation to

biological control of pests. Parasitology 84: 119-149.

Canning, E. H. and J. Lom. 1986. The Microsporidia of vertebrates. Academic Press, London.

Chapman, R. F. 1975. The insects, structure and function. New York: American Elsevier.

Chestukhina, G. G., I. A. Zalunin, L. I. Kostina, T. S. Kotova, S. P. Kattrukha and V. M. Stepanov. 1980. Crystal-forming proteins of *Bacillus thuringiensis*. Biochem. J. 187: 457-465.

Cheung, W. W. K. 1981. Ultrastructural and functional differentiation of the Malpighian tubules of the lantern bug, *Pyrops candelaria* Linn. (Homoptera: Fulgoridae). Cytologia 46: 241-254.

Cheung, W. W. K. and Y. F. Lam. 1993. Histochemical studies on normal and *Bacillus thuringiensis*-infected *Pieris canidia* larval midgut. Bull. Inst. Zool., Academia Sinica. 32: 12-22.

Cheung, W. W. K., Y. F. Lam and S. T. Chang. 1990. Histopathological effects of *Bacillus thuringiensis* on *Pieris canidia* larva: A transmission electron microscopic study. Acta Biol. Exp. Sinica. 23: 177-191.

Cheung, W. W. K. and A. T. Marshall. 1973a. Studies on water and ion transport in homopteran insects: Ultrastructure and cytochemistry of the cicadoid and cercopoid midgut. Tissue & Cell 5: 651-669.

Cheung, W. W. K. and A. T. Marshall. 1973b. Water and ion regulation in cicadas in relation to xylem feeding. J. Insect Physiol. 19: 1801-1816.

Cheung, W. W. K. and A. H. Purcell. 1993. Ultrastructure of the digestive system of the leafhopper *Euscelidoius variegatus* Kirshbaum (Homoptera: Cicadellidae), with and without congenital bacterial infections. Int. J. Insect Morphol. Embryol. 22: 49-61.

Church, B. D. and H. Halvorson. 1959. Dependence of the heat resistance of bacterial endospores on their dipicolinic acid content. Nature 183: 124-125.

Cooksey, K. E., C. Donninger, J. R. Norris and D. Shankland. 1969. Nerve-blocking effect of *Bacillus thuringiensis* protein toxin. J. Invert. Pathol. 13: 461-462.

Couch, T. L. and D. A. Ross. 1980. Production and utilization of *Bacillus thuringiensis*. Biotech. Bioeng. 112: 1297-1304.

Crowder, L. A. and D. L. Shankland. 1972. Structure of the Malpighian tubule muscle of the American cockroach *Periplaneta americana*. Ann. Entomol. Soc. Am. 65: 614-619.

DeLello, E., W. K. Hanton, S. T. Bishoff and D. W. Misch. 1984. Histopathological effects of *Bacillus thuringiensis* on the midgut of tobacco hornworm larvae (*Manduca sexta*): low doses compared with fasting. J. Invert. Pathol. 43: 169-181.

Donovan, W. P., C. C. Dankocsik, M. P. Gilbert and M. C. Gawron-Burke. 1988. Amino acid sequence and entomocidal activity of the P2 crystal protein. J. Biol. Chem. 263: 561-567.

Ebersold, H. R., P. Luthy, P. Geiser and L. Ettlinger. 1978. The action of the δ-endotoxin of *Bacillus thuringiensis*: An electron microscope study. Experientia 34: 1672.

Ebersold, H. R., P. Luthy and H. E. Huber. 1980. Membrane damaging effect of the δ-endotoxin of *Bacillus thuringiensis*. Experientia 36: 495-496.

Eichelberg, D. 1973. Elektronenmikroskopische untersuchung zur funktionsmorphologie des verdauungstraktes von *Ephydra riparia* unter besonderer berucksichtigung der Malpighisvchen gefabe und deren veranderungen unter verschiedenen aubenbedingungen sowie unter dem einflub von diuretika. Habil. Schrift. Gieben.

Eichelberg, D. and A. Wessing. 1975. Morphology of the Malpighian tubules of insect. Fortsch. Zool. 23: 124-147.

Ellar, D. J., B. H. Knowles, F. A. Drobniewski and H. Z. Haider. 1986. The insecticidal specificity and toxicity of *Bacillus thuringiensis* ?δ-endotoxin may be determined respectively by an initial binding to membrane specific receptors followed by a mechanism of cytolysis. In "Fundamental and Applied Aspects of Invertebrate Pathology". (Samson, R. A. Ed.), pp.7-10.

Endo, Y. and J. Nishiitsutsuji-Uwo. 1980. Mode of action of *Bacillus thuringiensis* δ-endotoxin: Histopathological changes in the silkworm midgut. J. Invert. Pathol. 36: 90-103.

English, L. H. and L. C. Cantley. 1985. Delta endotoxin inhibits Rb^+ uptake, lowers cytoplasmic pH and inhibits a K^+-ATPase in *Manduca sexta* CHE cells. J. Membrane Biol. 85: 199-204.

Ewen, A. B. and M. K. Mukerji. 1980. Evaluation of *Nosema locustae* (Microsporida) as a control agent of grasshopper populations in Saskatchewan. J. Invert. Pathol. 35: 295-303.

Fast, P. G. 1981. The crystal toxin of *Bacillus thuringiensis*. In "Microbial control of pests and plant diseases" (Burges, H. D. Ed.), pp. 223-248. Acdemic Press, London and New York.

Fast, P. G. and T. P. Donaghue. 1971. The δ-endotoxin of *Bacillus thuringiensis* II. On the mode of action. J. Invert. Pathol. 18: 135-138.

Fast, P. G. and I. K. Morrison. 1972. The δ-endotoxin of *Bacillus thuringiensis* IV. The effect of δ-endotoxin on ion regulation by midgut tissue of *Bombyx mori* larvae. J. Invert. Pathol. 20: 208-211.

Faust, R. M. 1968. In vitro chemical reaction of the δ-endotoxin produced by *Bacillus thuringiensis* var. *dendrolimus* with other proteins. J. Invert. Pathol. 11: 465-475.

Faust, R. M. and L. A. Bulla, Jr. 1982. Bacteria and their toxins as insecticides. In "Microbial and viral pesticides" (Kurstaki, E. Ed.), pp. 75-208. Marcel

Dekker, Inc. New York and Basel.

Fitz-James, P. C. 1953. The structure of spores as revealed by mechanical disruption. J. Bacteriol. 66: 312-319.

Fredricsson, B. 1952. A modification of the histochemical method for demonstration of alkaline phosphatase in which diffusion phenomenon is reduced. Experientia 8:139.

Gaugler, R. R. and W. M. Brooks. 1975. Sublethal effects of infection by *Nosema heliothidis* on the corn earthworm, *Heliothis zea*. J. Invert. Pathol. 26: 57-63.

Gingrich, R. E. 1968. A flotation procedure for producing spore-free crystals from commercial formations of *Bacillus thuringiensis*. J. Invert. Pathol. 10: 180-184.

Goodchild, A. J. P. 1963. Studies on the functional anatomy of the intestines of Heteroptera. Proc. Zool. Soc. Lond. 141: 851-910.

Goodman, N. S., R. J. Gotteried and M. H. Rogoff. 1967. Biophasic system for separation of spores and crystals of *Bacillus thuringiensis*. J. Bacteriol. 94: 485.

Gorske, S. F. and J. V. Maddox. 1978. A microsporidium, *Nosema pilicornis* sp. n., of the purslane sawfly, *Schizocerella pilicornis*. J. Invert. Pathol. 32: 235-243.

Gotz, P. and H. G. Boman. 1985. Insect immunity. In "Comprehensive insect physiology, biochemistry and pharmacology" (Kerkert, G. A. and L. I. Gilbert, Ed.), Vol. 3. pp. 453-485. Pergamm Press, Oxford.

Gouranton, J. 1968a. Composition, structure, et mode de formation des concretions minerals dans l' intestin moyen des Homopteres cercopides. J. Cell Biol. 2: 316-328.

Gouranton, J. 1968b. Observations histochimiques et histoenzymologiques sur mle tube digestif de quelques Homopteres cercopides et jassides. J. Insect Physiol. 14: 569-579.

Grace, T. D. C. 1962. Establishment of four strains of cells from insect tissue grown *in Vitro*. Nature. 195: 788-789.

Gringorten, J. L., D. P. Witt, R. E. Milne, P. G. Fast, S. S. Sohi and K. V. Frankenhuyzen. 1990. An in vitro system testing *Bacillus thuringiensis* toxins: The lawn assay. J. Invert. Pathol. 56: 237-242.

Gupta, B. L., J. A. T. Dow, T. A. Hall and W. R. Harvey. 1985. Electron probe X-ray microanalysis of the effects of *Bacillus thuringiensis* var. *kurstaki* crystal protein insecticide on ions in an electronic K^+-transporting epithelium of the larval midgut in the Lepidopteran, *Manduca sexta*, *in vitro*. J. Cell Sci. 74: 137-152.

Hannay, C. L. 1953. Crystalline inclusions in aerobic sporeforming bacteria. Nature 172: 1004.

Hannay, C. L. and P. Fitz-James. 1955. The protein crystal of *Bacillus thuringiensis* Berliner. Can. J. Microbiol. 1: 694-701.

Harvey, W. R., M. Cioffi, J. A. T. Dow and M. G. Wolfersberger. 1983. Potassium ion transport ATPase in insect epithelia. J. Exp. Biol. 106: 91-117.

Hayasaka, S. and T. Kawarabata. 1990. Cloning of a microsporidian, *Nosema bombycis* (Microsporida: Nosematidae) in insect cell cultures by a limiting dilution method. J. Invert. Pathol. 55: 35-40.

Hazard, E. I. and S. W. Oldacre. 1975. Revision of Microsporida (Protozoa) close to *Thelohania*, with descriptions of one new family, eight new genera, and thirteen new species. U. S. Dept. Agric. Techn. Bull. 1530: 1-104.

Hazelton, S., S. W. Parker and J. H. Spring. 1988. Excretion in the house cricket (*Acheta domesticus*): Fine structure of the Malpighian tubules . Tissue & Cell 20: 443-460.

Heimpel, A. M. and T. A. Angus. 1959. The site of action of crystalliferous bacteria in Lepidoptera larvae. J Insect Pathol. 1: 152-170.

Hill, D. S., P. M. Hore and I. W. B. Thornton. 1982. Insects of Hong Kong. pp. 274-279. Hong Kong University Press, Hong Kong.

Hill, R. E. and W. J. Gary. 1979. Effects of the microsporidium, *Nosema pyrausta*, on field populations of European corn borer in Nebraska. Environ. Ento. 8: 91-95.

Himeno, M. K., N. Koyama, T. Funato, and T. Komano. 1985. Mechanism of action of *Bacillus thuringiensis* insecticidal delta-endotoxin on insect cells in vitro. Agric. Biol. Chem. 49: 1461-1468.

Holmes, K. C. and R. E. Munro. 1965. Studies on the structure of parasporal inclusions from *Bacillus thuringiensis*. J. Mol. Biol. 14: 572.

Hsu, T. H., E. L. Hsu and D. F. Yen. 1991. Spore ultrastructure of a microsporidian species (*Nosema* sp.) from the tobacco cutworm *Spodoptera litura*. Chinese J. Entomol. 11: 242-251.

Ibarra, J. E. and B. A. Federici. 1956. Isolation of a relatively nontoxic 65-kilodalton protein inclusion from the parasporal body of *Bacillus thuringiensis* subsp. *israelensis*. J. Bacteriol. 165: 527-533.

Ignoffo, C. M. 1966. In " Insect pathology and microbial control" (P. A. Van der Laan, Ed.), North-Holland, Amsterdam. p. 91.

Irvine, H. B. 1969. Sodium and potassium secretion by isolated insect Malpighian tubules. American J. Physiol. 217: 1520-1527.

Ishihara, R. 1969. The life cycle of *Nosema bombycis* as revealed in tissue culture cells grown in vitro. Nature (London) 195: 788-789.

Iwano, H. and R. Ishihara. 1989. Intracellular germination of spores of a *Nosema* sp. immediately after their formation in culture cell. J. Invert. Pathol. 54: 125-127.

Iwano, H. and R. Ishihara. 1991. Dimorphism of spore of *Nosema* spp. in culture cell. J. Invert. Pathol. 57: 211-219.

Jarial, M. S. 1988. Fine structure of the Malpighian tubules of *Chironomus* larva in relation to glycogen storage and fate of hemoglobin. Tissue & Cell 20: 355-380.

Jarial, M. S. and G. G. E. Scudder. 1970. The morphology and ultrastructure of the Malpighian tubules and hindgut in *Cenocorixa bifida* Hung. (Hemiptera: Corixidae). Z. Morph. 68: 269-299.

Johnson, D. E. and L. I. Davidson. 1986. Specificity of cultured insect tissue cells for bioassay of entomocidal protein from B. t. In Vitro. 20: 66-70.

Johnson, D. L. and E. Pavlikova. 1986. Reduction of consumption by grasshoppers (Orthoptera: Acrididae) infected with *Nosema locustae* caning (Microsporida: Nosematidae). J. Invert. Pathol. 48: 232-238.

Kawarabata, T. and S. Hayasaka. 1987. An enzyme-linked immunosorbent assay to detect alkalisoluble spore surface antigens of strains of *Nosema bombycis*. J. Invert. Pathol. 50: 118-123.

Kawarabata, T. and R. Ishihara. 1984. Infection and development of *Nosema bombycis* (Microsporida: protozoa) in a cell line of *Antheraea eucalypti*. J. Invert. Pathol. 44: 52-62.

Kline, D. L., J. F. Kelly and E, A. Ellis. 1985. A *Nosema*-type microsporidian infection in larvae of *Culicoides* spp. from salt marshes in Florida. J. Invert. Pathol. 45: 60-65.

Knowles, B. H. and D. J. Ellar. 1987. Colloid-osmotic lysis is a general feature of the mechanism of action of *Bacillus thuringiensis* δ-endotoxins with different insect specificity. Biochim. Biophy. 924: 509-518.

Koefoed, B. M. 1971. Ultrastructure of the cryptonephridial system in the meal worm *Tenebrio molitor*. Z. Zellforsch. 116: 487-501.

Kurstak, E. 1982. Microbial and viral pesticides. Marcel Dekker, Inc. New York and Basel.

Kurstak, E. and P. Tijssen. 1982. Microbial and viral pesticides: Mode of action, safety, and future prospects. In "Microbial and viral pesticides" (Kurstak, E. Ed.), pp. 3-32. Marcel Dekker, Inc. New York.

Labaw, L. W. 1964. The structure of *Bacillus thuringiensis* Berliner crystals. J. Ultrastruct. Res. 10: 66.

Laemmli, U. K. 1970. Cleavage of structural proteins during the assembly of the head of bacteriophage T4. Nature 227: 680-685.

Lane, N. J., J. B. Harrison and W. M. Lee. 1989. Changes in microvilli and Golgi-associated membranes of Lepidopteran cells induced by an insecticidally active bacterial δ-endotoxin. J. Cell Sci. 93: 337-347.

Larsson, J. I. R. 1986. Ultrastructure, function and classification of Microsporidia. Progress in Protistol. 1: 325-390.

Larsson, J. I. R. 1989. On the ultrastructure of *Hyalinocysta expliatoria* (Microspora, Thelohaniidae) and the taxonomy of the species. J. Invert. Pathol. 54: 213-223.

Larsson, J. I. R. 1990. Description of a new microsporidium of the water mite *Limnochares aquatica* and establishment of the new genus *Napamichum* (Microspora, Thelohaniidae). J. Invert. Pathol. 55: 152-161.

Lecadet, M. M. 1965. La toxine figuree de *Bacillus thuringiensis*. Technique de separation et composition du acides amines. Compt. Rend. 261: 5693-5696.

Lecadet, M. M. 1970. *Bacillus thuringiensis*-The proteinacous crystal. In "Microbial toxins" (Montie, T. C. Ed.). Vol. 3. pp. 437-471. Academic Press. New York.

Lehninger, A. L. 1982. Principles of Biochemistry. Worth Publishers, Inc. New York.

Lewis, L. C. and R. E. Lynch. 1976. Influence on the European corn borer of *Nosema pyrausta* and resistance in maize to leaf feeding. Environ. Entomol. 5: 139-142.

Lewis, L. C., N. C. Snell and G. Alderton. 1964. Spores News Letter. 11: 5.

Lilley, M., R. N. Ruffell and H. J. Somerville. 1980. Purification of the insecticidal toxin in the crystal of *Bacillus thuringiensis*. J. Gen. Microbiol. 118: 1-11.

Lison, L. 1938. Cryptonephridic system in insects. C. R. Soc. Biol. 128: 801-803.

Liu, H. J. and F. L. McEwen. 1977. *Nosema blissi* sp. n. (Microsporida: Nosematidae), a pathogen of the chinch bug, *Blissus leucopterus hirtus* (Hemiptera: Lygaeidae). J. Invert. Pathol. 29: 141-146.

Luthy, P. 1973. Self-digestion of the gut epithelium: A possible explanation for the mode of action of the endotoxin of *Bacillus thuringiensis*. J. Invert. Pathol. 22: 130-140.

Luthy, P., J. L. Cordier and H. M. Fishcher. 1982. *Bacillus thuringiensis* as a bacterial insecticide: basic considerations and application. In "Microbial and viral pesticide" (Kurstaki, E. Ed.), pp. 35-74. Marcel Dekker, Inc. New York and Basal.

Macvean, C. M. and J. L. Capinera. 1991. Pathogenicity and transmission potential of *Nosema locustae* and *Vairimorpha* n. sp. (Protozoa: Microsporida) in mormon crickets (*Anabrus simplex*; Tettigoniidae): A laboratory evaluation. J. Invert. Pathol. 57: 23-36.

Maddrell, S. H. P. 1977. Insect Malpighian tubules. In "Transport of ions and water in animals" (Gupta, B. L., R. B. Moreton, J. L. Oschman and B. J. Wall, Ed.), pp. 541-569. Academic Press, New York.

Maddrell, S. H. P. and B. O. C. Gardiner. 1974. The passive permeability of insect Malpighian tubules to organic solutes. J. Exp. Biol. 8: 411-127.

Maddrell, S. H. P. and B. O. C. Gardiner. 1976. Excretion of alkaloids by Malpighian tubules of insects. J. Exp. Biol. 64: 267-281.

Maddrell, S. H. P. and J. E. Phillips. 1975a. Active transport of sulphate ions by the Malpighian tubules of larvae of the mosquito *Aedes campestris*. J. exp. Biol. 62: 367-378.

Maddrell, S. H. P. and J. E. Phillips. 1975b. Secretion of hypo-osmotic fluid by the lower Malpighian tubules of *Rhodnius prolixus*. J. exp. Biol. 62: 671-683.

Maddrell, S. H. P. and J, E. Phillips. 1976. Regulation of absorption in insect excretory system. In "Perspectives in Experimental Biology." Vol. 1: 179-185. Pergammon Press, Oxford.

Maddrell, S. H. P., G. Whittembury, R. L. Mooney, J. B. Harrison, J. A. Overton and B. Rodriguez. 1991. The fate of calcium in the diet of *Rhodnius prolixus*: Storage in concretion bodies in the Malpighian tubules. J Exp. Biol. 157: 483-502.

Mahillon, J. and J. Delcour. 1984. A convenient procedure for the preparation of highly purified parasporal crystals of *Bacillus thuringiensis*. J. Microbiol. Methods 3: 69-76.

Malone, L. A. 1984. Factors controlling *in vitro* hatching of *Vairimorpha plodiae* (Microspora) spores and their infectivity to *Plodia interpunctella*, *Heliothis virescens*, and *Pieris brassica*. J. Invert. Pathol. 44: 192-197.

Malone, L. A. and P. J. Wigley. 1981. Quantitative studies on the pathogenicity of *Nosema carpocapsae*, a microsporidian pathogen of the coding moth, *Cydia pomonella*, in New Zealand. J Invert. Pathol. 38: 330-334.

Marshall, A. T. 1974. Golgi body function and mucocomplex secretion in the Malpighian tubules of cercopoid larvae (Insecta: Homoptera). J. Ultrastructure Research 47: 95-105.

Marshall, A. T. and W. W. K. Cheung. 1970. Ultrastructure and cytochemistry of an extensive plexiform surface coat on the midgut cells of a fulgorid insect. J. Ultrastructure Research. 33: 161-172.

Marshall, A. T. and W. W. K. Cheung. 1973. Studies on water and ion transport in Homopteran insects: Ultrastructure and cytochemistry of the cicadoid and cercopoid hindgut. Tissue & Cell 5: 671-678.

Marshall, A. T. and W. W. K. Cheung. 1974. Studies on water and ion transport in Homopteran insects: Ultrastructure and cytochemistry of the cicadoid and cercopoid Malpighian tubules and filter chamber. Tissue & Cell 6: 153-171.

Martoja, R., C. Ballan-Dufrancais. 1984. The ultrastructure of digestive and excretory organs. In "Insect ultrastructure" (King, R. C. and H. Akai, Ed.), Academic Press, New York.

Mattes, D. 1927. Parasitare krankheieen der mehlmottenlarven und versuche

uber ihre verwendbarkeit als biologisches Bekamfungsmittel, Gesell. J. Beford. Ges. Naturw. Sitzber. Marburg. 62: 381.

Mclaughlin, R. E. 1971. In "Microbial control of insects and mites" (Burges, H. D. and N. W. Hussey, Eds.), Vol. 1. P. 151. Academic Press, New York.

Meenakshi, K. and K. Jayaraman. 1979. On the formation of crystal proteins during sporulation in *Bacillus thuringiensis* var. *thuringiensis*. Arch. Microbiol. 120: 9-14.

Milne, R., D. Murphy and P. G. Fast. 1977. *Bacillus thuringiensis* δ-endotoxin: An improved technique for the separation of crystals from spores. J. Invert. Pathol. 29: 230-231.

Milner, R. J. 1972. *Nosema whitei*, a microsporidian pathogen of some species of Tribolium. II. Ultrastructure. J. Invert. Pathol. 19: 239-247.

Moar, W. J., J. T. Trumble and B. A. Federici. 1989. Comparative toxicity of spores and crystals from the NRD-12 and HD-1 strains of *Bacillus thuringiensis* subsp. *kurstaki* to neonate beet armyworm (Lepidoptera: Noctuidae). J. Economic Entomol. 82: 1593-1603.

Mohd-Salleh, M. B. and L. C. Lewis. 1982. Toxic effects of spore/crystal ratios of *Bacillus thuringiensis* on European corn borer larvae. J. Invert. Pathol. 39: 290-297.

Munk, R. 1967. Zur morphologie des vergauungstraktes zweier jassiden (Homoptera Auchenorrhyncha) unter besonderer berucksichtigung der sogenannten filterkammmer. Z. Wiss. Zool. 175: 405-424.

Murray, E. D. and E. Y. Spencer. 1966. A simplified purification technique for parasporal inclusions from certain varieties of *Bacillus thuringiensis*. J. Invert. Pathol. 8: 418-420.

Nicolson, S. W. 1976. Diuresis in the cabbage white butterfly, *Pieris brassicae*: water and ion regulation and the role of the hindgut. J Insect Physiol. 22: 1623-1630.

Nishiitsutsuji-Uwo, J. and Endo, Y. 1979. Mode of action of *Bacillus thuringiensis* δ-endotoxin: Effect on TN-368 cells. J. Invert. Pathol. 34: 267-275.

Olsen, P. E., W. A. Rice and T. P. Liu. 1986. *In vitro* germination of *Nosema apis* spores under conditions favorable for the generation and maintenance of sporoplasms. J. Invert. Pathol. 47: 65-73.

Onstad, D. W. and J. V. Maddox. 1989. Modeling the effects of the microsporidium, *Nosema pyrausta*, on the population dynamics of the insect, *Ostrinia nubilalis*. J. Invert. Pathol. 53: 410-421.

Oron, U., M. Sokolover, A. Yawetz, M. Broza, B. Sneh and A. Honigman. 1985. Ultrastructural changes in the larval midgut epithelium of *Spodoptera littoralis* following ingestion of δ-endotoxin of *Bacillus thuingiensis* var. *entomocidus*. J. Invert. Pathol. 45: 353-355.

Oschman, J. L. and M. J. Berridge. 1971. The structural basis of fluid secretion. Federation Proceedings 30: 49-56.

Pang, A. S. D. and B. Mathieson. 1991. Peptide mapping of different *Bacillus thuringiensis* toxin gene products by CNBr cleavage in SDS-PAGE gels. J. Invert. Pathol. 57: 82-93.

Pearse, A. G. E. 1968. Histochemistry: Theoretical and applied, 3rd ed. London, Churchill.

Pendleton, I. R. and R. B. Morrison. 1966. Separation of the spores and crystals of *Bacillus thuringiensis*. Nature 212: 728-729.

Percy, J. and P. G. Fast. 1983. *Bacillus thuringiensis* crystal toxin: Ultrastructural studies of its effect on silkworm midgut cells. J. Invert. Pathol. 41: 86-98.

Purcell, A. H. and K. G. Suslow. 1987. Pathogenicity and effects on transmission of a mycoplasma-like organism of a transovarially infective bacterium on the leafhopper *Euscelidius variegatus* (Homoptera: Cicadellidae). J. Invert. Pathol. 50: 285-290.

Rahmet-Alla, M. and A. F. Rowley. 1989. Studies on the cellular defense reactions of the Medeira Cockroach, *Leucophaea maderae*: Nodule formation in response to injected bacteria. J. Invert. Pathol. 54: 200-207.

Ramsay, T. A. 1958. Excretion by the Malpighian tubules of the stick insect, *Dixippus morosus* (Orthoptera, Phasmidae): Calcium, magnesium, chloride, phosphate and hydrogen ions. J. Exp. Biol. 33: 697-708.

Ramsay, J. A. 1964. The rectal complex of the mealworm *Tenebrio molitor* L. (Coleoptera, Tenebrionidae). Phil. Trans. Roy. Soc. London, Ser. B 248: 279-314.

Ramsay, J. A. 1976. The rectal complex in the larvae of Lepidoptera. Phil. Trans. Roy. Soc. Lond. B274: 203-226.

Rao, C. D. and Y. Z. Shethna. 1980. A simple technique for purification of parasporal crystal of *Bacillus thuringiensis* var. *thuringiensis*. J. Ind. Insect Sci. 62: 1-11.

Ratcliffe, N. A. and A. F. Rowley. 1987. Insect responses to parasites and other pathogens. In "Immune response in parasitic infections: Immunology, immunopathology and immunoprophylaxis", Vol. IV, "Protozoa, arthropods and invertebrates" (Soulsby, E. J. Ed.), pp. 271-332. CRC Press, Florida.

Reisner, W. M., D. J. Feir, P. B. Lavrik and J. S. Ryerse. 1989. Effect of *Bacillus thuringiensis kurstaki* δ-endotoxin on insect Malpighian tubule structure and function. J. Invert. Pathol. 54: 175-190.

Ribier, J. and M. M. Lecadet. 1973. Etude ultrastructurale et cinetique de la sporulation de *Bacillus thuringiensis* var. *Berliner* 1715. Remarques sur la formation de l'inclusion paraspoirale, Ann. Microbiol. 124: 311

Rie, J. V., S. Jansens, H. Hofte, D. Degheele and H. V. Mellaert. 1990.

Receptors on the brush border membrane of the insect midgut as determinants of the specificity of *Bacillus thuringiensis* delta-endotoxin. App. Enviro. Microbiol. 56: 1378-1385.

Ross, H. H., C. A. Ross and J. R. Ross. 1982. A textbook of entomology. 4th ed. John Wiley & Sons, New York.

Ryerse, J. S. 1979. Developmental changes in Malpighian tubule cell structure. Tissue & Cell 11: 533-551.

Ryerse, J. S., Jr. J. R. Beck and P. B. Lavrik. 1990. Light microscope immunolocation of *Bacillus thuringiensis kurstaki* δ-endotoxin in the midgut and Malpighian tubules of the tobacco budworm, *Heliothis virescens*. J. Invert. Pathol. 56: 86-90.

Sato, R., M. Kobayashi and H. Watanabe. 1982. Internal ultrastructure of spores of microsporidians isolated from the silkworm, *Bombyx mori*. J. Invert. Pathol. 40: 260-265.

Schatz, G., E. Haslbrunner and H. Tuppy. 1964. Deoxyribonucleic acid associated with yeast mitochondria. Biochem. Biophy. Research Comm. 15: 127-132.

Schwemmler, W. and H. Muller. 1986. Role of insect lysozymes in endocytobiosis and immunity of leafhoppers. In "Hemocytic and humoral immunity in Arthropods. (A. P. Gupta, Ed.), pp. 440-460. Wiley, New York.

Seligman, A. M., K. C. Tsou, S. H. Rutenburg and R. B. Cohen. 1954. Histochemical demonstration of ß-D-glucuronidase with a synthetic substrate. J. Histochem. Cytochem. 2: 209-229.

Sharpe, E., K. W. Nickerson and L. A. Bulla, Jr. 1975. Separation of spores and parasporal crystals of *Bacillus thuringiensis* in gradients of certain X-ray contrasting agents. Applied Microbiol. 30: 1052-1053.

Siegel, J. P., J. V. Maddox and W. G. Ruesink. 1986. Lethal and sublethal effects of *Nosema pyrausta* on the European corn borer (*Ostrinia nubilalis*) in central Illinois. J. Invert. Pathol. 48: 167-173.

Sleigh, M. A. 1989. Protozoa and other protists. pp. 236-238. Edward Arnold, London.

Smirnoff, W. A. and W. H. Chu. 1968. Microsporidian infection and the reproductive capacity of the larch sawfly, *Pristophora erichsonii*. J. Invert. Pathol. 12: 388-390.

Smith, D. S. and V. C. Littau. 1960. Cellular specialization in the excretory epithelia of an insect, *Macrosteles fascifrons* Stal (Homoptera). J. Biophys. Biochem. Cytol. 8: 103-133.

Sohal, R. S. 1974. Fine structure of the Malpighian tubules in the housefly, *Musca domestica*. Tissue & Cell 6: 719-728.

Sohal, R. S., P. D. Peters and T. A. Hall. 1976. Fine structure and X-ray microanalysis of mineralized concretions in the Malpighian tubules of the

housefly, *Musca domestica*. Tissue & Cell 8: 447-458.

Sohal, R. S., P. D. Peters and T. A. Hall. 1977. Origin. structure, composition and age-dependence of mineralized dense bodies (concretion) in the midgut epithelium of the adult housefly, *Musca domestica*. Tissue & Cell 9: 87-102.

Solter, L. F., J. V. Maddox and D. W. Onstad. 1991. Transmission of *Nosema pyrausta* in adult European corn borers. J. Invert. Pathol. 57: 220-226.

Solter, L. F., D. W. Onstad and J. V. Maddox. 1990. Timing of disease-influenced processes in the life cycle of *Ostrinia nubilalis* infected with *Nosema pyrausta*. J. Invert. Pathol. 55: 337-341.

Somerville, H. J. 1971. Formation of the parasporal inclusion of *Bacillus thuringiensis*. Eur. J. Biochem. 18: 226.

Srivastava, P. N. 1962. Physiology of excretion in the larva of *Corcyra cephalonica* stainton (Lepidoptera, Pyralidae). J. Ins. Physiol. 8: 223-232.

Sutter, G. R. and E. S. Raun. 1967. Histopathology of European core borer larvae treated with *Bacillus thuringiensis*. J. Invert. Pathol. 9: 90-103.

Tamir, H. and C. Gilvarg. 1966. Density gradient centrifugation for the separation of sporulating form of bacteria. J. Bacteriol. Chem. 241: 1085-1090.

Tanabe, A. M. and M. Tamashiro. 1967. The biology and pathogenicity of a microsporidian (*Nosema trichoplusiae* sp. n.) of the cabbage looper, *Trichoplusia ni* (Hubner) (Lepidoptera: Noctuidae). J. Invert. Pathol. 9: 188-195.

Taylor, H. H. 1971a. Water and solute transport by the Malpighian tubules of the stick insect, *Carausius morosus*: The normal ultrastructure of the type 1 cells. Z. Zellforsch. 118: 333-368.

Taylor, H. H. 1971b. The fine structure of the type 2 cells in the Malpighian tubules of the stick insect, *Carausius morosus*. Z. Zellforsch. 122: 411-424.

Taylor, H. H. 1973. Structural and functional changes in the Malpighian tubules of *Carausius morosus* during dehydration and starvation. Z. Zellforsch. 141: 479-492.

Teigler, D. J. and H. J. Arnott. 1972. Crystal development in the Malpighian tubules of *Bombyx mori* L. Tissue and Cell 4: 173-185.

Tojo, A. 1986. Mode of action of bipyramidal δ-endotoxin of *Bacillus thuringiensis* subsp. *kurstaki* HD-1. Appl. Environ. Microbiol. 51: 630-633

Travers, R. S., R. M. Faust and C. F. Reichelderfer. 1976. Effects of *Bacillus thuringiensis* var. *Kurstaki* ?δ-endotoxin on isolated Lepidopteran mitochondria. J. Invert. Pathol. 28: 351-356.

Turbeck, B. O. 1974. A study of the concentrically laminated concretions, `spherites', in the regenerative cells of the midgut of Lepidopterous larvae. Tissue & Cell 6: 627-640.

Tyrell, D. J., L. A. Bulla, Jr., R. E. Andrews, Jr., K. J. Kramer, L. I.

Davidson and P. Nordin. 1981. Comparative biochemistry of entomocidal parasporal crystals of selected *Bacillus thuringiensis* strains. J. Bacteriol. 145: 1052-1062.

Undeen, A. H. 1983. The germination of *Varraia culicis* spores. J. Protozool. 30: 274-277.

Undeen, A. H. and Avery, S. W. 1984. Germination of experimentally nontransmissible Microsporidia. J. Invert. Pathol. 43: 229-301.

Undeen, A. H. and N. D. Epsky. 1990. *In vitro* and *in vivo* germination of *Nosema locustae* (Microspora: Nosematidae) spores. J. Invert. Pathol. 56: 371-379.

Vavra, J. and J. V. Maddox. 1976. Methods in microsporidiology. In " Comparative pathology" (Bulla, L. A. Jr. and T. C. Cheng. Eds.), pp. 281-320. Plenum Press. New York.

Wachstein, M. and E. Meisel. 1957. Histochemistry of hepatic phosphatase at a physiological pH with special reference to the demonstration of bile canaliculi. Amer. J. Clin. Pathol. 27: 13-23.

Wall, B. J. and J. L. Oschman. 1979. Insects. In "Comparative physiology of osmoregulation in Animals" (G. M. O. Maloiy, Ed), pp. 219-160. Academic Press, New York.

Wall, B. J., J. L. Oschman and B. A. Schmidt. 1975. Morphology and function of Malpighian tubules and associated structures in the cockroach *Periplaneta americana*. J. Morphol. 146: 265-306.

Waterhouse, D. F. 1957. Digestion in insects. Ann. Rev. Entomol. 2: 1-18.

Weiser, J. 1976. Microsporidia in invertebrates: Host-parasite relations at the organismal level. In "Comparative Pathology" (Bulla, L. A. Jr. and T. C. Cheng, Eds.), pp. 163-202. Plenum, New York.

Whiteley, H. R. and H. E. Schnepf. 1986. The molecular biology of parasporal crystal body formation in *Bacillus thuringiensis*. Ann. Rev. Microbiol. 40: 549-576.

Whitlock, V. H. and S. Johnson. 1990. Stimuli for the in vitro germination and inhibition of *Nosema locusta* (Microspora: Nosematidea) spores. J. Invert. Pathol. 56: 57-62.

Widner, W. R. and H. R. Whiteley. 1989. Two highly related insecticidal crystal proteins of *Bacillus thuringiensis* subsp. *kurstaki* possess different host range specificities. J. Bacteriol. 171: 965-974.

Wigglesworth, V. B. 1931. The physiology of excretion in a blood-sucking insect, *Rhodnius prolixus* (Hemiptera, Reduviidae). J. Exp. Biol. 8: 411-427.

Wigglesworth, V. B. 1972. The principles of insect physiology, 7th ed., London, Chapman & Hall.

Wigglesworth, V. B. and M. M. Salpeter. 1962. Histology of the Malpighian

tubules in *Rhodnius prolixus* stal (Hemiptera). J. Insect Physiol. 8: 299-307.

Wilson, G. G. 1974a. The effects of temperature and ultraviolet radiation on the infection of *Choristoneura fumiferana* and *Malacosoma pluviale* by a microsporidian parasite, *Nosema (Perezia) fumiferanae* (Thom.). Can. J. Zool. 52: 59-63.

Wilson, G. G. 1974b. Effects of larval age at inoculation, and dosage of microsporidian (*Nosema fumiferanae*) spores, on mortality of spruce budworm (*Choristoneura fumiferana*). Can. J. Zool. 52: 993-996.

Wilson, G. G. 1977. The effects of feeding microsporidian (*Nosema fumiferanae*) spores to naturally infected spruce budworm (*Choristoneura fumiferana*). Can. J. Zool. 55: 249-250.

Wilson, G. G. 1982. Protozoans for insect control. In "Microbial and viral pesticide" (Kurstak, E. Ed.), pp. 587-600.Marcel Dekker, Inc. New York and Basel.

Windels, M. B., H. C. Chiang and B. Furgala. 1976. Effects of *Nosema pyrausta* on pupa and adult stages of the European corn borer, Ostrinia nubilalis. J. Invert. Pathol. 27: 139-242.

Wise, T., A. Swanson and H. O. Halvorson. 1967. Dipicolinic acid-less mutants of *Bacillus cereus*. J. Bacteriol. 94: 2075-2076.

Wood, J. L. and R. B. Moreton. 1978. Refinements in the short-circuit technique and its application to active potassium transport across the *Cecropia* midgut. J. Exp. Biol. 77: 123-140.

Yamamoto, T. and T. Iizuka. 1983. Two types of Entomocidal toxins in the parasporal crystals of *Bacillus thuringiensis kurstaki*. Arch. Biochem. Biophy. 227: 233-241.

Yu, H., E. A. C. Almeida, P. J. Schulz and P. K. Chien. 1988. Electron microscopic and X-ray elemental analysis of spherical mineral concretions in the brine fly larva *Ephydra hians* say from the alkaline Mono Lake, California. The Wasmann J. Biol. 46: 49-65.

Zhao, X. K., W. D. Xie, X. Z. Wang, Q. X. Long and Z. L. Pu. 1990. A monoclonal antibody to *Nosema bombycis* and its use for identification of microsporidian spores. J. Invert. Pathol. 56: 395-400.

FIGURES AND TABLES

Fig 1. Diagrammatic representation of *Pieris* larval malpighian tubules (only one side drawn) and hindgut showing cryptonephric tubule (ct), rectal lead (rl), iliac plexus (ip), yellow region (yr), white region (wr), urinary bladder (ub), midgut (mg), ileum (il), colon (co) and rectum (re).

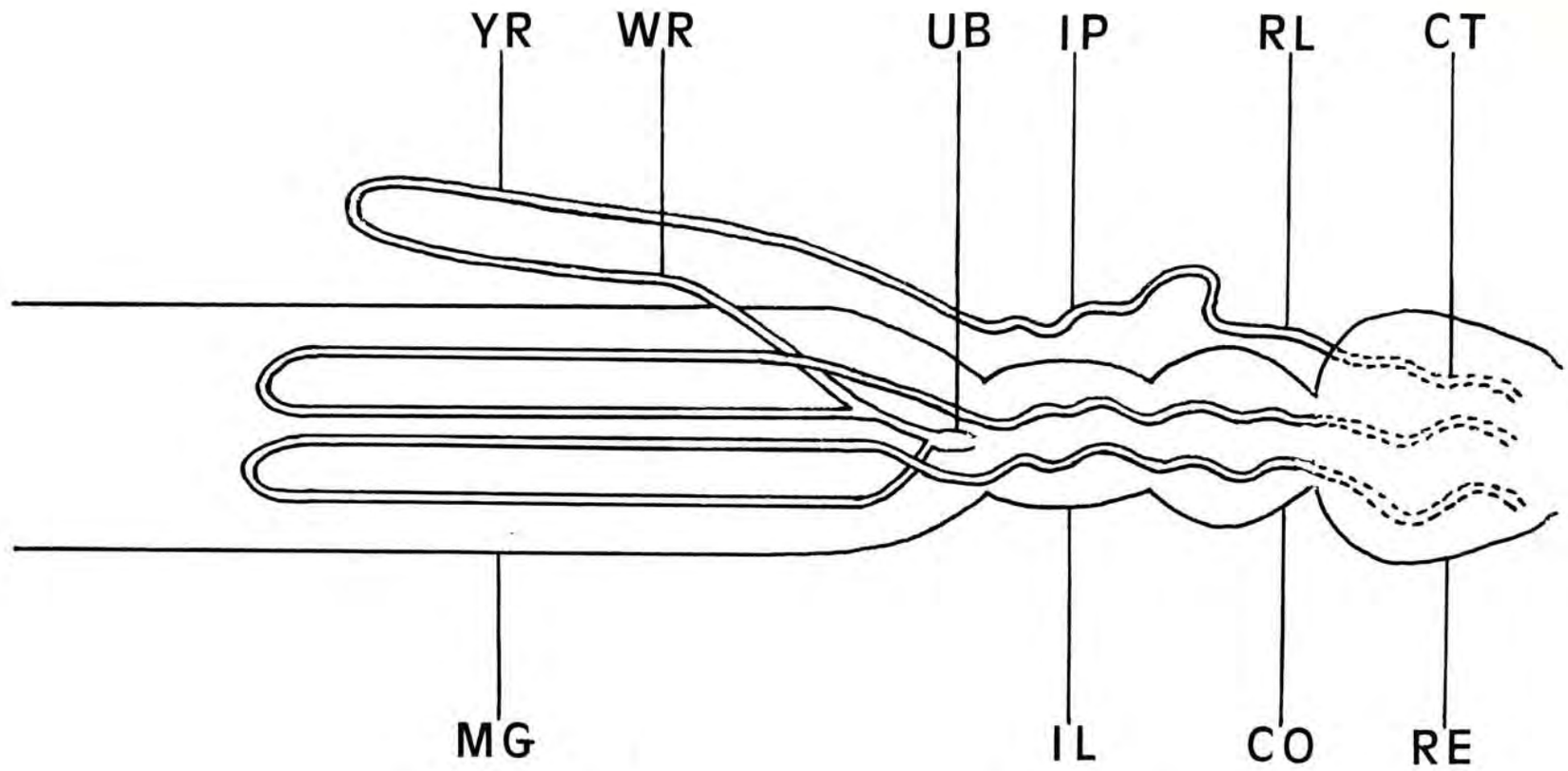

1

Fig. 2. Transverse section of rectal lead. Light micrograph of spurr resin section. Toluidine blue stained. Note a wide brush border. The basal infoldings formed by the basal membrane is prominent. x700.

Fig 3. Longitudinal section of rectal lead principal cell. Showing microvilli (mv) with mitochondria (m), lumen (l), vacuole (v), nucleus (n) and basement membrane (bm). x3960.

2

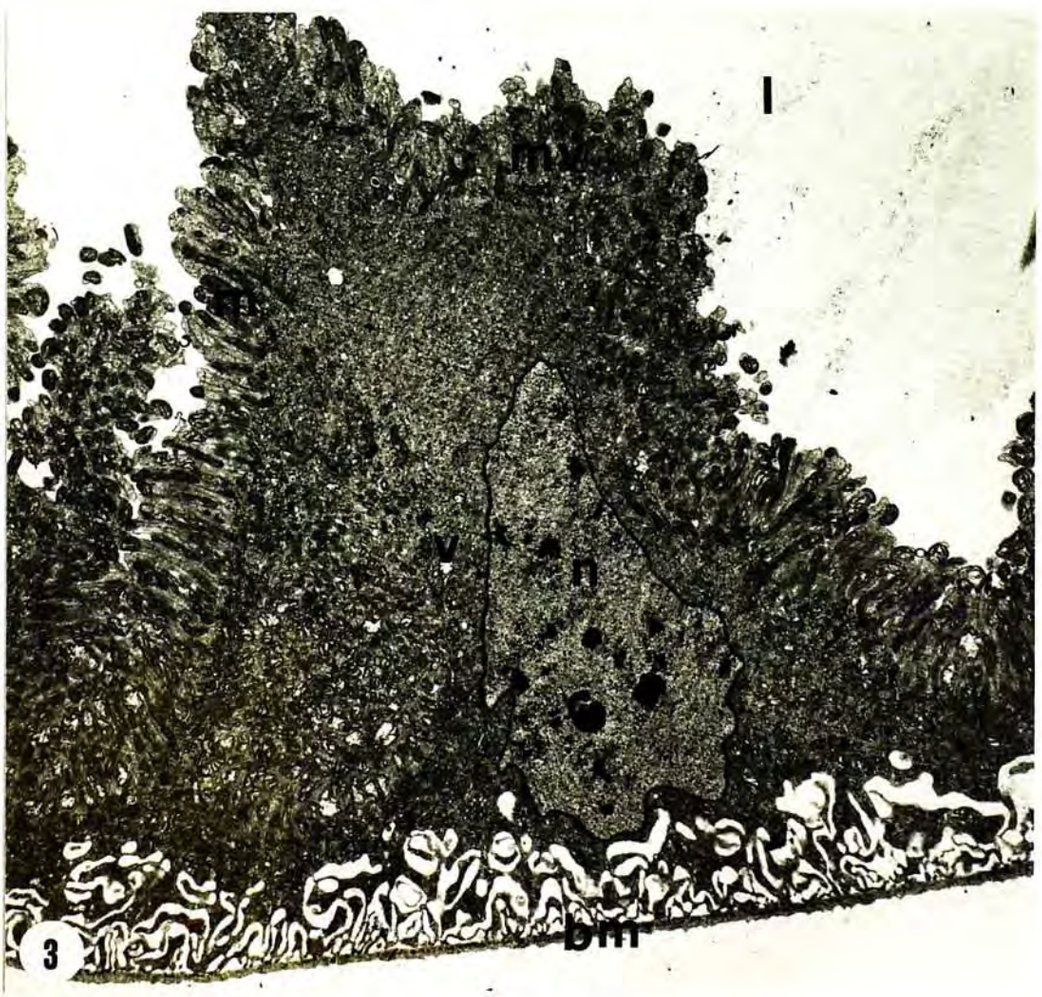

3

Fig 4. As above. High magnification of central region of principal cell. Showing rough endoplasmic reticulum (rer), vacuoles (v), golgi apparatus (g). x29400.

Fig. 5. As above. Showing microvilli (mv), tight cell junction (d) and basement membrane (bm). x3960.

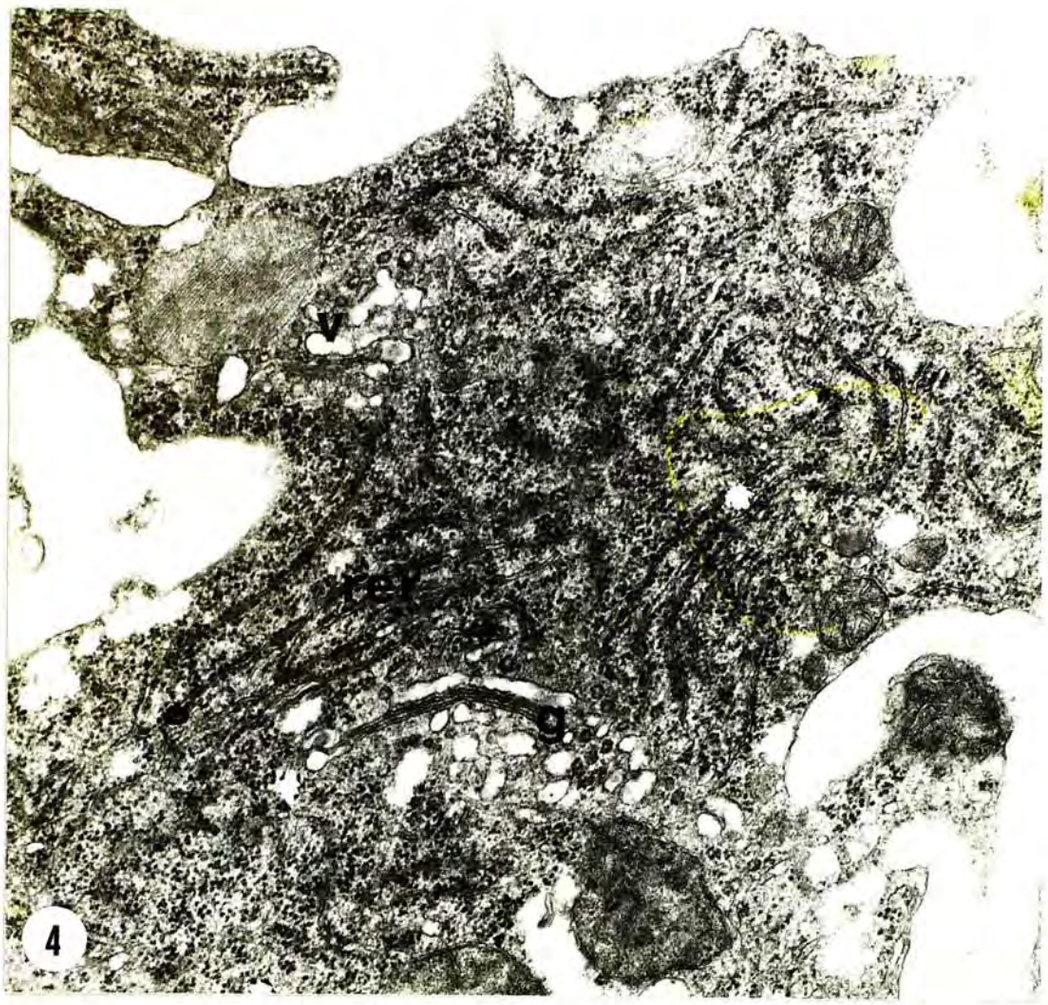
V
4


5

Fig. 6. As above. Showing microvilli (mv), tight cell junction (d) and mitochondria (m). x29400

Fig. 7. As above. High magnification of tight cell junction (d). x60900.

6

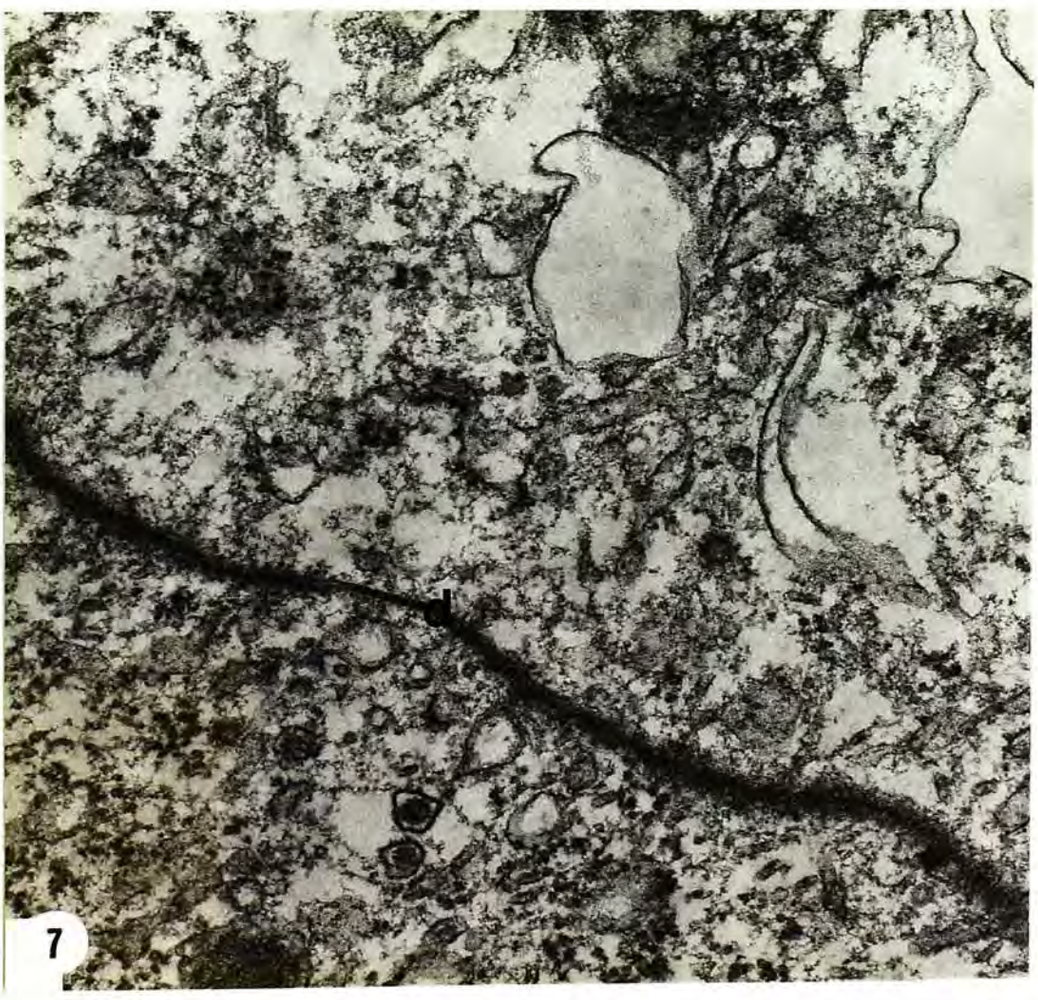

7

Fig. 8. Transverse section of iliac plexus. Light micrograph of spurr resin section. Toluidine blue stained. Note the basal infoldings. The apical surface area is further increased by the gross folding of the cell surface into canaliculi. x700.

Fig. 9. Longitudinal section of iliac plexus principal cell. Showing microvilli (mv), vacuoles (v), mitochondria (m) and basement membrane (bm). x3960.

8

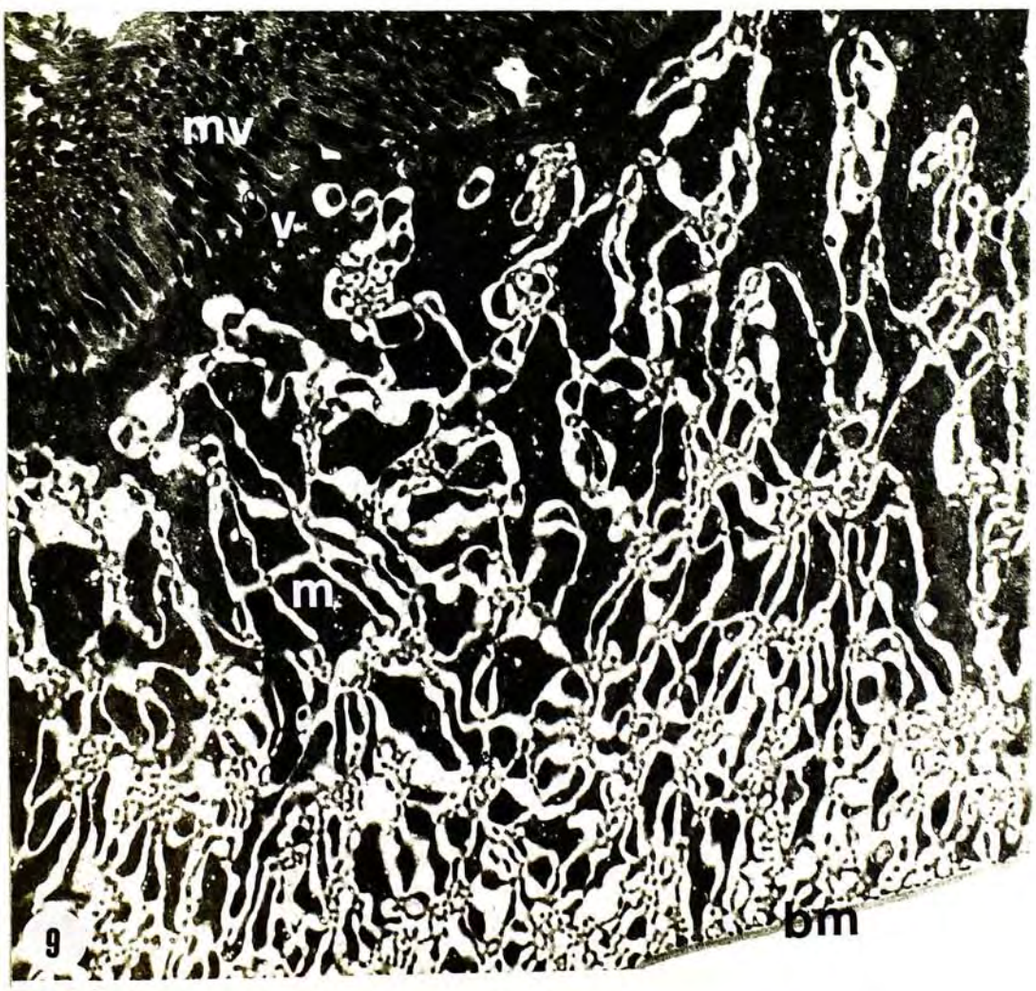

9

Fig. 10. As above. Showing rough endoplasmic reticulum (rer), vacuoles (v) and basement membrane (bm). x20900.

Fig. 11. Transverse section of yellow region. Light micrograph of spurr resin section. Toluidine blue stained. Note a brush border. The basal infoldings are prominent. There are numerous mineral spherites (or dense bodies) and clear vacuoles in the cytoplasm. x700.

10

11

Fig 12. As above. Longitudinal section of yellow region principal cell. Showing microvilli (mv), vacuoles (v), and basement membrane (bm). x3990.

Fig 13. As above. Showing mitochondria (m), rough endoplasmic reticulum (rer), vacuoles (v), gap junction (d) and multivesicular body (mb). x29400.

12

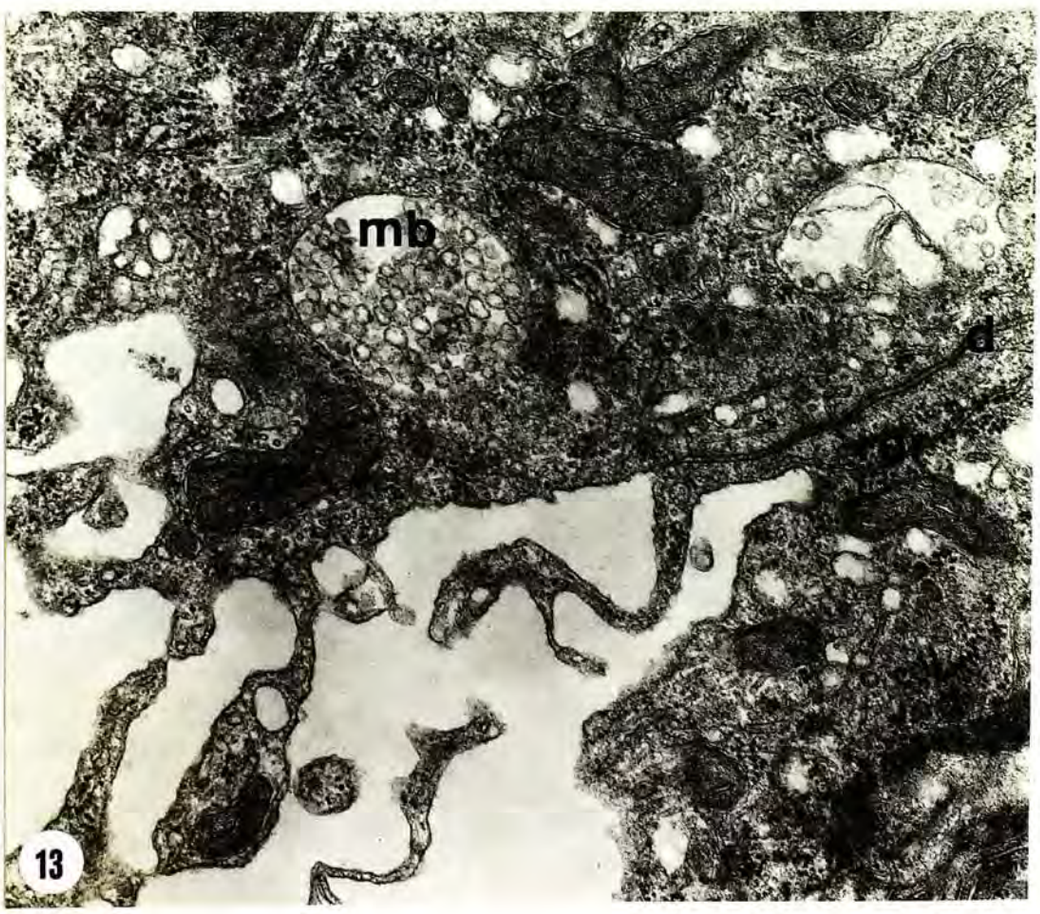

13

Fig 14. As above. High magnification of mineralized multivesicular body or young mineral spherite. x75000. (Courtesy of Dr. W. W. K. Cheung)

Fig. 15. As above. Showing young and old mineral spherite. Note cytoplasmic membrane (arrow). x75000. (Courtesy of Dr. W. W. K. Cheung)

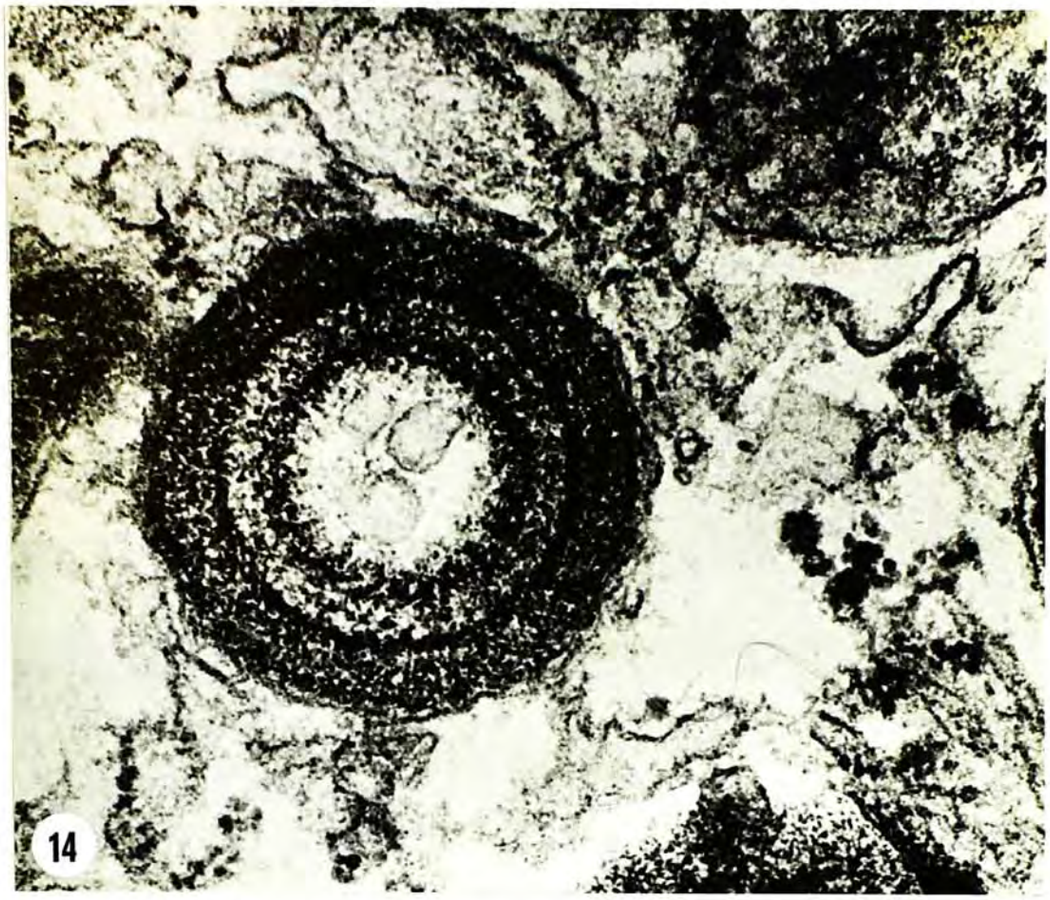
14

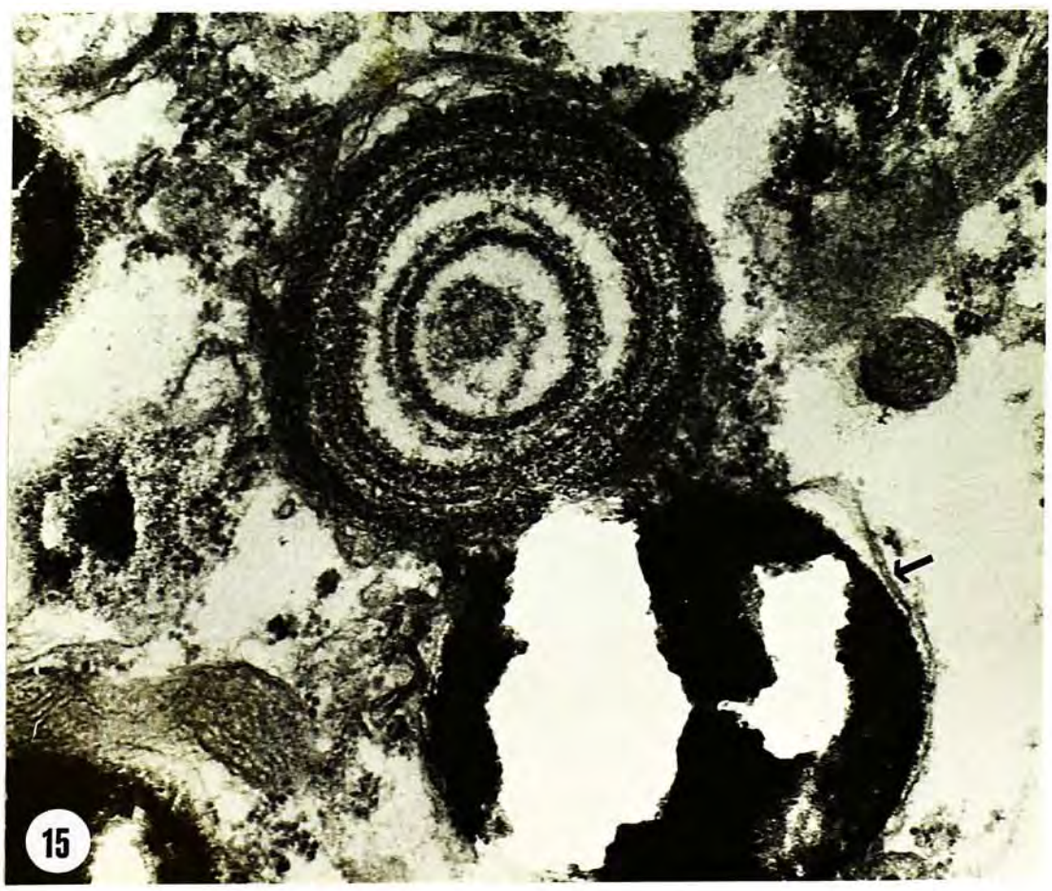
15

Fig. 16. Transverse section of white region. Light micrograph of spurr resin section. Toluidine blue stained. Note the brush border and basal infoldings. x700.

Fig. 17. Longitudinal section of white region principal cell. Showing microvilli (mv) with mitochondria, lumen (l), vacuoles (v), nucleus (n) and basement membrane (bm). x3780.

16

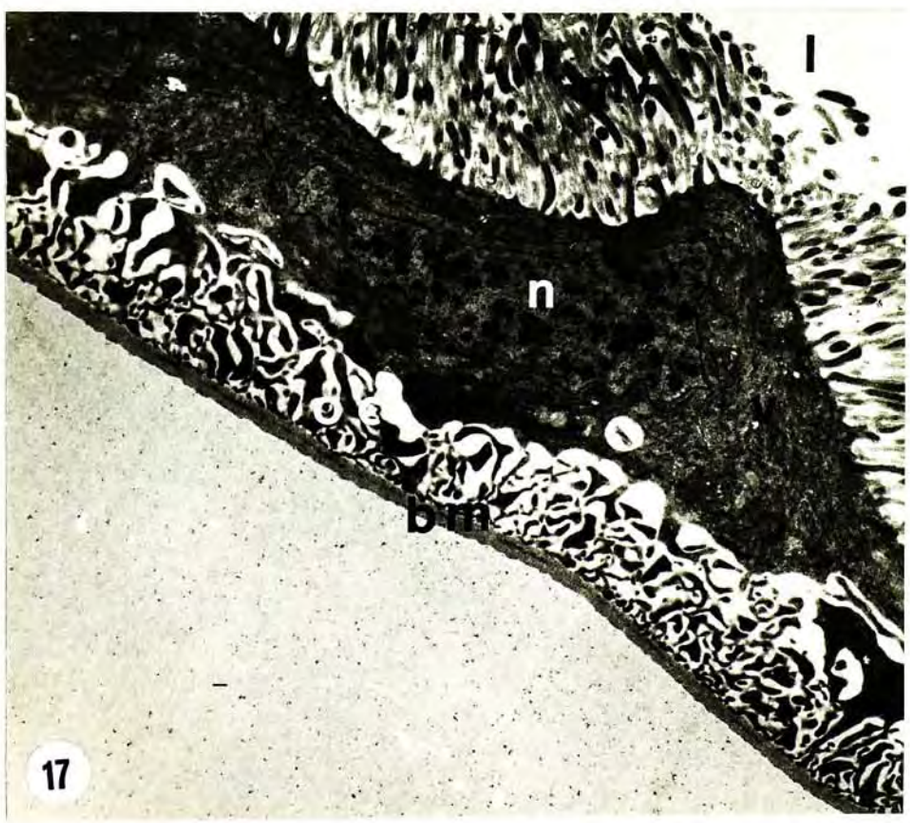

17

Fig. 18. As above. High magnification of basal region of principal cell. Showing nucleus (n), rough endoplasmic reticulum (rer) and mitochondria (m). x20900.

Fig. 19. As above. High magnification of apical region of principal cell. Showing microvilli (mv), nucleus (n), rough endoplasmic reticulum (rer) and golgi apparatus (g). x20900.


m
n
18

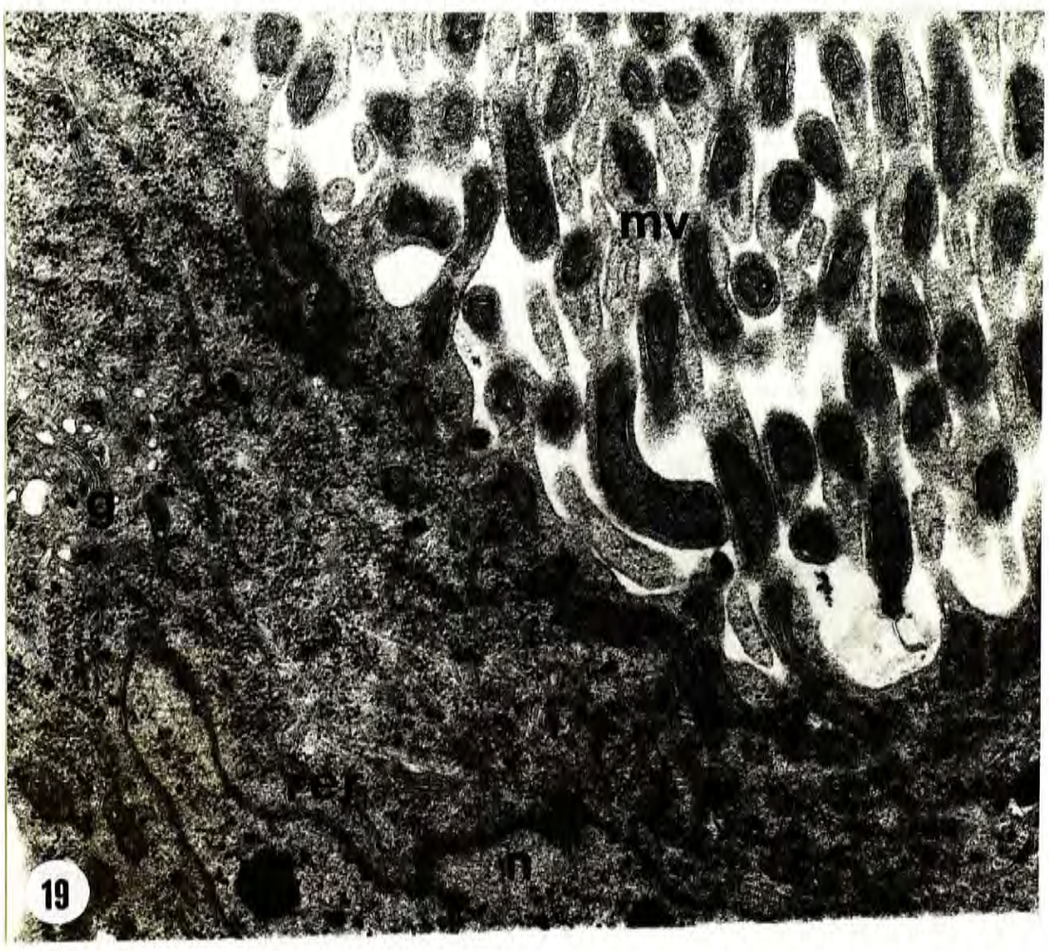
mv
g
rer
n
19

Fig. 20. Transverse section of *Pieris* Malpighian tubule; Toluidine Blue stained. Showing positively stained microvilli (mv), apical and basal cytoplasm of rectal lead cell. x700.

Fig. 21. Transverse section of *Pieris* Malpighian tubule; Mercury Bromophenol Blue stained. Showing positively stained proteins associated with microvilli (mv), apical and basal cytoplasm of rectal lead cell. x350.

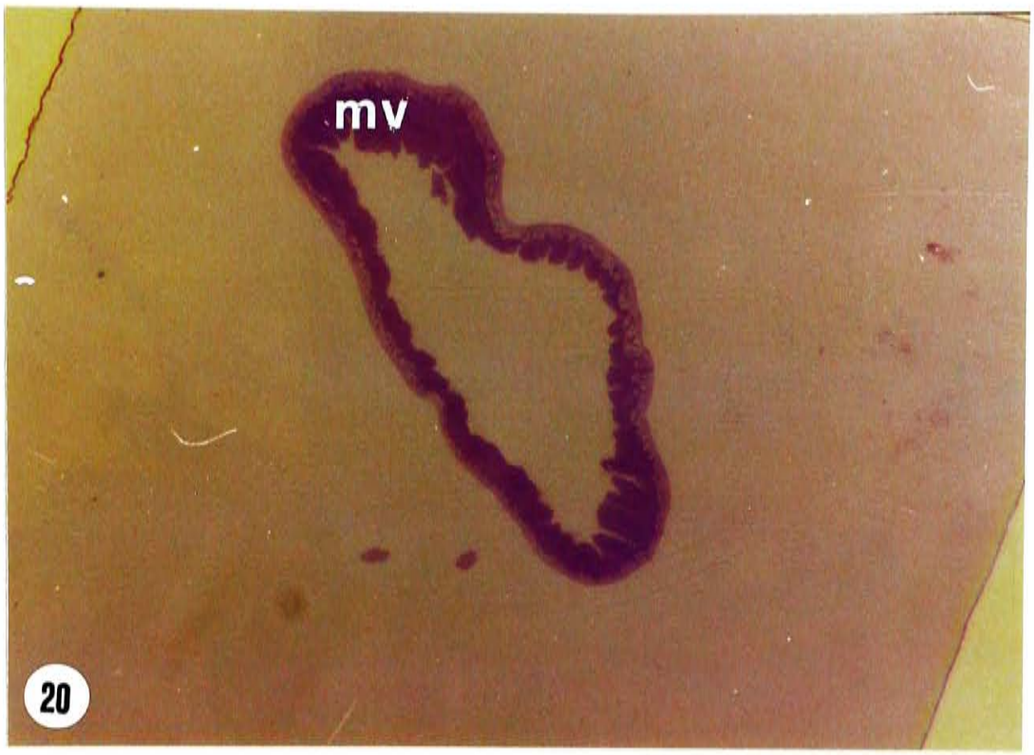
mv
20


mv
21

Fig. 22. Transverse section of *Pieris* Malpighian tubule; Toluidine Blue stained. Showing positively stained microvilli (mv), apical and basal cytoplasm of iliac plexus cell. x700.

Fig. 23. Whole mount of *Pieris* Malpighian tubule; Glucose-6-Phosphatase test. Showing reaction products of Glucose-6-Phosphatase associated with apical and basal cytoplasm of iliac plexus cell. x700.


mv
22

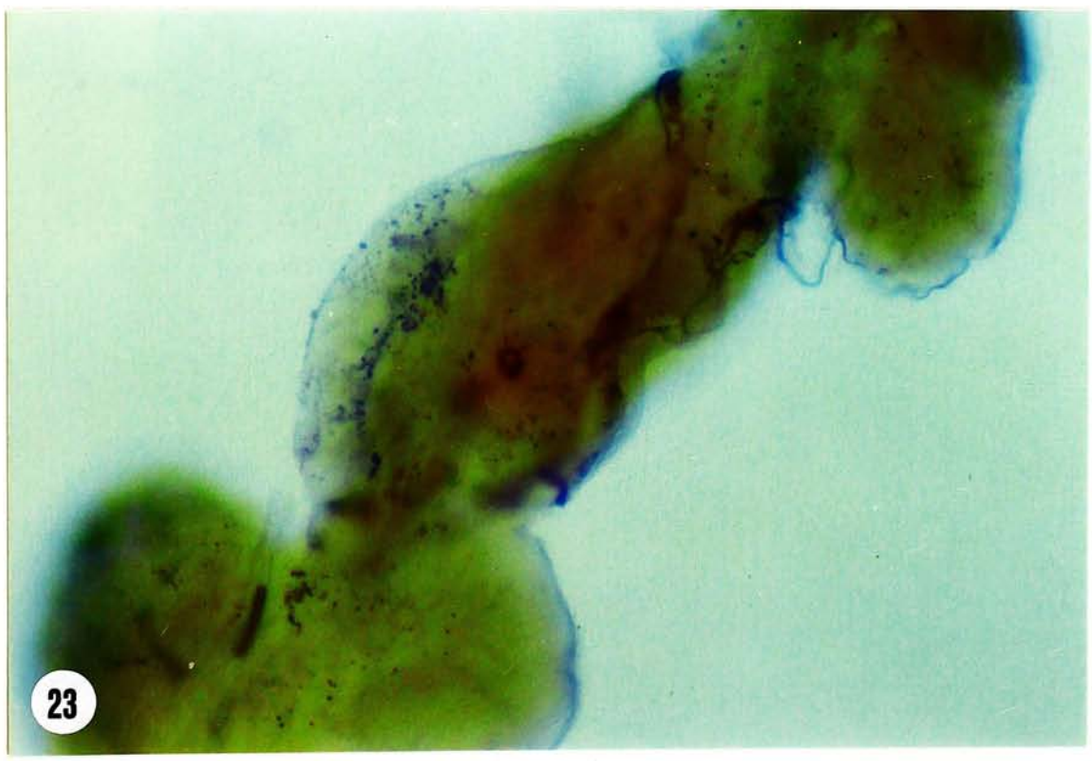
23

Fig. 24. Transverse section of *Pieris* Malpighian tubule; Toluidine Blue stained. Showing the microvilli (mv) of yellow region cell stained positive with τ-metachromasia which fainted on dehydration. x700.

Fig. 25. Whole mount of *Pieris* Malpighian tubule; ATPase test. Showing activity of ATPase (brownish black colour) localised at the microvilli, apical and basal cytoplasm of yellow region cell. x700.

24

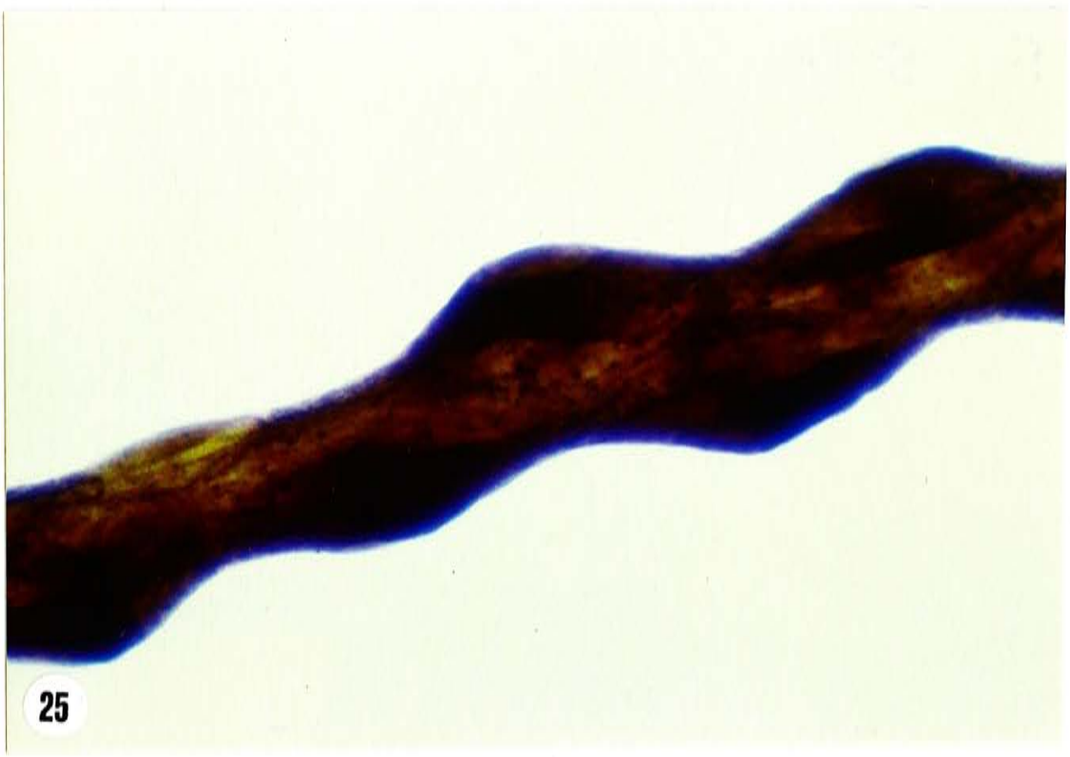

25

Fig. 26. Transverse section of *Pieris* Malpighian tubule; calcium test. The apical and basal cytoplasm of yellow region cell were stained orange-red with Alizarin Red. x700.

Fig. 27. Transverse section of *Pieris* Malpighian tubule; phosphate test. The apical cytoplasm of yellow region cell was stained positively in blue colour. x700.

26

27

Fig. 28. Transverse section of *Pieris* Malpighian tubule; ferric iron test. The apical cytoplasm of yellow region cell stained blue with Turnbull Blue. x700.

Fig. 29. Transverse section of *Pieris* Malpighian tubule; PAS stained. Showing positively stained microvilli (mv), apical and basal cytoplasm of white region cell. x700.

28

29

Fig. 30. Transverse section of *Pieris* Malpighian tubule; Toluidine Blue stained. The microvilli (mv), apical and basal cytoplasm of white region cell were stained positively in purple colour. x700.

Fig. 31. Transverse section of *Pieris* Malpighian tubule; Sudan Black B stained. Showing lipid localised in microvilli (mv), apical and basal cytoplasm of white region cell. x700.

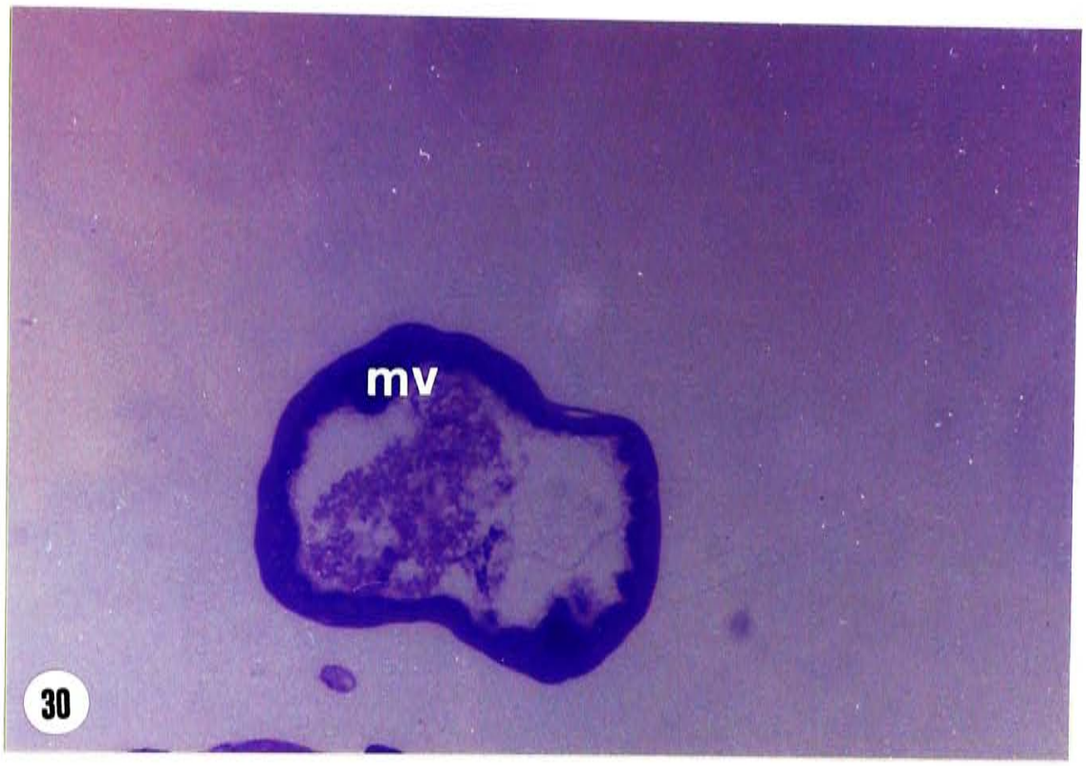
mv
30


mv
31

Fig. 32. Whole mount of *Pieris* Malpighian tubule; Succinic Dehydrogenase test. Showing Succinic Dehydrogenase associated with microvilli, apical and basal cytoplasm of white region cell. x700.

Fig. 33. Whole mount of *Pieris* Malpighian tubule; Alkaline Phosphatase test. The microvilli, apical and basal cytoplasm of white region cell were stained positively in black colour. x350.

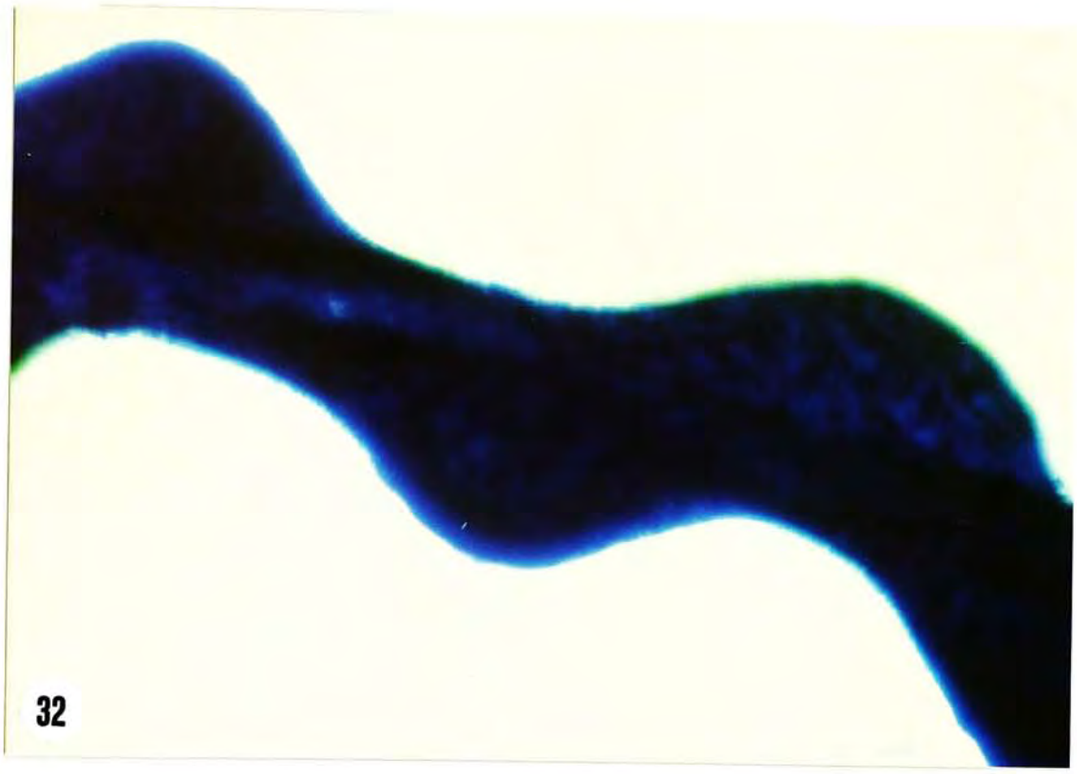

32

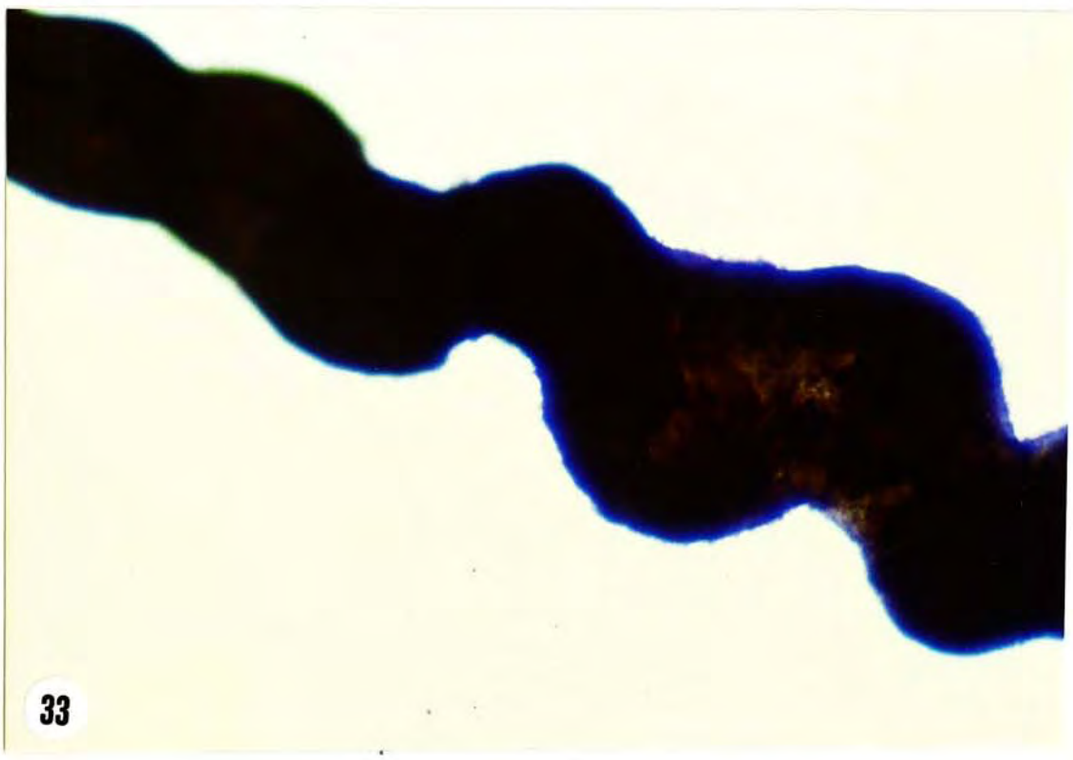

33

Fig. 34. Whole mount of *Pieris* Malpighian tubule; Acid Phosphatase test. Showing positively stained apical cytoplasm of white region cell. x350.

Fig. 35. Separation of the parasporal crystals, spores and cell debris of the HD-1 strain of *Bacillus thuringiensis* var. *kurstaki* in urografine gradients. cd: cell debris, c: crystals, s: spores.

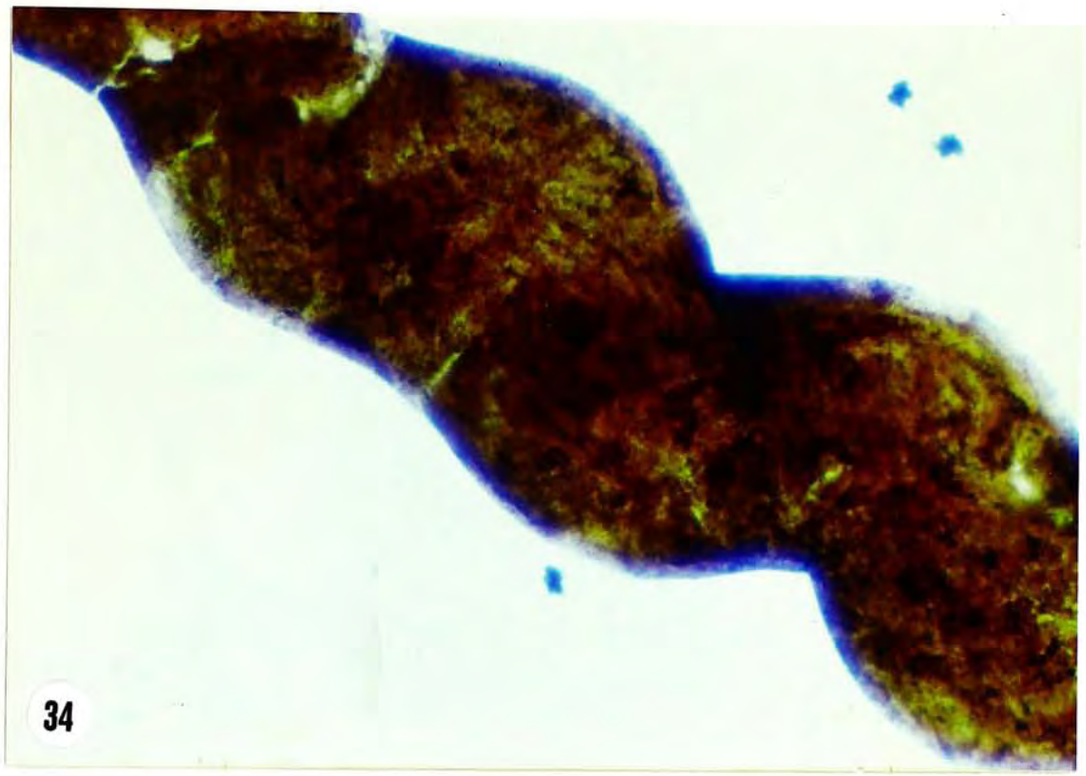

34

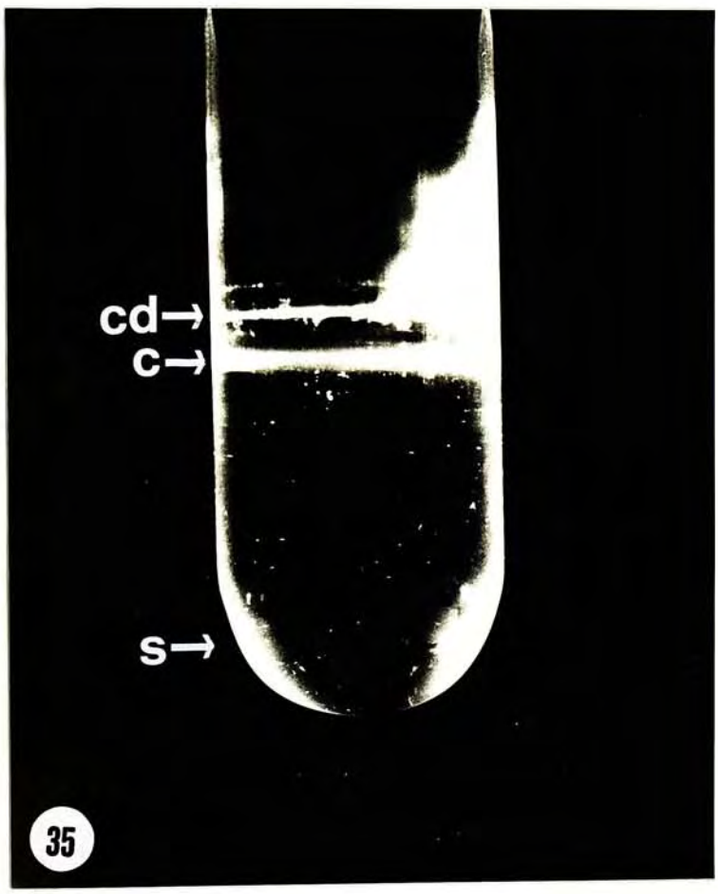

35

Fig. 36. Solublized products of the crystals analyzed on SDS-polyacrylamide gel electrophoresis. a and c. Molecular weight standards; myosin 200 KDa, ß-galactosidase 116.25 KDa, phosphorylase B 97.4 KDa, bovine serum albumin 66.2 KDa and ovalbumin 42.69 KDa. B. P1 134 kDa and P2 63 KDa toxin preparations.

Fig. 37. Scanning electron micrograph of P1 and P2 crystals after purification. Showing crystal morphology of *Bacillus thuringiensis* var. *kurstaki* strain HD-1.

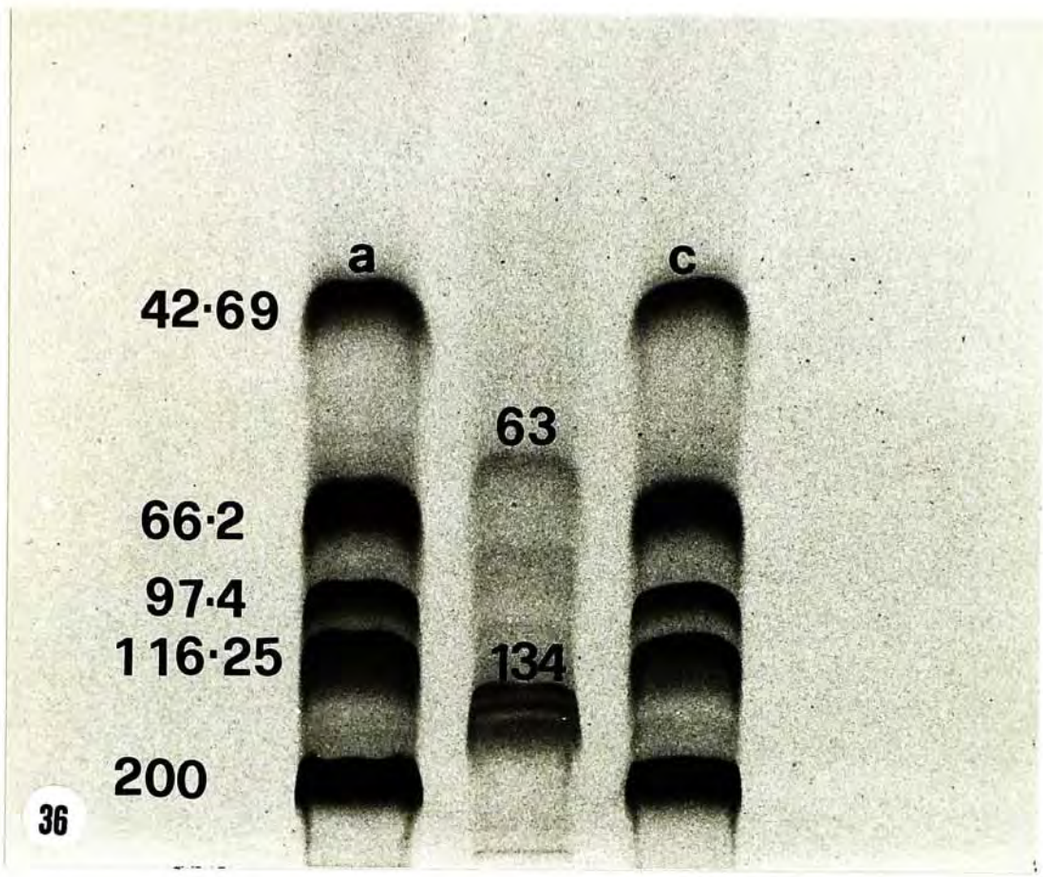

36

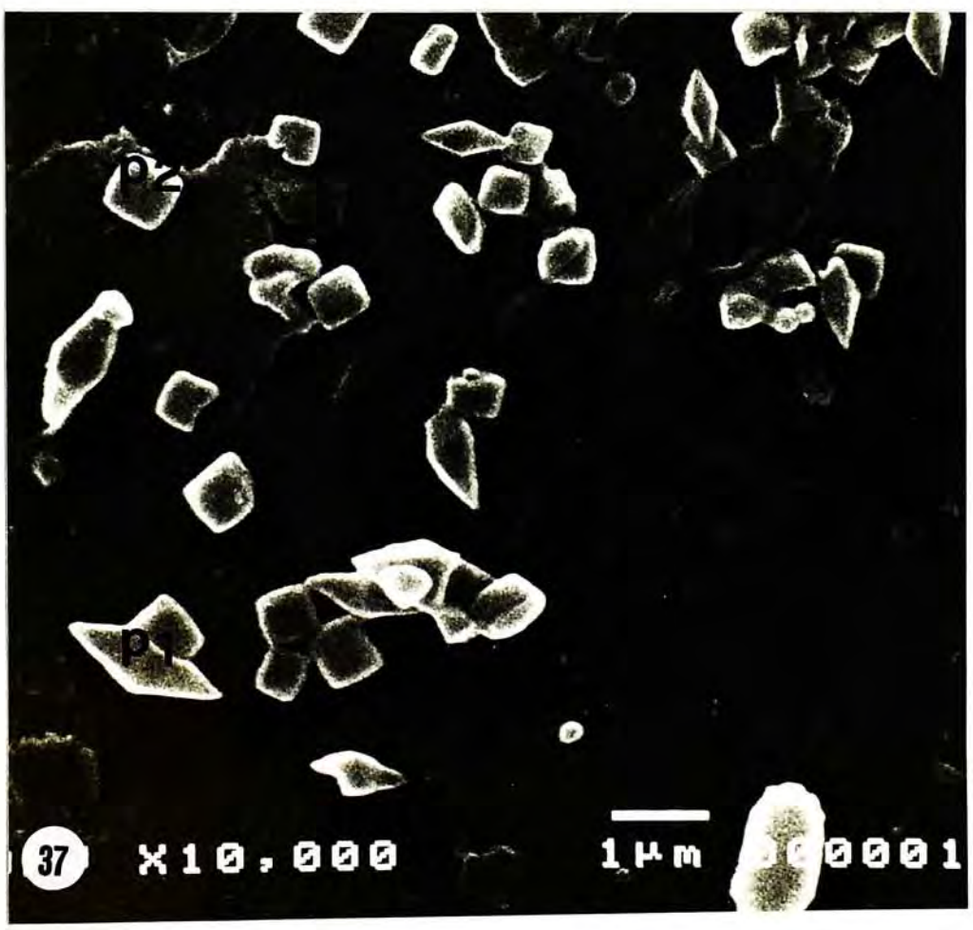

37

Fig. 38. As above, showing P1 crystals.

Fig. 39. As above, showing P2 crystals.


p1
38 X15,000
1µm 000005

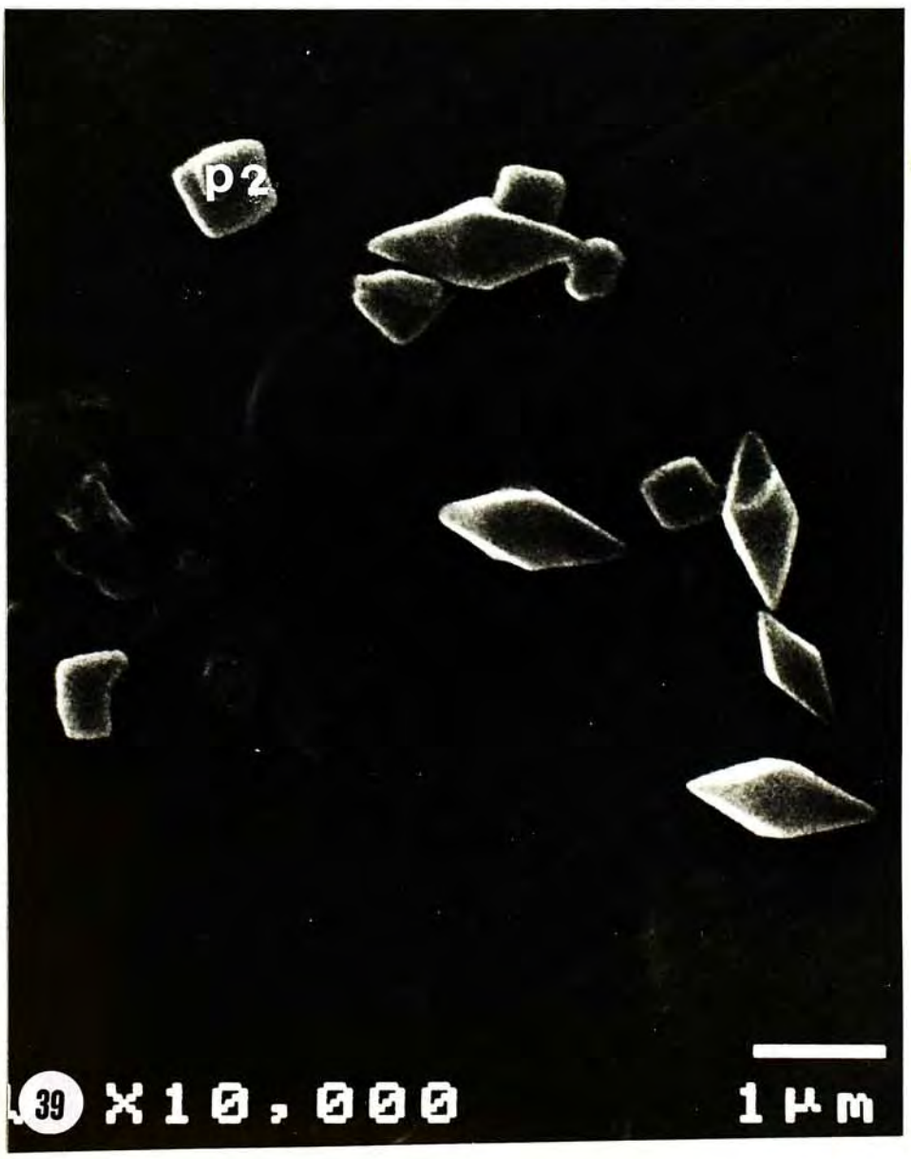
p2
39 X10,000
1µm

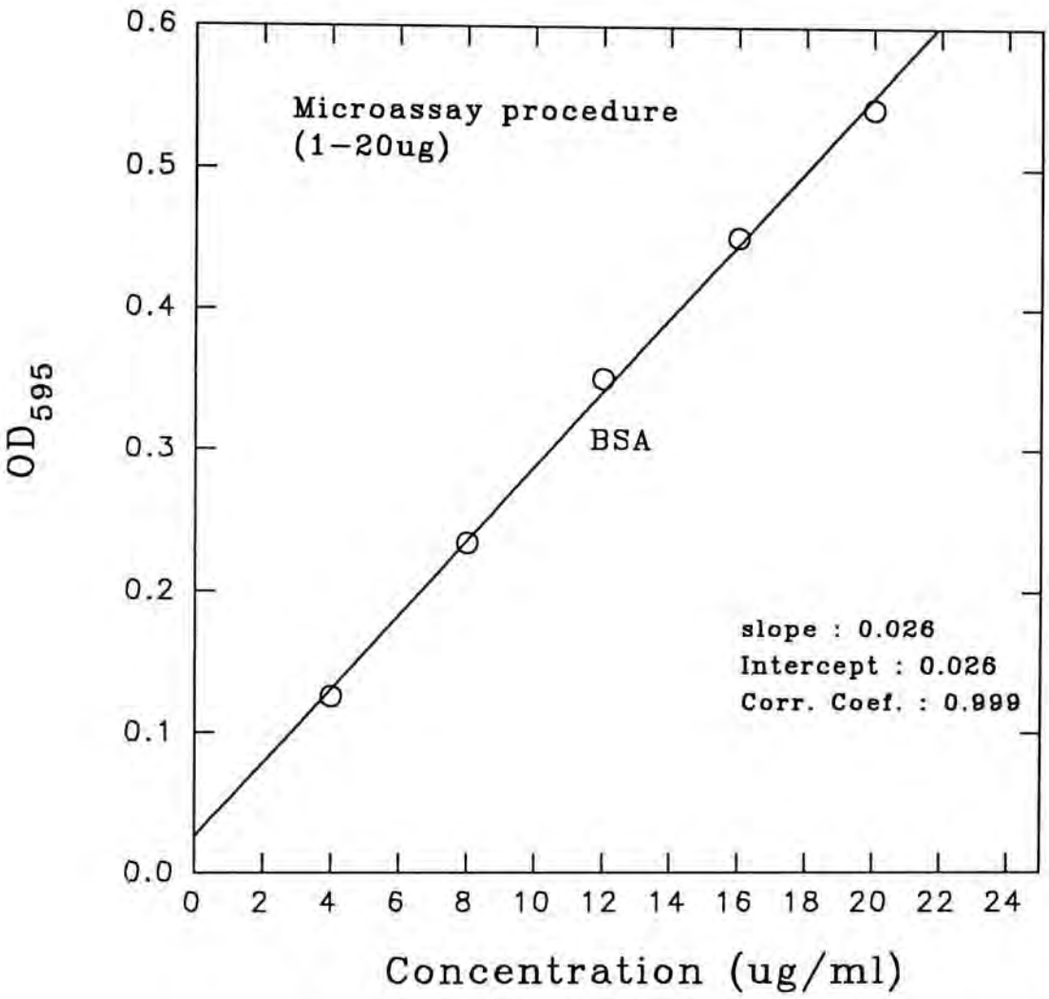

Figure 40. Standard curve of the Bio–Rad Protein Micro Assay (1–20ug/ml) : Bovine Serum Albumin.

Fig. 41. Mucosal exposure of principal cell treated with control CAPS buffer for 20 min. Showing microvilli (mv) with mitochondria (m), rough endoplasmic reticulum (rer), vacuoles (v), cytoplasmic spaces (cs) and basement membrane (bm). x10080.

Fig. 42. Mucosal exposure of principal cell treated with 0.00001 μg/ml toxin for 1 min. Showing numerous vacuoles (v), microvilli (mv) and nucleus (n) with dispersed chromatin materials. x3990.

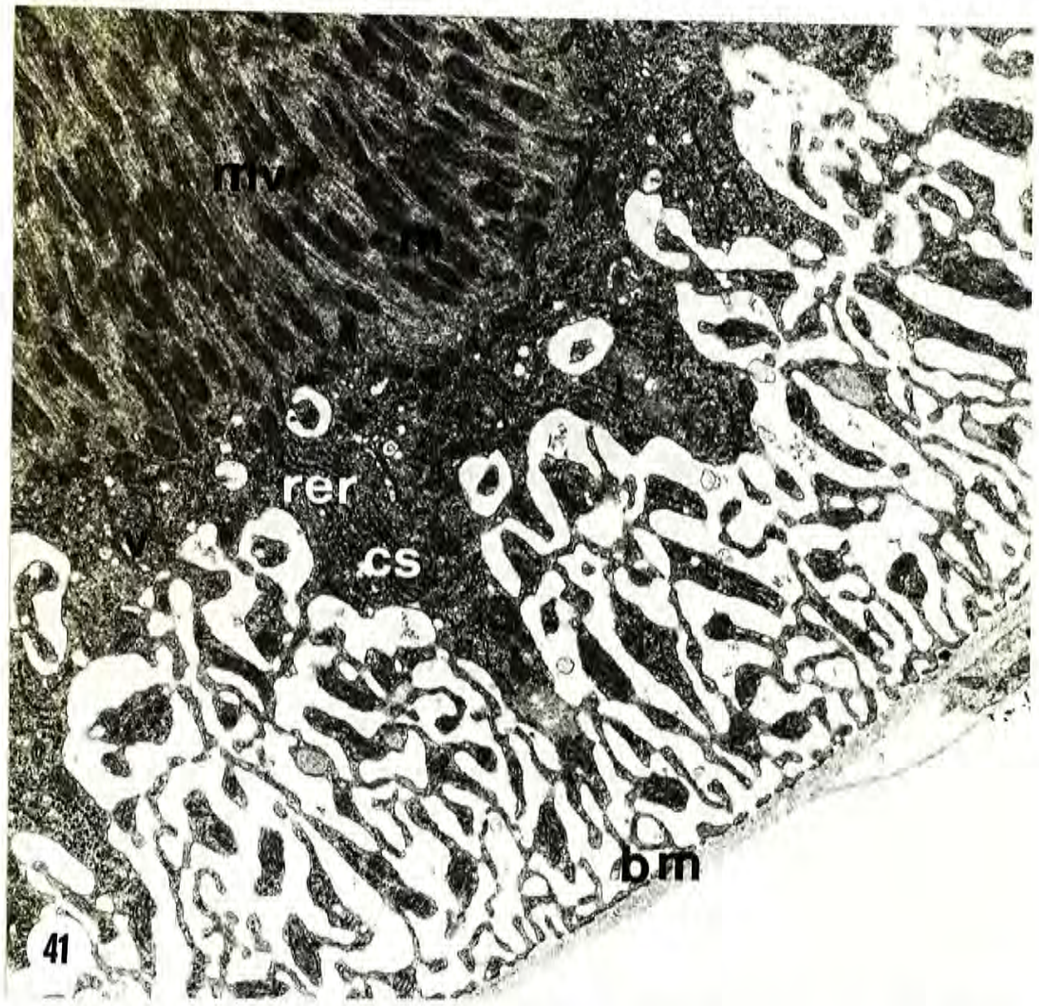
mv
m
rer
v
cs
bm
41

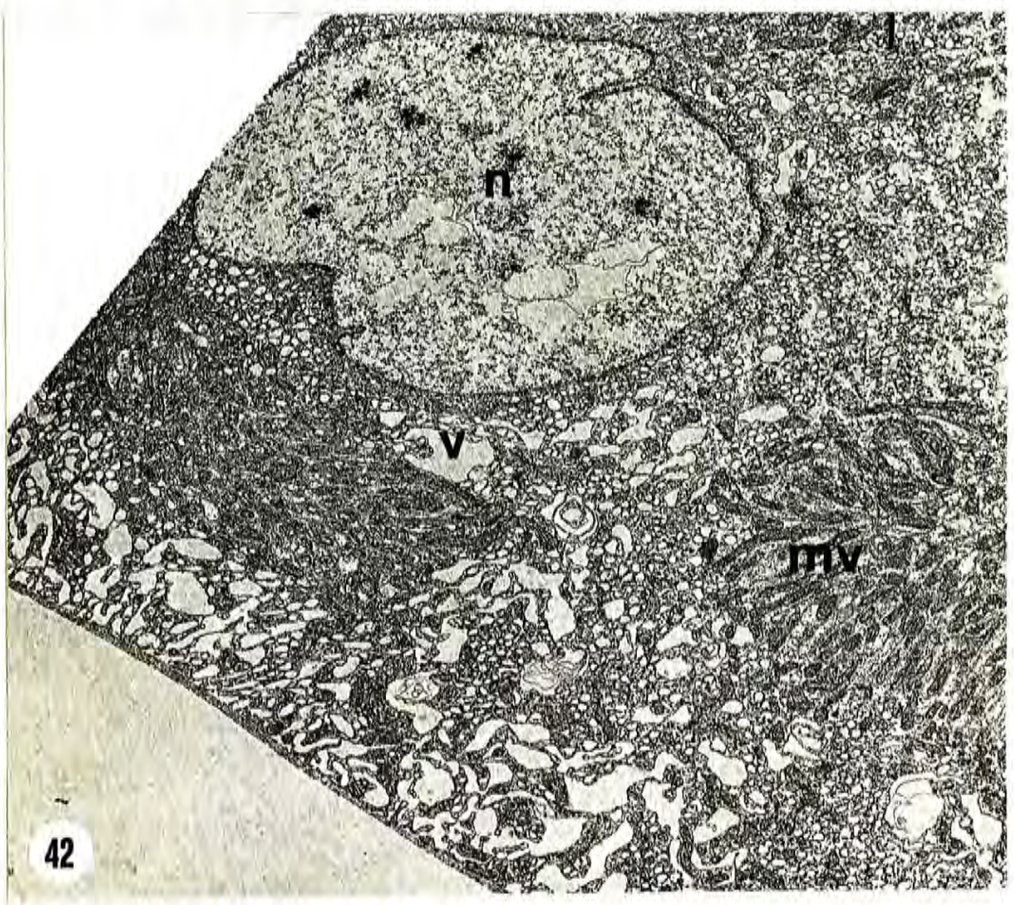
l
n
v
mv
42

Fig. 43. As above. Showing disorganized microvilli. x15120.

Fig. 44. As above. Showing numerous vacuoles (v), mitochondria (m) and tight cell junction (d). x10080.

43

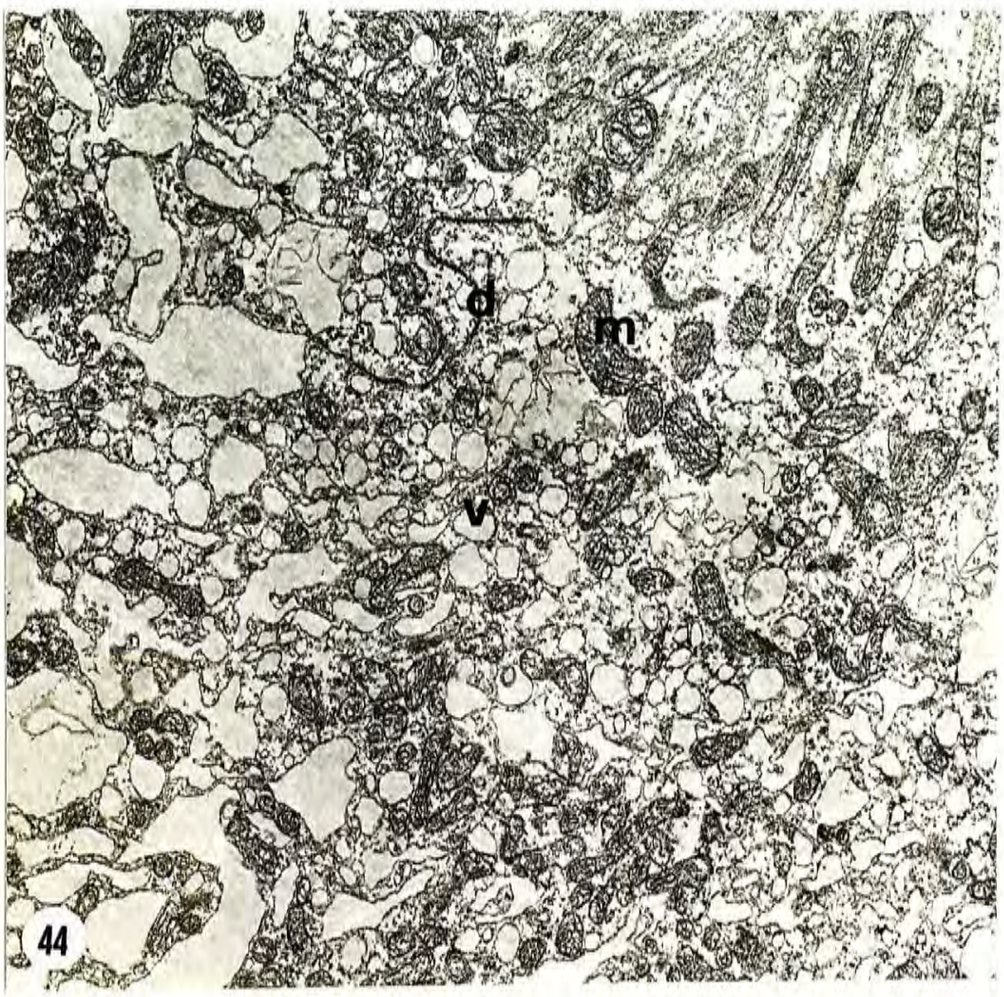

44

Fig. 45. As above. Showing microvilli (mv), vacuoles (v), mitochondria (m) and the nucleus (n) with dispersed chromatin materials. x6090.

Fig. 46. Mucosal exposure of principal cell treated with 0.00001 μg/ml toxin for 10 min. Showing damaged microvilli (mv), numerous vacuoles (v) and mitochondria (m). x6090.

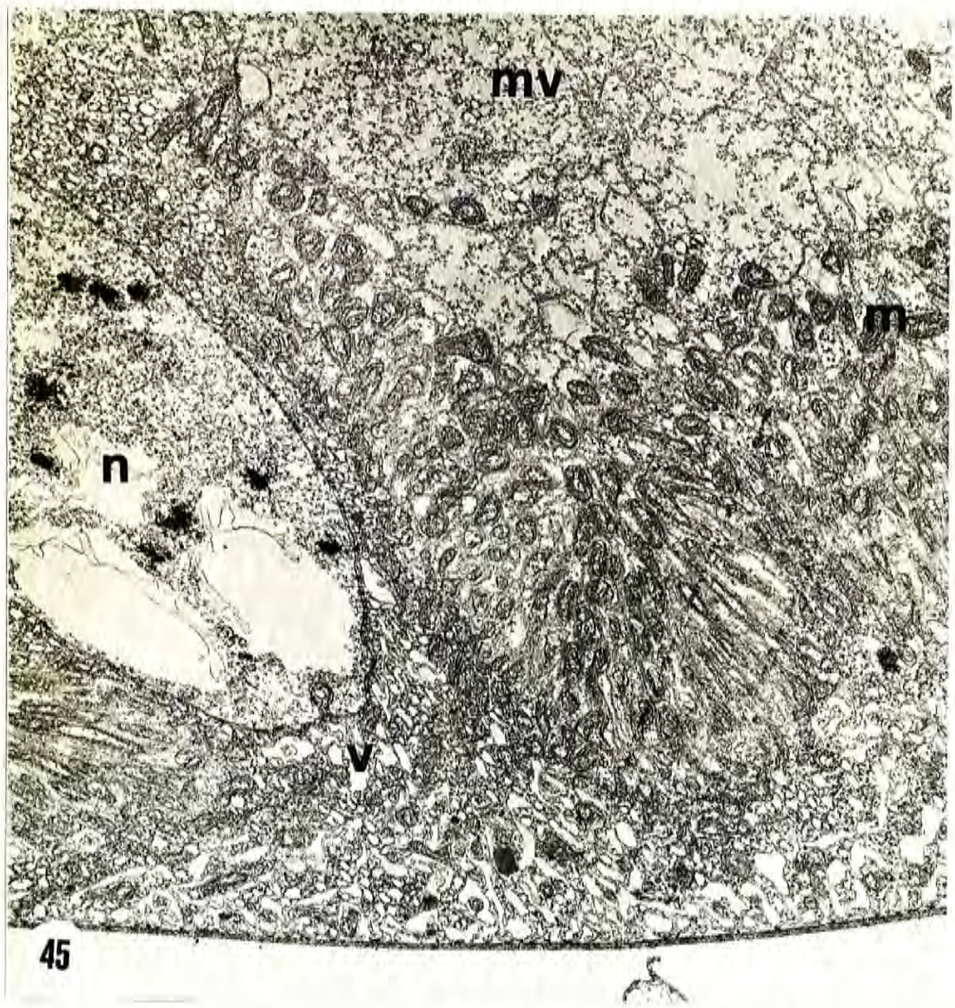

45

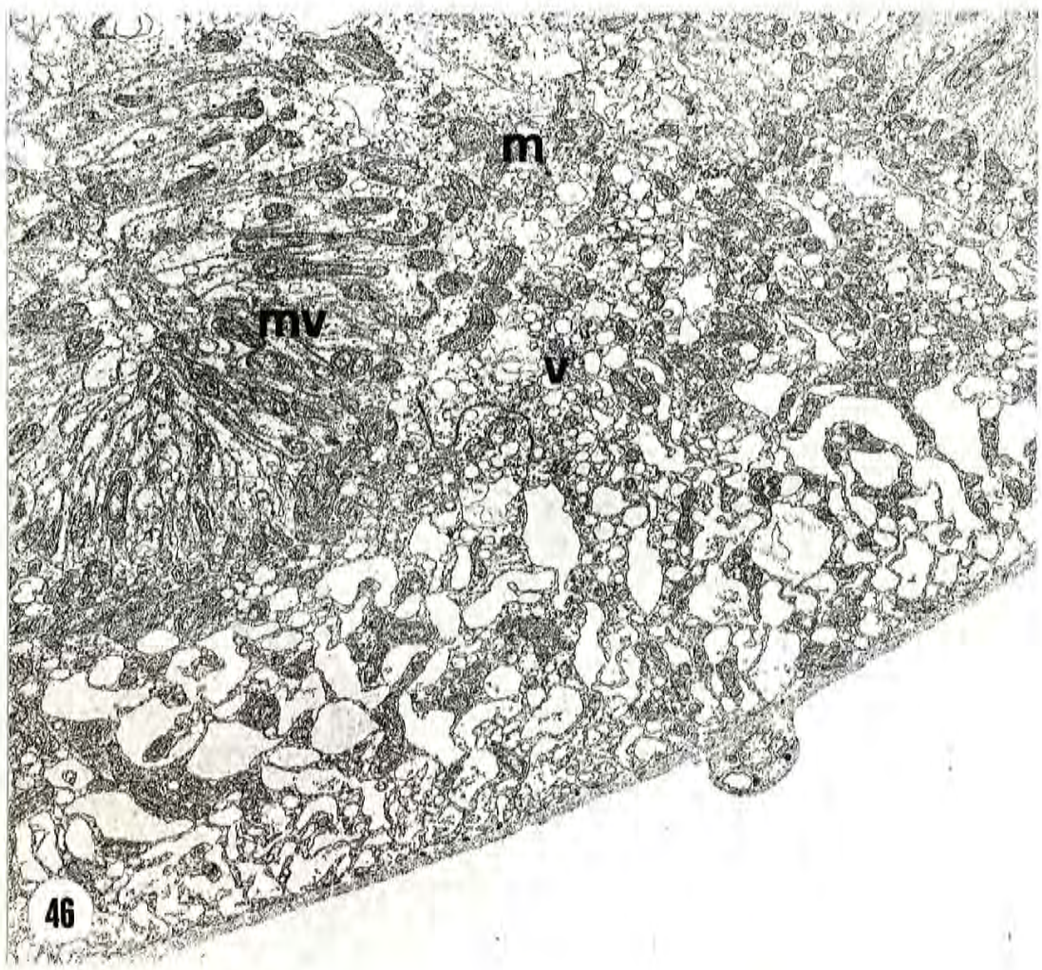

46

Fig. 47. As above. Showing distorted microvilli (mv). x12180.

Fig. 48. As above. Apical region. Showing lysed microvilli (mv) and mitochondria (m). x10100.

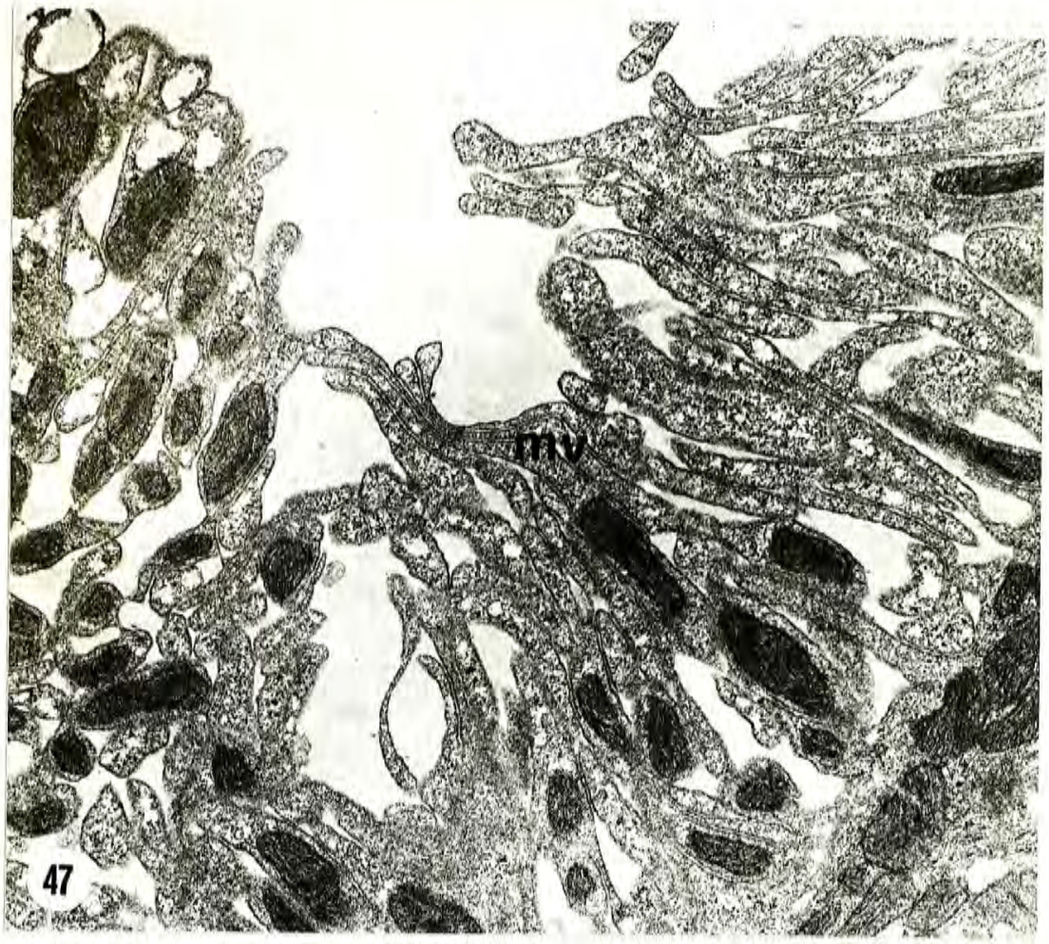
mv
47

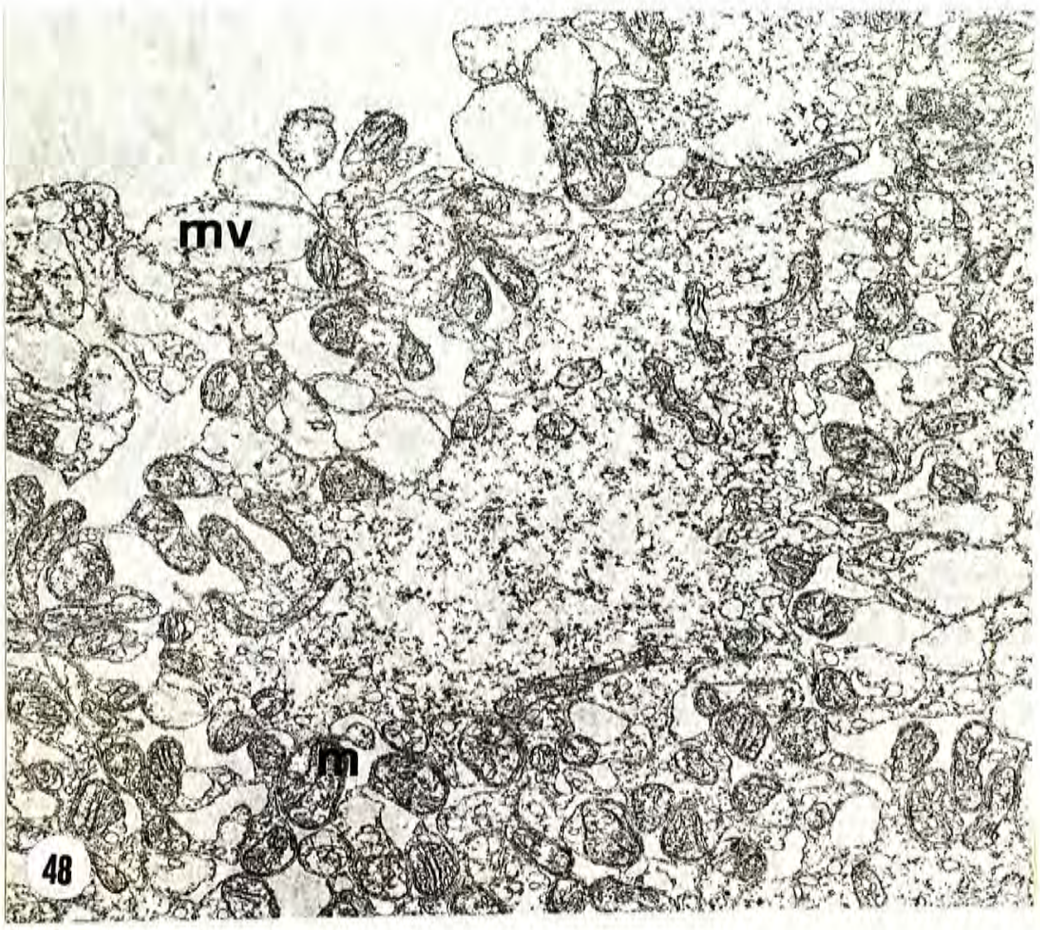
mv
m
48

Fig. 49. Mucosal exposure of principal cell treated with 0.00001 μg/ml toxin for 20 min. Showing damaged microvilli, mitochondria (m), vacuoles (v) and basement membrane (bm). x3990.

Fig. 50. As above. Apical region. Showing damaged microvilli (mv) and extrusion of apical cytoplasm with nucleus (n). x10080.

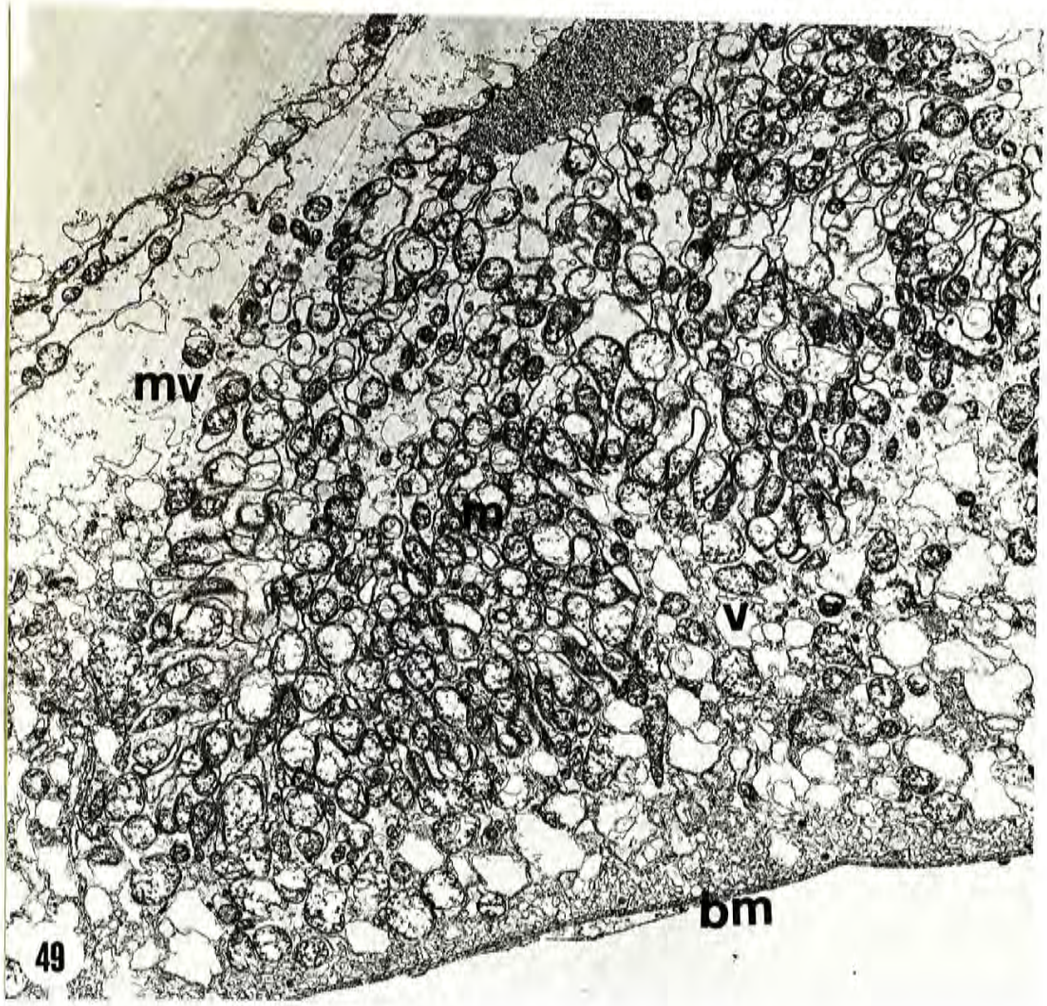

49

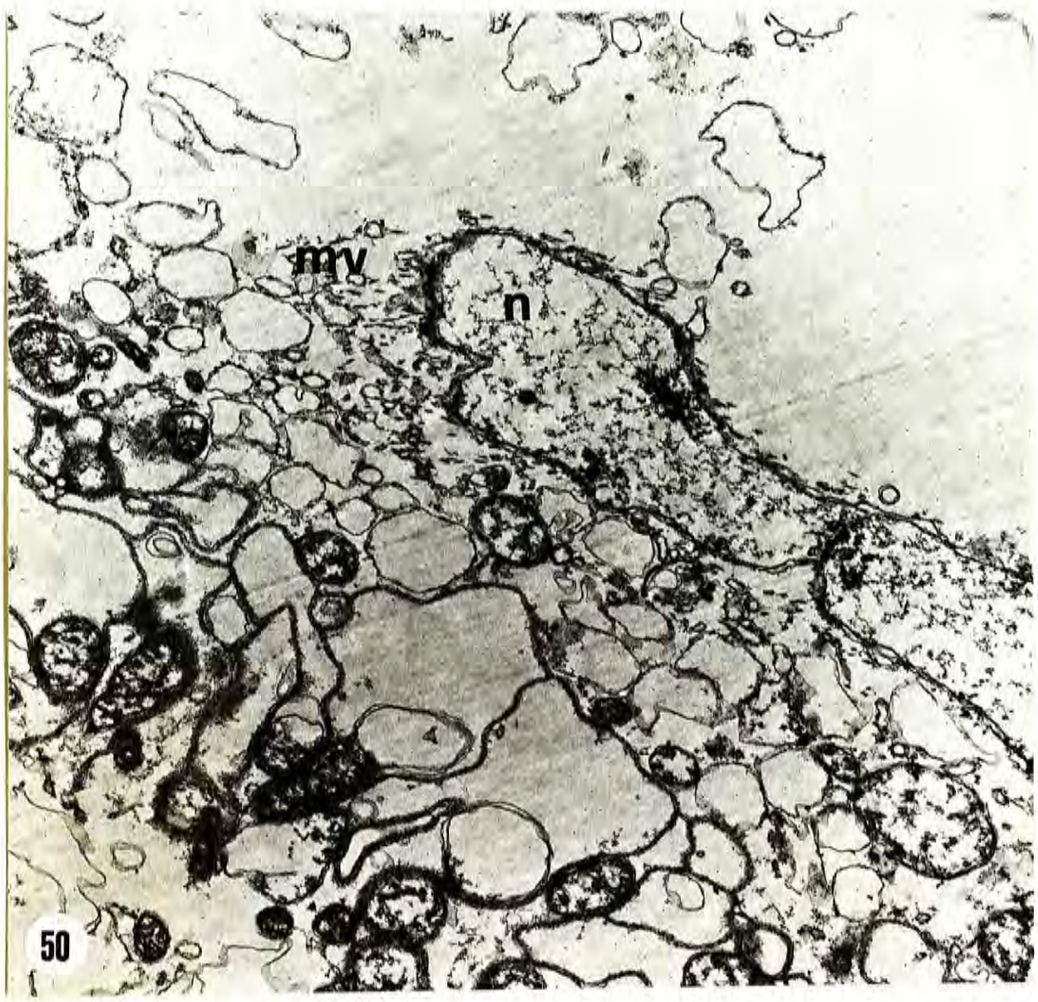

50

Fig. 51. As above. Showing mitochondria (m), vacuolated rough endoplasmic reticulum (rer) and golgi apparatus (g). x10080.

Fig. 52. As above. Basal region. Showing damaged basement membrane (bm), numerous vacuoles (v) and mitochondria (m) with cristae impaired. x15120.

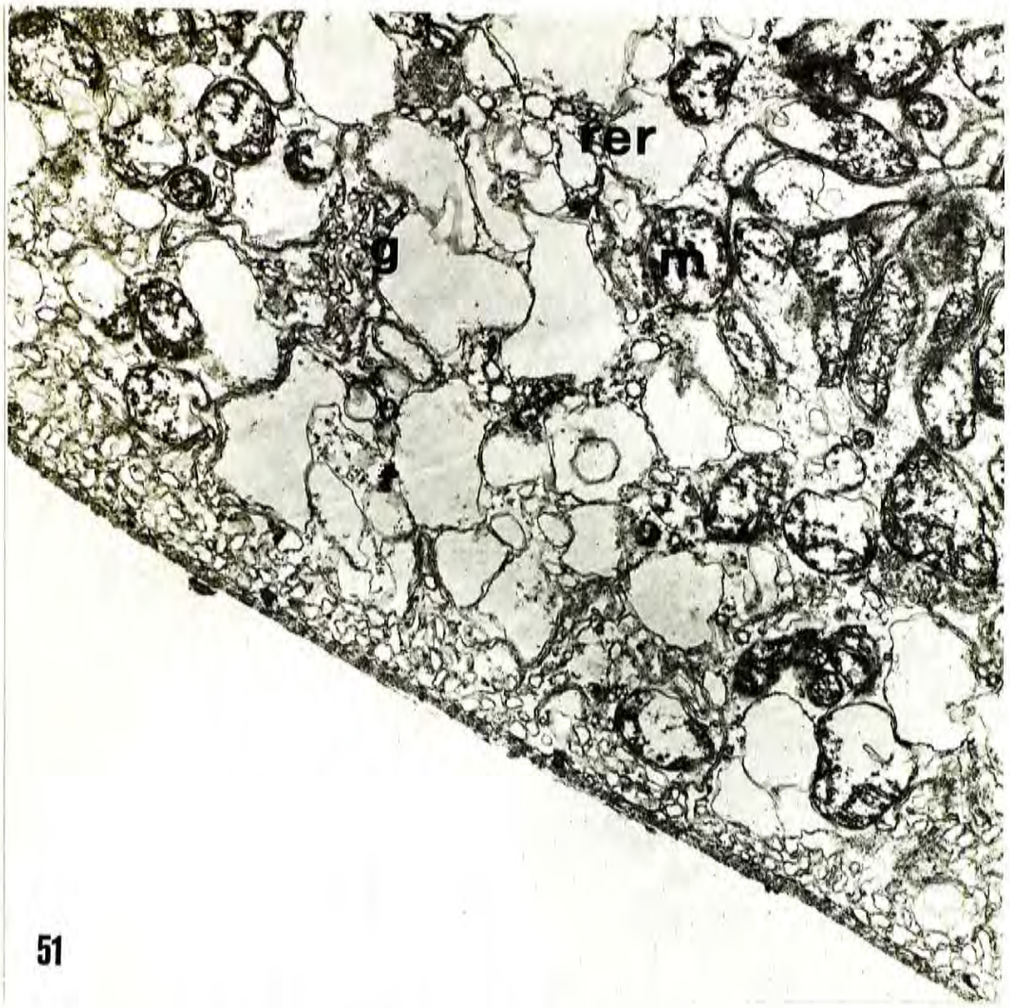

51

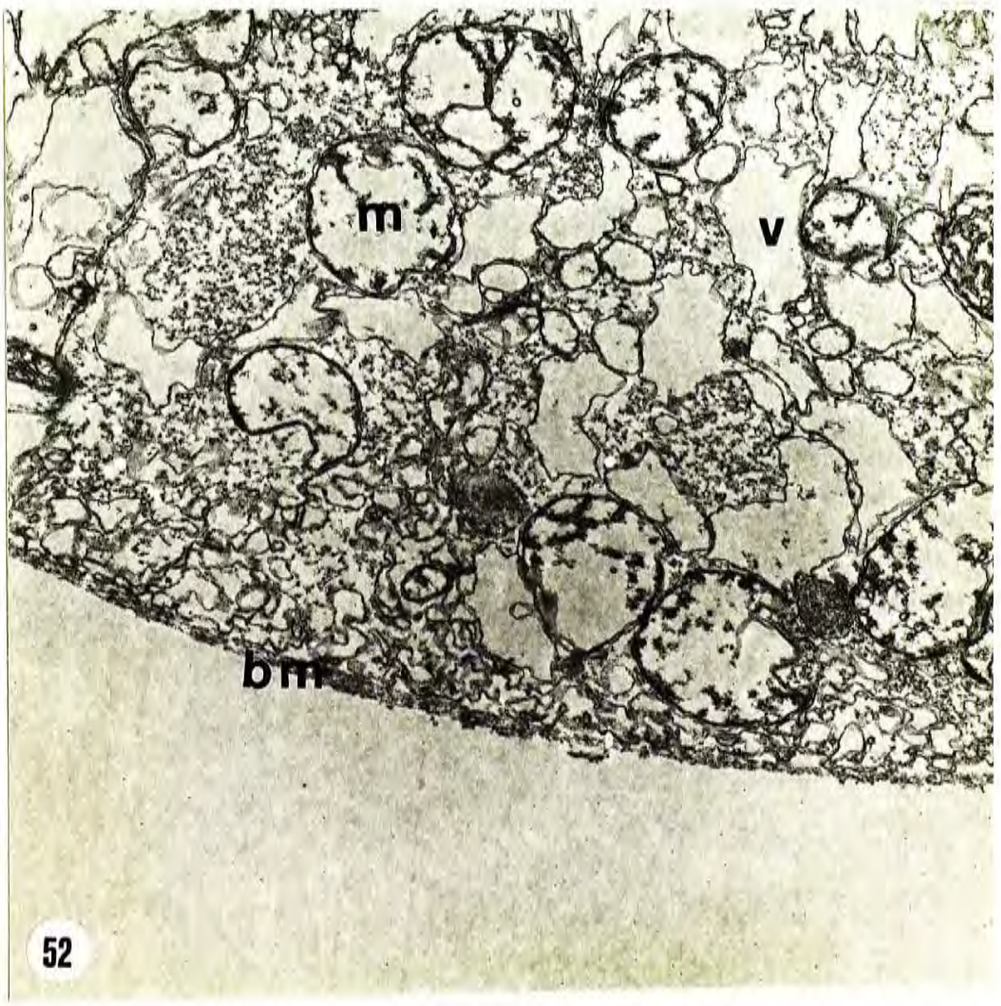

52

Fig. 53. As above. Showing mitochondria (m) with cristae impaired and undamaged tight cell junction (d). x15120.

Fig. 54. As above. Showing numerous vacuoles (v) and multivesicular body (mb). x15120.

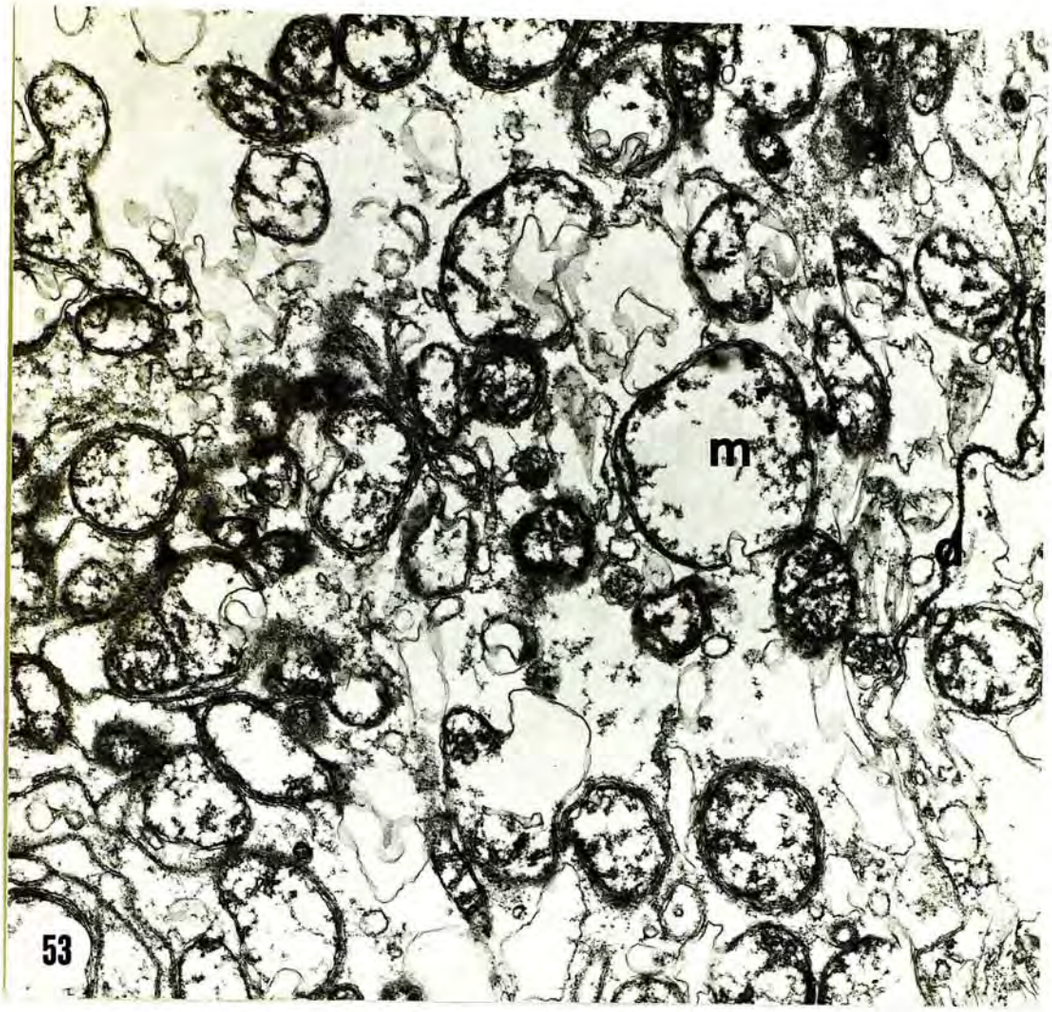
m
53

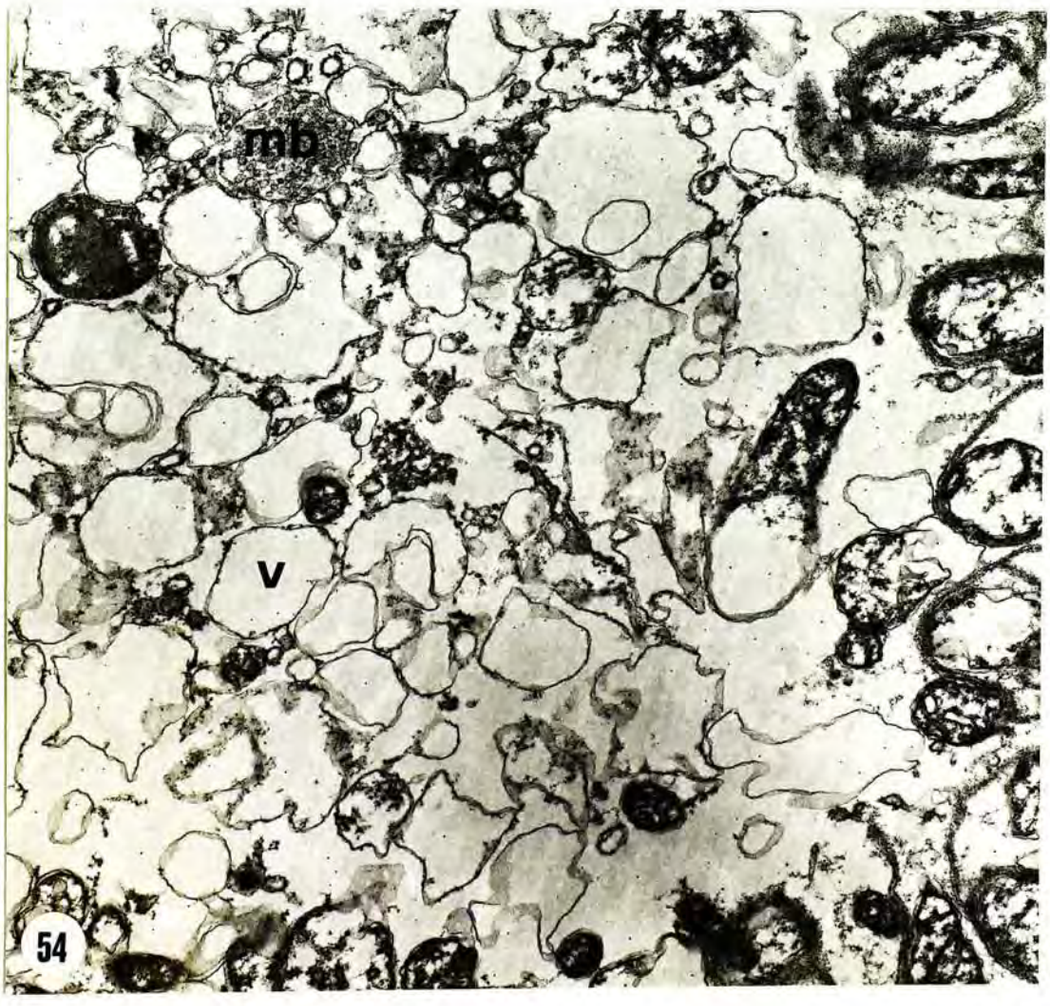
mb
v
54

Fig. 55. Serosal exposure of principal cell treated with control CAPS buffer for 20 min. Showing microvilli (mv), rough endoplasmic reticulum (rer), vacuoles (v) and basement membrane (bm). x10080.

Fig. 56. Serosal exposure of principal cell treated with 0.001 μg/ml toxin for 1 min. Showing numerous vacuoles (v), microvilli (mv), mitochondria (m) and basement membrane (bm). x6090.

55

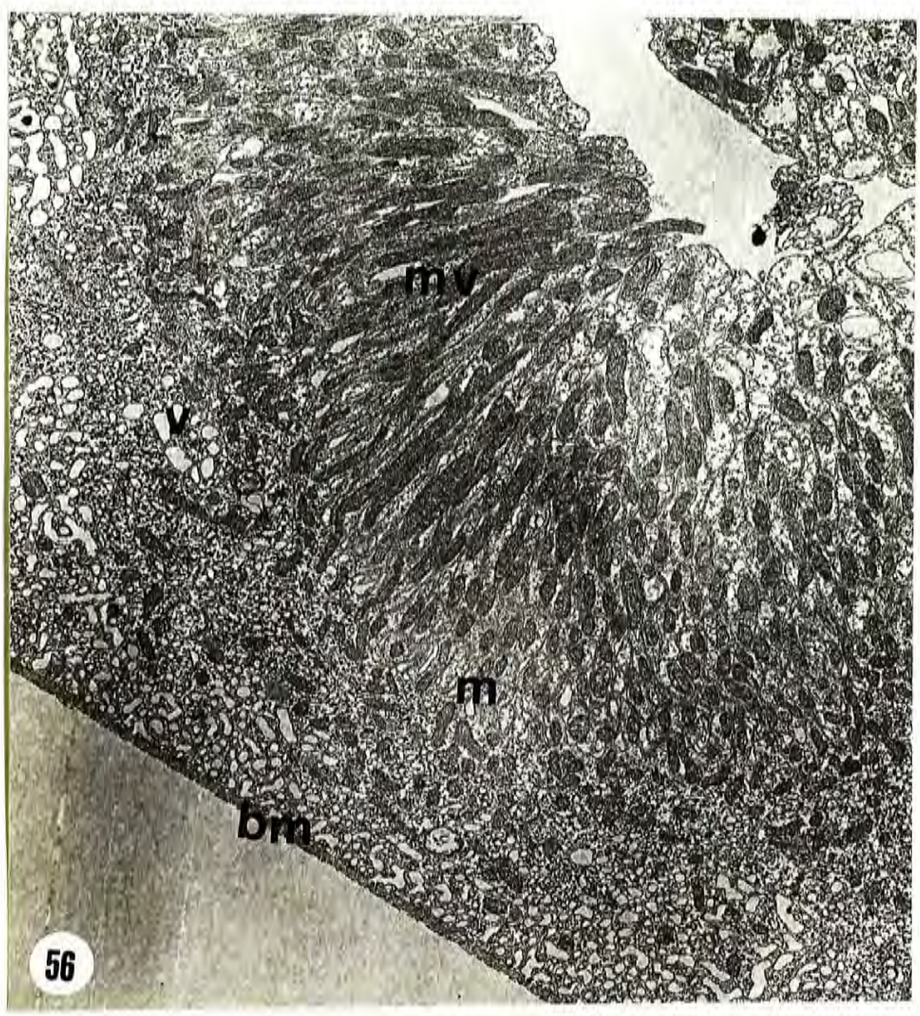

56

Fig. 57. As above. Showing numerous vacuoles (v), mitochondria (m) and tight cell junction (d). x15120.

Fig. 58. As above. Basal region. Showing disorganized basal infoldings and mitochondria (m). x9400.

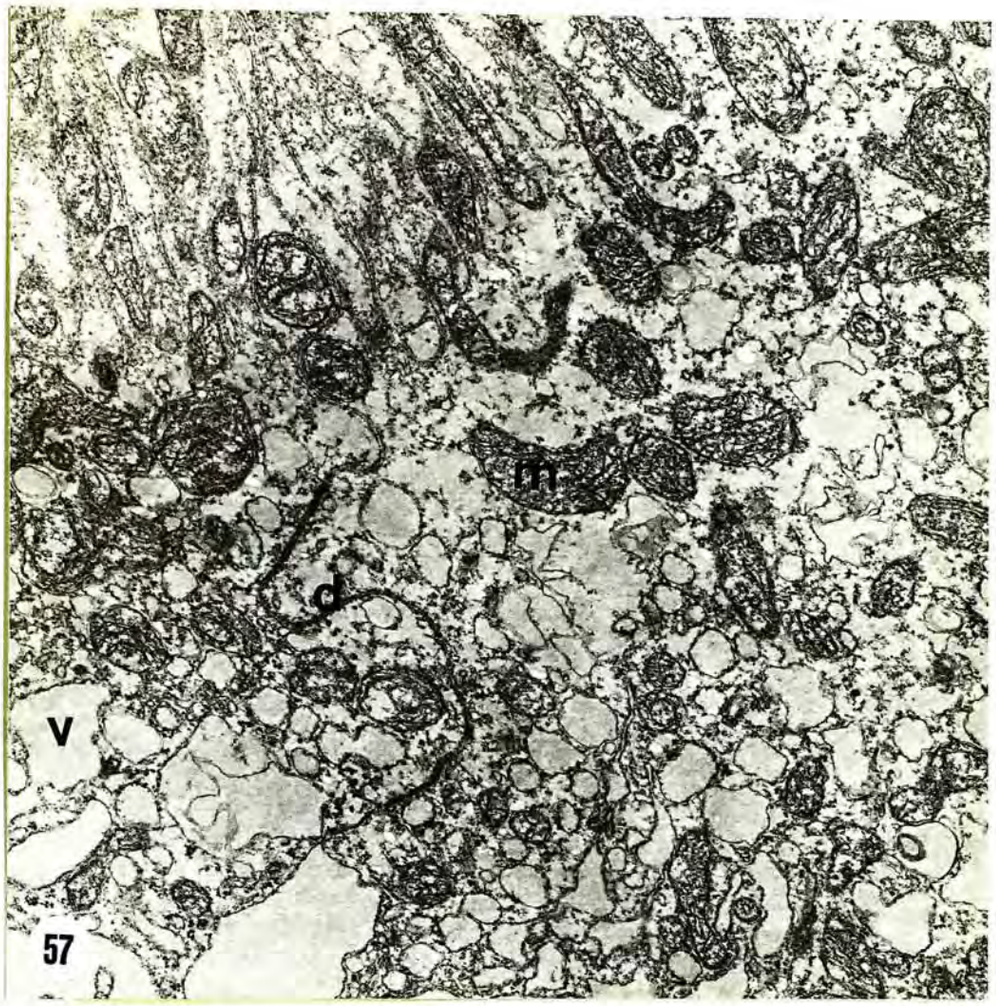
m
d
V
57

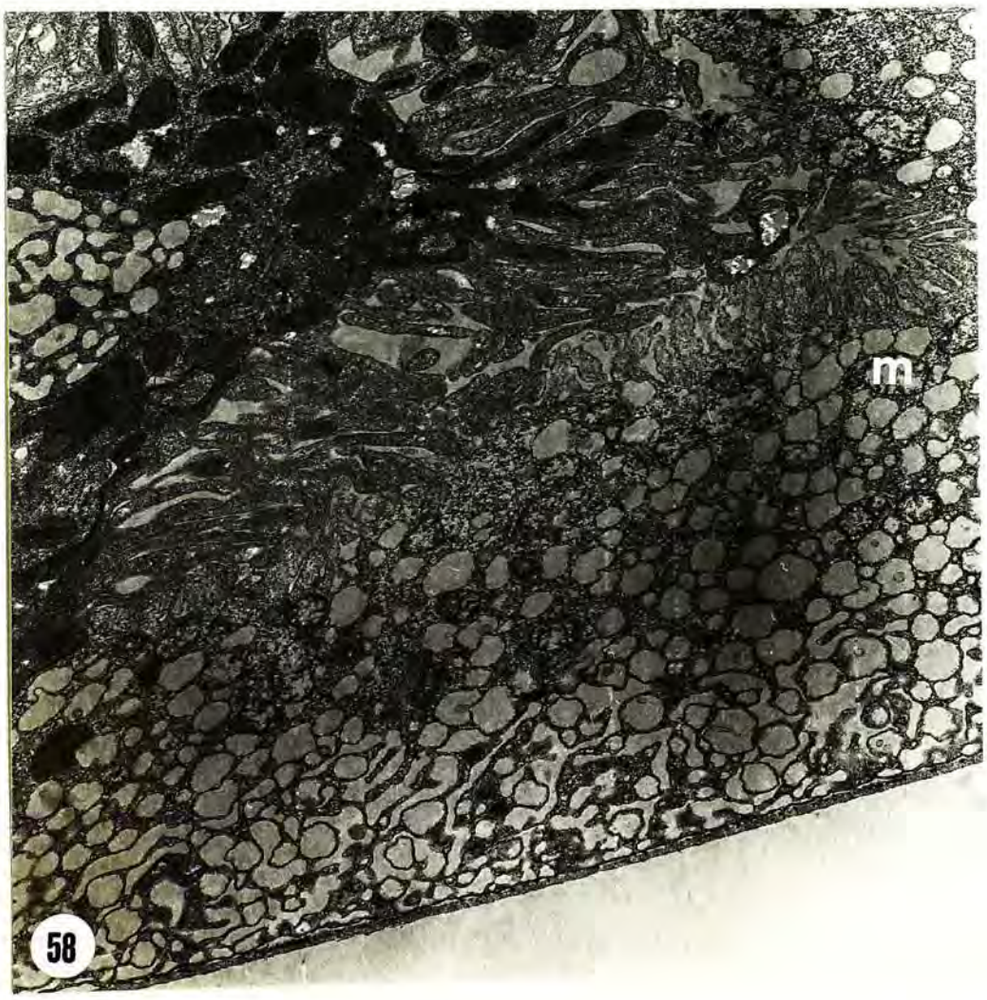
m
58

Fig. 59. Serosal exposure of principal cell treated with 0.001 μg/ml toxin for 10 min. Showing numerous vacuoles (v), mitochondria (m) with cristae damaged and basement membrane (bm). x21000.

Fig. 60. As above. Showing disorganized microvilli (mv) and mitochondria (m). x21000.

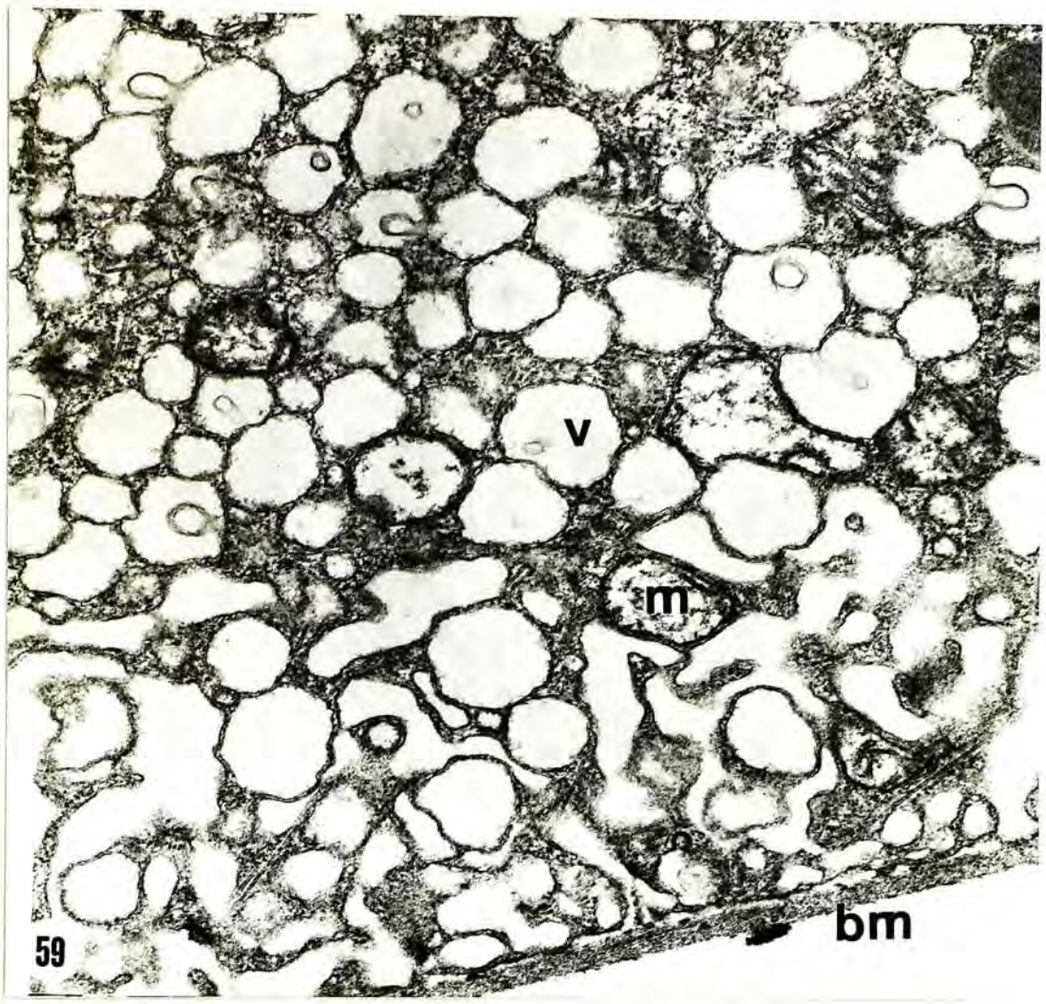
v
m
bm
59

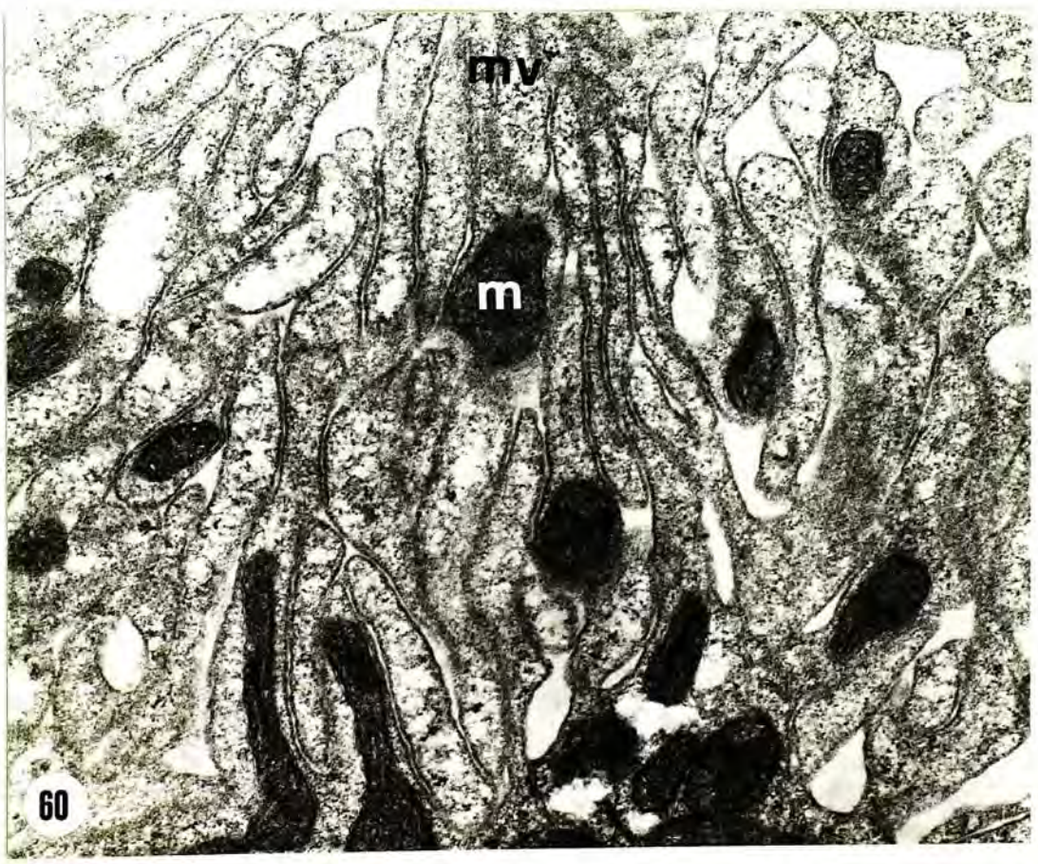
mv
m
60

Fig. 61. As above. Central region. Showing large vacuoles (v) and undamaged mitochondria (m). x21000.

Fig. 62. As above. showing damaged mitochondria (m) and nucleus (n) with dispersed chromatin materials. x7560.

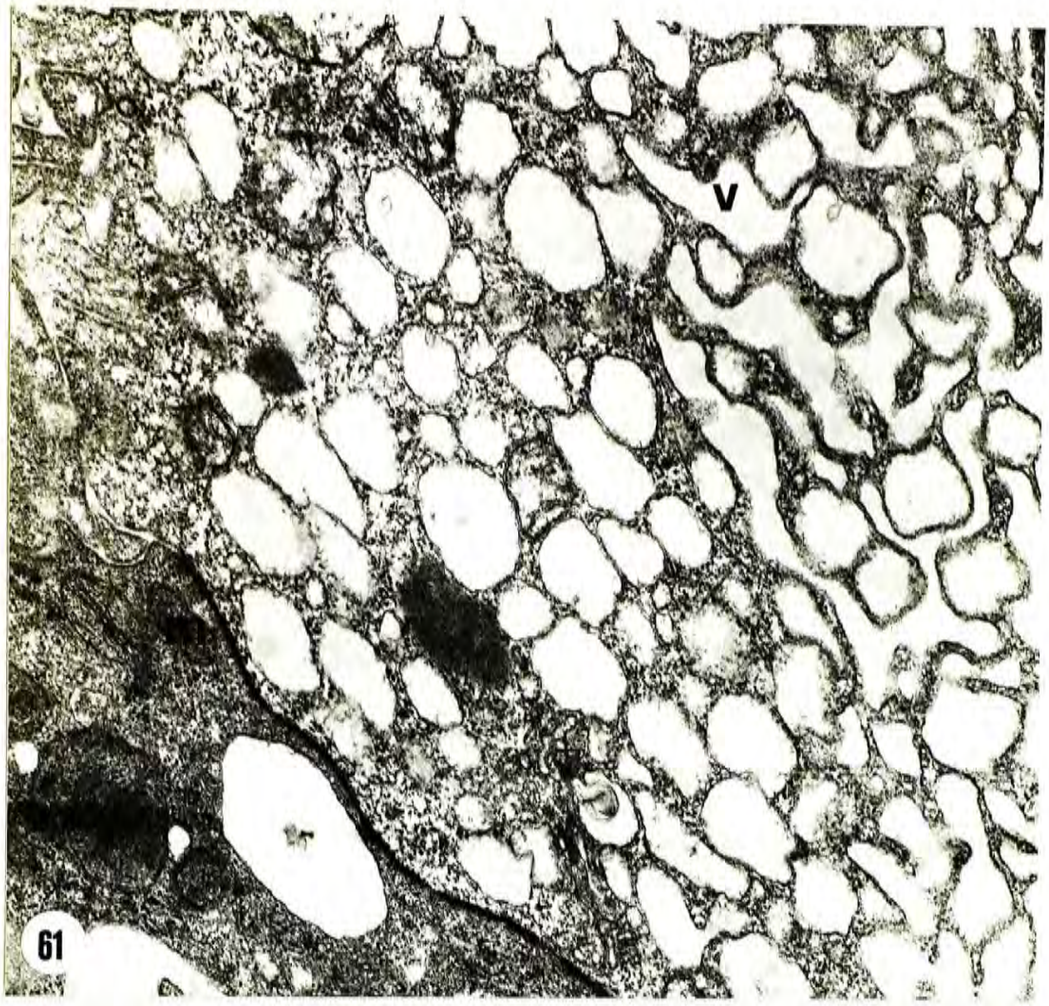
v
61

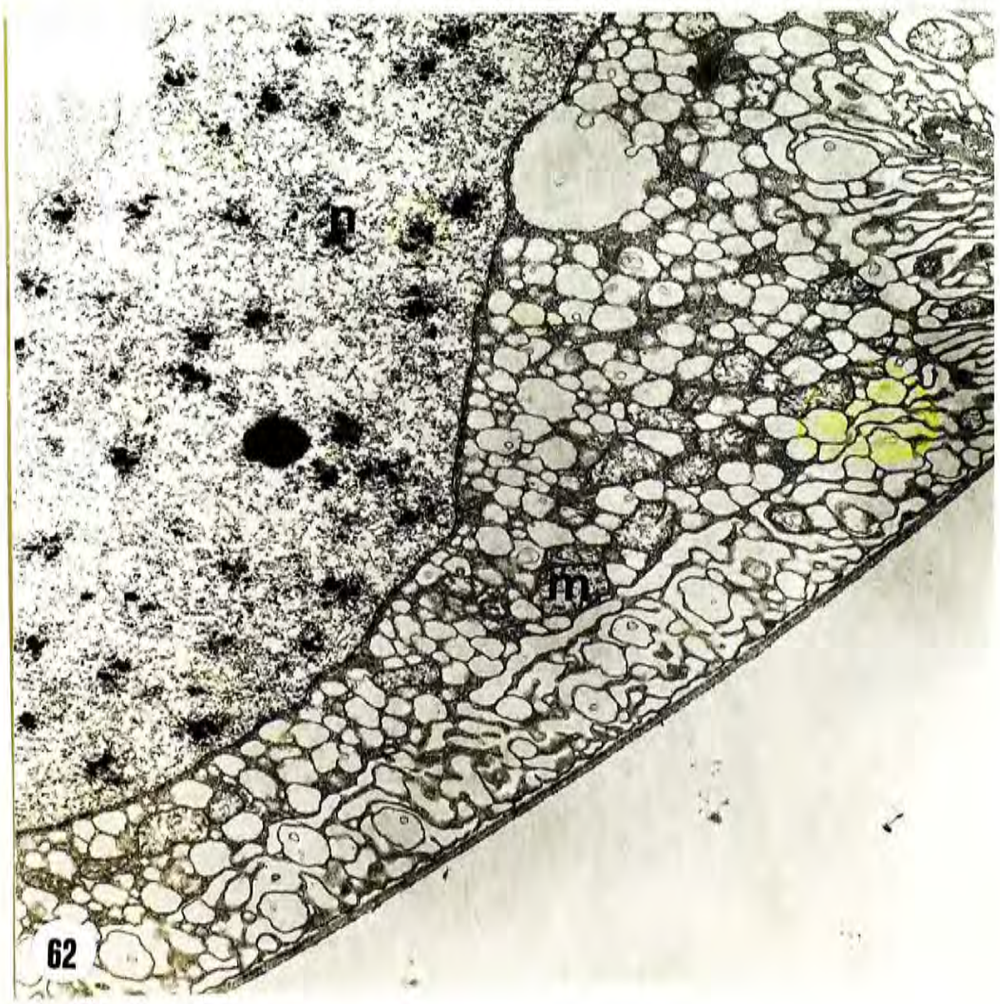
n
m
62

Fig. 63. Serosal exposure of principal cell treated with 0.001 μg/ml toxin for 20 min. Showing damaged microvilli (mv), mitochondria (m), vacuoles (v) and basement membrane (bm). x3990.

Fig. 64. As above. Showing damaged microvilli (mv), nucleus (n), mitochondria (m), vacuoles (v) and basement membrane (bm). x3990.

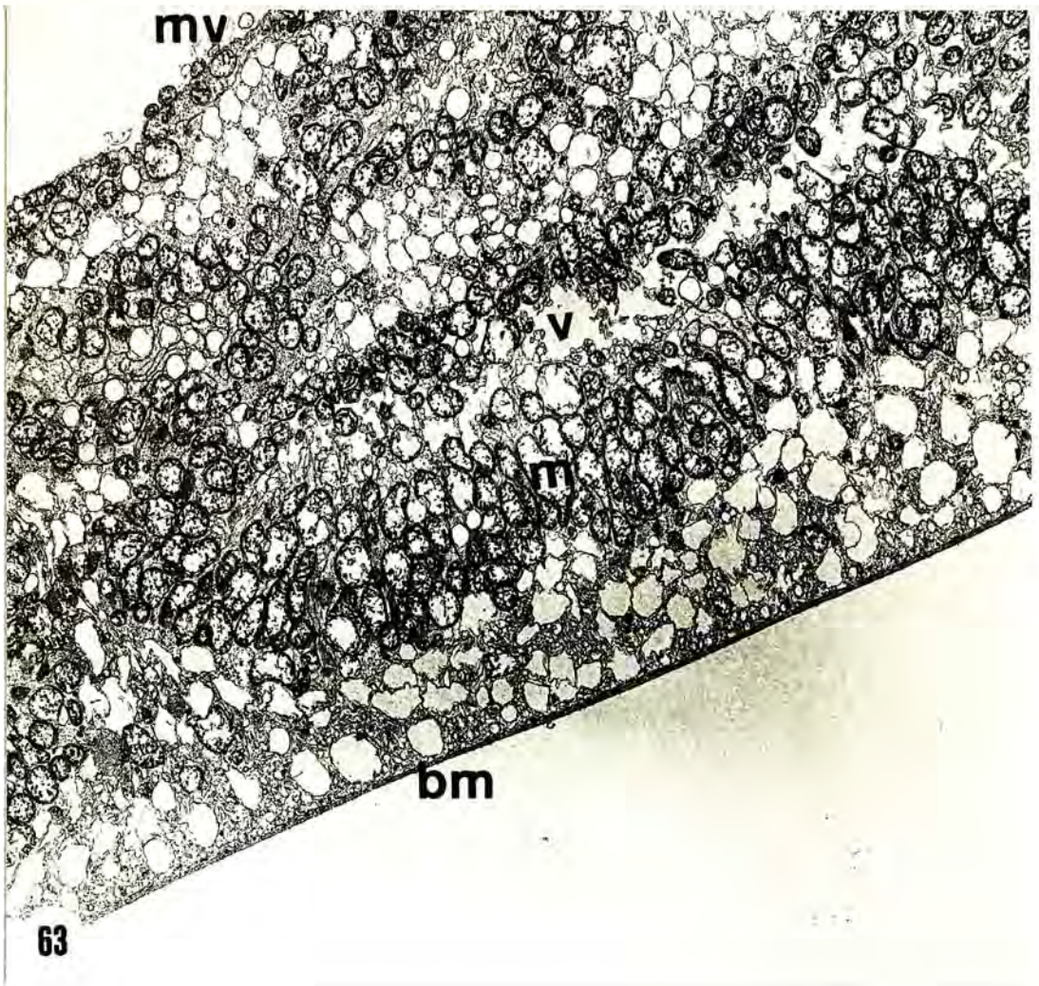

63

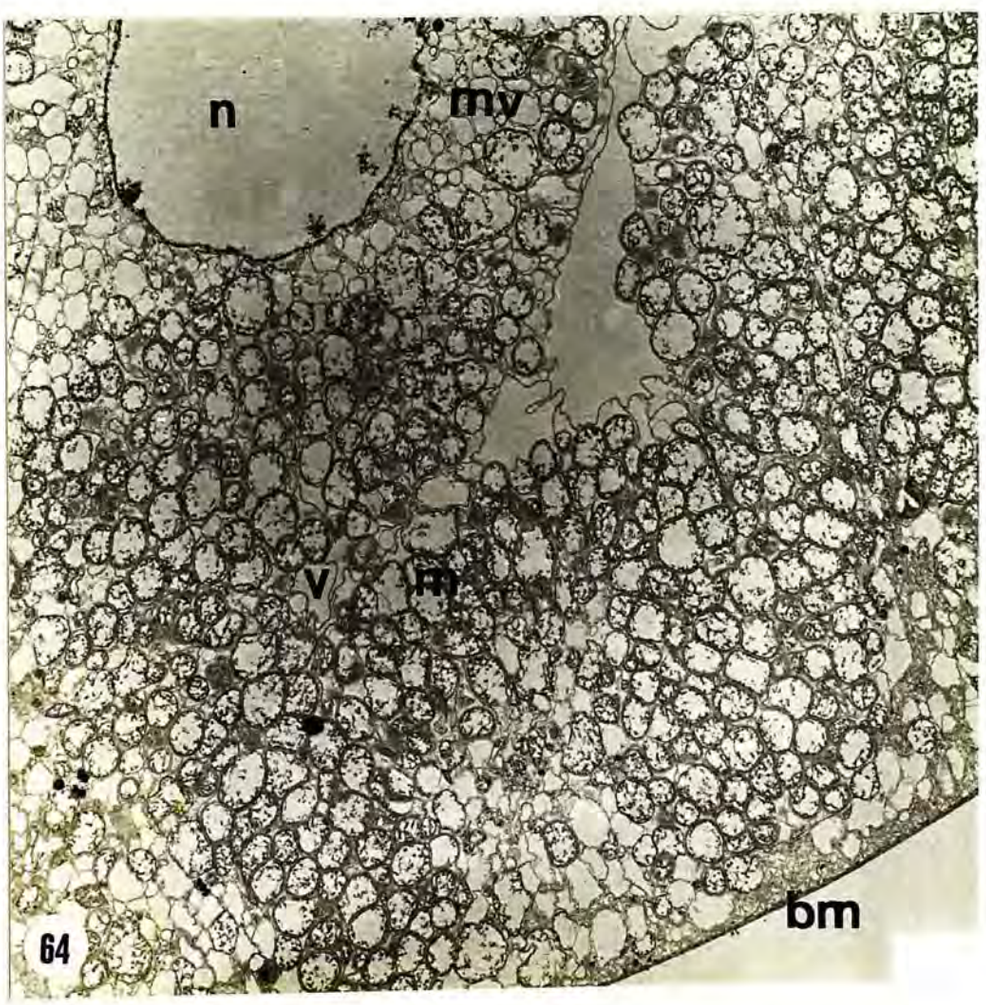

64

Fig. 65. As above. Showing mitochondria (m), large vacuoles (v), lysed rough endoplasmic reticulum (rer), multivesicular body (mb) and basement membrane (bm). x15120.

Fig. 66. As above. Basal region. Showing disorganized basal infoldings and myelin figure (mf). x15120.

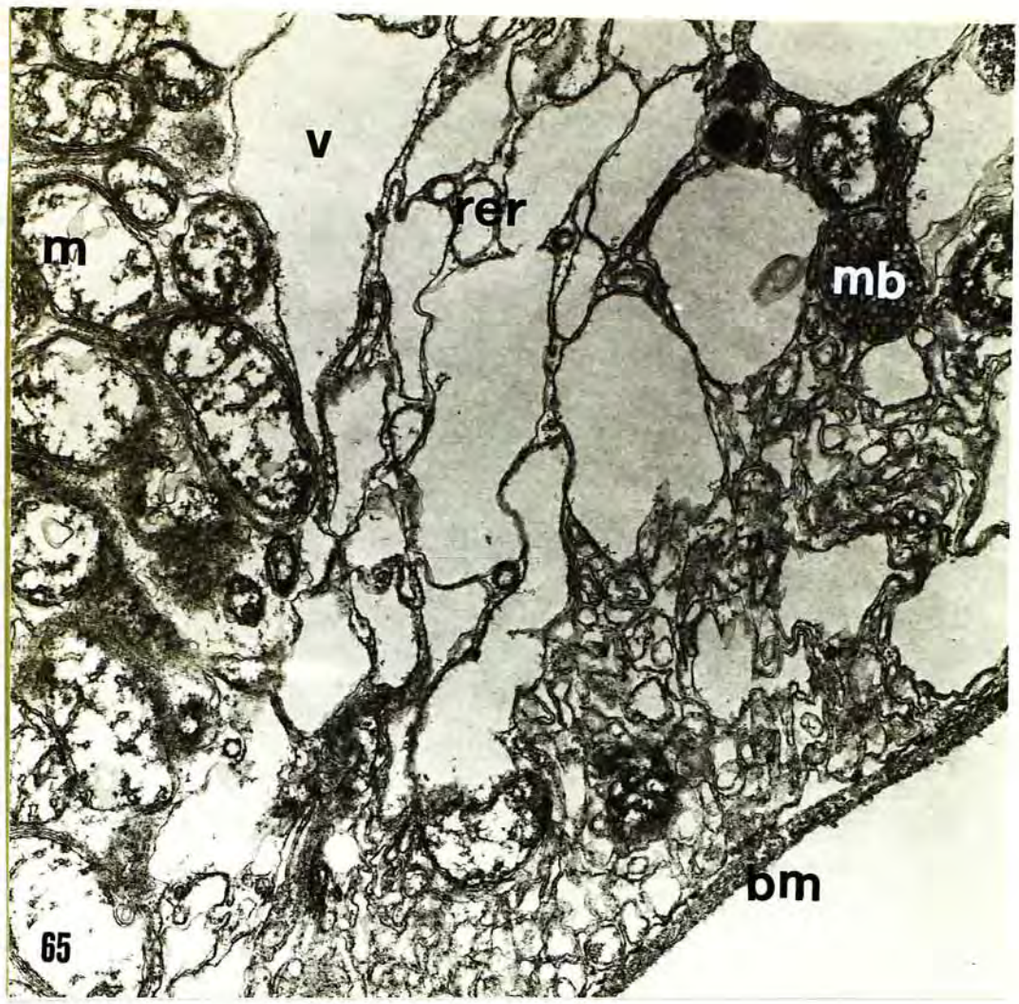

65

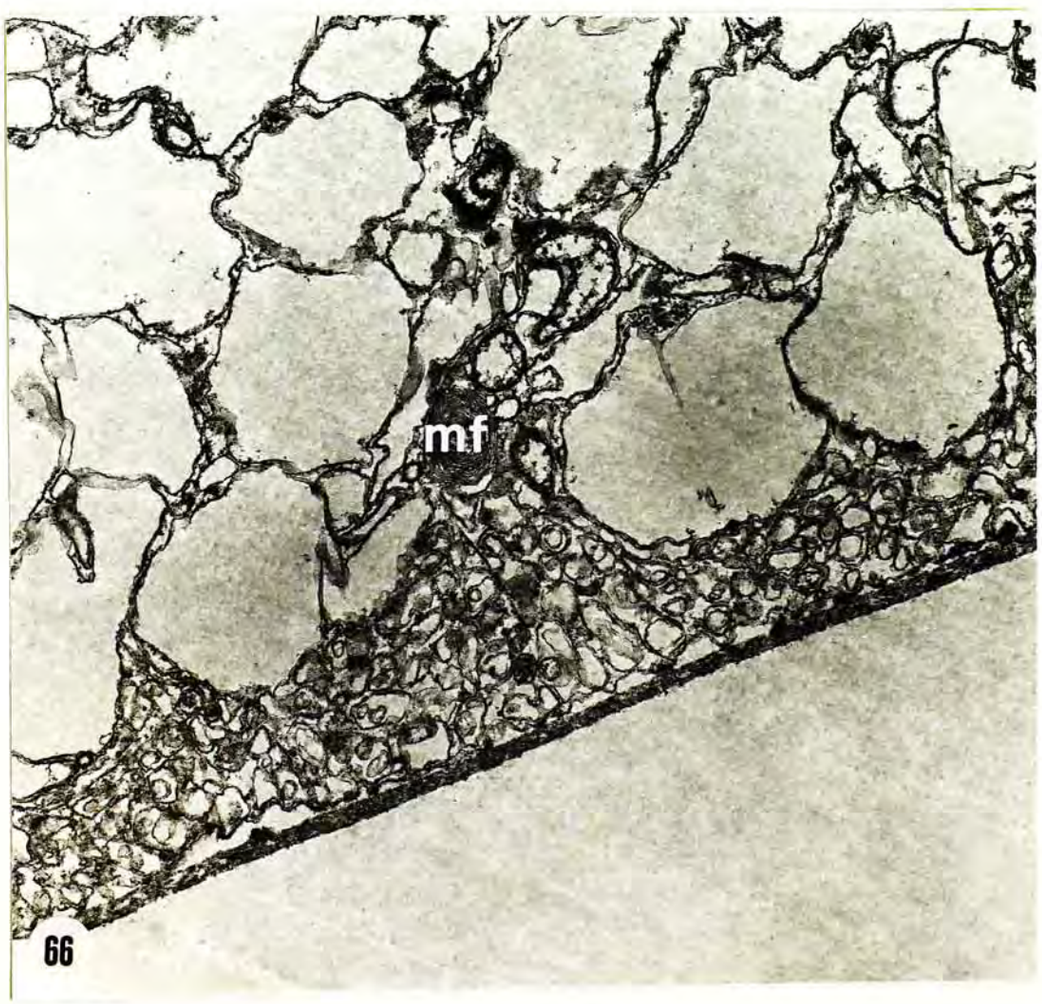

66

Fig. 67. As above. Part of nuclear region. Showing numerous vacuoles (v), damaged mitochondria (m) and nucleus (n) with chromatin materials lost. x7560.

Fig. 68. Trophozoite stage of *Nosema polyvora*. Showing dividing plasmodium (p), nuclei (n), merozoite (mz), mature spore (sp) and basal infoldings. x9660.

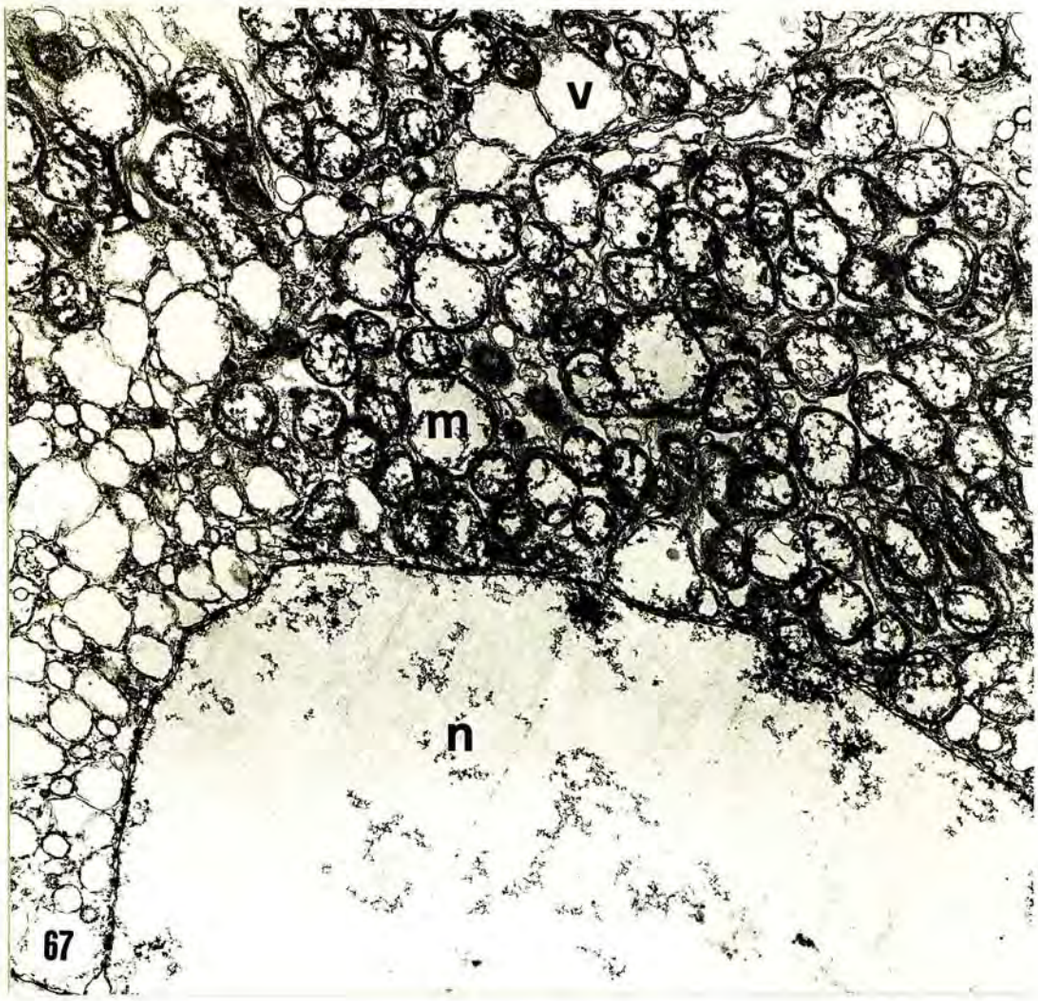
v
m
n
67

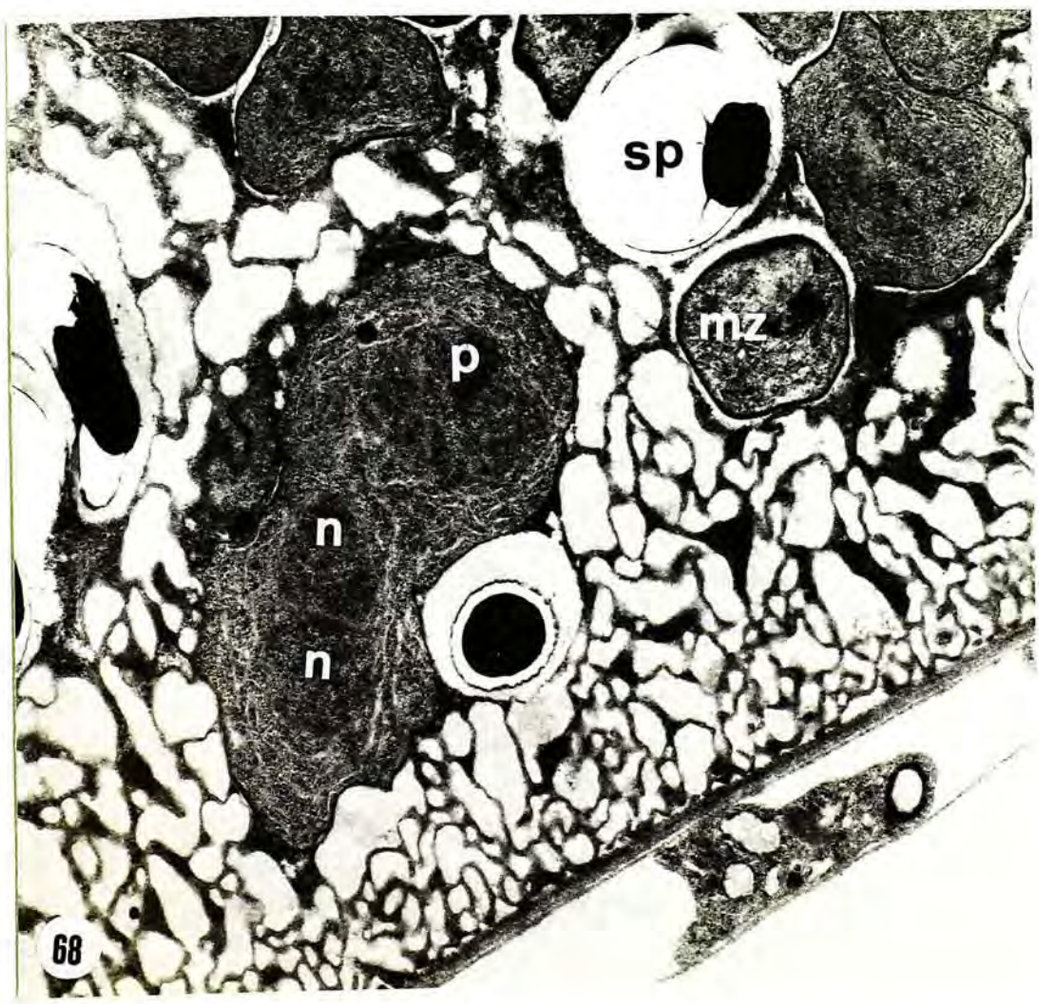
sp
mz
p
n
n
68

Fig. 69. A plasmodium undergoing binary fission to produce merozoites (mz). Mature spores (sp) are also shown. x10080.

Fig. 70. Sporont showing ribosomes (r), rough endoplasmic reticulum (rer), electron translucent spaces (s) formed between the sporoblast (sb), mature spore (sp) and host tissue. x21000.

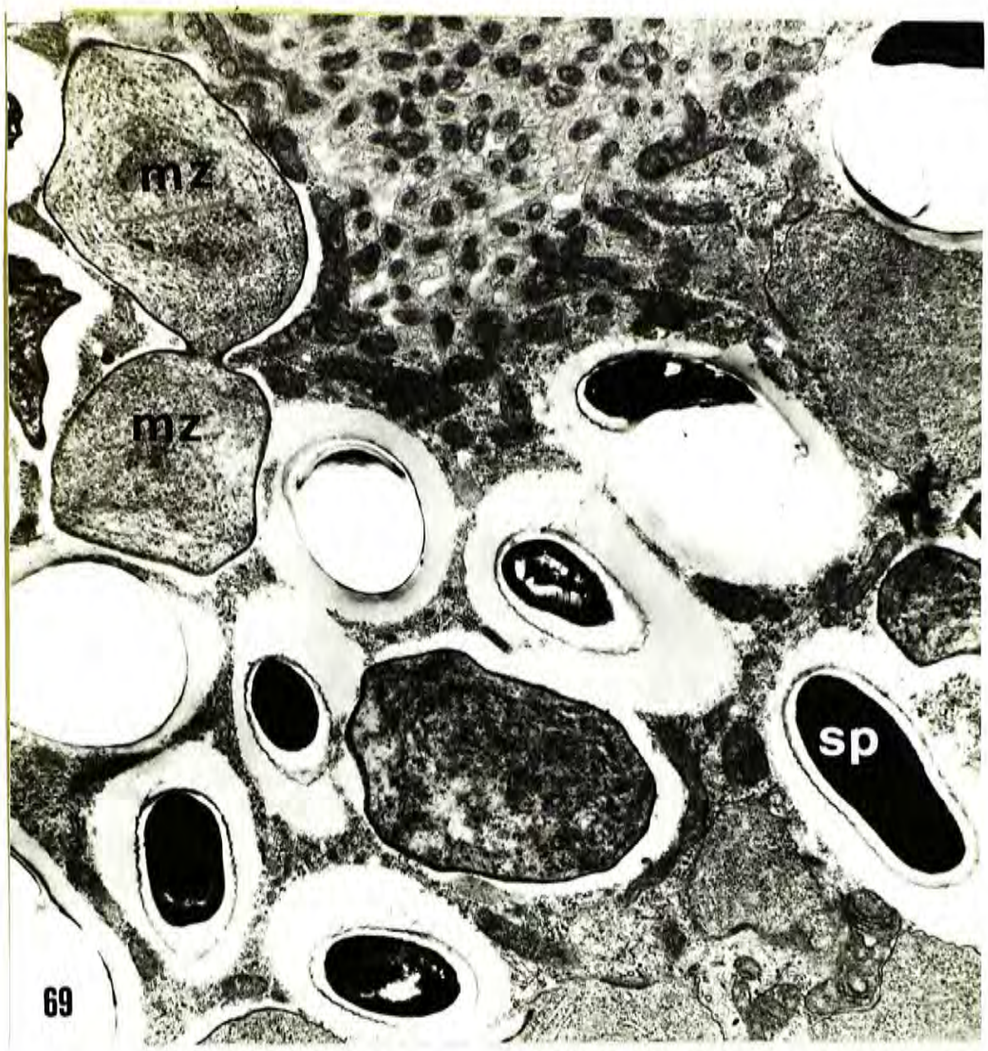

69

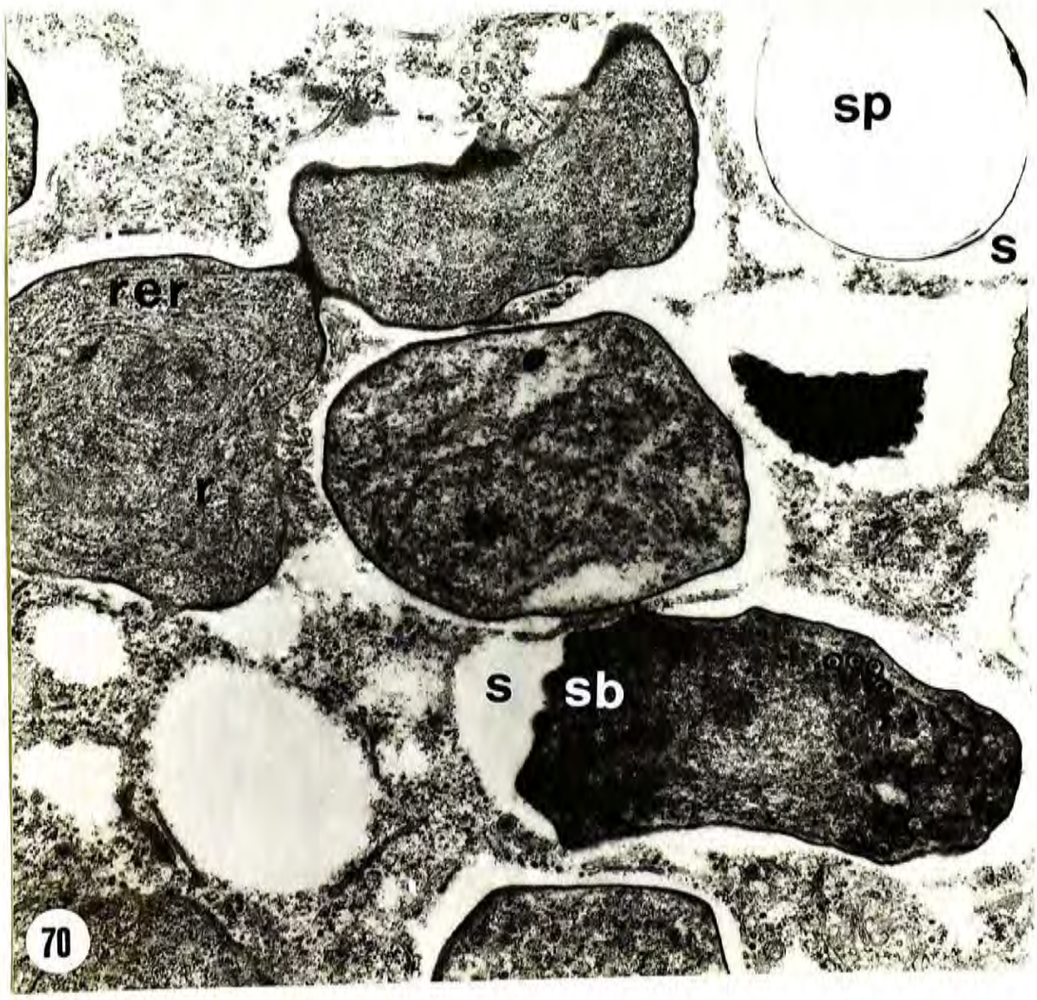

70

Fig. 71. Sporoblast showing developing polar coils (pc) and network structure (ns). x29400.

Fig. 72. Sporoblast showing a polar coil (pc) and network structure (ns). x19950.

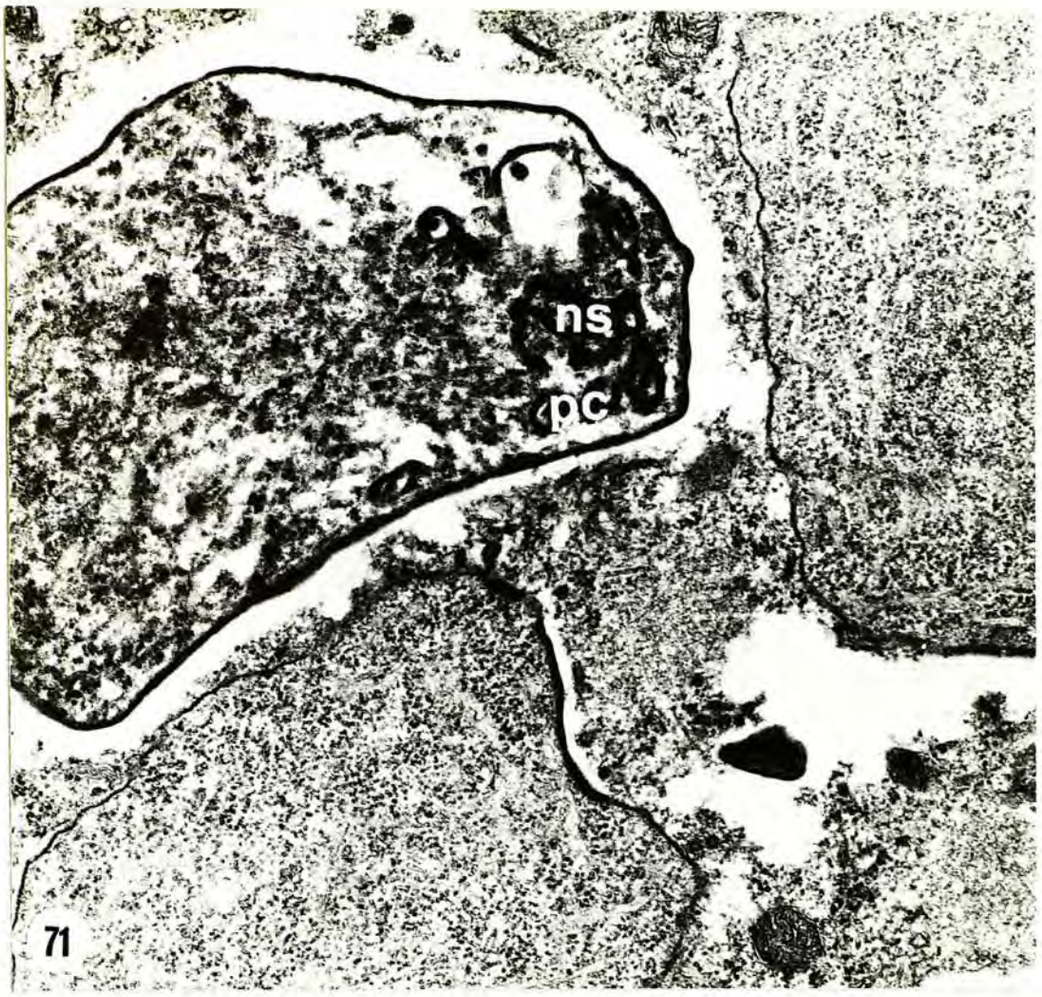

71

72

Fig. 73. High magnification of a sporoblast. Showing polar coils (pc) and network structure (ns). x75600.

Fig. 74. Low magnification of an infected principal cell. Showing microvilli (mv), numerous vacuoles (v), basement membrane (bm) and various stages of *Nosema*: merozoite (mz), sporoblast (sb) and mature spore (sp). x3990.

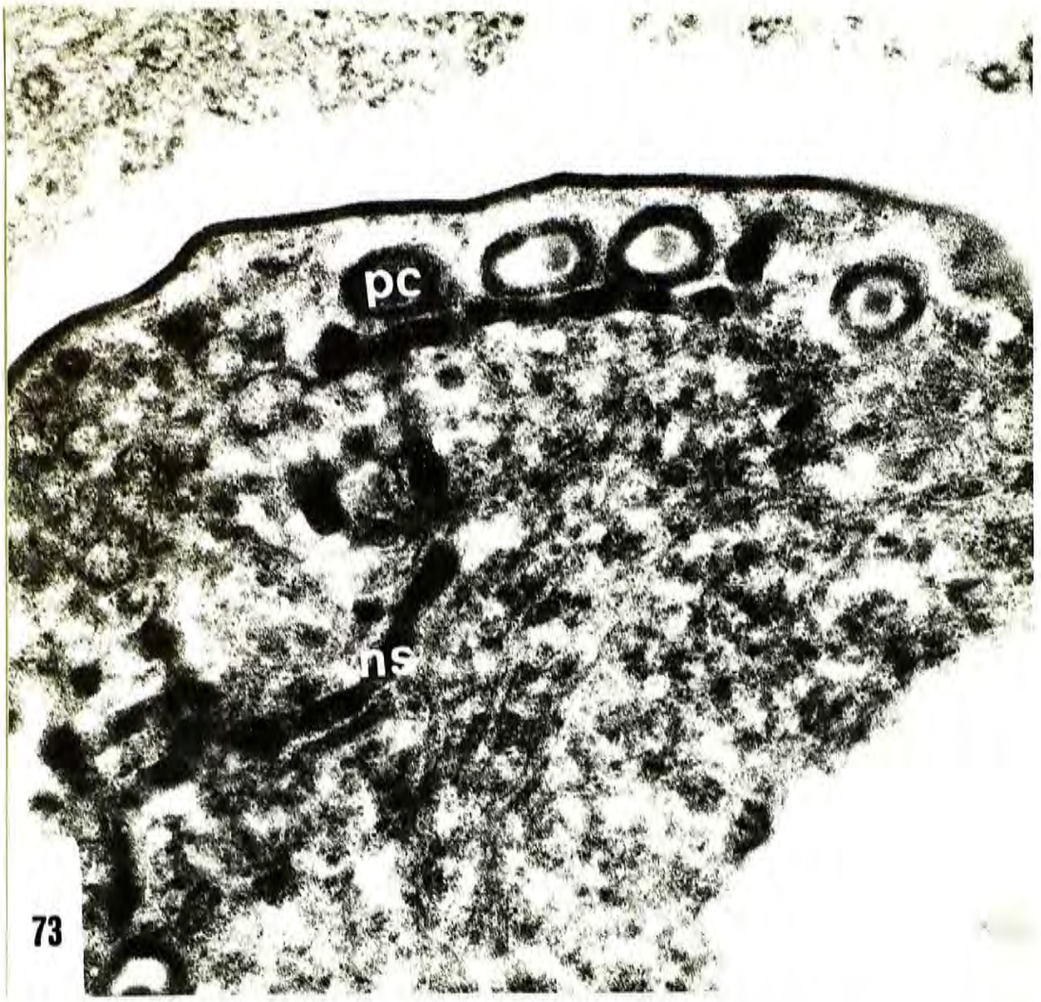

73

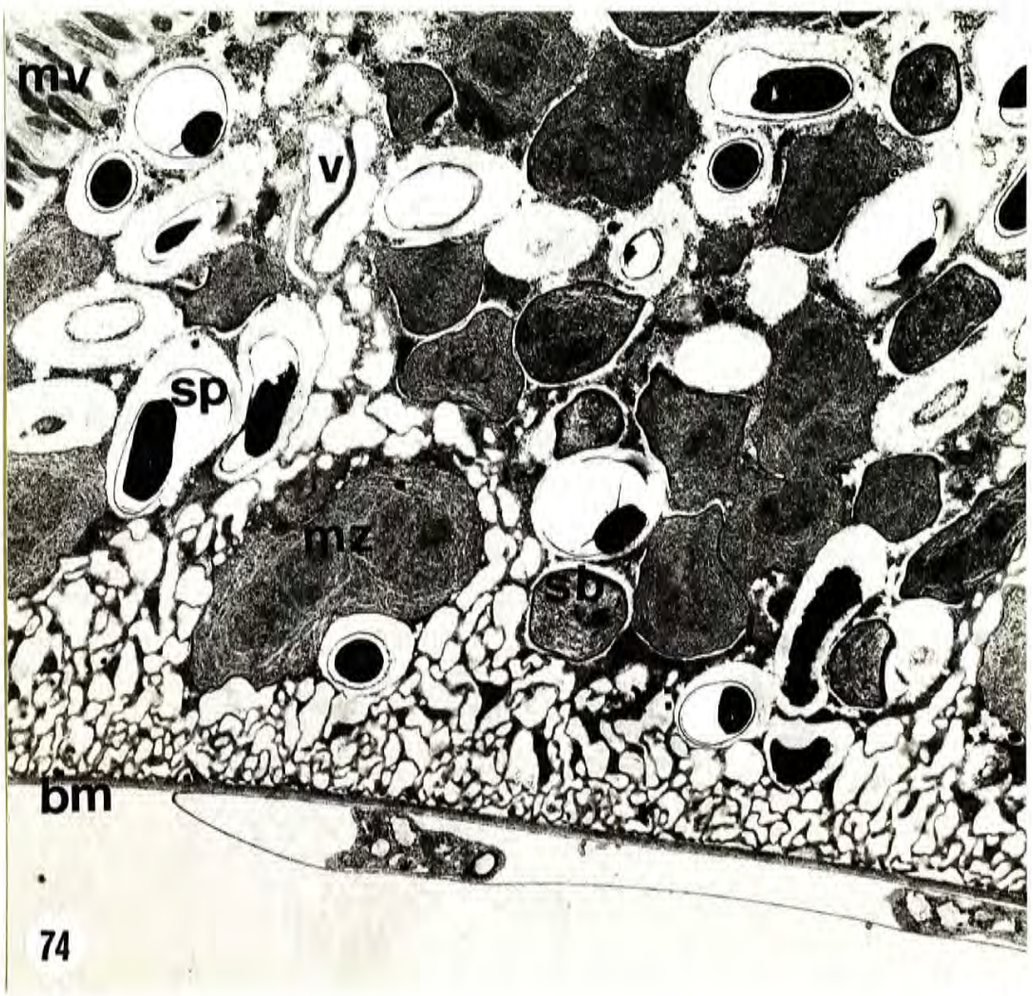

74

Fig. 75. As above. Showing microvilli (mv), vacuole-like structure (vs), sporoblast (sb) and mature spore (sp). x6090.

Fig. 76. Mature spore showing 11 pairs of polar coils (pc), polar filament (pf) and polaroplast (pp). x60900.

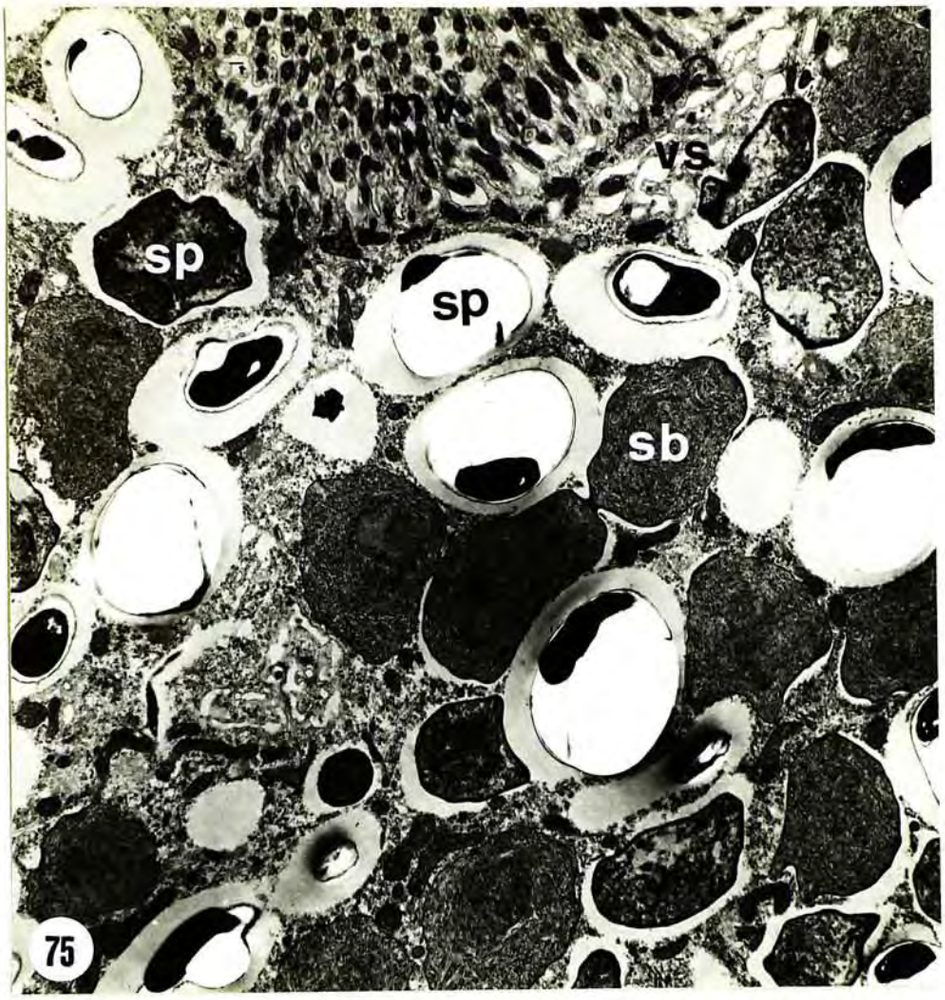
vs
sp
sp
sb
75


pc
pp
pf
76

Fig. 77. Anterior part of a mature spore. Showing polaroplast consisted of lamellar region (lr) and vesicular region (vr), polar sac (ps), anchoring disk (ad), polar filament (pf) and the layers of the spore wall: the plasma membrane (p), the endospore wall (e) and exospore wall (ex). x121800.

Fig. 78. High magnification of spore wall. Showing the exospore wall with three layers. x294000.

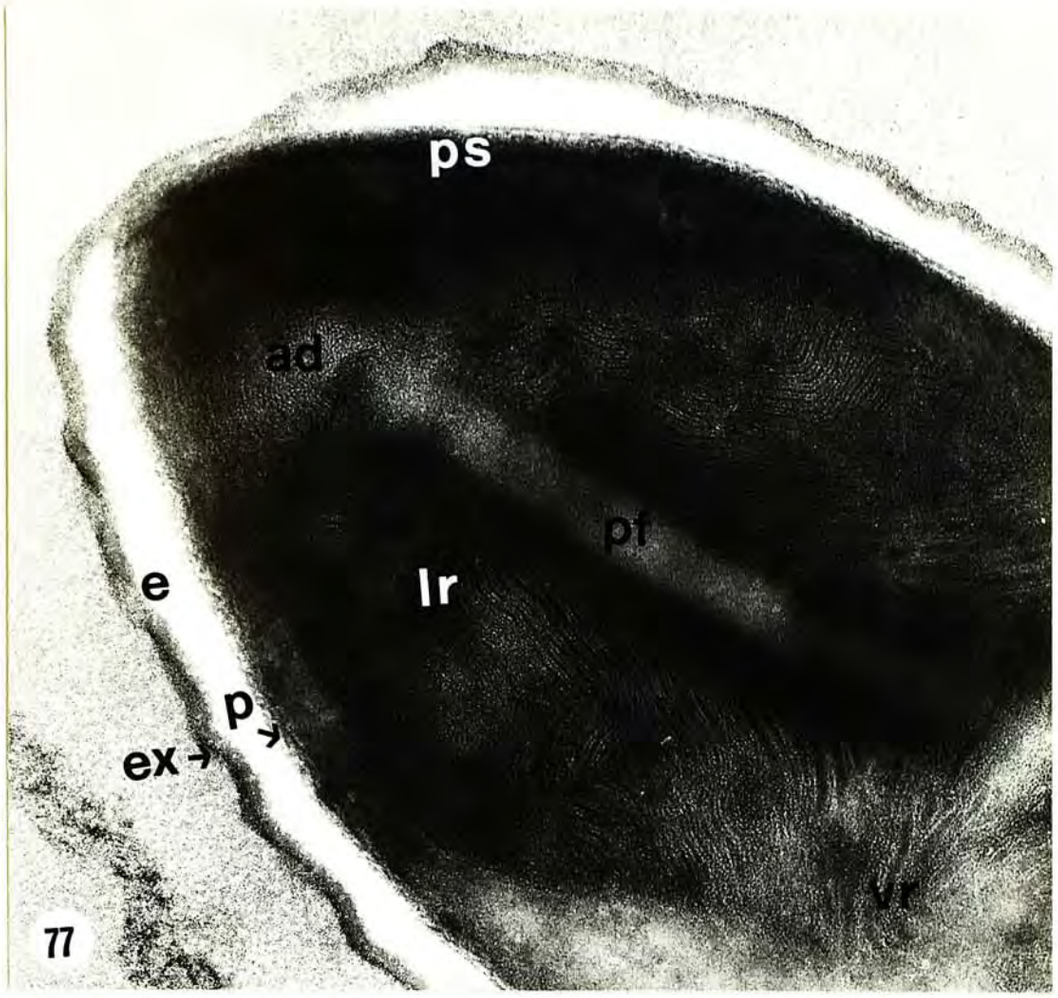

77

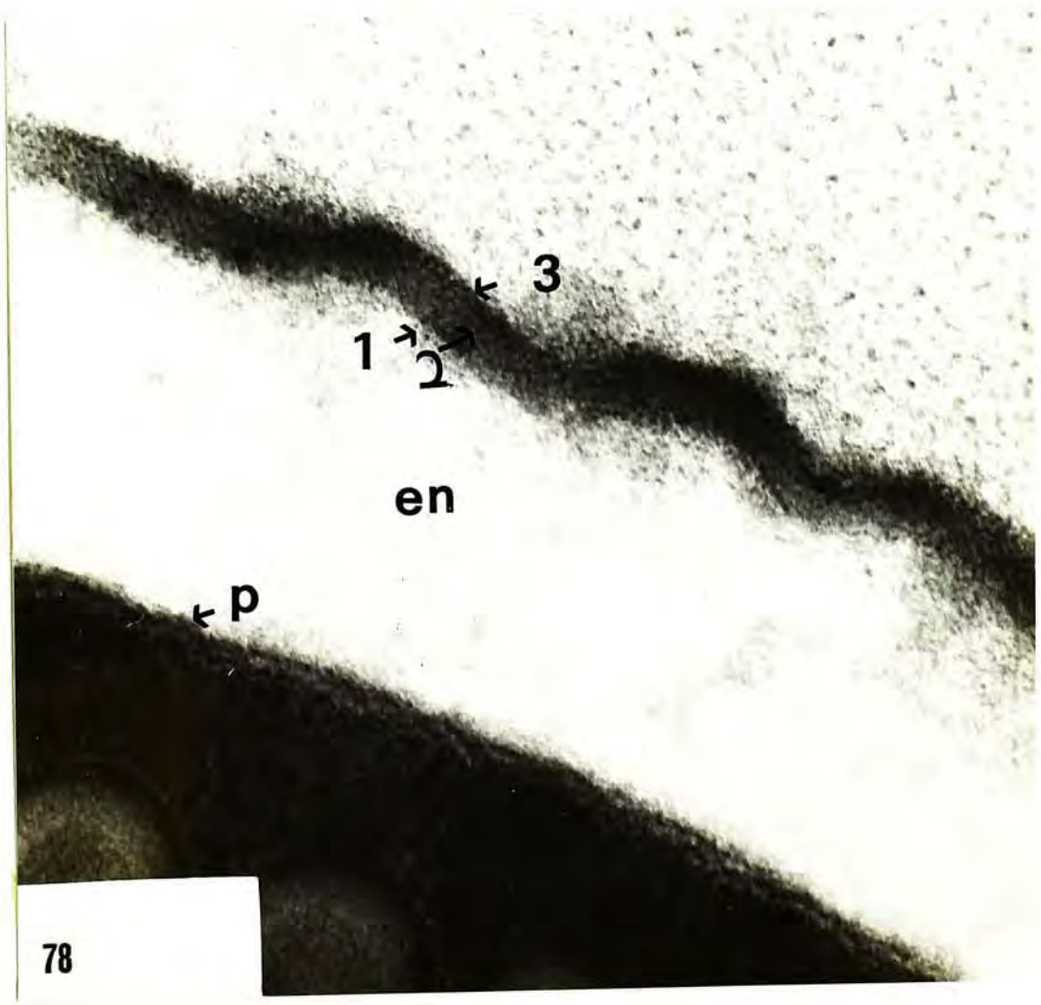

78

Fig. 79. Transverse section of coils of polar filament (pc). Showing four zones of filament and the layers of the spore wall: the plasma membrane (p), the endospore wall (e) and exospore wall (ex). x210000.

Fig. 80. Posterior part of a mature spore. Showing two nuclei (n) and rough endoplasmic reticula (rer) at the outside of nuclei. x60900.

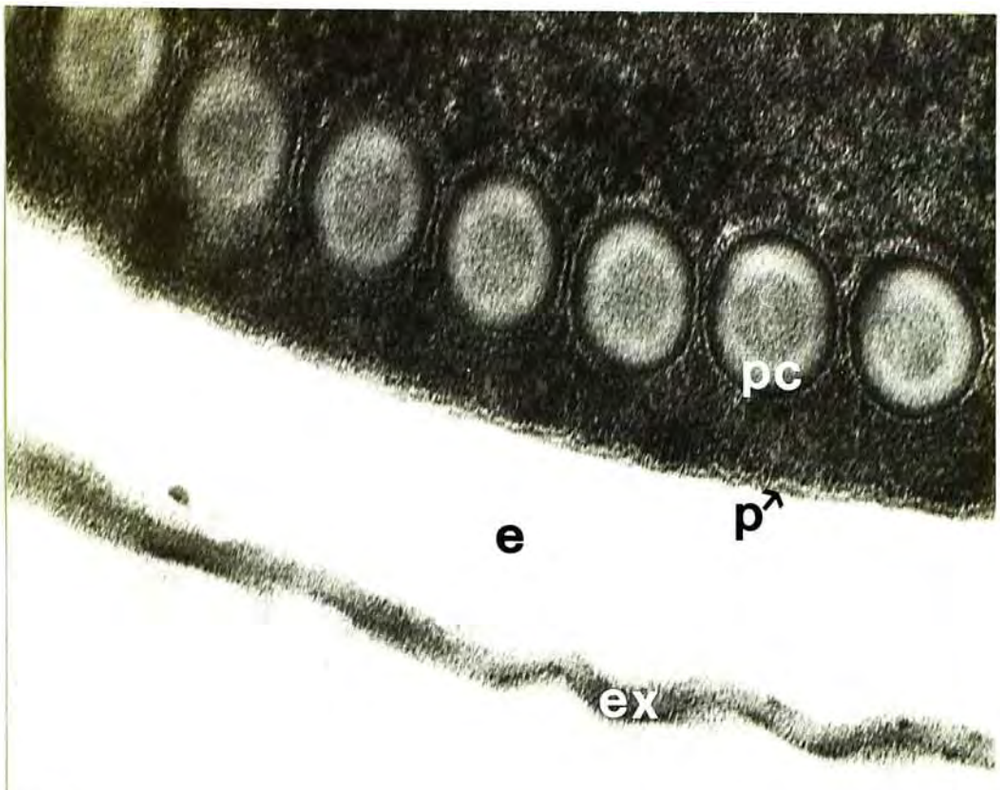

79

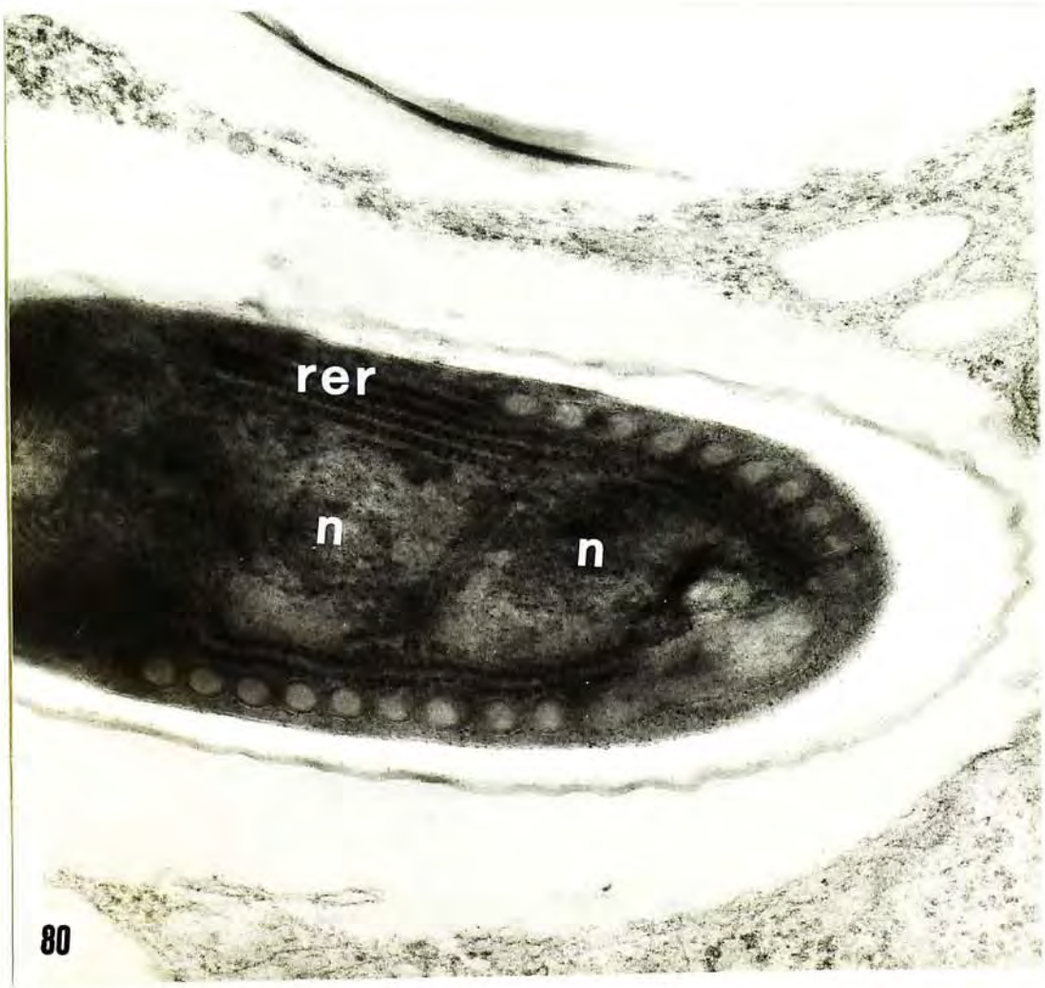

80

Fig. 81. As above. Showing a posterior vacuole (pv), polar coils (pc) and spore wall. x100800.

Fig. 82. As above. Showing three posterior vacuoles (pv), polar coils (pc) and spore wall. x100800.

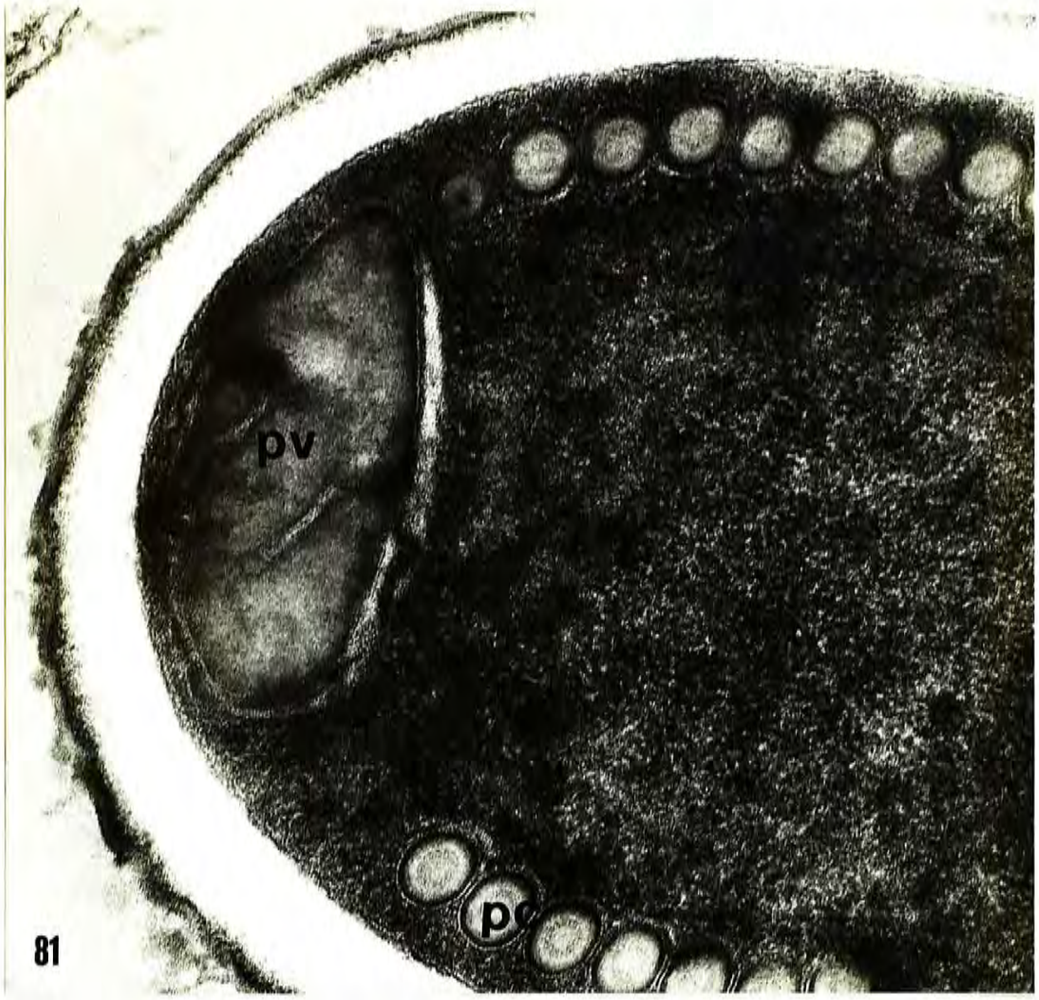

81

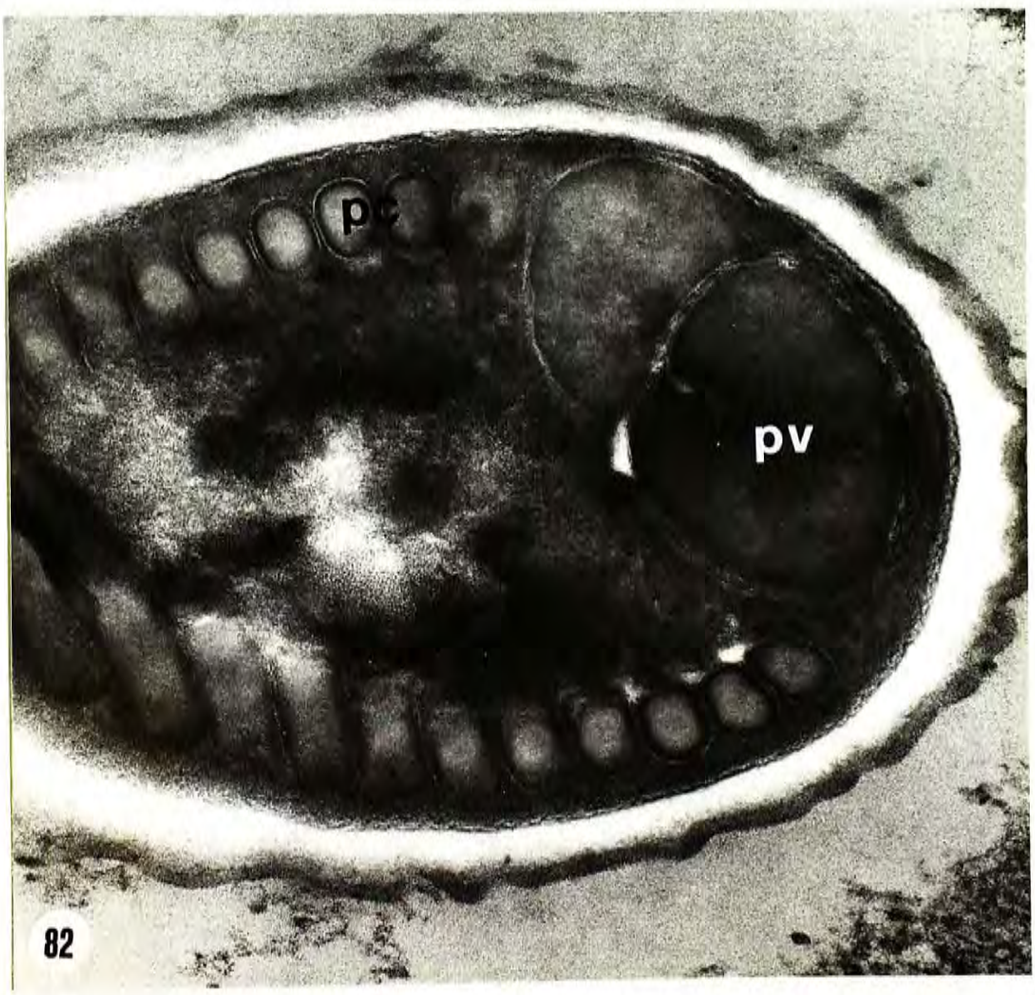

82

Fig. 83. Low magnification of an infected principal cell. Showing microvilli (mv), rough endoplasmic reticulum (rer) and cytoplasmic spaces (cs) around the spores. x9660.

Fig. 84. As above. Showing mucus secretions (ms) in the central region and apical region. x9660.

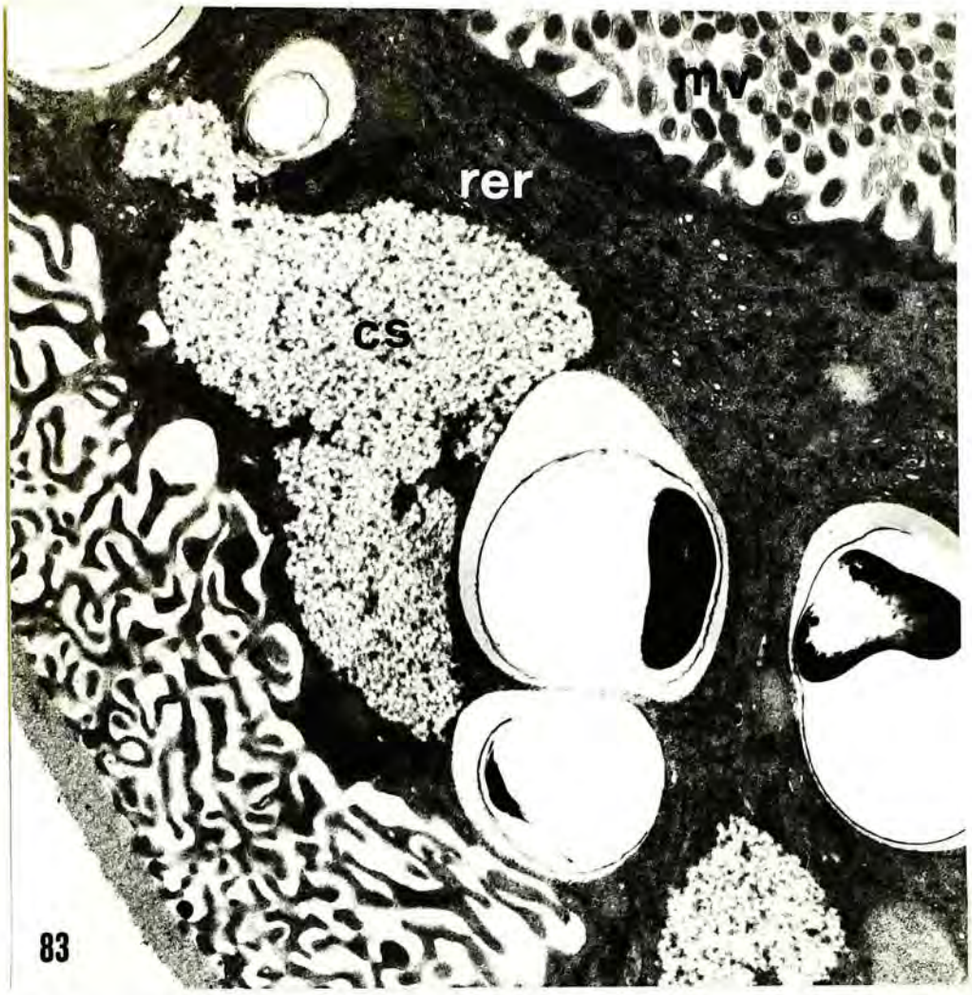

83

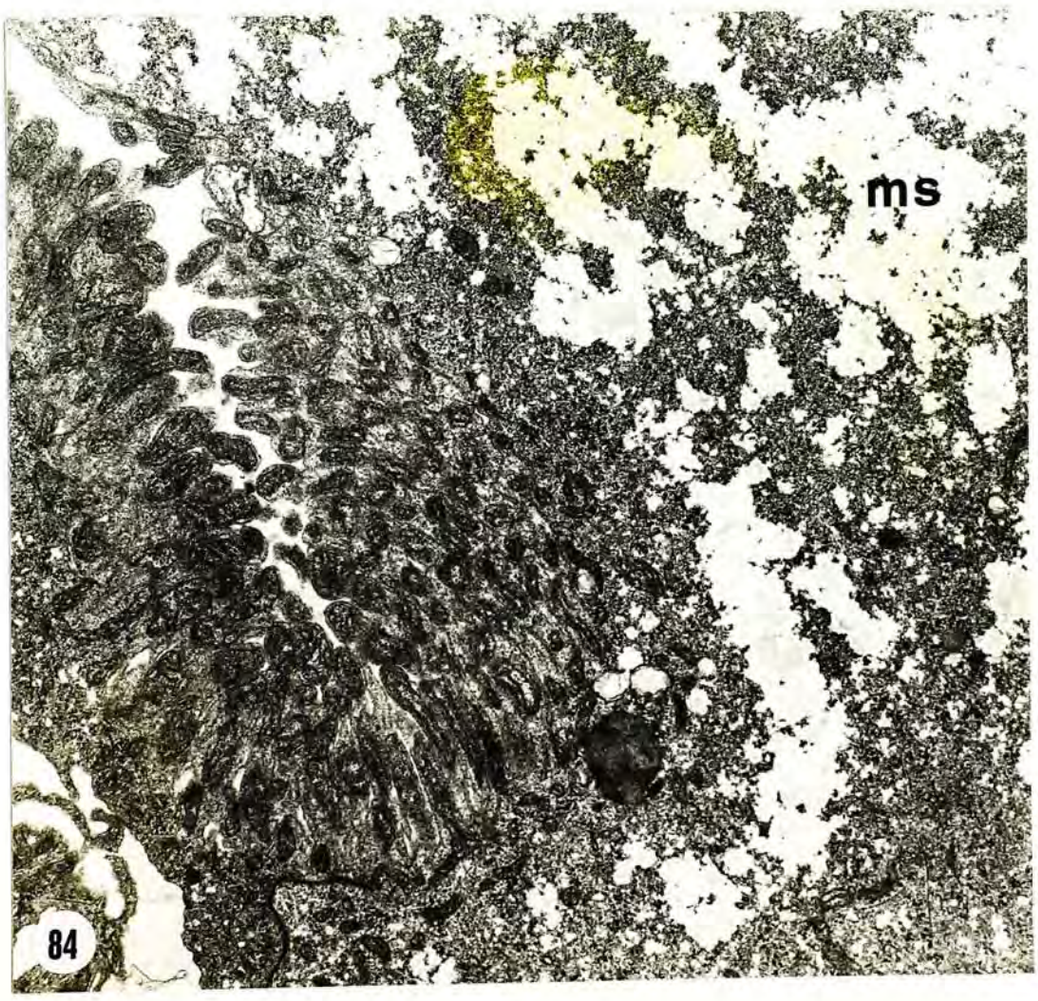

84

Fig. 85. As above. Showing microvilli (mv) and mucus secretion (ms) in apical region. x12180.

Fig. 86. High magnification of an infected principal cell. Showing mitochondria (m), rough endoplasmic reticulum (rer), golgi apparatus (g), mature spore (sp) and cytoplasmic spaces (cs). x19950.


mv
ms
85

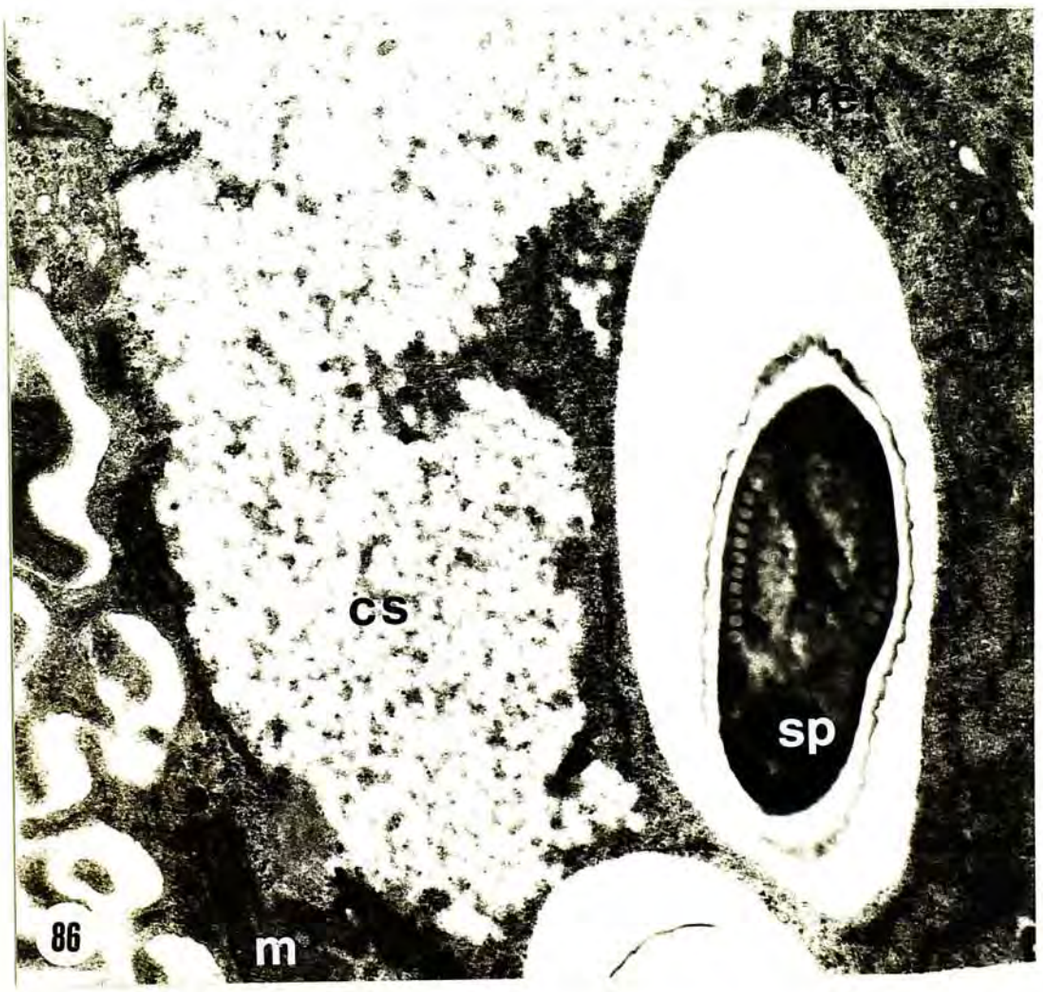
cs
sp
86
m

Fig. 87. Low magnification of an infected principal cell. Showing mechanical damages (md) formed in the cytoplasm. x9660.

Fig. 88. As above. Showing damaged microvilli (mv) and nuclei (n). x3780.

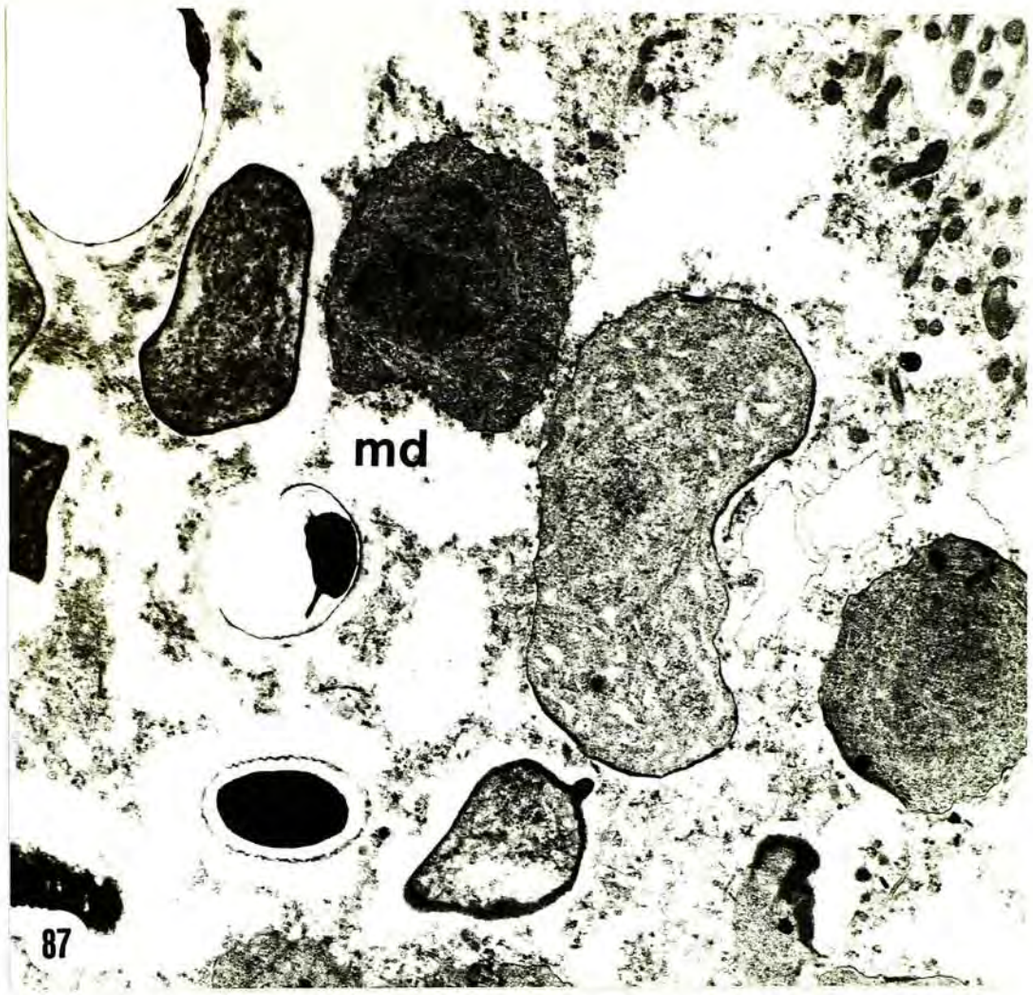
md
87

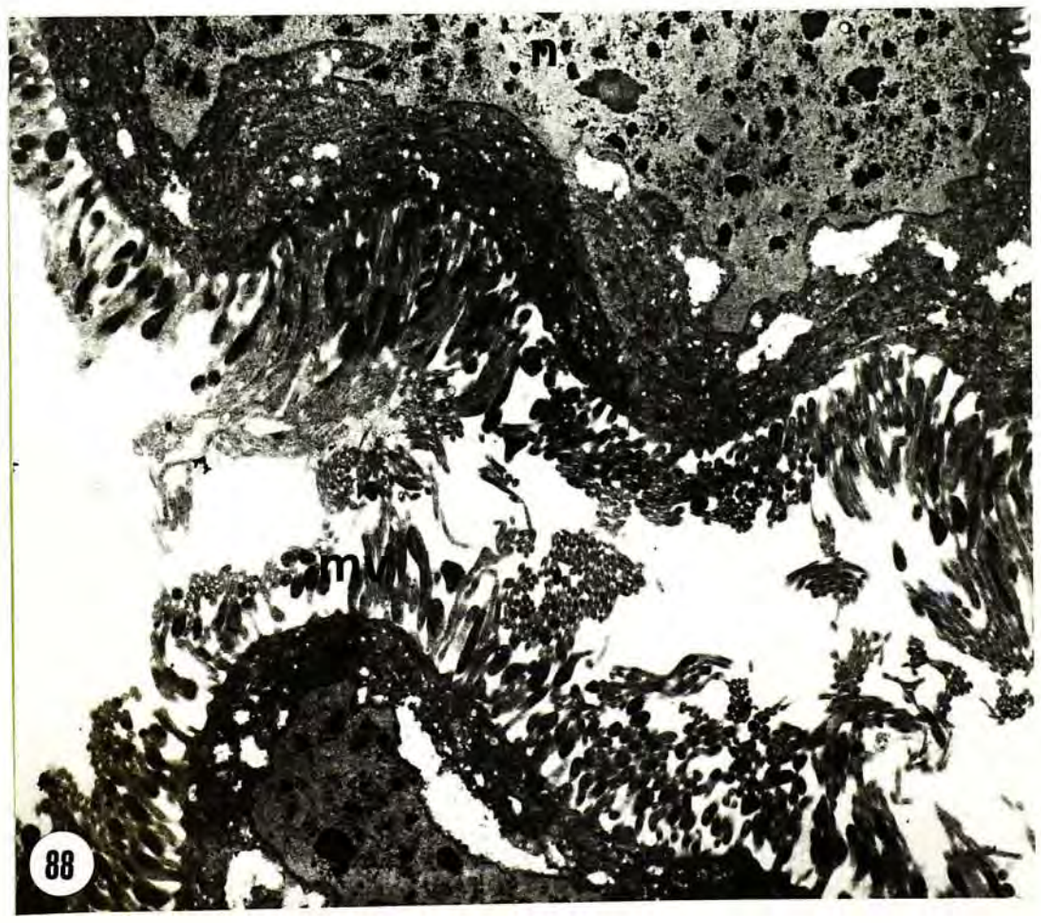
n
m
88

Fig. 89. High magnification of an infected principal cell. Showing basal infoldings and mitochondria (m) with damaged cristae. x19950.

Fig. 90. As above. Showing nucleus (n) of irregular outline, mature spore (s) and merozoite (mz). x9660.

89

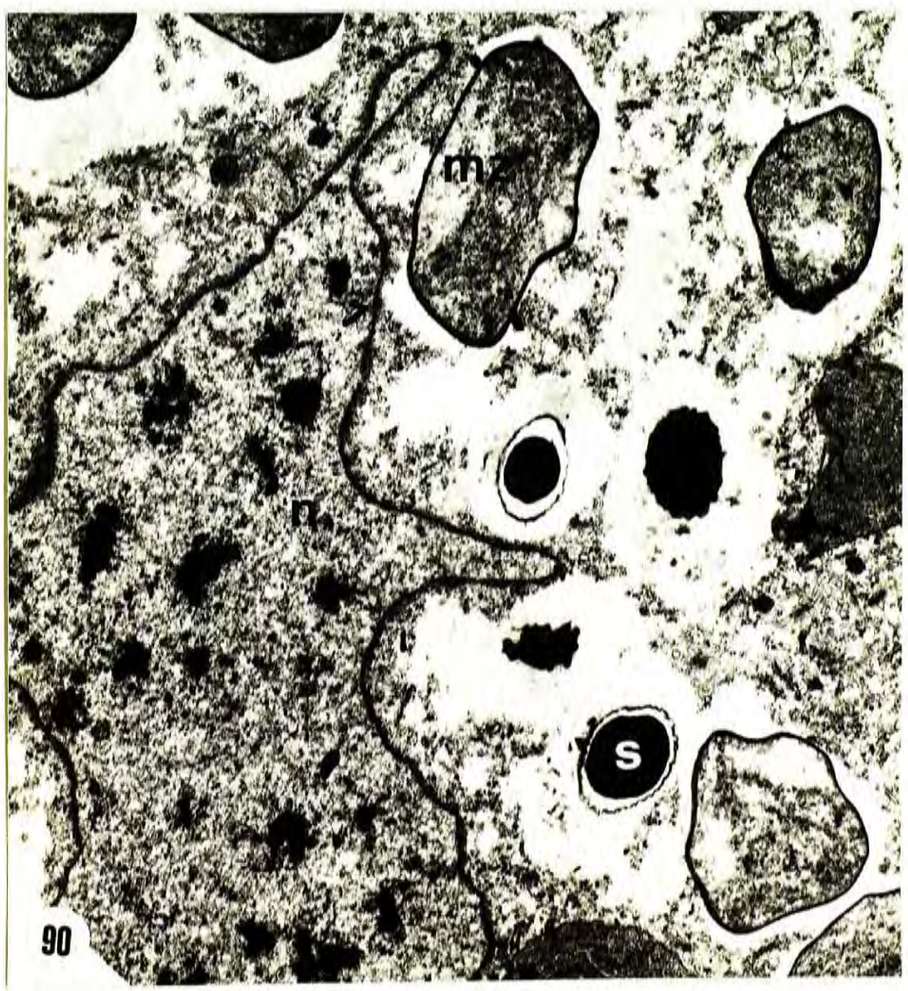

90

Table 1. Histochemical tests on the rectal lead of the Malpighian tubules of *Pieris* larva

	Rectal lead		
	Microvilli	Apical cytoplasm	Basal cytoplasm
Alcian Blue	0	0	0
Toluidine Blue	++	++	+
PAS	0	+	0
Acid Solochrome Cyanine	++	+	+
Mercury-Bromophenol Blue	+++	++	++
Sudan Black B	+	+	+
Alkaline Phosphatase	+	+	+
ATPase	+	+	+
Glucose-6-Phosphatase	0	++	0
Acid Phosphatase	0	+	+
Succinic Dehydrogenase	++	+++	+++
β-Glucuronidase	0	+	+
Calcium	0	+	0
Magnesium	0	0	0
Phosphate	0	0	+
Ferric iron	0	+	0
Carbonate	0	0	0
Uric acid	0	0	0

'+' indicates positive reaction, the number of +'s being proportional to the intensity of the reaction;
'0' indicates a negative reaction

Table 2. Histochemical tests on the iliac plexus of the Malpighian tubules of *Pieris* larva

	Iliac Plexus		
	Microvilli	Apical cytoplasm	Basal cytoplasm
Alcian Blue	0	0	0
Toluidine Blue	++	+	+
PAS	0	+	0
Acid Solochrome Cyanine	++	+	+
Mercury Bromophenol Blue	+++	++	++
Sudan Black B	++	+	+
Alkaline Phosphatase	+	+	+
ATPase	+	0	0
Glucose-6-Phosphatase	0	++	++
Acid Phosphatase	0	+	+
Succinic Dehydrogenase	++	+++	+++
β-Glucuronidase	0	0	0
Calcium	0	++	0
Magnesium	0	0	0
Phosphate	0	+	0
Ferric iron	0	+	0
Carbonate	0	0	0
Uric acid	0	0	0

'+' indicates positive reaction, the number of +'s being proportional to the intensity of the reaction;
'0' indicates a negative reaction

Table 3. Histochemical tests on the yellow region of the Malpighian tubules of *Pieris* larva

	Yellow region		
	Microvilli	Apical cytoplasm	Basal Cytoplasm
Alcian Blue	0	0	0
Toluidine Blue	++	0	0
PAS	+	0	0
Acid Solochrome Cyanine	++	++	+
Mercury Bromophenol Blue	+++	++	+
Sudan Black B	++	+	+
Alkaline Phosphatase	+++	+	++
ATPase	+	++++	++
Glucose-6-Phosphatase	0	++	0
Acid Phosphatase	0	+	+
Succinic Dehydrogenase	+++	+++	++
β-Glucuronidase	0	0	0
Calcium	0	++++	+++
Magnesium	0	++	0
Phosphate	0	++	0
Ferric iron	0	+	0
Carbonate	0	0	0
Uric acid	0	0	0

'+' indicates positive reaction, the number of '+'s being proportional to the intensity of the reaction;
'0' indicates a negative reaction

Table 4. Histochemical tests on the white region of the Malpighian tubules of *Pieris* larva

	White region		
	Microvilli	Apical cytoplasm	Basal cytoplasm
Alcian Blue	0	0	0
Toluidine Blue	++	+	+
PAS	+	+	+
Acid Solochrome Cyanine	+	0	0
Mercury Bromophenol Blue	+++	++	++
Sudan Black B	++	+	+
Alkaline Phosphatase	++	+	+
ATPase	++	+	+
Glucose-6-Phosphatase	0	++	0
Acid Phosphatase	0	+	+
Succinic Dehydrogenase	++	++	++
β-Glucuronidase	0	0	0
Calcium	0	++	0
Magnesium	0	0	0
Phosphate	0	+	0
Ferric iron	0	+	0
Carbonate	0	0	0
Uric aciid	0	0	0

'+' indicates positive reaction, the number of +'s being proportional to the intensity of the reaction;
'0' indicates a negative reaction

Table 5. Bio-Rad Protein Micro Assay Standard Curve

Standard	Conc. (ug/ml)	Abs. (595nm)
1	4.00	0.126
2	8.00	0.234
3	12.00	0.350
4	16.00	0.451
5	20.00	0.542
Sample 1	**10.07**	**0.290**
Sample 2	**10.57**	**0.303**